

**The role of membrane transporters in the
pharmacokinetics of psychotropic drugs: *in vitro* studies
with special focus on organic cation transporters**

Doctoral Thesis

In partial fulfillment of the requirements for the degree
“Doctor rerum naturalium (Dr. rer. nat.)”
in the Molecular Medicine Study Program
at the Georg-August University Göttingen

submitted by

João Nuno dos Santos Pereira

born in 1989, Torres Novas, Portugal

November 2014

Members of the Thesis Committee:

Supervisor:

Name, Institute: **Prof. Dr. med. Jürgen Brockmüller**, Institute for Clinical Pharmacology, University Medical Center, Georg-August University Göttingen

Second member of the thesis committee:

Name, Institute: **Prof. Dr. med. Gerhard Burckhardt**, Institute for Vegetative Physiology, University Medical Center, Georg-August University Göttingen

Third member of the thesis committee:

Name, Institute: **Prof. Dr. rer. nat. Uwe-Karsten Hanisch**, Institute for Neuropathology, University Medical Center, Georg-August University Göttingen

Date of Disputation: 30.01.2015

AFFIDAVIT

Here I declare that my doctoral thesis entitled “**The role of membrane transporters in the pharmacokinetics of psychotropic drugs: *in vitro* studies with special focus on organic cation transporters**” has been written independently with no other sources and aids than quoted.

João Nuno dos Santos Pereira

Göttingen, November 2014

List of Publications:

Dos Santos Pereira, João N., Tadjerpisheh, Sina, Abed, Manar Abu, Saadatmand, Ali R., Weksler, Babette, Romero, Ignacio A., Couraud, Pierre-Olivier, Brockmüller, Jürgen, & Tzvetkov, Mladen V. **2014**. The Poorly Membrane Permeable Antipsychotic Drugs Amisulpride and Sulpiride Are Substrates of the Organic Cation Transporters from the SLC22 Family. *The AAPS journal*, 16(6), 1247–1258.

Tzvetkov, Mladen V., Dos Santos Pereira, João N., Meineke, Ingolf, Saadatmand, Ali R., Stingl, Julia C., & Brockmüller, Jürgen. **2013**. Morphine is a substrate of the organic cation transporter OCT1 and polymorphisms in OCT1 gene affect morphine pharmacokinetics after codeine administration. *Biochemical pharmacology*, 86(5), 666–678.

*“We shall allow only one wrong thing to exist: the absolute truth”*¹

Afonso Cruz, *Where the umbrellas go*, 2013

¹Original: “Faremos com que exista apenas uma coisa errada: a verdade absoluta”, Afonso Cruz, *Para onde vão os guarda chuvas*, 2013

Contents

Contents	v
Acknowledgements	ix
Abstract	x
List of Figures	xii
List of Tables	xv
1 Introduction	1
1.1 Efficacy of the treatment of major depression, schizophrenia and bipolar disorder	1
1.2 Drug absorption, distribution, metabolism and excretion	2
1.2.1 General principles of pharmacokinetics	2
1.2.2 Absorption and distribution	2
1.2.3 Metabolism and excretion	3
1.3 Transport across cellular membranes	5
1.3.1 Passive diffusion	8
1.3.2 Carrier-mediated transport	10
1.4 Influence of membrane transporters on drug pharmacokinetics	12
1.4.1 Drug transport and drug transporters at the blood-brain barrier	15
1.4.2 Factors affecting drug transporter activity: genetic polymorphisms and drug-drug interactions	15
1.5 OCT1 - A highly polymorphic membrane transporter important for drug pharmacokinetics	16
1.5.1 Drug-binding to OCT1	16
1.5.2 Genetic variation on the OCT1 gene	17
1.6 Variability on the pharmacokinetics of psychotropic drugs	18
1.7 Aims of this work	20
2 Materials	21
2.1 Reagents	21
2.2 Antibodies	24
2.3 Consumables	24
2.4 Cell lines	25

2.5	Equipment	25
2.6	Software	26
3	Methods	27
3.1	Parallel artificial membrane permeability assay (PAMPA)	27
3.2	Gene expression analysis	29
3.2.1	Reverse transcription	29
3.2.2	Gene expression analysis with TaqMan [®] low density gene expression arrays	30
3.3	DAB-Immunostaining of paraffin-embedded sections on glass	31
3.4	Cell culture	31
3.4.1	HEK293 cells	31
3.4.2	hCMEC/D3 cells	32
3.4.3	MDCK II cells	32
3.5	Uptake measurements in HEK293 cells	33
3.5.1	Uptake measurements in 12-well plates	33
3.5.2	Uptake measurements of amisulpride in Petri dishes	34
3.6	Uptake measurements in hCMEC/D3 cells	34
3.7	LC-MS/MS quantification of tiapride, sultopride and amisulpride	35
3.8	Quantification of total cellular protein by the bicinchoninic acid (BCA) assay	35
3.9	Stable integration of the pFRT/LacZeo plasmid on the MDCK II cell line	36
3.9.1	Plasmid midi-prep: Isolation of plasmid DNA by solid extraction with a commercial kit	36
3.9.2	Plasmid linearization and gel extraction	37
3.9.3	Transfection and Selection of MDCK II clones	38
3.9.4	TEER (transepithelial electrical resistance) measurements	39
3.9.5	β -Galactosidase assay	40
3.10	Data analysis	41
3.10.1	Enzyme kinetics	41
3.10.2	Estimation of maximal drug concentration in the portal vein	42
3.10.3	Prediction of drug chemical properties	42
3.10.4	Statistics	43
4	Results	44
4.1	Membrane permeability of psychotropic drugs	44
4.1.1	Computer based prediction of the physicochemical properties of drugs	44
4.1.2	Transporter independent membrane permeability	46
4.2	Gene expression analysis of membrane drug transporters	47
4.2.1	Validation of the TaqMan [®] low density array microfluidic cards	48
4.2.2	Gene expression analysis in organs relevant for drug pharmacokinetics	49
4.2.3	Gene expression analysis in primary human brain cells	52
4.2.4	Donor to donor variation in the expression of drug transporters in primary human brain microvascular endothelial cells	56

4.2.5	Gene expression analysis in the HEK293-pcDNA5, HEK-OCT1 and hCMEC/D3 cell lines	58
4.3	Immunohistochemistry of brain tissue	61
4.4	Validation of the HEK293 cell lines expressing OCT1, OCT2, OCT3, OCTN1 and OCTN2 with typical substrates	63
4.5	Transport of the poorly membrane permeable antipsychotics amisulpride, sulpiride, sultopride and tiapride by organic cation transporters	65
4.5.1	Uptake of amisulpride by the organic cation transporters of the <i>SLC22</i> family	65
4.5.2	Uptake of sulpiride by the organic cation transporters of the <i>SLC22</i> family	68
4.5.3	Uptake of sultopride and tiapride by the organic cation transporters of the <i>SLC22</i> family	69
4.5.4	Effect of polymorphisms on the OCT1 (<i>SLC22A1</i>) gene on the uptake of amisulpride by OCT1	72
4.5.5	Uptake of amisulpride by the MATE1 and MATE2-K transporters	72
4.6	Uptake of amisulpride and sulpiride in the human brain endothelial cell line hCMEC/D3	74
4.7	Interaction between psychotropic drugs with high membrane permeability and OCT1	76
4.7.1	Lack of uptake of clozapine, lamotrigine, amantadine and citalopram by OCT1	76
4.7.2	Characterization of the interactions between amitriptyline and OCT1	78
4.7.3	Drug-drug interactions involving psychiatric drugs which affect the OCT1-mediated uptake of morphine	83
4.8	The cellular uptake of tyramine is affected by genetic polymorphisms in OCT1	86
4.9	Establishment of a MDCK II cell line for targeted chromosomal gene integration	89
5	Discussion	92
5.1	Membrane permeability of psychotropic drugs	92
5.2	Amisulpride and sulpiride are substrates of the organic cation transporters of the <i>SLC22</i> family and MATEs	94
5.3	The role of carrier-mediated transport of amisulpride and sulpiride at the blood-brain barrier	95
5.4	Transport of amisulpride and sulpiride in hCMEC/D3 cells	96
5.5	Organic cation transporters may influence the pharmacokinetics of amisulpride and sulpiride	98
5.6	Role of polymorphisms in organic cation transporters on the pharmacokinetics of amisulpride and sulpiride	100
5.7	Sultopride and Tiapride are not substrates of the organic cation transporters of the <i>SLC22</i> family	101
5.8	Gene expression analysis of drug membrane transporters in tissues relevant for drug distribution and primary brain cells	102
5.9	Interaction between psychotropic drugs with high membrane permeability and OCT1	106

5.9.1	The interaction of amitriptyline with OCT1	107
5.9.2	Inhibition of OCT1-mediated morphine uptake by antidepressants and other drugs	109
5.10	Genetic variants in OCT1 affect the uptake of the biogenic amine tyramine	110
5.11	Establishment of a MDCK II cell line for targeted chromosomal integration	110
6	Conclusion	112
A	Assays used on the custom-made TaqMan[®] low density arrays	115
B	Step-by-step protocol for DAB-immunostaining of paraffin-embedded sections on glass	117
C	Gene expression of membrane transporters - Tables	120
	Bibliography	128

Acknowledgements

This work is the end of a path which has been as much influenced by myself, as by the people surrounding me.

I am grateful to Prof. Jürgen Brockmöller for supervising my work, and for giving me the opportunity to spend the last few years in Göttingen at the Institute for Clinical Pharmacology. His consideration, very accurate observations, and constructive advice were always very much appreciated.

I owe my development into a better scientist to the supervision and support of Dr. Mladen Tzvetkov. His great knowledge, advice and also critic, were invaluable for my development. Last but not least, his critical reading of this manuscript significantly contributed to its improvement.

I would like to thank Prof. Gerhard Burckhardt and Uwe–Karsten Hanisch for being in my thesis committee and for the always pleasant meetings with vivid discussions, which were very helpful.

I am also grateful to Dr. Oliver Wirths and Petra Tucholla for their invaluable help in doing immunological stainings.

I am thankful to the colleagues from the Institute for Vegetative Physiology who organized a great meeting every year, where I had the chance to present my work, and learn from experience people in the field. Additionally, I would like to thank Yohannes Hagos and Anette Kühne from PortaCellTec biosciences without whom some parts of this work would not have been possible.

I thank my colleagues in our institute for the good mood and for making sure that birthdays, cake and chocolate were never forgotten. A special thanks to Ellen Bruns, for her fantastic support and technical skills with the mass spectrometry. Sven Müller for his great support, and finally Bernd Zirk, who was even lent me some of his equipment to write this thesis. A special thanks goes also to Helen, Nawar and Mohammad for proof-reading this manuscript.

The greatest influence always came from my family and friends. From the ones who are far away, and the ones who are close by. They were, are, and will always be, the key to personal, academic and professional success.

Abstract

The role of membrane transporters in the pharmacokinetics of psychotropic drugs: *in vitro* studies with special focus on organic cation transporters

The treatment of common psychiatric disorders like major depression, schizophrenia and bipolar disorder is characterized by low efficacy and variability in the case of depression and bipolar disorder, and of undesirable side effects in the case of schizophrenia. One of the explanations is that the drug may not be reaching its site of action, at concentrations that are high enough to provoke a response. On the other hand, poor elimination of the drug from the body may lead to high plasma concentrations, which may cause undesirable side effects.

Variations in membrane transport at the blood-brain barrier might affect the concentration of psychotropic drugs at their site of action. In organs such as the liver and kidney, variations in membrane transport may affect drug elimination.

Using a parallel artificial membrane assay, 31 commonly used psychotropic drugs were screened for their ability to penetrate cell membranes by passive diffusion. Using custom made TaqMan[®] low-density gene expression arrays, the mRNA expression of 90 drug transporters was analyzed in organs relevant for drug pharmacokinetics and in human primary brain cells. HEK293 cells overexpressing organic cation transporters were used to study the transporter-mediated cellular uptake of psychotropic drugs. Finally, the immortalized human brain microvascular endothelial cell line, hCMEC/D3, was used as a blood-brain barrier model to study influx transport.

In human primary brain microvascular endothelial cells (HBMECs), the expression of organic cation transporters was substantially lower than in other organs like the liver and the kidney. Nonetheless organic cation transporters were detected in HBMECs. OCTN2 was the organic cation transporter with the highest expression, followed by OCTN1, OCT1 and OCT3.

Amisulpride, sulpiride, sultopride and tiapride were identified as drugs with low membrane permeability, which may require influx transport to reach their site of action in the brain. Amisulpride and sulpiride were identified *in vitro* as substrates of the organic cation transporters of the SLC22 family and may depend on organic cation mediated transport to cross the blood-brain barrier. The presence of a carrier-mediated transport mechanism for the uptake of amisulpride and sulpiride was confirmed in the brain endothelial cell line model hCMEC/D3.

Furthermore, absorption and elimination of amisulpride and sulpiride may also depend on organic cation transporters. OCT1 may contribute to the biliary elimination of amisulpride and sulpiride. In addition, the transporters OCT2, MATE1 and MATE2-K may contribute for the renal elimination of amisulpride and sulpiride in the proximal tubule epithelium. Common genetic polymorphisms on the OCT1 gene were found to affect the cellular uptake of amisulpride and sulpiride.

The majority of the psychotropic drugs, like amitriptyline, have high membrane permeability and may not benefit from drug transporters to permeate cellular barriers in the *in vitro* models used in this work. However, these drugs can still interact strongly with membrane transporters, like OCT1. Clinical studies, providing *in vivo* evidence for the interaction of high permeability drugs with membrane transporters, will be needed in the future. Weak basic psychotropic drugs may inhibit the OCT1-mediated uptake of other important drugs, like morphine. The psychotropic drugs amitriptyline, clomipramine, imipramine and fluoxetine, and also irinotecan, ondansetron and verapamil, inhibited the OCT1-mediated uptake of morphine at therapeutically relevant concentrations.

Furthermore, the effect of genetic polymorphisms in the OCT1 gene on the OCT1-mediated uptake of the biogenic amine tyramine was studied. In addition, an MDCK II cell line carrying a site for targeted chromosomal gene integration was developed. This model should in the future enable the analysis of the effects of genetic polymorphisms on drug transport by efflux transporters, which are present at the blood-brain barrier.

In conclusion, this study demonstrates that influx transporters may mediate the uptake of psychotropic drugs with low membrane permeability like amisulpride and sulpiride, and may influence their pharmacokinetics and distribution to the brain. This work, and the tools which were developed here, can serve as a basis for further work on the role of organic cation transporters at the blood-brain barrier, and to study in more detail the role of organic cation transporters in the pharmacokinetics of amisulpride and sulpiride.

List of Figures

1.1	Absorption, distribution, metabolism and elimination of orally administered compounds	3
1.2	Major routes of drug elimination	4
1.3	Routes of permeation of a drug through a cell membrane illustrated by an example of intestinal absorption	7
1.4	Schematic drawing of key cellular barriers important for drug absorption, distribution, metabolism and excretion.	8
1.5	Passive diffusion of weak acids and weak bases	9
1.6	Methods to determine the passive membrane permeability of compounds	9
1.7	Mechanisms of carrier-mediated transport	11
1.8	Co-existence of carrier-mediated transport and passive diffusion	11
1.9	Membrane transporters which are important for drug absorption, distribution and elimination	13
1.10	Pharmacophore describing drug binding to OCT1	17
3.1	A schematic representation of a PAMPA assay	28
3.2	The pFRT/LacZeo plasmid	36
3.3	Selection of MDCK II cells transfected with the pFRT/LacZeo plasmid	39
4.1	Carrier-independent membrane permeabilities of commonly used psychotropic drugs	46
4.2	Correlation between P_e and $\log D_{7.4}$ and $\log P$ of psychotropic drugs	47
4.3	Validation of the cDNA synthesis and TaqMan [®] microfluidic cards	48
4.4	Comparison of the Ct values obtained with TaqMan [®] single assays and TaqMan [®] microfluidic cards	48
4.5	Gene expression analysis of membrane transporters in the liver and in the kidney	50
4.6	Gene expression analysis of membrane transporters in the intestine and in the brain	51
4.7	Distribution of the expression of membrane transporters in primary cells from the human brain	53
4.8	Gene expression analysis of membrane transporters in primary human astrocytes and choroid plexus epithelial cells	54
4.9	Expression of membrane transporters in primary human brain microvascular endothelial cells (HBMECs)	55
4.10	mRNA expression of organic cation transporters in HBMECs	56
4.11	mRNA expression of LAT-1, BCRP and MDR-1 in HBMECs	57
4.12	Comparison of the gene expression analysis in primary HBMECs RNA obtained from different donors	57

4.13	Expression of membrane transporters in the HEK-pcDNA5 and HEK-OCT1 cell lines	59
4.14	Expression of membrane transporters in the hCMEC/D3 cell line	60
4.15	Immunostaining of BCRP in paraffin-fixed brain tissue slides	61
4.16	Immunostaining of MDR-1 in paraffin-fixed brain tissue slides	62
4.17	Lack of Immunostaining of OCTN2 and OCT1 in brain blood vessels	62
4.18	Validation of the HEK-OCT1 and HEK-OCT3 cell lines with the substrate MPP ⁺	64
4.19	Validation of the HEK-OCT1 HEK-OCT2, HEK-OCTN1 and HEK-OCTN2 cell lines with the substrate TEA ⁺	64
4.20	Chemical structures of amisulpride and sulpiride	65
4.21	Cellular uptake of amisulpride at a concentration of 5 μ M in cells over-expressing OCT1, OCT2, OCT3, OCTN1 and OCTN2	66
4.22	Concentration dependence of amisulpride uptake by OCT1, OCT2, OCT3, OCTN1 and OCTN2	67
4.23	Cellular uptake of sulpiride at a concentration of 5 μ M in cells over-expressing OCT1, OCT2, OCT3, OCTN1 and OCTN2	68
4.24	Concentration dependence of sulpiride uptake by OCT1, OCT2, OCT3, OCTN1 and OCTN2	69
4.25	Lack of transport of sultopride and tiapride by the organic cation transporters of the <i>SLC22</i> family.	70
4.26	Inhibition of the OCT1 mediated MPP ⁺ uptake by amisulpride, sulpiride, sultopride and tiapride	71
4.27	Uptake of amisulpride and sulpiride by the OCT1 genetic variants	72
4.28	Uptake of amisulpride and sulpiride in cell lines expressing MATE-1 and MATE2-K	73
4.29	Concentration and temperature dependant uptake of amisulpride and sulpiride in the human brain microvascular endothelial cell line hCMEC/D3	74
4.30	Inhibition of the uptake of amisulpride and sulpiride in the human brain microvascular endothelial cell line hCMEC/D3	75
4.31	Inhibition of the uptake of ³ H-MPP ⁺ on the hCMEC/D3 cell line by 1 mM of non-labeled MPP ⁺	76
4.32	Lack of uptake of clozapine, citalopram, lamotrigine and amantadine by the human OCT1	77
4.33	Inhibition of the OCT1 mediated MPP ⁺ uptake by amitriptyline	79
4.34	Time dependent uptake of amitriptyline by OCT1	80
4.35	The role of human serum on the uptake of amitriptyline by OCT1	81
4.36	Inhibition of amitriptyline uptake by MPP ⁺ , desipramine and NH ₄ Cl	82
4.37	Inhibition of the OCT1 mediated morphine uptake by commonly co-administrated drugs: Codeine, amitriptyline, verapamil, irinotecan, fluoxetine	84
4.38	Inhibition of the OCT1 mediated morphine uptake by commonly co-administrated drugs: Ondasetron, clomipramine, imipramine, tropisetron	85
4.39	Inhibition of the OCT1 mediated MPP ⁺ uptake by tyramine	87
4.40	Kinetics of the OCT1 mediated tyramine uptake	87
4.41	Uptake of tyramine in cell lines expressing OCT1 genetic variants	88
4.42	Characterization of the MDCK II cell lines cloned with the pFRT/LacZeo plasmid - TEER	90

4.43	Characterization of the MDCK II cell lines cloned with the pFRT/LacZeo plasmid - β -Galactosidase activity	91
5.1	Tranlycypromine - a drug with low LogD and high permeability in the PAMPA assay	93
5.2	Localization of the membrane transporters which may play a role on the pharmacokinetics of amisulpride	99
5.3	Comparison of the chemical structures of sulpiride, amisulpride, sultopride and tiapride.	101
5.4	Principal component analysis of gene expression in tissues and primary cells	103
5.5	Comparison of the gene expression analysis in primary HBMECs with the study of Geier <i>et al.</i> (2013a)	104
5.6	Comparison of the gene expression analysis in primary HBMECs with the study of Geier <i>et al.</i> (2013a) - Part 2	105

List of Tables

1.1	Key cellular barriers for drug absorption, distribution, metabolism and excretion in the human body	6
1.2	Membrane transporters important for drug absorption, distribution and elimination	14
1.3	The haplotype combinations of the five most frequent loss of function polymorphisms and their frequencies in Caucasians	18
2.1	Reagents used shown in alphabetical order (A-C)	21
2.2	Reagents used shown in alphabetical order (D-O)	22
2.3	Reagents used shown in alphabetical order (P-Z)	23
2.4	Antibodies	24
2.5	Consumables	24
2.6	Cell lines	25
2.7	Equipment	25
2.8	Software	26
3.1	Protocol for reverse transcription	29
3.2	Master mix for cDNA synthesis	29
3.3	Real-Time PCR conditions	30
3.4	Antibodies for the detection of OCT1, BCRP and MDR-1 by DAB-Immunostaining	31
3.5	Cell lysis and quantification of intracellular drug amounts in 12-well plate assays	33
3.6	Mass transitions and retention times used for LC-MS/MS detection of amisulpride, sultopride and tiapride	35
3.7	Linearization of Plasmid DNA	37
4.1	Physicochemical properties of psychotropic drugs at pH 7.4	45
4.2	Kinetics of the uptake of TEA ⁺ and MPP ⁺ by organic cation transporters of the <i>SLC22</i> family	63
4.3	Kinetics of amisulpride and sulpiride transport by organic cation transporters of the <i>SLC22</i> family	69
4.4	Inhibition of the OCT1-mediated MPP ⁺ uptake by amisulpride, sulpiride, sultopride and tiapride: Half-maximal inhibition constants, <i>IC</i> ₅₀	71
4.5	Kinetics of amisulpride and sulpiride transport by the MATE-1 and MATE2-K transporters	74
4.6	Previous evidence for the interaction of the psychotropic drugs analyzed in this study, with OCT1	77

4.7	Inhibition of OCT1-mediated morphine uptake by drugs commonly co-administered with morphine.	86
5.1	Clinically relevant drugs shown to be OCT1 substrates	100
A.1	Reference numbers of the assays used on the custom made TaqMan [®] low density arrays	116
C.1	Gene expression analysis in tissues and primary cells - Part 1	121
C.2	Gene expression analysis in tissues and primary cells - Part 2	122
C.3	Gene expression analysis in human brain microvascular endothelial cells - Donor 1	123
C.4	Gene expression analysis in human brain microvascular endothelial cells - Donor 2	124
C.5	Gene expression analysis in human brain microvascular endothelial cells - Donor 3	125
C.6	Gene expression analysis in the hCMEC/D3 cell line	126
C.7	Gene expression analysis in the HEK-OCT1 and HEK-pcDNA5 cell lines .	127

1

Introduction

“A compound must get in, move about, hang around, and then get out.”

– Hodgson (2001) *Nature Biotechnology*

1.1 Efficacy of the treatment of major depression, schizophrenia and bipolar disorder

Major depression, schizophrenia and bipolar disorder are among the most common psychiatric diseases worldwide.

The efficacy of drug treatment of mild to moderate depression is very low, with patients presenting only small changes from the baseline HRSD Scores (Hamilton Rating Scale for Depression) in comparison to placebo. The treatment of severe depression is more efficient, showing significant differences from the baseline after treatment, but response to the same medication varies between clinical trials (Kirsch *et al.* (2008)).

The administration of several antipsychotics in the treatment of schizophrenia is associated with a range of undesirable neurologic effects, and many patients suffering from bipolar disorder have a poor treatment outcome. A third of the patients suffer chronic symptoms and 13-24% of the patients develop rapid cycling disorder, and have four or more episodes per year. The recognised risk of completed suicide is 15% in patients suffering from bipolar disorder (Young *et al.* (2000)).

A possible reason for non-response to the therapy may be the drug not reaching its site of action. On the other hand, poor elimination of the drug may lead to higher drug concentrations in the blood and undesired drug side-effects.

1.2 Drug absorption, distribution, metabolism and excretion

1.2.1 General principles of pharmacokinetics

The term *pharmacokinetics* was first described by the German physician F.H. Dost (Dost (1953)). It studies the time course of the absorption, distribution, metabolism and excretion (ADME) of a drug or compound. These four processes affect the concentration of a specific drug at its site of action and are depicted on figure 1.1.

After an oral dose, a compound is absorbed in the gastrointestinal tract before it reaches the portal vein. In the intestine, it can already be subject to enzymatic metabolism. From the portal vein, it will be delivered into the liver, where first pass metabolism and biliary elimination may occur. If a compound is eliminated through the biliary route, it may be re-absorbed in the intestine (a process known as entero-hepatic circulation). If a compound is delivered intravenously, it will be first found in the venous circulation, and therefore not be subject to first pass metabolism. Once a compound reaches the arterial circulation it will be distributed throughout the body. When a drug is in the peripheral circulation, the two most common routes of elimination are hepatic metabolism (liver), and excretion into the urine by the kidney. The concentration at which a compound reaches its site of action will depend on all these factors. If the target of a certain compound is the brain, it also has to cross the blood-brain barrier (Figure 1.1) (Fan & de Lannoy (2014)).

1.2.2 Absorption and distribution

In order for an orally administered drug to be absorbed and reach the blood, it has to cross the intestinal epithelium. Distribution takes place mainly through the systemic circulation, and compounds present in the blood stream will be delivered to all relevant tissues, at a rate which will depend on the organ/tissue blood flow. The brain, however, is separated from the systemic circulation by two main barriers, the blood-brain barrier (BBB) and the blood-cerebrospinal fluid barrier (BCSFB). The BBB is made of endothelial cells which build tight junctions and do not allow the paracellular diffusion of compounds. The BCSFB is formed by an epithelial cell layer which lines the choroid plexus (Hammarlund-Udenaes *et al.* (2008)). Compounds may cross the BBB and the BCSFB through simple diffusion or carrier mediated transport. The specificities of drug transport at the BBB will be addressed in section 1.4.1.

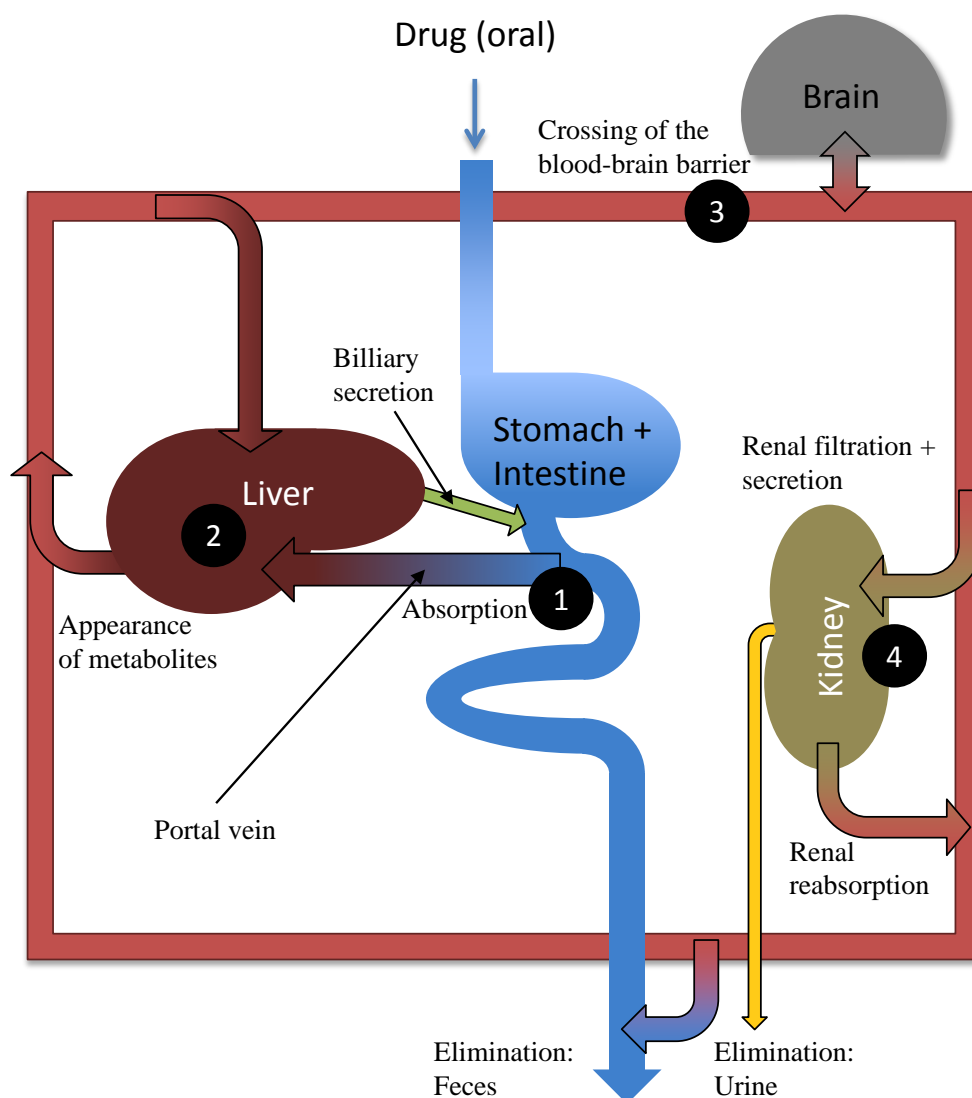


FIGURE 1.1: Absorption, distribution, metabolism and excretion of orally administered compounds. A compound is first absorbed into the portal vein (1), it is exposed to first-pass metabolism in the liver or intestine (1 and 2) and it is distributed by the peripheral blood circulation throughout the body, including to the brain (3). It is eliminated in the liver or kidney by metabolism or excretion (2 and 4). Based on Schwenk (1987) and Fan & de Lannoy (2014)

1.2.3 Metabolism and excretion

The elimination of a drug from the body is due to either metabolism, excretion, or both processes together. An important pharmacokinetic parameter, clearance, introduced by F.H. Dost (Dost (1949)), describes the rate of elimination of a drug from the blood. Clearance (CL) describes the volume of blood from which all the drug is removed, per unit of time (i.e. $mL\ min^{-1}$). It may be divided into metabolic clearance, renal clearance (excretion), biliary clearance (excretion) and other (for example, exhalation through breathing):

$$CL_{total} = CL_{metabolic} + CL_{renal} + CL_{bile} + CL_{other} \quad (1.1)$$

For most of the molecules with a molecular weight under 500 Daltons, the metabolic and renal elimination pathways are the most relevant which greatly simplifies this equation by removing the parameters CL_{bile} and CL_{other} (Pandit & Soltis (2011)).

Metabolism is by far the most important of the clearance pathways, followed by renal clearance (Figure 1.2) (Wienkers & Heath (2005)). Biliary clearance is the major clearance mechanism for only a small number of drugs.

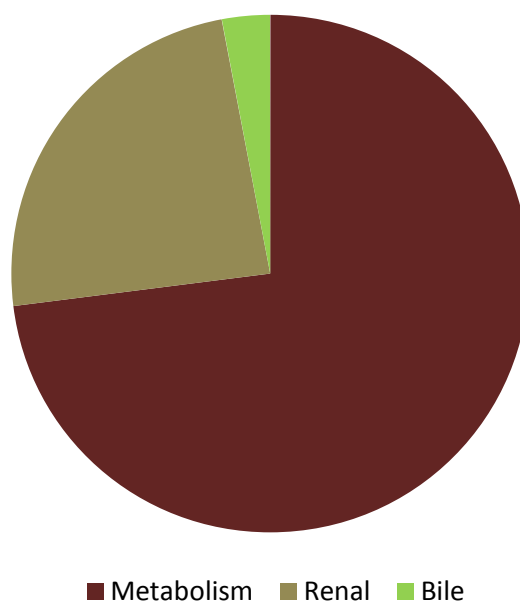


FIGURE 1.2: Major routes of drug elimination. Adapted from Wienkers & Heath (2005)

The organ where most of drug metabolism occurs is the liver, although other tissues may also play a role. Drug metabolism is also known to occur in the intestine, kidney, lung, plasma, blood cells and in the brain. Enzymatic metabolism has the goal of turning compounds into more hydrophilic substances, in order to facilitate their excretion through the kidney and the bile (Fan & de Lannoy (2014)).

The human body has two major routes for drug excretion: Kidney excretion and biliary excretion. Renal excretion is by far the most important excretion mechanism in the human body (Figure 1.2) and it is usually due to one or more distinct processes which happen in the kidney: glomerular filtration, tubular secretion and reabsorption (Kwon (2001)).

Glomerular filtration is the process through which blood is filtered through the glomerulus to form urine. Only small molecules which are not bound to plasma proteins are

filtered in the glomerulus. The GFR (glomerular filtration rate), measures kidney function and is normally determined by measuring the renal clearance of substances which have low binding to plasma membrane proteins (i.e. creatinine). The normal GFR for humans is 120-130 mL/min (Stevens *et al.* (2006)). The rate of glomerular filtration for a specific drug can be determined by multiplying the fraction the drug which is not bound to plasma proteins, f_u , by the GFR (i. e. a substance which is 90% bound to plasma, will have a $f_u \times GFR = 0.1 \times 125 mL/min$, on a healthy adult kidney).

Tubular secretion is a carrier-mediated transport process, where membrane transporters play a major role. Several organic anion transporters (OAT1, OAT3), organic cation transporters (OCT2, MATE1 and MATE-2K) and efflux pumps (MDR-1, MRP4 and MRP2) are involved in this process (Kusuhara & Sugiyama (2009)).

Compounds can also be reabsorbed from the urine into the blood. The fraction of the compound which is reabsorbed (F_R) from the urine into the blood depends on the lipophilicity of the compound. The more lipophilic a compound is, the greater the extent of the reabsorption. Influx transporters may also contribute to the reabsorption process, and efflux transporters may prevent it (Feng *et al.* (2010)).

A simple way to illustrate how glomerular filtration, tubular secretion and tubular reabsorption influence the renal clearance of a drug is:

$$CL_{renal} = (f_u \times GFR + CL_{secretion}) \times (1 - F_R) \quad (1.2)$$

After comparing the renal clearance of a substance with its $f_u \times GFR$, one can characterise the mechanism of renal clearance. If the renal clearance is lower than the filtration rate ($CL_{renal} < f_u \times GFR$), it normally means that a greater fraction (F_R) of the drug is reabsorbed, indicating a net reabsorption mechanism. If the renal clearance is similar to the filtration rate ($CL_{renal} \approx f_u \times GFR$), reabsorption and secretion mechanisms will probably not play a role in renal excretion. If the renal clearance is higher than the filtration rate ($CL_{renal} > f_u \times GFR$), more drug is excreted as it is filtered, indicating a net secretion clearance mechanism which is likely mediated by carrier mediated transport (Fan & de Lannoy (2014)).

1.3 Transport across cellular membranes

As soon as a drug enters the human body, it comes directly into contact with cellular barriers. The way it crosses these cellular barriers will influence its pharmacokinetics

(i.e. its absorption, distribution, metabolism and excretion - ADME). There are several key cellular barriers which influence ADME processes (Table 1.1).

TABLE 1.1: Key cellular barriers for drug absorption, distribution, metabolism and excretion in the human body

Organ/Tissue	Cellular barrier
Intestine	Intestinal epithelium
Liver	Sinusoidal and canicular membrane of hepatocytes
Kidney	Proximal and distal tubular epithelium
Brain	Microvascular endothelial cells Choroid plexus epithelial cells

For a compound which is orally administered to reach the blood it has to first be absorbed in the intestine, and to cross the intestinal epithelium (Figure 1.3). In order to be metabolized in the liver, it has to cross the sinusoidal membrane of the hepatocytes (blood) and to be eliminated through the bile, it has to exit the hepatocytes through their canicular membrane (Figure 1.4 A). In the kidney, compounds may be secreted and reabsorbed in the tubules, where they have to cross the interstitial (blood side), and the luminal (urine side) cell membrane of tubular epithelial cells (Figure 1.4 B). At the blood-brain barrier (Figure 1.4 C), drugs have to cross the luminal and basolateral membranes of the microvascular endothelial cells which make up the blood vessels in the brain.

A compound may permeate a cell membrane by four different processes, paracellular diffusion, transcellular diffusion, facilitated diffusion and active transport (Figure 1.3 and Schwenk (1987)). Paracellular diffusion is the process through which substances permeate a cell layer through the spaces between cells. In the case of the intestinal epithelium, depicted on figure 1.3, the presence of leaky tight junctions allows small hydrophilic molecules (like water) and electrolytes to use the paracellular pathway to cross cell membranes. Most pharmaceutical compounds are absorbed through the transcellular route. An explanation is given by Nellans (1991): The tight junctions in the intestine are large enough to allow compounds up to a size of 3500 Dalton to go through but they only represent 0.1% of the epithelial surface available for drug absorption. Even hydrophilic pharmaceutical compounds ($LogD = -0.5$) are lipophilic enough to benefit from the $1000 \times$ greater surface area available for the transcellular pathway (more on $LogD$ on section 1.3.1, figure 4.1.2).

The transcellular pathway is the major absorption pathway for small molecule pharmaceuticals and is dominated by the ability of a compound to penetrate the cell membrane which can be either by passive diffusion, or by carrier-mediated transport.

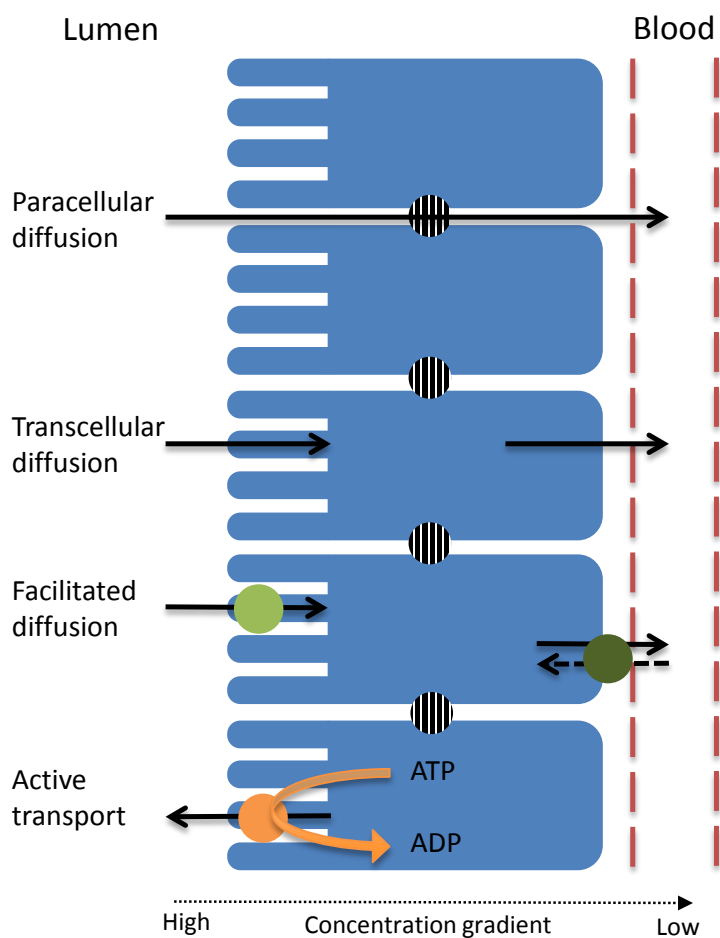


FIGURE 1.3: Routes of permeation of a drug through a cell membrane illustrated by an example of intestinal absorption. Note: Endocytosis is also an important process of membrane permeation, which was left out of this work, as it is mostly important for larger molecules. Based on an illustration by Schwenk (1987).

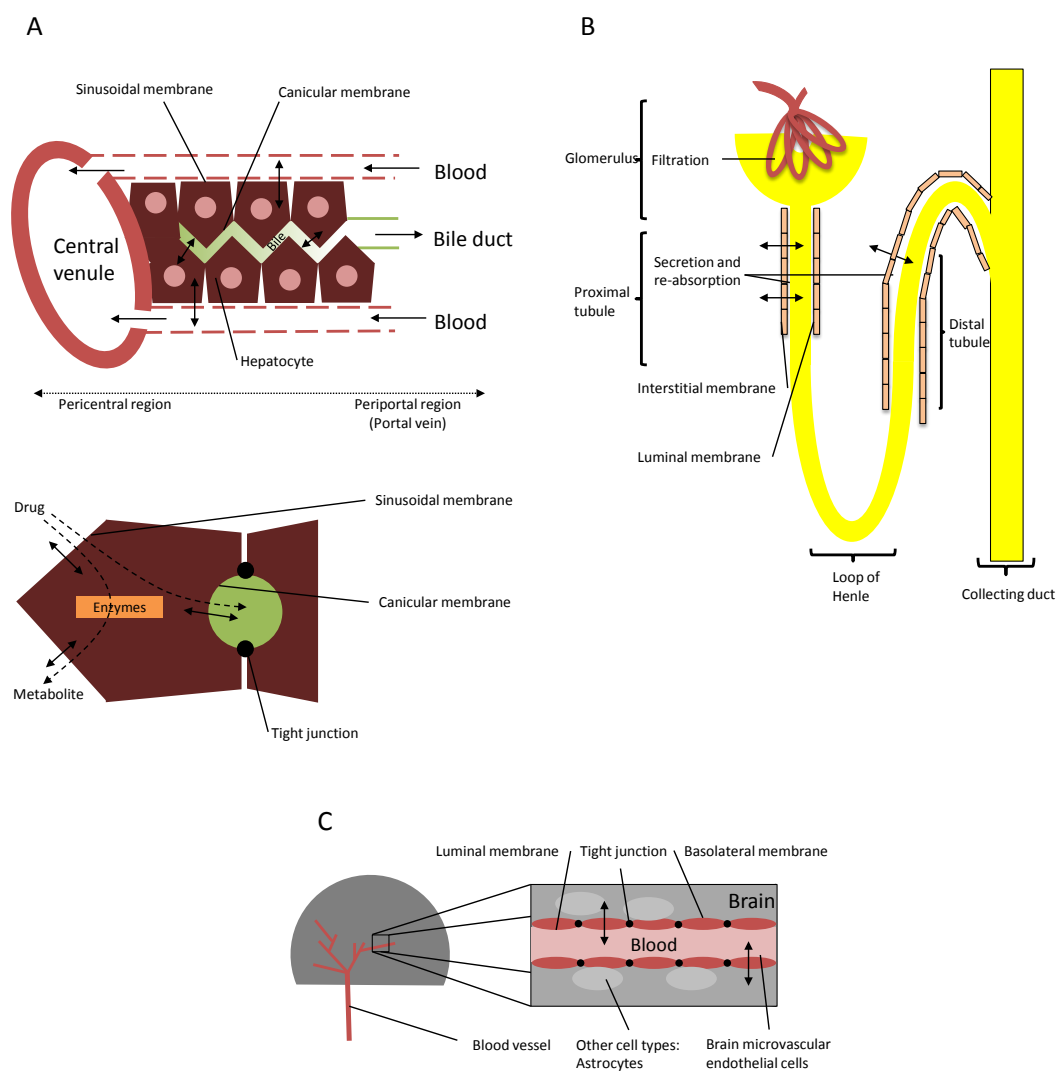


FIGURE 1.4: Schematic drawing of key cellular barriers important for drug absorption, distribution, metabolism and excretion. Shown is the cellular organisation in the liver (A), the localisation of renal elimination systems (B), and a scheme of the blood-brain barrier showing the brain microvascular endothelial cells and their tight junctions (C). Based on illustrations by Schwenk (1987) and Cecchelli *et al.* (2007).

1.3.1 Passive diffusion

Simple diffusion, also known as passive diffusion is the unspecific diffusion of compounds through the cellular membrane and it is the main pathway responsible for the cellular uptake of very lipophilic compounds. Over 100 years ago, Overton and Meyer, proposed that the membrane permeability (related to the efficacy of anaesthetics) of a molecule could be predicted from its partition between an aqueous phase and an organic phase (Meyer (1899), Overton (1901) and Missner & Pohl (2009)). Overton also found that neutral molecules cross the cell membrane faster than charged molecules, and that the

diffusion occurred according to a concentration gradient. Weak bases and weak acids may also cross the cell membrane by passive diffusion. In this case, the substances, either give up (weak bases) or pick-up (weak acids) a proton before crossing the cell membrane (Figure 1.5 and Missner & Pohl (2009)).

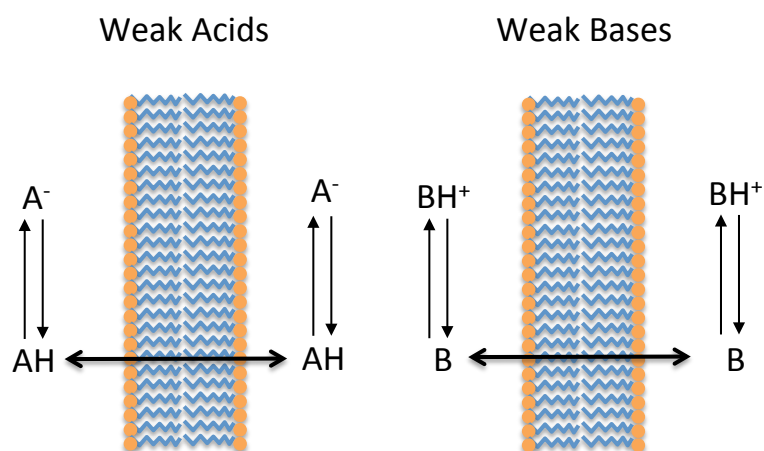


FIGURE 1.5: Passive diffusion of weak acids and weak bases. A represents a weak acid, and A^- its deprotonated form. B represents a weak base and BH^+ its protonated form.

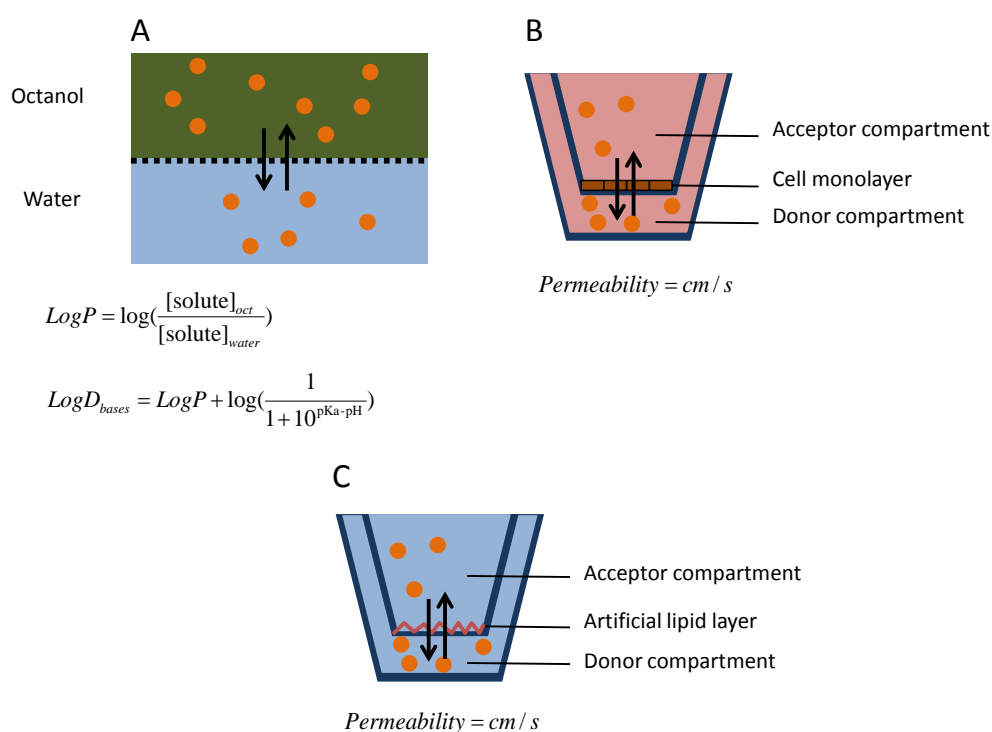


FIGURE 1.6: Methods to determine the passive membrane permeability of compounds. A) Partition coefficient between octanol and water (Meyer (1899) and Overton (1901)). B) Cell permeability assay (usually Caco-2 cells, Artursson (1990)) C) PAMPA assay - Parallel artificial membrane permeability assay (Kansy *et al.* (1998)).

In pharmaceutical research, three methods can be used to assess the passive diffusion of a compound. The simplest one is the determination of the $LogP$ of a substance, which is the partition coefficient between octanol and water. In the case of weak acids and weak bases, $LogD_{7.4}$ can be measured, which also accounts for the pKa , and the dissociation of a drug at the physiological pH of 7.4 (Figure 1.6 A). This follows the principles established by Meyer (1899) and Overton (1901) who used vegetable oil instead of octanol (Franks & Lieb (1978)). The second method takes advantage of the ability of certain cell lines, usually the Caco-2 cell line, to form monolayers, which allows the measurement of membrane permeability across a cellular barrier (Artursson (1990)) (Figure 1.6 B). Because cell lines express membrane transporters, some artefacts may occur when a substance is a substrate for a membrane transporter in Caco-2 cells. The third model, the PAMPA - Parallel artificial membrane permeability assay (Figure 1.6 C), was developed in order to measure membrane permeability without having to go through the tedious process of establishing cell monolayers (Kansy *et al.* (1998)). The fact that no membrane transporters are present in the PAMPA membranes is also an advantage of this method.

1.3.2 Carrier-mediated transport

Carrier-mediated transport of drugs was not known to Meyer (1899) and Overton (1901), when the process of passive diffusion was proposed. Later, it was discovered that drugs may also penetrate the cellular membranes in the kidney, liver and intestine, by carrier-mediated transport.

Facilitated diffusion occurs in the direction of the concentration gradient and is an energy independent process (Schwenk (1987)). In the case of clinically relevant drugs, carrier mediated transport is the major form of facilitated diffusion (Giacomini *et al.* (2010)). Active transport is another form of carrier-mediated transport, and is an energy dependent process, where a compound is transported against a concentration gradient (Figure 1.7).

There are several types of carrier proteins, which can transport from small ions up to small peptides (Dobson & Kell (2008)). Carrier mediated transport can facilitate a compound's passage through a cell membrane (facilitated diffusion), or actively transport it against a concentration gradient. Carrier-mediated transport in the direction of the concentration gradient, may take place through uniport, antiport, or symport mechanisms (Figure 1.7 and (Dobson & Kell (2008))).

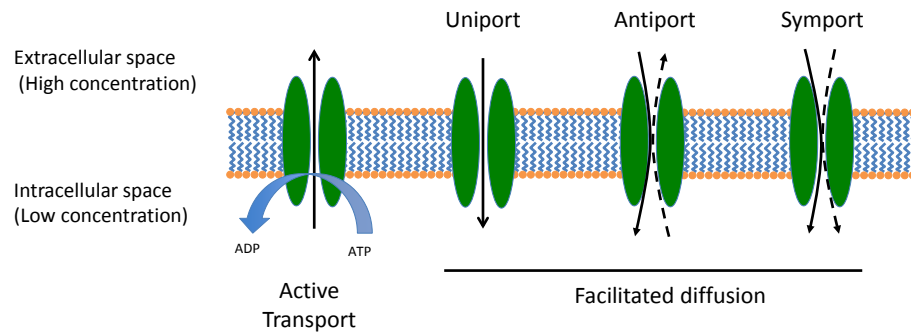


FIGURE 1.7: Mechanisms of carrier-mediated transport. Uniport: passive transporter, antiport: exchanger, symport: coupled transport.

Today it is accepted that both passive diffusion and carrier-mediated transport mechanisms co-exist and contribute to the permeability of substances through a cell membrane (Sugano *et al.* (2010)). Passive diffusion is not a saturable process. In contrast, carrier-mediated transport is saturable, and follows Michaelis-Menten Kinetics (Figure 1.8).

As of this date, the TransportDB website lists 1022 membrane transporters for *H. Sapiens*. With a genome size of 3150 Mb, this leads to a number of 0.32 membrane transporter per Mb of genome (<http://www.membranetransport.org>, Ren *et al.* (2007), as of November 2014). In 2007, the total number of known transporters was 758 (Dobson & Kell (2008)). The transporters of the SLC family (total of 395, Hediger *et al.* (2013)) and of the ABC family (total of 48, Tarling *et al.* (2013)) have become very important in the study of human health and disease, including drug therapy.

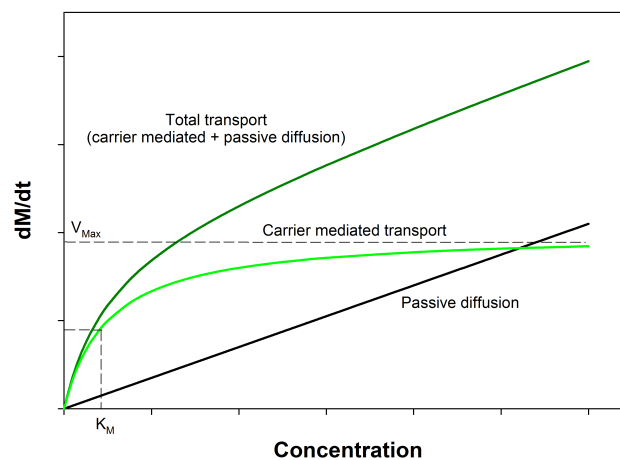


FIGURE 1.8: Coexistence of carrier-mediated transport and passive diffusion. $dM/dt = \frac{V_{Max} \times C}{K_m + C} + C \times D$. Carrier-mediated transport follows Michaelis-Menten kinetics. dM/dt is the total mass transported per unit of time, which is equal to the sum of carrier-mediated transport $\frac{V_{Max} \times C}{K_m + C}$ and passive diffusion $C \times D$. C is the concentration of the substance, K_M and V_M are the Michaelis-Menten constants, and D is the rate of simple diffusion.

1.4 Influence of membrane transporters on drug pharmacokinetics

As mentioned before, cellular membranes in the human body play a major role in drug pharmacokinetics. Because membrane transporters can facilitate the permeation of drugs through cell membranes, they are important for drug absorption, distribution and elimination. Although the SLC and ABC families consist of large number of transporters, only a restricted number of transporters within these families are known to play a role in drug pharmacokinetics (Hillgren *et al.* (2013)). The international transporter consortium (ITC) has released a list of membrane transporters which should be considered during drug development (Figure 1.9 and Table 1.2). This list represents a broad review of the literature and does not account for new developments in membrane transporter research (i.e. the recent identification of OCT1 at the apical membrane (intestine side) of human enterocytes (Han *et al.* (2013)), the accumulating data for the expression of OCT1 in the kidney (Tzvetkov *et al.* (2009)), or the expression of organic cation transporters at the blood-brain barrier which will be addressed in the next section).

In the ITC list of transporters which should be regarded during drug development (Hillgren *et al.* (2013)), no pathways for the intestinal transport and thus absorption of cationic drugs are depicted (Figure 1.9 A). In contrast, the kidney has several organic anion transporters which are expressed on the basolateral membrane (blood) of its proximal tubules (OAT1, OAT2, OAT3, OATP4C1), but only one on the luminal membrane (urine) (OAT4). In the kidney proximal tubules, there is a major organic cation transporter (OCT2) located on the basolateral membrane, and five (MATE1, MATE2, MATE2-K, OCTN1 and OCTN2) on the luminal membrane (Figure 1.9 B).

As in the kidney, in the liver there is only one major organic cation transporter on the basolateral/sinusoidal membrane (OCT1), and several organic anion transporters (OAT2, OAT7, OATP1B1 and OATP1B3). On the cannicular membrane (bile), there is only one major organic cation transporter (MATE1) and no organic anion transporters. However, efflux transporters like MDR1, BCRP and MRP2, may also contribute to biliary secretion of drugs.

At the blood-brain barrier, no organic cation transporters are depicted. In contrast, four efflux transporters are shown to be present at the blood-brain barrier (BCRP, MRP4, MRP5 and MDR1). These transporters are suggested to be expressed at the luminal membrane of brain microvascular epithelial cells and to transport drugs back to the blood.

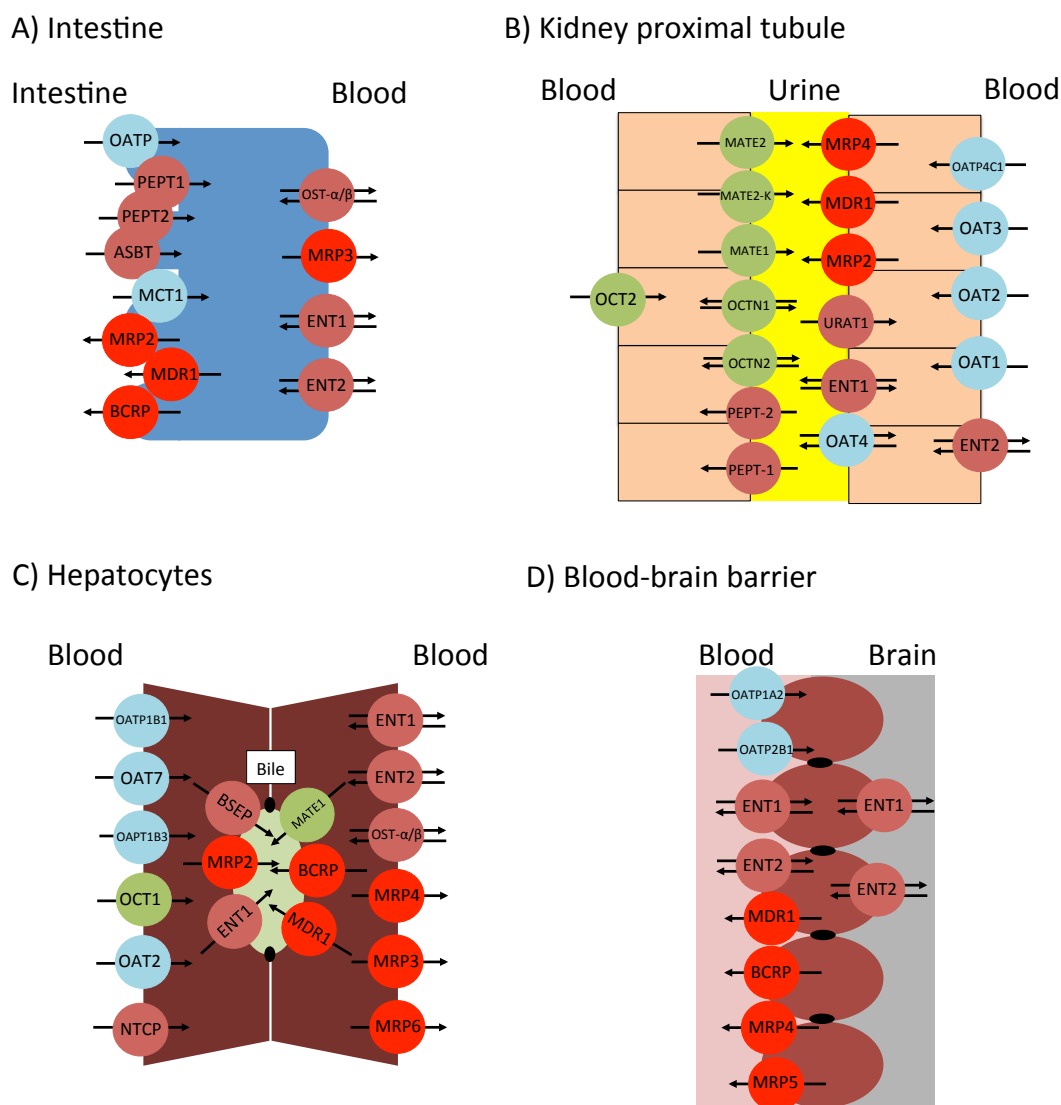


FIGURE 1.9: Membrane transporters which are important for drug absorption, distribution and elimination, according to the international transporter consortium (ITC). Organic cation transporters are shown in green, organic anion transporters are shown in blue, drug efflux transporters are shown in red, other transporters are shown in dark red. Arrows indicate the direction of the transport. *Note: The intestine epithelium expresses one or more transporters of the OATP family.* According to Hillgren *et al.* (2013) with modifications.

TABLE 1.2: Membrane transporters important for drug absorption, distribution and elimination according to the international transporter consortium (ITC) (Hillgren *et al.* (2013)).

Transporter	Type of transporter	Gene name	Expression
OCT1	Organic cation transporter	SLC22A1	Liver
OCT2	Organic cation transporter	SLC22A2	Kidney
OCTN1	Organic cation transporter	SLC22A4	Kidney
OCTN2	Organic cation transporter	SLC22A5	Kidney
MATE1	Organic cation transporter	SLC47A1	Liver, Kidney
MATE2	Organic cation transporter	SLC47A2	Kidney
MATE2-K (Kidney isoform)	Organic cation transporter	SLC47A2	Kidney
OAT1	Organic anion transporter	SLC22A6	Kidney
OAT2	Organic anion transporter	SLC22A7	Liver, Kidney
OAT3	Organic anion transporter	SLC22A8	Kidney
OAT4	Organic anion transporter	SLC22A11	Kidney
OAT7	Organic anion transporter	SLC22A9	Liver
OATP1B1	Organic anion transporter	SLCO1B1	Liver
OATP1B3	Organic anion transporter	SLCO1B3	Liver
OATP2B1	Organic anion transporter	SLCO2B1	Liver
OATP4C1	Organic anion transporter	SLCO4C1	Kidney
BCRP	Efflux transporter	ABCG2	Liver, Intestine Blood-brain barrier
MDR1	Efflux transporter	ABCB1	Kidney, Blood-brain barrier Kidney, Blood-brain barrier
MRP2	Efflux transporter	ABCC2	Liver, Intestine Kidney
MRP3	Efflux transporter	ABCC3	Liver, Intestine Kidney
MRP4	Efflux transporter	ABCC4	Liver, Kidney Blood-brain barrier
MRP5	Efflux transporter	ABCC5	Blood-brain barrier
MRP6	Efflux transporter	ABCC6	Liver
MCT1	Monocarboxylate transporter	SLC16A1	Intestine
ENT1	Nucleoside transporter	SLC29A1	Liver, Intestine Kidney, Blood-brain barrier
ENT2	Nucleoside transporter	SLC29A2	Liver, Intestine Kidney, Blood-brain barrier
PEPT1	Peptide transporter	SLC15A1	Liver, Intestine Kidney
PEPT2	Peptide transporter	SLC15A2	Liver, Intestine Kidney
URAT1	Urate transporter	SLC22A12	Kidney
ASBT	Bile acid transporter	SLC10A2	Intestine
NTCP	Bile acid transporter	SLC10A1	Liver
OST- α/β	Bile acid transporter	SLC51A / SLC51B	Liver, Intestine
BSEP	Bile salt efflux pump	ABCB11	Liver

1.4.1 Drug transport and drug transporters at the blood-brain barrier

For a psychotropic drug to exert its action, it has first to be delivered to the brain. Psychotropic drugs usually act on neural receptors or on a transporter specific for the pre-synaptic uptake of neurotransmitters. A number of factors contribute to the effective concentration of a psychotropic drug at its site of action. These include influx and efflux through the blood-brain barrier (BBB), drug distribution within the brain and binding to brain tissue (Hammarlund-Udenaes *et al.* (2008)). The limiting step in reaching the brain is the crossing of the blood-brain barrier. The paracellular diffusion of compounds through the BBB is restricted due to the presence of tight-junctions between the endothelial cells, which make the brain capillaries. The transcellular diffusion of compounds is limited by the presence of efflux transporters. However, small molecules, for example nutrients, are still transported into the brain by specific solute carriers (Strazielle & Ghersi-Egea (2013))

As previously stated, figure 1.9 is based on a broad literature review and ignores several recent research developments. It does not, for example, depict any organic cation transporter at the blood-brain barrier. It has been recently suggested that organic cation transporters like OCT1, OCT2, OCT3, OCTN2 and MATE1 are expressed at the human blood-brain barrier (Kido *et al.* (2001), Lin *et al.* (2010) and Geier *et al.* (2013a)). MCT1 (depicted here only on the intestinal epithelia), as well as LAT-1, are also known to be highly expressed at the blood-brain barrier (Geier *et al.* (2013a)) and LAT-1 has recently been shown to be able to transport psychotropic drugs (Geier *et al.* (2013b)).

1.4.2 Factors affecting drug transporter activity: genetic polymorphisms and drug-drug interactions

Because drug transporters play a major role in drug absorption, distribution and elimination, factors which lead to a decrease in their activity may dramatically change drug pharmacokinetics. These can be for example, genetic polymorphisms leading to a decrease, or absence of transporter activity (Kerb (2006)), or drug-drug interactions, which may also lead to a decrease in transporter activity (König *et al.* (2013)).

Membrane transporters for which important genetic variants have been identified include MDR1 (*ABCB1*), BCRP (*ABCB1*), OCT1 and OCT2 (*SLC22A1* and *SLC22A2*), MATE1 (*SLC47A1*), MATE2 (*SLC47A2*) OAT1 (*SLC22A6*) and OATPs (*SLCO*) (Kerb (2006), Ha Choi *et al.* (2009) and Stocker *et al.* (2013a)).

A notable example is the genetic variability in the OATP1B1 transporter, highly expressed in human hepatocytes and responsible for the uptake of several statins (simvastatin, pravastatin, atorvastatin, etc.) in the liver. If OATP1B1 is inactive, the elimination of statins in the liver will be reduced. Polymorphisms in this gene have been found to result in remarkably increased plasma concentrations of statins, and were associated with increased risk of statin-induced myopathy (for review, see Niemi *et al.* (2011)). OCT1, the major liver transporter for organic cations, has been shown to be important for the hepatic uptake of cationic drugs which are metabolized in the liver. Lack of OCT1 activity will lead to increase drug plasma concentrations (for review, Brockmüller & Tzvetkov (2013)). Within the efflux transporters, polymorphisms in MDR1 have been shown to be associated with changes in drug pharmacokinetics (Kerb (2006)).

Inhibition of drug transporters by co-administered substances can also alter the pharmacokinetics of the victim drug. For example, the inhibition of the hepatic OATPs has a similar effect to genetic polymorphisms on drug pharmacokinetics, resulting in an increase in the blood concentration of the victim drug. In the kidney, the inhibition of OATs, and OCTs also leads to an increase in the plasma drug concentrations of drugs. Cimetidine is a known inhibitor of the organic cation transport system in the kidney, and co-administration of cimetidine has been shown to reduce the elimination of drugs like metformin (Somogyi *et al.* (1987)). It has been demonstrated that renal drug-drug interactions with cimetidine are likely due to the intracellular inhibition of the MATE transporters at the luminal membrane (urine), and not of OCT2 at the basolateral membrane (blood) (Ito *et al.* (2012)). On the other hand, the inhibition of intestinal OATPs, has the effect of lowering drug concentrations, as less drug is absorbed (König *et al.* (2013)). The inhibition of MDR1 (an efflux transporter) at the blood-brain barrier has been shown in mice to increase the concentration of drugs in the brain (Fellner *et al.* (2002)).

1.5 OCT1 - A highly polymorphic membrane transporter important for drug pharmacokinetics

1.5.1 Drug-binding to OCT1

OCT1 is a polyspecific organic cation transporter (Koepsell *et al.* (2007)) which has affinity for structurally different substances. Inhibition of a membrane transporter by a compound gives an idea of its affinity to the transporter, and is an indication that the compound may also be a substrate. A positive charge and the increasing size of

tetraalkyl-ammonium compounds (the bigger the alkyl chains, the larger the hydrophobicity) was shown to correlate to the inhibition of MPP^+ uptake by organic cation transporters (Ullrich (1997)). An interesting model has also been proposed by Moaddel *et al.*, which states that an ion pair interaction (protonation site), a H-bond donor (hydrogen bonds) and a hydrophobic moiety are important for binding to OCT1 (Figure 1.10 and Moaddel *et al.* (2005)). This is present in substances like morphine, O-desmethyl-tramadol, which have been identified as OCT1 substrates (Tzvetkov *et al.* (2011), Tzvetkov *et al.* (2013)). On the other hand, Ahlin *et al.* (2008) proposes that many hydrogen bonds are negatively correlated with OCT1 inhibition. The different structural specificities identified by different authors for the binding to OCT1 reflects the polyspecificity of OCT1, and the likely presence of multiple binding sites for different substrates.

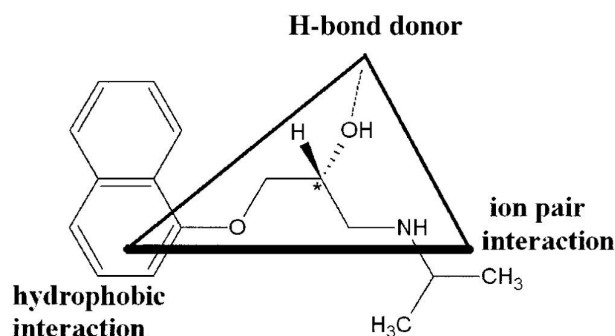


FIGURE 1.10: Pharmacophore describing drug binding to OCT1. Figure obtained without changes from Moaddel *et al.* (2005).

1.5.2 Genetic variation on the OCT1 gene

The organic cation transporter 1, OCT1 (*SLC22A1*), is the most expressed transporter in the human liver (Hilgendorf *et al.* (2007), Schaefer *et al.* (2012)) and is able to transport organic cations which include clinically relevant drugs (Koepsell (2013)). The OCT1 gene is highly polymorphic and in the caucasian population, 30% of the individuals carry a loss-of-function mutation on at least one of its alleles (Table 1.3). This means that circa 9% of the caucasian population will have two copies of an inactive OCT1 allele, and circa 40% will have only one functional allele, leading to reduced OCT1 activity.

Loss of function polymorphisms on the OCT1 gene have been shown to affect the pharmacokinetics of drugs which are metabolized in the liver like tramadol, tropisetron and morphine (Tzvetkov *et al.* (2011), Tzvetkov *et al.* (2012) and Tzvetkov *et al.* (2013)). If drugs cannot enter the liver, they will not be a metabolized, and plasma concentrations will increase. This may lead to unwanted drug adverse effects during therapy, or treatment failure in case the drug needs to be activated in the liver via metabolism.

Recently, the global variability in the OCT1 gene in 54 populations worldwide was analysed. Interestingly, while caucasians have 9% loss of OCT1 activity, asians lacked any of the known loss-of-function polymorphisms. In contrast, in a small population of native american indians, 70% of the individuals were homozygous carriers of loss-of-function mutations in OCT1, while 30% were heterozygous carriers of loss-of-function mutations (Stalman *et al.* (2014)). Pharmaceutical drugs have been around for a very short time considering the time span of the evolution of the human species. Food, and exposure to naturally occurring xenobiotics may be one of the explanations for the worldwide variability observed in the OCT1 gene. In this context, it is very interesting to study, not only drugs, but also natural substances which are liver metabolized and may depend on OCT1 to enter the liver.

TABLE 1.3: The haplotype combinations of the five most frequent loss of function polymorphisms and their frequencies in Caucasians. From Tzvetkov *et al.* (2013)

Haplotype	Codon					Allele freq	
	61	88	401	420	465	[%]	
OCT1*1	Arg	Cys	Gly	Met	Gly	Fully active	70.3
OCT1*2	Arg	Cys	Gly	del	Gly	Deficient	14.8
OCT1*3	Cys	Cys	Gly	Met	Gly	Deficient	10.1
OCT1*4	Arg	Cys	Ser	Met	Gly	Deficient	2.4
OCT1*5	Arg	Cys	Gly	del	Arg	Deficient	1.8
OCT1*6	Arg	Arg	Gly	del	Gly	Deficient	0.6

1.6 Variability on the pharmacokinetics of psychotropic drugs

The variability in the treatment with psychotropic drugs may be explained by variable drug pharmacokinetics. In order for a psychotropic drug to reach its target, it has to be absorbed, go through first pass metabolism, and be distributed to the brain. The rate of elimination of a drug also influences its plasma concentrations and concentration at the site of action. Genetic polymorphisms in drug metabolising enzymes have been shown to affect the plasma concentrations of antidepressants (Kirchheiner *et al.* (2004) and Rau *et al.* (2004)). However, the plasma concentration of psychotropic drugs poorly correlates with their efficacy (Hendset *et al.* (2006)).

One possible hypothesis is that variable distribution of drugs to the brain may also affect treatment efficacy. The presence of efflux transporters in the brain and their influence on the distribution of psychotropic drugs to the brain has been already demonstrated (Abaut *et al.* (2009), Grauer & Uhr (2004) and Uhr *et al.* (2008)). Not much is known about how changes in influx membrane transport at the blood-brain barrier may influence the efficacy of psychotropic drugs. Indeed, little is known about which influx transporters at the blood-brain barrier are important for the blood-brain barrier permeation of psychotropic drugs.

1.7 Aims of this work

The aim of this work is to evaluate the extent to which carrier-mediated influx transport may modulate the pharmacokinetics and efficacy of psychotropic drugs, by influencing their distribution and elimination. Specifically, it is hypothesised that organic cation transporters present at the blood-brain barrier mediate the uptake of psychotropic drugs into the brain. It is also hypothesized that carrier-mediated uptake through OCT1 may mediate the hepatic uptake of psychotropic drugs which are liver metabolized. In this case, polymorphisms in OCT1 would lead to lower hepatic uptake, and slower elimination of these drugs. Thus, genetic polymorphisms in and drug-drug interactions with OCT1, and other cation transporters may affect the distribution and elimination of psychotropic drugs and influence therapy efficacy.

The specific aims of this project were to:

- Identify psychotropic drugs which may benefit from carrier-mediated transport to cross cellular membranes
- Study the gene expression of membrane transporters at the blood-brain barrier
- Evaluate to what extent organic cation transporter mediated drug uptake contributes to the transport of drugs through the blood-brain barrier
- Evaluate to what extent carrier-mediate transport through OCT1 contributes to the hepatic uptake and further metabolism of psychotropic drugs
- Investigate how genetic polymorphisms and drug-drug interactions at membrane transporters may influence the pharmacokinetics of psychotropic drugs
- Establish and develop cellular models for the study of drug transport at the blood-brain barrier

2

Materials

2.1 Reagents

TABLE 2.1: Reagents used shown in alphabetical order (A-C)

Substance	Manufacturer	Use
¹⁴ C-Tetraethylammonium (TEA+)(55mCi/mmol)	Hartmann Analytic	Uptake experiments
¹⁴ C-Tyramine(55mCi/mmol)	Hartmann Analytic	Uptake experiments
³ H Amantadine (439 mCi/mmol)	Hartmann Analytic	Uptake experiments
³ H Clozapine (80mCi/mmol)	Hartmann Analytic	Uptake experiments
³ H-1-Methyl-4-phenylpyridinium(MPP+) (80 Ci/mmol)	Hartmann Analytic	Substrate uptake assays
³ H-Amitriptyline (60 Ci/mmol)	Hartmann Analytic	Uptake experiments
³ H-Citalopram (85Ci/mmol)	Hartmann Analytic	Uptake experiments
³ H-Lamotrigine (5Ci/mmol)	Hartmann Analytic	Uptake experiments
³ H-Morphine (80 Ci/mmol)	Hartmann Analytic	Substrate uptake assays
³ H-Sulpiride (80,6 Ci/mmol)	Hartmann Analytic	Uptake experiments
Acetonitrile	Merck	Lysis Buffer and LC-MS/MS
Amisulpride	Sigma-Aldrich	Uptake experiments
Amitriptyline	Sigma-Aldrich	Uptake experiments
Atropine	Sigma-Aldrich	Uptake experiments
Bicinchoninic Acid solution (B9643)	Sigma-Aldrich	BCA assay
Bovine Serum Albumin (BSA)	Sigma-Aldrich	BCA assay
Citalopram	Sigma-Aldrich	Uptake experiments
Clomipramine	Sigma-Aldrich	Uptake experiments
Clozapine	Sigma-Aldrich	Uptake experiments
Codeine	Sigma-Aldrich	Uptake experiments
Cultrex rat collagen I	R&D Systems	Cell culture (hCMEC/d3)
Cupric sulfate pentahydrate	Sigma-Aldrich	BCA assay

TABLE 2.2: Reagents used shown in alphabetical order (D-O)

Substance	Manufacturer	Use
DAB (3,3'- Diaminobenzidine)	Sigma-Aldrich	Immunostaining
Desipramine	Sigma-Aldrich	Uptake experiments
DMEM	Life Technologies	Cell culture
DMSO	Sigma-Aldrich	Freezing of mammalian cells
dNTPs	Thermo Scientific	Reverse transcripion
Doxepine	Sigma-Aldrich	Uptake experiments
Duloxetine	Sigma-Aldrich	Uptake experiments
EndoGRO-MV (SMCE-004)	Merck	Cell culture (hCMEC/d3)
Eukitt Quick hardening mdium	Sigma-Aldrich	Immunostaining
Fetal Calf Serum (FCS)	Life Technologies	Cell culture
Fluoxetine	Sigma-Aldrich	Uptake experiments
Flupentixol	Sigma-Aldrich	Uptake experiments
Fluphenazine	Sigma-Aldrich	Uptake experiments
Formic Acid	Sigma-Aldrich	Running buffer LC-MS/MS, Lysis buffer
GFP plasmid (pIRES2-EGFP)	Addgene	Controlling transfection efficiency
H_2O_2	Carl Roth GmbH	Immunostaining
Haloperidol	Sigma-Aldrich	Uptake experiments
HBMEC RNA Lots 7686, 6221, 5803	ScienCell	Gene expression analysis
HBSS (with phenol red)	Life Technologies	Transport experiments
HBSS (without phenol red)	Life Technologies	Cell culture (hCMEC/d3)
Hematoxylin	Sigma-Aldrich	Immunostaining
HEPES	Sigma-Aldrich	Buffer for cell culture
Human basic fibroblast growth factor	Sigma-Aldrich	Cell culture (hCMEC/d3)
Imipramine	Sigma-Aldrich	Uptake experiments
Irinotecan	Sigma-Aldrich	Uptake experiments
Lamotrigine	Sigma-Aldrich	Uptake experiments
Lipid pen	Sigma-Aldrich	Immunostaining
Lipofectamine 2000	Life Technologies	Transfection reagent
Melperon	Sigma-Aldrich	Uptake experiments
Methanol	Merck	LC-MS/MS
Methylphenidate	Sigma-Aldrich	Uptake experiments
Milk powder	Carl Roth GmbH	Immunostaining
Milnacipram	Sigma-Aldrich	Uptake experiments
Mirtazapine	Sigma-Aldrich	Uptake experiments
MPP+ 1-Methyl-4-phenylpyridinium	Sigma-Aldrich	Uptake experiments
NaOH	Sigma-Aldrich	Cell lysis buffer, Mini-prep buffer 2
Nortriptyline	Sigma-Aldrich	Uptake experiments
Olanzapine	Sigma-Aldrich	Uptake experiments
Ondansetron	Sigma-Aldrich	Uptake experiments
OptiMEM	Life Technologies	Transfection MDCK II cells

TABLE 2.3: Reagents used shown in alphabetical order (P-Z)

Substance	Manufacturer	Use
Paroxetine	Sigma-Aldrich	Uptake experiments
Penicillin-Streptomycin (10000 U/mL)	Life Technologies	Cell culture
Perazine	Sigma-Aldrich	Uptake experiments
Perphenazine	Sigma-Aldrich	Uptake experiments
pFRT/LacZeo	Life Technologies	Transfection MDCK II cells
poly-D-lysine (1-4 kDa)	Sigma-Aldrich	Cell culture
Potassium dihydrogen phosphate	Sigma-Aldrich	Lysis buffer
Promethazine	Sigma-Aldrich	Uptake experiments
Quetiapine	Sigma-Aldrich	Uptake experiments
Random hexanucleotide primers	Roche	Reverse transcriptipion
Recombinant human placenta RNase inhibitor	Affymetrix	Reverse transcriptipion
Risperidone	Sigma-Aldrich	Uptake experiments
RNA Ch.Plex.Epithelial cells	ScienCell	Gene expression analysis
RNA primary astrocytes	ScienCell	Gene expression analysis
SacI-HF restriction enzyme	NEB	Transfection MDCK II cells
SDS	Sigma-Aldrich	Cell lysis buffer, Mini-prep buffer 2
Sodium citrate	Sigma-Aldrich	Immunostaining
Sulpiride	Sigma-Aldrich	Uptake experiments
Sultopride	Santa Cruz Biotechnology	Uptake experiments
Sumatriptan	Sigma-Aldrich	Uptake experiments
Sumatriptan-d6	Santa Cruz Biotechnology	Internal standard LC-MS/MS
SuperScript II reverse transcriptase	Life Technologies	Reverse transcriptipion
TaqMan® Universal PCR Master Mix 2x	Life Technologies	Gene expression analysis
Tiapride	Sigma-Aldrich	Uptake experiments
Total intestine RNA	Ambion	Gene expression analysis
Total kidney RNA	Ambion	Gene expression analysis
Total liver RNA	Life Technologies	Gene expression analysis
Tranlycypromine	Sigma-Aldrich	Uptake experiments
Triton	Sigma-Aldrich	Immunostaining
Tropisetron	Sigma-Aldrich	Uptake experiments
Trypan Blue	Sigma-Aldrich	Reagent for assessing cell viability
TrypLE Express	Life Technologies	Cell culture
Trypsin 0.25% EDTA	Life Technologies	Cell culture (hCMEC/d3)
Tyramine	Sigma-Aldrich	Uptake experiments
Vectastain ABC Kit (PK-6100)	Linaris	Immunostaining
Verapamil	Sigma-Aldrich	Uptake experiments
Xylene	Sigma-Aldrich	Immunostaining
Zeocin	Life Technologies	Cell culture

2.2 Antibodies

TABLE 2.4: Antibodies

Anitbody	Manufacturer	Use
Goat polyclonal antibody for OCTN2 (H-13) sc-19822	Santa Cruz Biotechnology	Immunostaining - Primary antibody
Mouse monoclonal anti-OCT1 (2C5)	Novus Biologics	Immunostaining - Primary antibody
Mouse Monoclonal antibody (BXP-21) BCRP	Abcam	Immunostaining - Primary antibody
Anti-ABCB1 antibody (HPA002199-100UL)	Sigma-Aldrich	Immunostaining - Primary antibody
Polyclonal rabbit anti-goat IgG Biotinylated	Dako	Immunostaining -Secondary antibody
Polyclonal rabbit anti-mouse IgG Biotinylated	Dako	Immunostaining -Secondary antibody
Polyclonal swine anti-rabbit IgG Biotinylated	Dako	Immunostaining -Secondary antibody

2.3 Consumables

TABLE 2.5: Consumables

Consumable	Manufacturer	Use
PAMPA 96-well plates	BD Biosciences	PAMPA assay
96-well Costar UV plates	Corning	PAMPA assay
96-Well RNase free plates	Sarstedt	cDNA synthesis
Thermo-Fast 384er Plate (qPCR)	Thermo Scientific	Gene expression assay
Absolute qPCR Seal (Optically Clear)	Thermo Scientific	Gene expression assay
Nunclon TM 12-well cell culture plates	Nunc	Cell culture
6 well plates Corning (Cat 3506)	Corning	Cell culture of hCMEC/D3 cells
Cell culture flasks 75mm	Sarstedt	Cell culture HEK293 and MDCK II cells
Cell culture flasks (Cat 430641)	Corning	Cell culture of hCMEC/D3 cells
Liquid Scintillation flasks	Zinsser Analytics	Liquid scintillation counting
AQUASAFE 500 Plus	Zinsser Analytics	Liquid scintillation counting
Petri dishes 100mm (5 μ m, 4 \times 12.50 mm)	Sarstedt	Cell culture HEK293 and MDCK II cells
Brownlee SPP RP-Amide column (4.6x100 mm, 2.7 μ m)	Perkin Elmer	LC-MS/MS
SecurityGuard Standard precolumn (C18, ODS, 4 mm x 2 mm, KJO-4282)	Phenomenex	LC-MS/MS
96-well plates sterile clear	Sarstedt	BCA assay
Phosphate Buffer Saline (PBS) Powder	Sigma-Aldrich	PAMPA assay
Transwell permeable supports 12-well format	Corning	MDCK II cell culture
QUIAGEN Plasmid Plus Midi Kit	Quiagen	Midi-prep:Isolation of plasmid DNA
Beta-Gal assay kit	Life Technologies	Assessing of Beta-galactosidase activity
QUIAGEN QIAquick Gel Extraction Kit	Quiagen	DNA gel extraction
QUIAGEN RNeasy plus mini kit	Quiagen	RNA extraction

2.4 Cell lines

TABLE 2.6: Cell lines

Cell Line	Obtained from:
HEK-OCT1	Institute for Clinical Pharmacology - UMG Göttingen
HEK-OCT2	Institute for Clinical Pharmacology - UMG Göttingen
HEK-OCT3	Prof. Koepsell and Dr. Gorboulev, University of Würzburg, Germany
HEK-OCTN1	Institute for Clinical Pharmacology - UMG Göttingen
HEK-OCTN2	Institute for Clinical Pharmacology - UMG Göttingen
HEK-pcDNA5	Institute for Clinical Pharmacology - UMG Göttingen
hCMEC/D3	PO Couraud, INSERM Paris
MDCK-II cell line canine	European Collection of Cell Cultures (ECACC) Cat No. 00062107, Lot No. 13A022, 24 May 2013, P 28
HEK-MATE1	PortaCellTec biosciences, Göttingen, Germany
HEK-MATE2	PortaCellTec biosciences, Göttingen, Germany
HEK-OCT1 variants	Institute for Clinical Pharmacology - UMG Göttingen

2.5 Equipment

TABLE 2.7: Equipment

Equipment	Manufacturer	Use
TECAN Ultra Microplate Reader	TECAN	PAMPA assay, BCA assay, Beta-gal assay
Beckman LS5000TD	Beckman Coulter	Liquid scintillation counting
PerkinElmer/Sciex HPLC system	Perkin Elmer	LC-MS/MS
API4000 tandem mass spectrometer	Applied Biosystems	LC-MS/MS
7900HT Fast Real-Time PCR System	Applied Biosystems	Gene expression analysis
TaqMan [®] Array Micro Fluidic Card Thermal Cycling Block	Applied Biosystems	Gene expression analysis
Neubauer chamber	Geier	Chamber for cell counting
Microscope	Zeiss	Cell observation and counting
BX51 Microscope with DP-50 camera	Olympus	Imaging of immunostained slides
2 mm electroporation cuvette	PeqLab	Transformation of bacteria
Centrifuge 5810 R	Eppendorf	Centrifuge
Multifuge X3R	Thermo Scientific	Microfluidic cards
Microfluidic card holders (75015679)	Heraeus	Centrifuge Buckets
Biofuge pico	Heraeus	Bench-top centrifuge
Spectrophotometer	Eppendorf	Quantification of RNA and DNA
EVOM meter with STX2 electrode	World Precision Instruments	Measurement of TEER
TaqMan [®] Array Micro Fluidic Card Sealer	Life Technologies	Card sealer
BioPhotometer	Eppendorf	Quantification of nucleic acids
Nanodrop cuvette	Implen	Quantification of nucleic acids
PTC-200 Thermal Cycler	Biorad	Thermal cycler

2.6 Software

TABLE 2.8: Software

Software	Manufacturer	Use
ADMET Predictor 5.5	Simulations Plus	Prediction of LogD, logP and pKa
SDS 2.4	Life Technologies	Gene expression analysis
RQ-Manager 1.2.1	Life Technologies	Gene expression analysis
SigmaPlot 12	Systat Software Inc.	Determination of IC_{50} , V_{Max} , K_M and data visualisation
IBM SPSS Statistics version 21.0	IBM Corporation	Statistics

3

Methods

3.1 Parallel artificial membrane permeability assay (PAMPA)

Parallel artificial membrane permeability assays (PAMPA) were performed using PAMPA 96-well plates (BD Biosciences) according to the manufacturer's instructions. Briefly, 300 μL of PBS (pH 7.4) with increasing concentrations of the drug to be analyzed were pipetted into the donor wells. Two hundred μL of PBS (pH 7.4) without drug were pipetted into the acceptor wells. Each concentration was measured in duplicate.

The PAMPA plates were incubated at room temperature for 5 h. Equal volumes of 150 μL , from the donor and acceptor well, as well as from the initial drug solution (C_0), was transferred into a Corning UV plate (Figure 3.1). It is important to use these plates, as they are made of a plastic which has no UV absorption. Drug concentrations from both the donor and acceptor wells were determined by UV absorption in a TECAN Ultra Microplate Reader (TECAN, Crailsheim, Germany). The following wavelengths were used: 230 nm for amitriptyline, citalopram, clomipramine, doxepine, fluoxetine, haloperidol, methylphenidate, nortriptyline and paroxetine; 260 nm for desipramine, fluphenazine, imipramine, lamotrigine, melperon, milnacipram, perphenazine and tranlycypromine; and 280 nm for amisulpride, clozapine, duloxetine, flupentixol, mirtazapine, olanzapine, paliperidone, perazine, promethazine, quetiapine, risperidone, sulpiride, sultopride and tiapride. Membrane permeability (P_e) was calculated as follows:

$$P_e = \frac{-\ln(1 - C_A / (1 - (0.3 \times C_D + 0.2 \times C_A) / 0.3 \times C_0))}{(A \times (1/V_D + 1/V_A) \times t)} \quad (3.1)$$

- C_0 is the initial concentration in the donor well

- C_D and C_A are the end concentrations in the donor and acceptor wells, respectively
- A represents the area of each well (0.3 cm^2)
- V_D is the volume of the acceptor well ($0,2 \text{ mL}$)
- t is the time of incubation in seconds ($18\ 000 \text{ seconds} = 5 \text{ hours}$)

The assays were performed using three different concentrations for each drug and average P_e values were calculated.

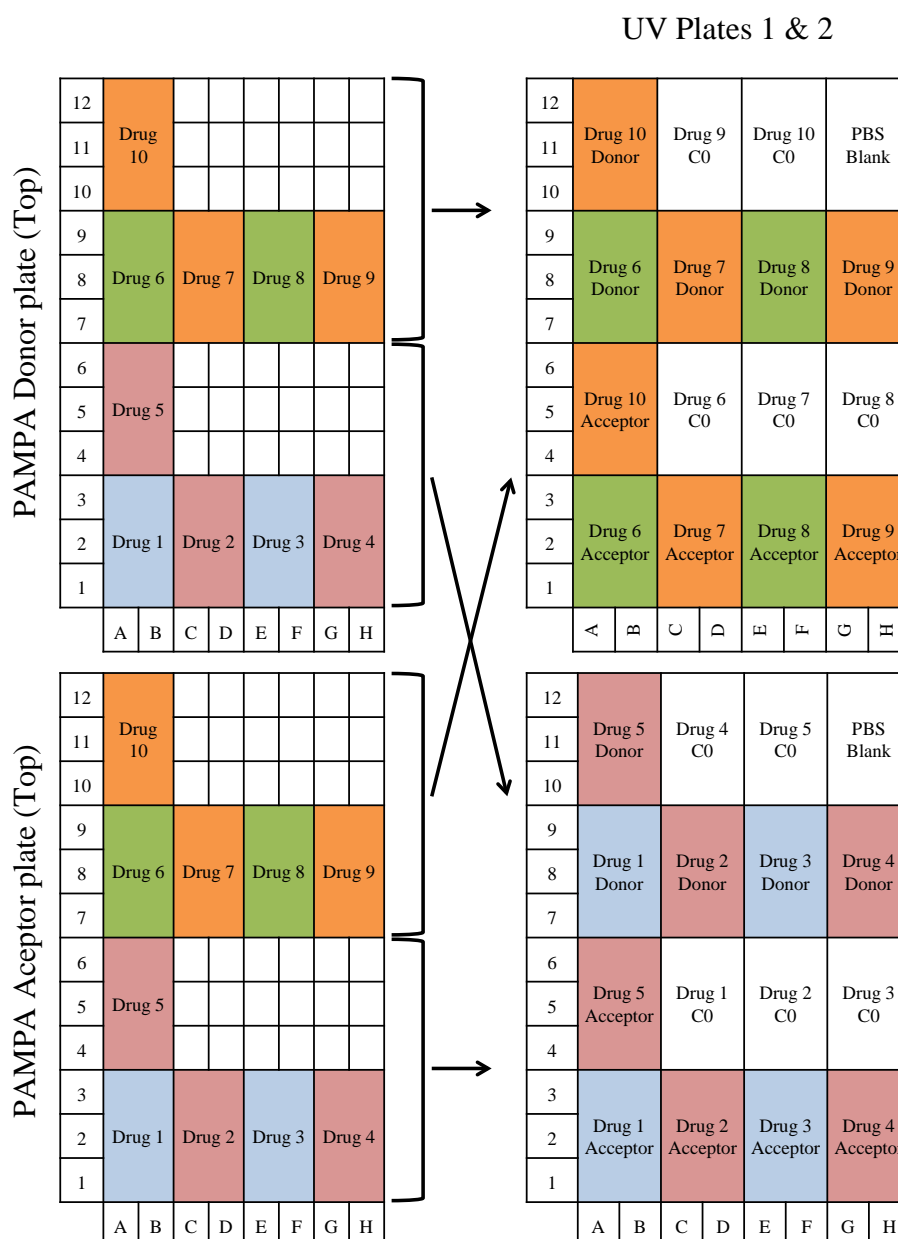


FIGURE 3.1: Schematic representation of a PAMPA assay showing the PAMPA acceptor and donor plates, and the cross-pipetting scheme to the Costar® UV plates

3.2 Gene expression analysis

The procedures described in this section were used to synthesise copy DNA (cDNA) and to study the gene expression of membrane transporters in cell lines and tissues. RNA was either obtained commercially, or isolated from hCMEC/D3 and HEK293 cells with the RNeasy Plus Mini Kit (QUIAGEN) according to the manufacturer's instructions. RNA was quantified by photometry in an BioPhotometer (Eppendorf) with a Nanodrop cuvette (Implen) using 3 μL of RNA solution. A 260nm/280nm ratio above 1.9 was considered good for RNA.

3.2.1 Reverse transcription

To synthesize cDNA, 1 μg of RNA was diluted in 17,75 μL of RNase free water. The reaction was performed in a thermal cycler, by first incubating the cDNA at 42°C with random hexanucleotide primers for 10 min. After cooling down at room temperature for 5 to 10 min, the reverse transcription master mix was added, and incubated for an additional 60 min at 72°C. At the end of the reaction, 70 μL of H₂O was added to the cDNA. This procedure is described in Table 3.1. The reverse transcription master mix is described on Table 3.2.

TABLE 3.1: Protocol for reverse transcription

Reagent	Volume added	Time	Temperature
Random hexanucleotide primers	1 μL	10 min	72°C
X	X	5-10 min	Cooling down at room temperature
Reverse transcription Master Mix	11,25 μL	60 min	42°C

TABLE 3.2: Master mix for cDNA synthesis

Reagent	Volume
SuperScript® II reverse transcriptase	0,25 μL
RNase inhibitors	0,5 μL
10 mM dNTPs	1 μL
0,1 M DTT	3,5 μL
5x RT Buffer	6 μL

3.2.2 Gene expression analysis with TaqMan[®] low density gene expression arrays

Gene expression analysis were carried out using customized TaqMan[®] low density gene expression arrays, in a 384-well format, designed to analyze the gene expression of 90 different transporter genes (Appendix A on Table A.1). The gold standard TaqMan[®] single assays were used to validate the gene expression arrays (assays used are also listed on table A.1). The gene expression analysis using single assays was carried out by mixing 3 μL of cDNA with 5.1 μL of H_2O , 0.9 μL of the TaqMan[®] gene expression assay and 9 μL of TaqMan[®] Universal PCR Master mix. The gene expression analysis using microfluidic cards was carried out according to the manufacturers instructions. Twenty μL of cDNA were mixed with 80 μL H_2O and 100 μL TaqMan[®] Universal PCR Master Mix. The mixture was pipetted into two wells of the microfluidic card (100 μL per well, 4 samples per microfluidic card). The cards were centrifuged at $331\times g$ for 1 min (Thermo Scientific Multifuge X3R, using the Heraeus microfluidic card holders). The cards were sealed with the TaqMan[®] array micro fluidic card sealer.

Both for the single assays, as well as for the microfluidic cards, the qPCR was performed using a 7900HT Fast Real-Time PCR System equipped with the 384-well thermo cycling block (single assays) or the TaqMan[®] array micro fluidic card thermal cycling block using the conditions listed on Table 3.3.

TABLE 3.3: Real-Time PCR conditions

Temperature	Time
50°C	2 min
94,5°C	10 min
97°C	30 sec
59,7°C	1 min
	(40 cycles)

Data analysis and calculation of the Ct values was performed using SDS version 2.4 and RQ-manager version 1.2.1. Gene expression was normalized to the arithmetic mean of the expression of 6 housekeeping genes (GADPH, ACTB, HPRT1, MVP, TBP, and UBC) included in the TaqMan[®] Array microfluidic cards (Table A.1). Gene expression was calculated with the equation:

$$\text{Relative gene expression} = 2^{-(Ct_{\text{gene of interest}} - Ct_{\text{average house keeping genes}})} \quad (3.2)$$

3.3 DAB-Immunostaining of paraffin-embedded sections on glass

The immunostaining of paraffin-embedded sections on glass was performed following a protocol provided by Dr. Oliver Wirths (Wirths *et al.* (2002), with modifications). The method is based on the oxidation of DAB (3,3'-diaminobenzidine) in the presence of a peroxidase enzyme and hydrogen peroxide. The product of the oxidation is a brown precipitate which stays at the site of enzymatic activity and is insoluble in alcohol. First, the tissue slides are incubated with a primary antibody which binds to the protein to detect. In a second step, a biotinilated secondary antibody binds to the primary antibody. The detection is made with the VECTASTAIN[®] ABC kit, which is comprised of a peroxidase enzyme bound to avidin (avidin binds to the biotinilated secondary antibody). The primary and secondary antibodies used for this procedure are listed on Table 3.4. Imaging was performed with a Olympus BX51 Microscope. The full staining method is described on Appendix.B.

TABLE 3.4: Antibodies for the detection of OCT1, BCRP and MDR-1 by DAB-Immunostaining

Protein	Primary antibody	Secondary antibody	Reference
BCRP	Mouse monoclonal for BCRP (BXP-21)	Polyclonal rabbit anti-mouse IgG / Biotinylated	Budak <i>et al.</i> (2005)
MDR-1	Rabbit polyclonal (HPA002199) anti-ABCB1 antibody	Polyclonal swine anti-rabbit IgG / Biotinylated	Uhlen <i>et al.</i> (2010)
OCTN2	Goat polyclonal antibody for OCTN2 (sc-19822)	Polyclonal rabbit anti-goat IgG / Biotinylated	Chang <i>et al.</i> (2011)
OCT1	Mouse monoclonal anti-OCT1 (2C5)	Polyclonal rabbit anti-mouse IgG / Biotinylated	Saadatmand (2012)

3.4 Cell culture

3.4.1 HEK293 cells

All HEK293 cell lines were routinely cultured in DMEM medium supplemented with 10% FCS and 1% Penicillin/Streptomycin (100 *U/mL*) in 75 mm flasks. A dissociation reagent was not used for routine sub-cultivation of HEK293 cell lines. Before plating cells for uptake experiments, cells were treated with 3.5 *mL* of TrypLE[™]Express for 3 to 5 minutes. Adding 10 *mL* of cell culture medium stopped the action of TrypLE[™]Express. After centrifugation at 300×*g* for 3 min, cells were re-suspended in fresh cell culture medium, counted on a Neubauer chamber using trypan blue staining, and used for

further experiments. To store HEK293 cells, cell stocks were frozen in FCS with 10% DMSO.

3.4.2 hCMEC/D3 cells

hCMEC/D3 cells were routinely cultured (Weksler *et al.* (2005), with modifications) in EndoGRO™ medium (including kit supplements) additionally supplemented with 1% Penicillin/Streptomycin (100 *U/mL*) and 1 *ng/mL* of human basic fibroblast growth factor (Table 2.2). After the addition of supplements, the cell culture medium was stable for at least 1 month. Before subcultivation, or plating, cells were washed once with sterile HBSS, and incubated with 0.25% trypsin for no more than 5 min (controlled under the microscope, until cells round-up). Adding cell culture medium stopped the action of trypsin. After centrifugation at $288 \times g$ for 5 min, cells were re-suspended in fresh cell culture medium, counted on a Neubauer chamber using trypan blue staining, and used for further experiments. The hCMEC/D3 cell line was grown in Corning® tissue culture treated 75mm flasks and 6-well plates, coated with rat collagen I. Before use, the collagen was dissolved at concentration of 150 $\mu g/mL$ in sterile water. Enough collagen to cover the whole cell culture surface was added to the flask or well and the cell culture surface was incubated at 37°C for one hour. The collagen was removed, the surface was washed with sterile PBS and cell culture medium was added to the cell culture surface (so that the collagen coating does not dry). To store the hCMEC/D3 cell line, cell stocks were frozen in 95% FCS and 5% DMSO. To use frozen vials, cells were quickly thawed and placed in culture in EndoGRO™ medium in a 25mm flask. A medium exchange to remove the DMSO was performed after 4 to 5 hours when cells have attached.

3.4.3 MDCK II cells

MDCK II cells, obtained from the European Collection of Cell Cultures (ECACC), were routinely cultured in DMEM medium supplemented with 10% FCS and 1% Penicillin/Streptomycin (100 *U/mL*) in 75mm flasks. MDCK II cells attach strongly to the cell culture surfaces. Therefore, before subcultivation or plating of the MDCK II cell line, cells were treated with 3,5 *mL* of TrypLE™ Express for 15 to 20 minutes. Adding 10 *mL* of cell culture medium stopped the action of TrypLE™ Express. A cell scraper was used to further de-attach the cells from the cell culture surface. After centrifugation at $300 \times g$ for 3 min, cells were re-suspended in fresh cell culture medium, counted on a Neubauer chamber using trypan blue staining (to determine cell viability), and used for further experiments. To store the MDCKII cell line, cell stocks were frozen in FCS

with 10% DMSO. The MDCKII-LacZeo/FRT cell line was cultured in the same way as the parent MDCKII cell line, and Zeocin was added to the cell culture medium at the concentration of 250 $\mu\text{g}/\text{mL}$.

3.5 Uptake measurements in HEK293 cells

3.5.1 Uptake measurements in 12-well plates

TABLE 3.5: Summary of the methods used for cell lysis and quantification of drug uptake in assays performed in 12-well plates

	Dilution (labeled: non-labeled)	Lysis Bufer	Detection method
^3H -sulpiride(80,6 Ci/mmol)	1:4000		
^3H -morphine(80 Ci/mmol)	Only labeled		
^{14}C -tyramine(55 mCi/mmol)	Only labeled (5 - 20 μM)		
	1:3.6 (50 - 200 μM)		
	1:39.6 (500 - 1000 μM)		
^3H -MPP ⁺ (80 Ci/mmol)	Only labeled (5 $n\text{M}$)	500 μL 0.1 NaOH solution containing 0.1% SDS	Liquid Scintillation Counting. 400 μL of cell lysate plus 9 mL of AQUASAFE 500 Plus TM
	1:40000 (10 - 800 μM)		
^{14}C -TEA ⁺ (55 mCi/mmol)	1:50		
^3H -clozapine(80 Ci/mmol)	Only labeled		
^3H -lamotrigine(5 Ci/mmol)	Only labeled		
^3H -amantadine(439 mCi/mmol)	Only labeled		
^3H -citalopram(85 Ci/mmol)	Only labeled		
^3H -amitriptyline(60 Ci/mmol)	Only labeled (<100 $n\text{M}$)		
	1:100 (0.1 and 1 μM)		
Amisulpride	Not Applicable	500 μL of	High-performance liquid chromatography coupled with a tandem mass spectrometer (LC-MS/MS)
Tiapride	Not Applicable	80% acetonitrile, 20%water	
Sultopride	Not Applicable	containing 10 ng/mL of sumatriptan-d6	

To measure the uptake of sulpiride, amisulpride, tiapride and sultopride in 12-well plates, 0.6 million HEK293 cells were cultured in a single well pre-coated with poly-D-lysine (1-4 kDa). Cells were cultured for two days to reach complete confluence. All uptake measurements were performed at pH 7.4. The cells were washed with 1 ml 37°C Hank's Buffered Salt Solution (HBSS). The reaction was started by adding 400 μL 37°C HBSS containing the drug at different concentrations. The reaction was stopped after exactly 2 min by adding 2 ml ice-cold HBSS. The cells were washed twice with 2 ml ice-cold HBSS and lysed with 500 μL of the lysis buffer (Table 3.5). Liquid scintillation counting was used to quantify ^3H and ^{14}C label substances, according to table 3.5. Amisulpride, tiapride and sultopride were quantified by LC-MS/MS according to table 3.5. The intracellular drug concentrations were normalized to the total protein amount, as determined using the bicinchoninic acid (BCA) assay. HEK293 cells expressing the MATE-1 and

MATE-2K transporters were incubated with HBSS supplemented with 40 *mM* NH_4Cl for 30 min at 37°C before the start of uptake measurements.

3.5.2 Uptake measurements of amisulpride in Petri dishes

Nine million cells were plated in Petri dishes, which were pre-coated with poly-D-lysine. Cells were incubated for 48 h until confluent. Before starting the uptake, cells were washed with 10 *ml* 37°C HBSS. The uptake was initiated by adding 5 *ml* 37°C HBSS supplemented with amisulpride and the reaction was stopped after 2 min by adding 20 *ml* ice-cold HBSS. Cells were washed twice with 20 *ml* ice-cold HBSS and transferred to a 2 *ml* tube. At this point, an aliquot was stored for protein quantification. The remaining cells were lysed in 1 *ml* of Lysis buffer (80% acetonitrile and 20% 30 *mM* potassium dihydrogen phosphate buffer (pH 6,5)). The intracellular concentration of amisulpride was determined as described in Dos Santos Pereira *et al.* (2014). The intracellular amount of amisulpride was normalized to the total protein content of the sample as determined by the bicinchoninic acid (BCA) assay.

3.6 Uptake measurements in hCMEC/D3 cells

One million hCMEC/D3 cells were plated in a single well of a 6-well plate coated with rat collagen I, and cultured for two days to reach complete confluence. Before the uptake assay, cells were washed with 2 *ml* 37°C Hank's Buffered Salt Solution (HBSS). The reaction was started by adding 1 *mL* 37°C HBSS containing sulpiride or amisulpride at the concentrations of 1 μM , 5 μM and 25 μM . Sulpiride was used in a mixture of ^3H -labeled and non-radiolabeled in a molar ratio of 1:400. The reaction was stopped after 2 min by adding 5 *ml* ice-cold HBSS. For quantifying the intracellular amount of sulpiride, cells were lysed with 1 *mL* of a 0.1 *N* NaOH solution containing 0.1% SDS. Eight hundred (800) μL of the cell lysates were mixed with 15 *ml* liquid scintillator (AQUASAFE 500 Plus™). The total amount of sulpiride was quantified by liquid scintillation counting. For quantifying the intracellular amount of amisulpride, sultopride and tiapride, cells were lysed with 1 *mL* of a lysis solution (80% acetonitrile, 20% water) containing 10 *ng/mL* of sumatriptan-d6, which was used as internal standard. The cell lysate was used for the quantification of intracellular drug accumulation by LC-MS/MS. The uptake measurements at 4°C were performed after pre-incubating the cells for 15 *min* on ice and the uptake reaction was carried out with ice-cold HBSS buffer. The intracellular drug concentrations were normalized to the total protein amount, as determined using the bicinchoninic acid (BCA) assay.

3.7 LC-MS/MS quantification of tiapride, sultopride and amisulpride

Tiapride, sultopride and amisulpride were quantified by LC-MS/MS by adapting previously described methods (Fisher *et al.* (2013), Moon *et al.* (2004)). Ten μL of the sample were injected into a PerkinElmer/Sciex HPLC system coupled with an API4000 tandem mass spectrometer (Applied Biosystems, Darmstadt, Germany). Separation was carried out in a Brownlee SPP RP-Amide column (4.6x100 mm, 2.7 μm particle size; Perkin Elmer, Waltham, MA, USA) with a Phenomenex SecurityGuard Standard precolumn (C18, ODS, 4mmx2mm, KJO-4282, Phenomenex, Aschaffenburg, Germany). Isocratic elution was performed with a mobile phase of 0,1% formic acid, 6,9% acetonitrile, and 1,1% methanol at a flow rate of 0.3 mL/min . Detection was performed with the mass transitions and retention times listed on table 3.6.

TABLE 3.6: Mass transitions and retention times used for LC-MS/MS detection of amisulpride, sultopride and tiapride

Drug	Mass transition (m/z)	Retention time (min)
Tiapride	329.4>256.1	6.6
Sultopride	355.5>227.3	10.7
Amisulpride	370.2>242.1	16.0

3.8 Quantification of total cellular protein by the bicinchoninic acid (BCA) assay

The bicinchoninic acid was first described by Smith *et al.* (1985). After cell lysis with a 0.1 N NaOH solution containing 0.1% SDS, 10 μL of the cell lysate were incubated with 200 μL of a commercial bicinchoninic acid solution (Sigma-Aldrich), supplemented with 4 μL of a 4% cupric sulfate pentahydrate solution (2 mg of $\text{CuSO}_4 \times 5\text{H}_2\text{O}$ in 50 mL of H_2O). The cell lysate was incubated with the BCA solution for 25 min at 37°C and absorbance at 570 nm was measured in a TECAN plate reader using 96-well sterile clear plates (Sarsted). The total protein amount was determined through a standard curve containing 1-10 μg of bovine serum albumin (from a 1 $\mu\text{g}/\mu\text{L}$ BSA solution in water).

3.9 Stable integration of the pFRT/LacZeo plasmid on the MDCK II cell line

This section describes the procedures used to transfect and select MDCK II cell lines stably expressing the pFRT/LacZeo plasmid. The pFRT/LacZeo plasmid was obtained from Life Technologies and is shown schematically on Figure 3.2.

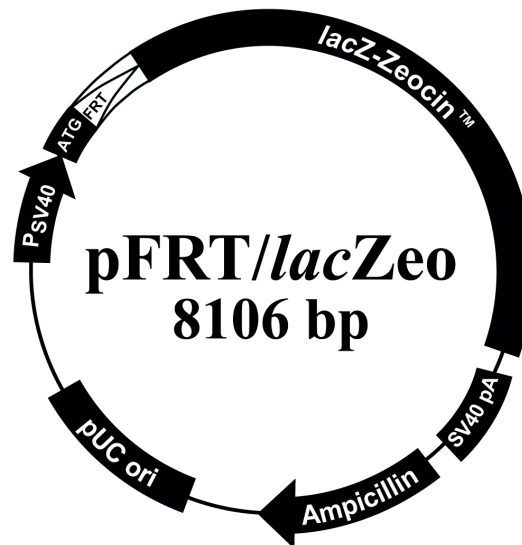


FIGURE 3.2: The pFRT/LacZeo plasmid. *SV40* is the early promoter; *ATG* is the initiation codon. *LacZ-Zeocin™* is the β -Galactosidase - Zeocin™ fusion gene. *SV40 pA* is the polyadenylation signal; *Ampicillin* is the ampicillin resistance gene; *pUC origin* is the plasmid origin of replication

3.9.1 Plasmid midi-prep: Isolation of plasmid DNA by solid extraction with a commercial kit

The isolation of plasmid DNA by solid extraction is the preferred method to obtain higher amounts of high purity plasmid DNA. This method is used to prepare plasmid DNA for a transfection of mammalian cells. The commercial kit used was the QUIAGEN® Plasmid Plus Midi Kit according to the manufacturer's instructions. Briefly, bacteria were grown in a pre-culture of 5 mL of LB medium containing antibiotics (ampicillin 100 $\mu\text{g}/\text{mL}$) for 5 hours. After this period, 5 mL of the pre-culture were transferred into a 500 mL autoclaved glass bottle containing 20 mL of LB medium with ampicillin (100 $\mu\text{g}/\text{mL}$). The 25 mL bacterial culture was grown overnight. The bacterial suspension was harvested by centrifugation at 4000 rpm for 15 min. Buffers P1, P2, S3, ETR, PE and EB were obtained from the QUIAGEN® Plasmid Plus Midi Kit. The cells were re-suspended in 2 mL of buffer P1.

Then, 2 *mL* of buffer P2 were added, and the tubes gently mixed by inversion, and incubated for 3 min at room temperature. During the incubation time, QIAfilter cartridges are placed in 50 *mL* tubes. After 3 min, 2 *mL* of buffer S3 were added to the lysate and mixed by inverting 4-6 times. The lysate was transferred to the QIAfilter cartridges and incubated at room temperature for 10 min. During the incubation time, QUIAGEN Plasmid Plus spin columns with tube extenders were placed into the QIAvac 24 Plus (vacuum). With the aid of the supplied plunger, the lysate was passed through the filter into the 15 *mL* tube and the filter cartridges were disposed of. Then, 2 *mL* of the BB buffer were added to the cleared lysate (in the 50 *mL* tube) and mixed by inverting 4-6 times. The lysate was added to the QUIAGEN Plasmid Plus spin column (with the tube extender) and vacuum was applied until all the liquid has been drawn into the column.

The column (where the DNA was now bound) was washed with 0.7 *mL* of ETR buffer followed by 0.7 *mL* of PE buffer. Vacuum was applied until all the buffer had passed through the column. To remove the residual buffer in the column, the QUIAGEN Plasmid Plus spin column was centrifuged for 1min at 10000×g in a bench top centrifuge (Biofuge pico). Finally, to elute the DNA, 200 μL of Buffer EB was added to the column, incubated for 1 min, and centrifuged for 1 min into a collection tube. DNA was quantified by photometry in an BioPhotometer (Eppendorf) with a Nanodrop cuvette (Implen) using 3 μL of DNA. A 260nm/280nm ratio above 1.6 was considered good for DNA.

3.9.2 Plasmid linearization and gel extraction

Before transfecting MDCK II cells, the plasmid DNA obtained from a midi-prep (Section 3.9.1) was linearised with the *SacI* enzyme. The restriction reaction was performed for 3h (1h, with additional 2h) at 37°C with the components listed on (Table 3.7). After linearisation, the plasmid was run on an 0.8% agarose gel, and isolated with the QIAquick Gel Extraction Kit.

TABLE 3.7: Linearization of Plasmid DNA

Reagent	Volume (μL)
SacI-HF	5
10x Enzyme buffer	5
Plasmid DNA	40
SacI-HF (after 1h)	2
	incubate for 2h

3.9.3 Transfection and Selection of MDCK II clones

MDCK II cells were seeded at 0.4 million cells/well in a 6-well plate and cultured for 48 hours (MDCK II cells are considered difficult to transfect cells. For a successful transfection, it is important that the cells are less than 80% confluent). On the day of transfection, 14 μg of the linearised plasmid DNA was diluted in 150 μL of OptiMEM medium in a 1,5 mL tube (supplemented with 100 U/mL of penicillin and streptomycin (1%) and without serum). In another tube, 9 μL of Lipofectamine 2000 was added to 141 μL of OptiMEM medium. The 150 μL of medium containing Lipofectamine 2000 was added to the tube containing the plasmid DNA and incubated for 5 min (Lipofectamine® 2000 reagent protocol, No. MAN007824 Rev. 1.0, Life Technologies) at room temperature. The Lipofectamine-DNA complexes were formed at this point. Then, the cell culture medium covering the MDCK II cells in the 6-well plates was removed, and 300 μL of OptiMEM medium containing the Lipofectamine-DNA complexes, are added to the each well. Next, 700 μL of OptiMEM medium are added to each well, to a final volume of 1000 μL per well. It is important to make the DNA complexes in a smaller volume of medium, and then diluting them to a bigger volume (therefore, 300 μL + 700 μL). A plasmid containing the gene encoding for GFP (green fluorescence protein) should be transfected in another well at the same time as the plasmid to be integrated. A GFP-overexpressing plasmid was transfected in an independent well under the same conditions in order to control for transfection efficiency. After 24h, cells are controlled for GFP expression and are harvested from the 6-well plate (with the help of TrypLE® Express and a cell scraper) and transferred into a Petri dish (10 cm diameter) with fresh DMEM medium (10% FCS, 1% PenStrep) without antibiotics. After 5-6 hours, cells had attached to the Petri dish and the medium was replaced with fresh cell culture medium containing Zeocin (250 $\mu\text{g}/\text{mL}$). Medium (with Zeocin) was replaced on day 4 after transfection. At day 7 after transfection the first single clones are observed and a medium exchange is performed. At day 10 after transfection, a medium exchange was also performed, and at day 11 after transfection, isolated cell colonies are picked. A concentration of 250 $\mu\text{g}/\text{mL}$ of Zeocin in the medium yielded single colonies.

Zeocin™'s method of killing the cells is different from other eukaryotic antibiotics including hygromycin, G418 and blasticidin. Zeocin sensitive cells do not de-attach from the cell surface. Instead, cells increase in size and show an abnormal cell shape (Flp-In™system user manual, Version E, 9 November 2010, 25-0306, Invitrogen). Single colonies of Zeocin resistance clones were identified (Figure 3.3) and labelled with a pen from the outside of the Petri dish. Then, a cell scraper was used to de-attach the labelled colonies from the plate by carefully scrapping only the cells inside of the colony (Zeocin sensitive cells colonies were big enough and had a different opacity in the Petri dish,

that could be seen with the naked eye). The de-attached cells were collected from the Petri dish by pipetting up and down with a pipette containing $10\ \mu\text{L}$ fresh medium. The Zeocin resistant cells were further propagated in a 12-well plate with medium containing $250\ \mu\text{g}/\text{mL}$ of Zeocin.

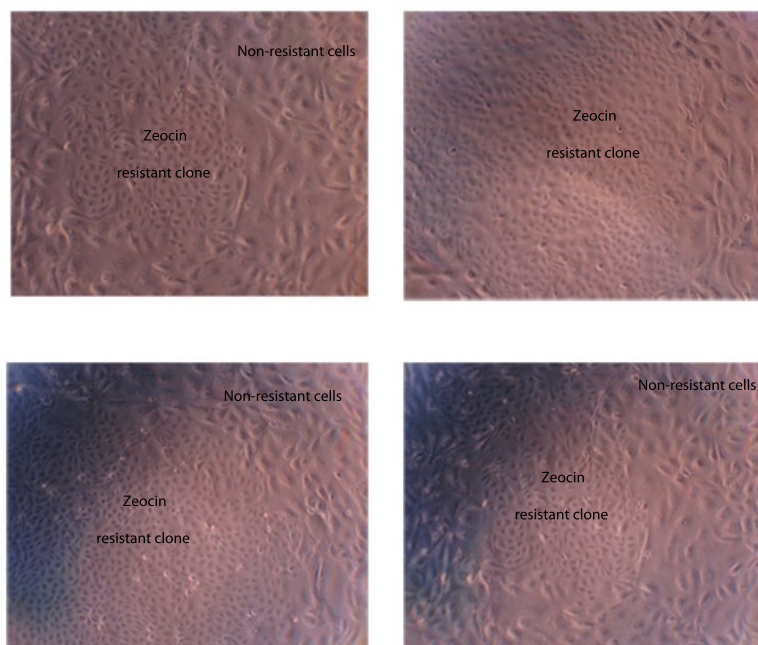


FIGURE 3.3: Selection of MDCK II cells transfected with the pFRT/LacZeo plasmid. MDCK II cells were transfected with the pFRT/LacZeo plasmid and selected in medium containing $250\ \mu\text{g}/\text{mL}$ of Zeocin. Cells which are resistant to Zeocin have the normal cell shape of the original MDCK II cells, whereas Zeocin sensitive cells have an elongated phenotype, and appear to be bigger.

3.9.4 TEER (transepithelial electrical resistance) measurements

MDCK II cells form tight junctions and allow the study of drug transport through polarized cell monolayers. In order to assess whether the cells have formed a monolayer, the transepithelial electrical resistance (TEER) can be measured by placing an electrode on the basolateral side of the monolayer and an electrode on the apical side of the monolayer.

For this purpose, cells were seeded at a density of 100,000 cells/well on a single well of a Transwell[®] 12-well plate (1 mL of medium on the bottom well and 0.6 mL of medium on the top well). The resistance between the two sides of the monolayer was measured with an EVOM[®] Volt/Ohmmeter coupled with a STX2 electrode (Table 2.7, Section 2.5).

3.9.5 β -Galactosidase assay

The β -Galactosidase assay assesses the activity of the pFRT/LacZeo plasmid when transfected into mammalian cells. The assay is based on the hydrolysis of o-Nitrophenyl- β -D-galactopyranosid (ONPG), a synthetic substrate of the enzyme β -galactosidase. The β -gal assay kit (Life Technologies) was used according to the manufacturers instructions with slight modifications. Briefly, MDCK II cells growing on a 10 cm Petri dish were collected with a cell scraper and diluted in 1 mL PBS. The cells were centrifuged for 5 min at $250 \times g$ and the supernatant was removed. The cell pellet was re-suspended in 100 μL of 1X lysis buffer and samples were snap-frozen on liquid nitrogen, and then thawed at $37^\circ C$. This was repeated twice. The insoluble cell material was pelleted by centrifugation at maximum speed for 5 min on a bench-top centrifuge. From each sample, 1, 5 and 10 μL of the supernatant (containing the soluble cell lysate) were transferred into a new 1,5 μL tube, and diluted to 30 μL with deionized water. To each tube, 70 μL of ONPG and 200 μL of 1X cleavage buffer were added. The tubes were mixed by gently flicking the bottom of the tube and short centrifugation. After incubation for 30 min at $37^\circ C$, the reaction was stopped by adding 500 μL of stop buffer and absorbance was read at 405 nm. As a control, a sample of non-transfected MDCK II cells was also assayed. The β -Galactosidase activity was normalized to the total protein amount as determined by the BCA assay. Specific activity was calculated based on the following equations:

$$\text{Specific activity} = \text{nmoles of ONPG hydrolysed} / t / \text{mg protein} \quad (3.3)$$

- t is the time of incubation at $37^\circ C$
- mg protein is the protein amount determined by the BCA assay

$$\text{nmoles of ONPG hydrolysed} = \frac{OD_{405} \times \text{Volume}(nL)}{\text{extinction coefficient} \times 1 \text{ cm}} \quad (3.4)$$

- OD_{405} is the absorption at 405 nm
- Volume is the total volume of the assay $8 \times 10^5 nL$ (800 μL total volume)
- The $\text{extinction coefficient}$ of the hydrolysed ONPG is 4500 $nl/nmoles - cm$

3.10 Data analysis

3.10.1 Enzyme kinetics

The membrane transporter dependent uptake was calculated by subtracting the uptake in cells transfected with the empty vector ($uptake_{emptyvector}$) from the uptake in cells expressing a membrane transporter ($uptake_{transporter}$):

$$Transporter\ dependent\ uptake = uptake_{transporter} - uptake_{emptyvector} \quad (3.5)$$

The Michaelis-Menten constants, V_{Max} and K_M , and the half-maximal inhibition constants, IC_{50} , were calculated using non-linear regressions with Sigma Plot 12 (Systat Software Inc., Erkrath, Germany).

V_{Max} and K_M were determined according to the Michaelis-Menten equation, where $[S]$ represents the substrate concentration:

$$Transporter\ dependent\ uptake = \frac{V_{Max} \times [S]}{K_M + [S]} \quad (3.6)$$

The intrinsic clearance of the transporter, CL_{Int} , was determined by:

$$CL_{Int} = \frac{V_{Max}}{K_M} \quad (3.7)$$

The half-maximal inhibition constants, IC_{50} were determined by measuring the uptake at a single concentration of the substrate, with different concentrations of the inhibitor drug, and fitting the data into the equation:

$$Y([S]) = Y_{min} + \frac{Y_{max} - Y_{min}}{1 + ([S]/IC_{50})^{-H}} \quad (3.8)$$

- Y is the percent of uptake at different concentrations of the inhibitor
- S is the concentration of the inhibitor
- Y_{max} is the Y value at the top plateau of the curve (maximum uptake value)
- Y_{min} is the Y value at the bottom plateau of the curve (minimum uptake value)
- IC_{50} is the concentration of the drug between the top and bottom plateaus
- H is the Hill slope, which describes the steepness of the inhibition curve

3.10.2 Estimation of maximal drug concentration in the portal vein

The plasma concentration of drugs which are metabolised in the liver, may be higher in the portal vein than in the rest of the body. This is due to the fact that drugs reach the liver directly after being absorbed in the intestine and have not yet suffered any kind of liver metabolism. The theoretical maximal plasma unbound drug concentration in the portal vein, $C_{MAXPort,Unb.}$, was calculated with the following equation, derived from Ahlin *et al.* (2011) and Ito *et al.* (1998).

$$C_{MAXPort,Unb.} = f_u \times \left(C_{Max} + \frac{k_a \times D \times F_a}{Q_h} \right) \quad (3.9)$$

- f_u is the fraction of unbound drug in the plasma
- C_{Max} is the maximal plasma concentration
- k_a is the absorption rate constant (set to $0,1 \text{ min}^{-1}$)
- D is the dose in *nmol*
- F_a is the fraction from the drug which is absorbed into the portal vein (set to 0,99)
- Q_h is the hepatic blood flow (set to 1610 mL/min)

3.10.3 Prediction of drug chemical properties

The $\text{Log}D_{7,4}$ and pKa values of the drugs analyzed were estimated based on their chemical structures using ADMET Predictor 5.5 (Simulations Plus, Lancaster, CA, USA). Using the estimated pKa, the percentage of drug which is protonated at pH 7,4 ($\%[BH^+]$) was calculated according to the Henderson-Haselbach equation, as follows:

$$pH = pKa + \log \frac{[B]}{[BH^+]} \quad (3.10)$$

$$\frac{[B]}{[BH^+]} = 10^{pH-pKa} \quad (3.11)$$

and

$$100\% = \%[BH^+] + \%[B] \quad (3.12)$$

$$\%[BH^+] = \frac{100\%}{\frac{[B]}{[BH^+]} + 1} \quad (3.13)$$

3.10.4 Statistics

The Student's t-test was used for two independent group comparisons. ANOVA was used for multiple group comparisons followed by post-hoc pair-wise comparisons using Tukey's HSD test. Spearman's correlation was used to analyze the correlation between the estimated $LogD_{7.4}$ and the measured membrane permeability (P_e) values. The statistical analyses were performed with IBM SPSS Statistics version 21.0 (IBM Corporation, Ehningen, Germany).

4

Results

4.1 Membrane permeability of psychotropic drugs

Systematic screens were performed in order to identify psychotropic drugs with low membrane permeability by passive diffusion. These drugs may benefit from carrier-mediated transport to penetrate the cell membrane. First the membrane permeability of psychotropic drugs was estimated by calculating their physicochemical properties, and secondly, experimentally determined by means of a PAMPA assay (parallel artificial membrane permeability assay).

4.1.1 Computer based prediction of the physicochemical properties of drugs

The membrane permeability of drugs was first assessed by *in silico* prediction of their physicochemical properties. Table 4.1 shows the $LogD$ at pH 7.4, $LogP$ and pKa of several psychiatric drugs obtained by simulation with the Software ADMET Predictor 5.5. The fraction of the drug protonated at pH 7.4 was obtained with the Henderson-Hasselbach equation. Out of the 31 drugs tested, 22 were estimated to be above 90% positively charged at pH 7.4 (Table 4.1). However, only 6 out of the 31 drugs tested were estimated to have low $logD_{7.4}$ values, lower than 0: tranlycypromine, sulpiride, clozapine, amisulpride, tiapride and milnacipram. A low $logD_{7.4}$ means that a drug is more hydrophilic, and a high $logD_{7.4}$ means that a drug is more hydrophobic. The most hydrophilic drug was tranlycypromine ($LogD = -0.53$), and the least hydrophilic drug, clomipramine ($LogD = -3.93$). Drugs with low $logD_{7.4}$ are expected to have low membrane permeability and to profit from carrier mediated transport to penetrate cellular membranes.

TABLE 4.1: Physicochemical properties of psychotropic drugs at pH 7.4. The $\log D_{7.4}$, $\text{Log}P$ and pK_a values were obtained by simulation with the Software ADMET Predictor 5.5. The fraction of the drug protonated at pH 7.4 was calculated with the Henderson-Hasselbach equation.

Drug	$\log D_{7.4}$	$\text{Log}P$	pkA	Fraction protonated at pH 7,4 (%)
Tranlycypromine	-0.53	1.72	9.65	99.4
Sulpiride	-0.51	0.91	8.80	96.2
Clozapine	-0.38	2.65	10.43	99.9
Amisulpride	-0.29	1.32	9.00	97.5
Tiapride	-0.23	2.37	8.83	96.4
Milnacipram	-0.07	2.09	9.56	99.3
Sultopride	0.09	1.70	8.95	97.3
Methylphenidate	0.82	2.19	8.75	95.7
Paliperidone	1.2	1.83	7.92	76.8
Melperon	1.43	3.49	9.46	99.1
Citalopram	1.82	3.57	9.14	98.2
Paroxetine	1.83	3.77	9.34	98.9
Desipramine	1.85	4.32	9.87	99.7
Nortriptyline	1.96	4.57	10.01	99.8
Lamotrigine	1.99	1.99	3.41	0.0
Risperidone	2.16	2.83	7.97	78.8
Duloxetine	2.26	4.51	9.65	99.4
Fluoxetine	2.37	4.73	9.76	99.6
Olanzapine	2.43	3.00	7.84	73.4
Quetiapin	2.47	2.81	7.48	54.6
Mirtazapine	2.49	2.71	7.23	40.3
Doxepine	2.65	4.35	9.09	98.0
Haloperidol	2.83	3.93	8.46	92.0
Perazine	3.18	4.28	8.46	92.0
Imipramine	3.25	4.81	8.95	97.3
Amitriptyline	3.25	4.99	9.13	98.2
Perphenazine	3.32	4.02	8.00	79.9
Promethazin	3.37	4.44	8.43	91.5
Fluphenazine	3.47	4.18	8.02	80.7
Flupentixol	3.91	4.74	8.16	85.2
Clomipramin	3.93	5.40	8.86	96.6

4.1.2 Transporter independent membrane permeability

The PAMPA (parallel artificial membrane permeability assay) assay is an experimental method of determining the membrane permeability of a drug. The PAMPA membranes are composed of a mixture of artificial phospholipids, which represent a cellular membrane better than the partition coefficient $LogP$, and allow for an estimation of the permeability coefficient (P_e) of a drug.

The psychotropic drugs listed on Table 4.1 were ranked by their permeability coefficient on the PAMPA assay in Figure 4.1.

Amisulpride and sulpiride were the least permeable drugs, within the drugs tested. Amisulpride had a P_e of $0.36 \times 10^{-6} \text{ cm/s}$ and sulpiride had a P_e of $1.19 \times 10^{-6} \text{ cm/s}$. The most permeable drug was doxepine, with a P_e of $24.9 \times 10^{-6} \text{ cm/s}$. Interestingly, the drug with the lowest predicted $\log D$, tranylcypromine, had a P_e of $9.5 \times 10^{-6} \text{ cm/s}$.

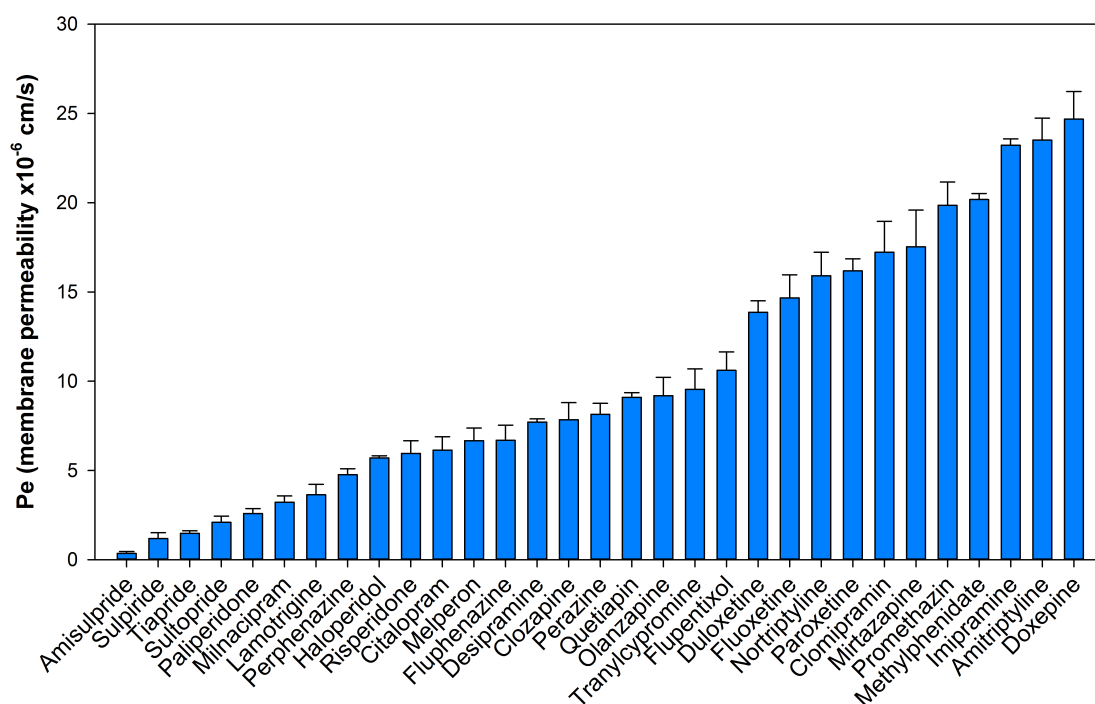


FIGURE 4.1: Comparison of the carrier-independent membrane permeabilities of commonly used psychotropic drugs. Shown are means and standard error of the means of at least two independent PAMPA experiments.

Drugs which have a lower $\log D_{7.4}$ value, should be less membrane permeable and have a lower P_e value. However, only 26% of the variability in the drug membrane permeabilities could be explained by the variations in the $\log D_{7.4}$ values ($r^2 = 0.26$, Figure 4.2 A). The variation in the $\log P$ explained 36% of the variability in drug membrane permeability (Figure 4.2 B).

Sulpiride, amisulpride, tiapride and sultopride are weak bases, which are more than 96% protonated at the physiological pH of 7.4 (Table 4.1). Their low membrane permeability (Figure 4.1) and their weak basic properties suggest that these drugs may benefit from carrier-mediated influx transport by organic cation transporters to penetrate cell membranes. This will be further explored in this work.

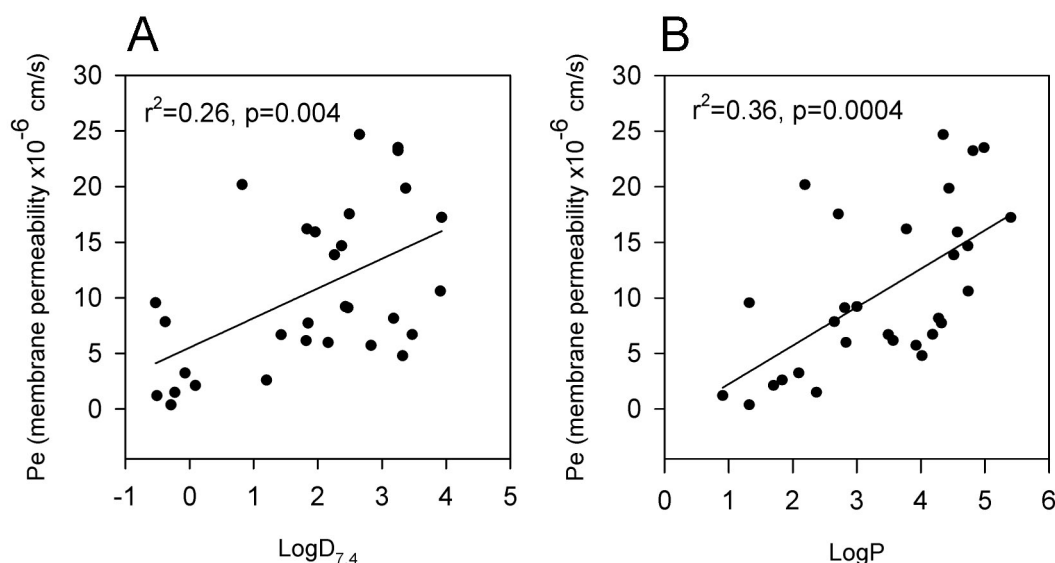


FIGURE 4.2: Correlation between experimentally determined P_e and the predicted $\log D_{7.4}$ (A) and $\log P$ (B) of psychotropic drugs

4.2 Gene expression analysis of membrane drug transporters

The expression of membrane drug transporters was analysed in tissues relevant for the distribution and elimination of psychotropic drugs. The aim was to identify the transporters which support the penetration of the psychotropic drugs, identified in the previous section (Section 4.1.2), through cellular barriers, especially through the blood-brain barrier. Custom designed Taqman[®] microfluidic cards were used to study the expression of 85 potentially relevant membrane transporter genes in tissues important for the distribution and elimination of psychotropic drugs, such as the liver, kidney, intestine and brain.

The expression of membrane transporter genes was also studied in primary cells isolated from human brain tissue. In addition, the expression of membrane transporter genes was studied in HEK293 cell lines stably expressing the gene of the organic cation transporter OCT1(*SLC22A1*) and the empty vector and in the immortalised human brain endothelial cell line, hCMEC/D3.

4.2.1 Validation of the TaqMan[®] low density array microfluidic cards

To validate the cDNA synthesis method used in this work, as well as the TaqMan[®] microfluidic cards, replicates of the cDNA synthesis were performed and run on different arrays (Figure 4.3 A). Furthermore, one of the cDNA samples was analysed in two independent cards, in order to evaluate inter-array variability (Figure 4.3). There was a good correlation ($r > 0.96$) between the replicates of both the cDNA synthesis (Figure 4.3 A), as well as between different arrays (Figure 4.3 B). In addition, some of the transporter genes which were included in the TaqMan[®] microfluidic cards were also analysed with the gold standard TaqMan[®] single gene expression assay. The correlation between the Ct values of both these assays was very good ($r = 0.93$, Figure 4.4).

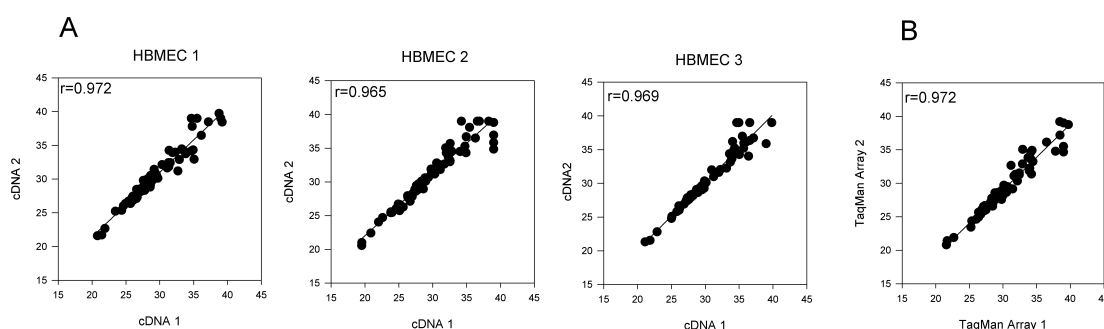


FIGURE 4.3: Validation of the cDNA synthesis and TaqMan[®] microfluidic cards. A) Variation between different cDNA synthesis reactions of the same RNA sample. B) Same cDNA run on two different TaqMan[®] microfluidics cards. Shown are the Ct values for each of the 90 transporters tested. The data used for this correlation is shown in tables C.3, C.4 and C.5 in Appendix C.

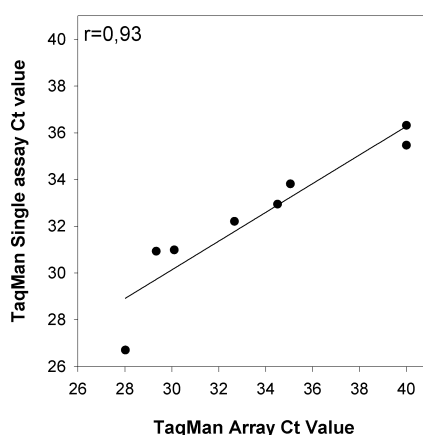


FIGURE 4.4: Comparison of the Ct values obtained with TaqMan[®] single assays and TaqMan[®] microfluidic cards. Shown is the correlation of the Ct values for the transporters OCT1 (*SLC22A1*), OCT2 (*SLC22A2*) and OCTN2 (*SLC22A5*), as well as housekeeping gene TBP in the samples HBMEC1 and HBMEC2 (Tables C.3, C.4).

4.2.2 Gene expression analysis in organs relevant for drug pharmacokinetics

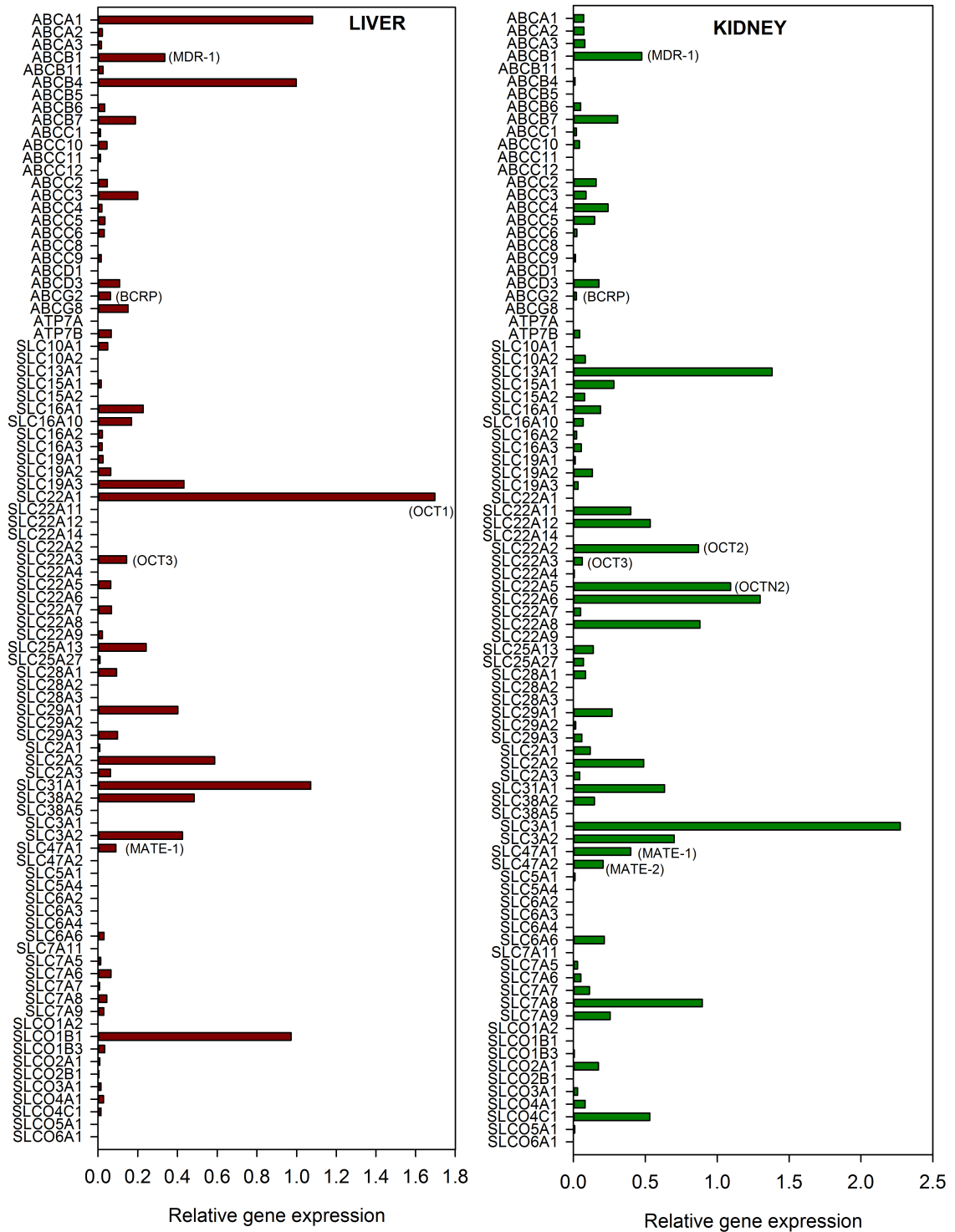
The expression of membrane transporter genes was studied in RNA samples obtained from liver, kidney, intestine and brain tissue, the organs which are most important for drug absorption, distribution and elimination.

The major organs where drug eliminations occurs are the liver and the kidney. The organic cation transporter 1, OCT1 (*SLC22A1*), was the transporter which showed the highest expression in the liver sample. The expression of OCT1 was 2.9-fold higher than the expression of GLUT-2 (*SLC2A2*), the major glucose transporter in the liver, and 1.7-fold higher than OATP1B1 (*SLCO1B1*), the major anion transporter in the liver (Figure 4.5 A). The second and third organic cation transporters with the highest expression in the liver were OCT3 (*SLC22A3*) and MATE1 (*SLC47A1*), respectively.

In contrast to the liver, where the major organic cation transporter is OCT1, the kidney has several OCTs which were expressed at high levels. The most expressed organic cation transporters in the kidney were OCTN2 (*SLC22A5*) and OCT2 (*SLC22A2*), followed by MATE-1 (*SLC47A1*) and MATE-2 (*SLC47A2*) respectively. The organic anion transporters OAT1 (*SLC22A6*) and OAT3 (*SLC22A8*) were also expressed at high levels in the kidney (Figure 4.5 B).

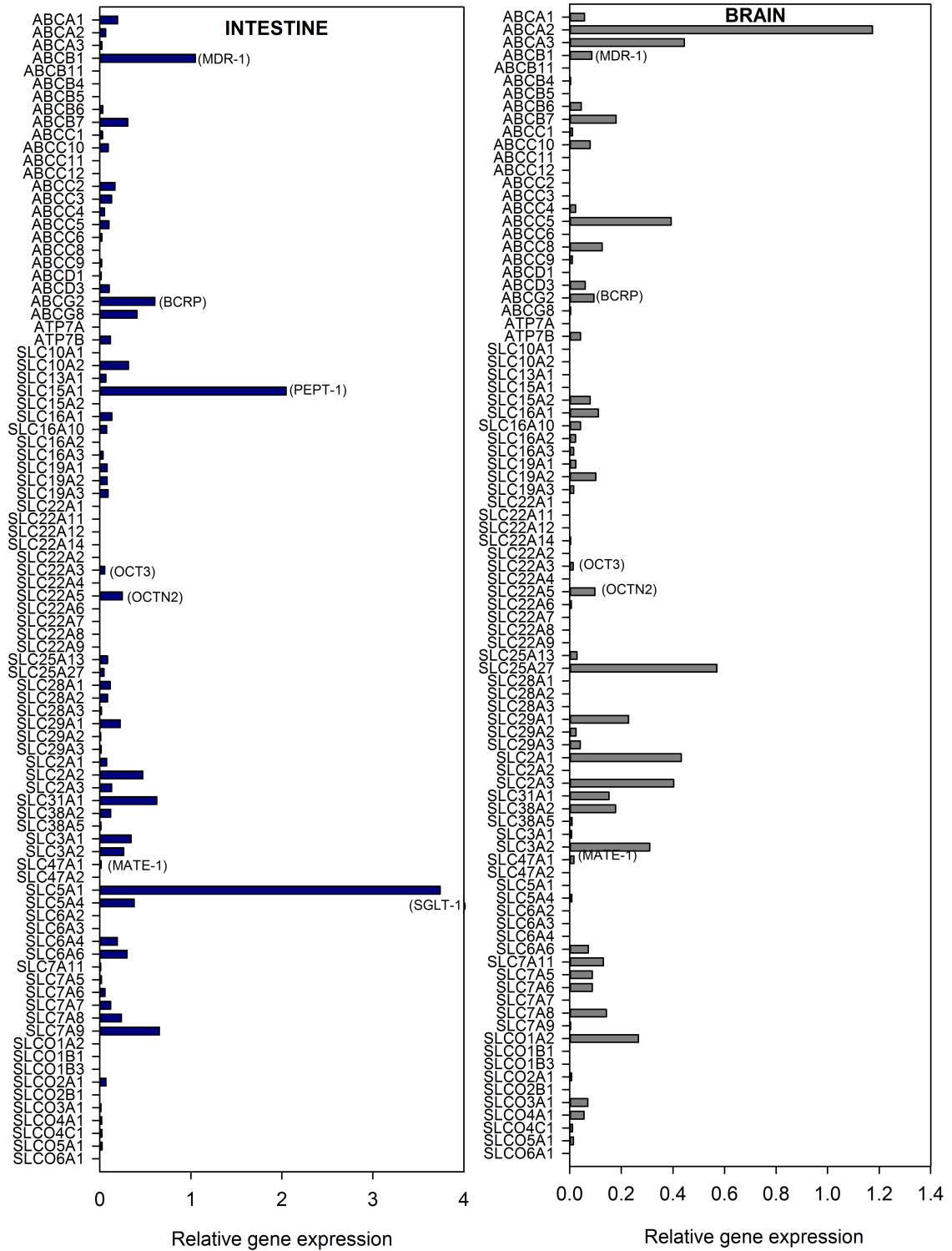
The expression of organic cation transporters in the intestine was lower compared to the liver and kidney. OCTN2 was the most expressed organic cation transporter in the intestine, followed by OCT3 and MATE-1. High expression of PEPT-1 (*SLC15A1*), a peptide transporter which is also able to transport drugs, was detected. The efflux transporters MDR-1 and BCRP were also among the most expressed transporters in the intestine. By far the transporter with the highest gene expression was the glucose-sodium co-transporter SGLT-1 (*SLC5A1*)(Figure 4.6 A).

The expression of organic cation transporters in the brain was lower than in the liver, kidney and intestine. However, OCTN2 mRNA was clearly detected in the brain. In addition, MATE-1 and OCT3 were also detected in the brain, although at low levels (Figure 4.6 B).



(A) Expression of membrane transporters in the liver (B) Expression of membrane transporters in the kidney

FIGURE 4.5: Gene expression analysis of membrane transporters in liver and kidney tissue using TaqMan[®] Low density Array microfluidic cards. The expression is normalised to the arithmetic mean of the expression of 6 housekeeping genes (GADPH, ACTB, HPRT1, MVP, TBP, UBC). The data represented in this figure is shown in tables C.1 and C.2 in Appendix C.



(A) Expression of membrane transporters in the intestine (B) Expression of membrane transporters in the brain

FIGURE 4.6: Gene expression analysis of membrane transporters in intestine and brain tissue using TaqMan[®] Low density Array microfluidic cards. The expression is normalised to the arithmetic mean of the expression of 6 housekeeping genes (GADPH, ACTB, HPRT1, MVP, TBP, UBC). The data represented in this figure is shown in tables C.1 and C.2 in Appendix C.

4.2.3 Gene expression analysis in primary human brain cells

The brain is a complex organ composed of several cell types. Here, the RNA expression of drug transporters was studied in different types of primary human brain cells in order to dissect which drug transporters may facilitate the entry of psychotropic drugs into the brain.

The endothelial cells which form the blood vessels in the brain and the cells which form the choroid plexus epithelium are the first barriers which drugs have to face before they reach the brain. Primary microvascular endothelial cells from the brain were studied in order to identify transporters relevant for penetrating the blood-brain barrier (BBB), and choroid plexus epithelial cells for penetrating the blood-CSF barrier (BCSFB). Astrocytes are one of the most abundant cell types in the brain, and were also studied for membrane transporter expression.

Within the three cell types analysed, transporter expression was the highest in brain microvascular endothelial cells (HBMECs). As shown in Figure 4.7, the number of transporters with high gene expression is higher in human brain microvascular than in astrocytes and choroid plexus epithelial cells.

The expression of drug membrane transporters in primary astrocytes was low, with OCTN2 being the most expressed organic cation transporter. MATE-1 was also detected at very low amounts (Figure 4.8 A).

In choroid plexus epithelial cells, the expression of drug membrane transporters was higher than in astrocytes, but lower than in microvascular endothelial cells. OCTN2 was, like in astrocytes, the most expressed cation transporter in choroid plexus epithelial cells (Figure 4.8 A).

OCTN2 was the most expressed organic cation transporter in human brain microvascular endothelial cells (HBMECs) (Figure 4.9). OCT3, OCT1, OCTN1 and MATE-1 were also detectable, at low levels (Appendix C, tables C.1 and C.2). Their expression levels were comparable with the expression of ENT2 (*SLC29A2*), a nucleotide transporter known to be expressed at the blood-brain barrier (Young *et al.* (2013)).

Worth mentioning, was the high expression of the breast cancer resistance protein (BCRP) in HBMECs (*ABCG2*) (Figure 4.9). The efflux transporter BCRP was highly expressed in primary microvascular endothelial cells and intestine (Figures 4.6 and 4.9), two of the major drug barriers in the human body. In contrast, MDR-1 (*ABCB1*) an important efflux transporter, is detectable in most of the tissues studied (Figures 4.5, 4.6, 4.8 and 4.9). LAT-1, an amino-acid transporter that is known for its high expression

at the blood-brain barrier (Boado *et al.* (1999)) also showed a high expression in our sample (Figure 4.9).

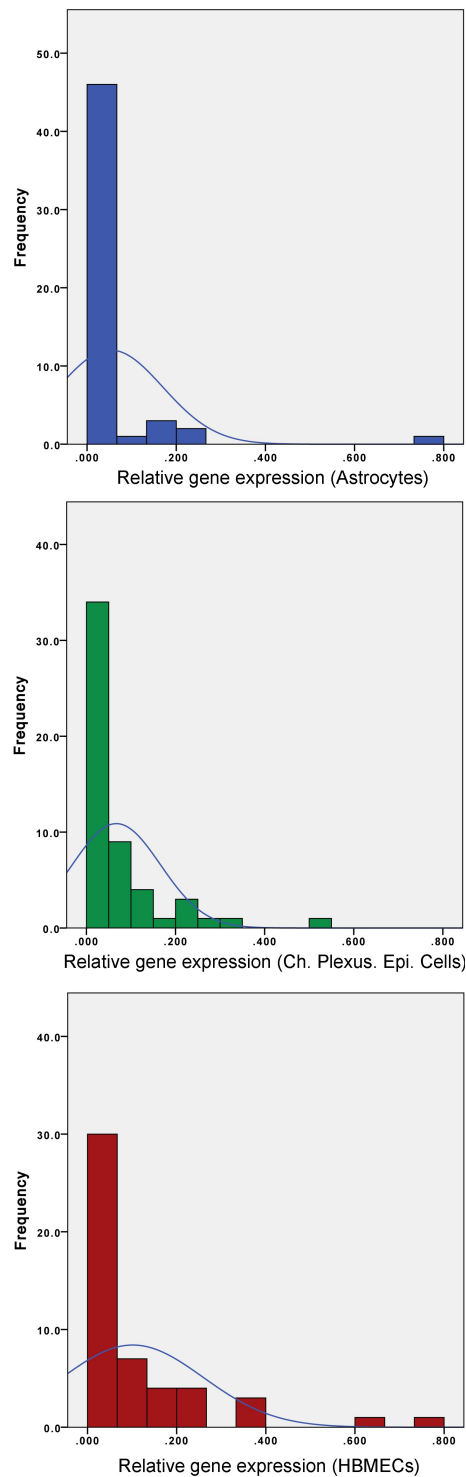


FIGURE 4.7: Distribution of the expression of membrane transporters in primary cells from the human brain. Only the transporters with relative gene expression higher than 0 were used for this analysis. The analysis was performed with SPSS version 21.0 using data from tables C.1 and C.2 from Appendix C.

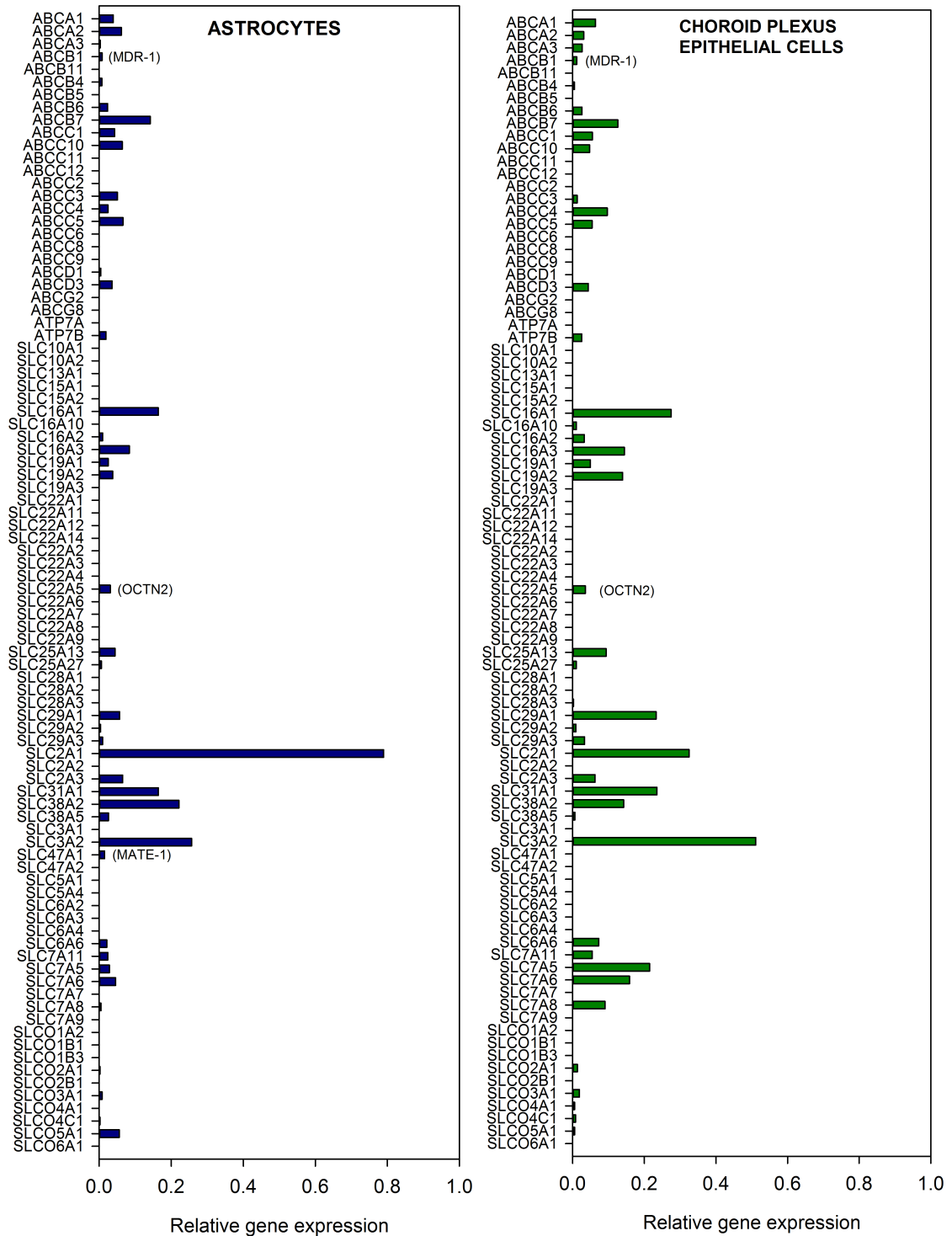


FIGURE 4.8: Gene expression analysis of membrane transporters using TaqMan® Low density Array microfluidic cards. Gene expression analysis of membrane transporters in Intestine and brain tissue using TaqMan® Low density Array microfluidic cards. The expression is normalised to the arithmetic mean of the expression of 6 housekeeping genes (GADPH, ACTB, HPRT1, MVP, TBP, UBC). The data represented in this figure is shown in tables C.1 and C.2 in Appendix C.

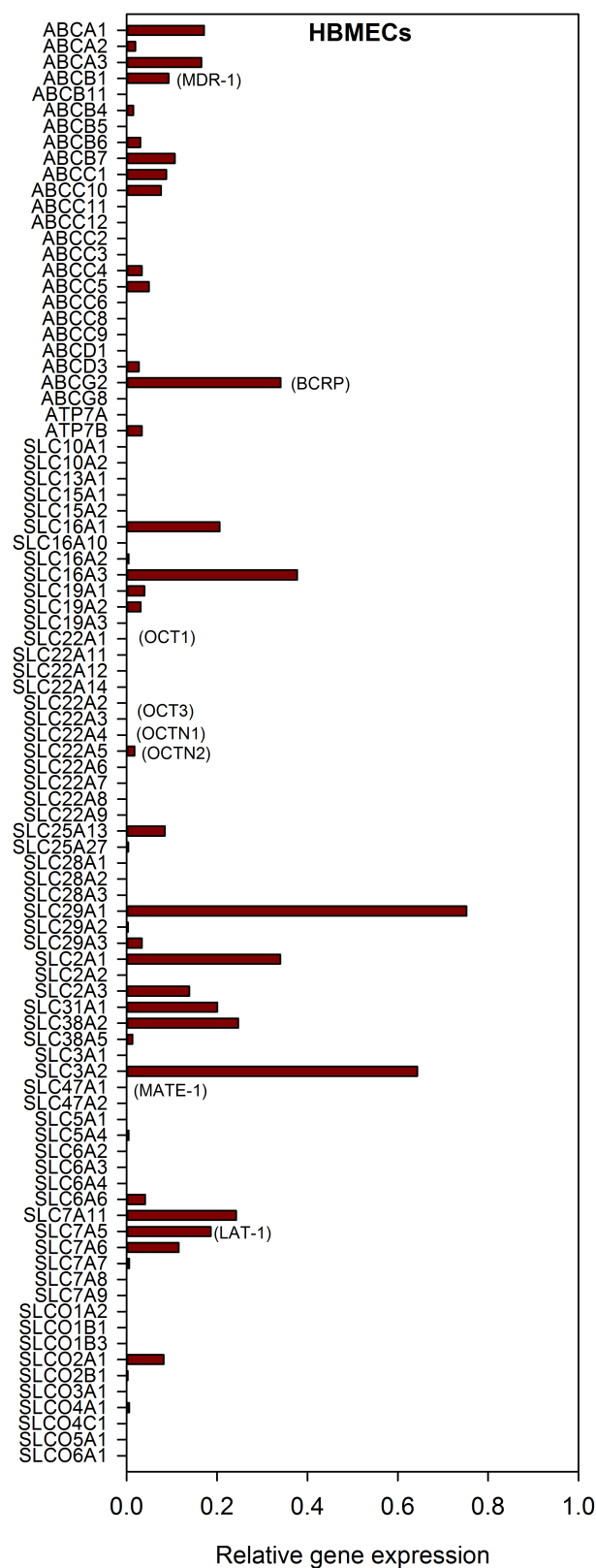


FIGURE 4.9: Gene expression analysis of membrane transporters in primary human brain microvascular endothelial cells (HBMECs) using TaqMan[®] low density array microfluidic cards. The expression is normalised to the arithmetic mean of the expression of 6 housekeeping genes (GADPH, ACTB, HPRT1, MVP, TBP, UBC).. The data represented in this figure is shown in tables C.1 and C.2 in Appendix C.

4.2.4 Donor to donor variation in the expression of drug transporters in primary human brain microvascular endothelial cells

The commercially obtained mRNA used in this study was isolated from primary human brain microvascular endothelial cells (HBMECs) which were isolated from three unrelated donors. The results of the gene expression analysis for the three different donors are shown for all the analyzed genes in tables C.3, C.4 and C.5 in Appendix C. At the low expression levels observed for organic cation transporters, there was inter-individual variability in the expression of OCT1 and OCT3 and less inter-individual variability in the expression of OCTN1, OCTN2 and MATE-1 (Figure 4.10).

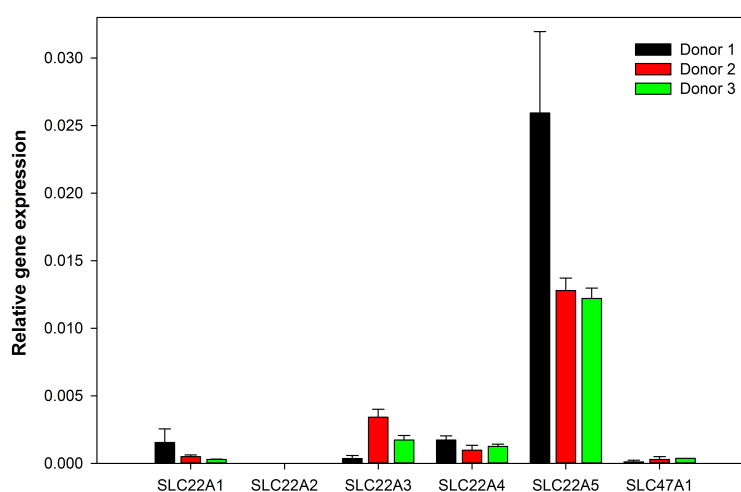


FIGURE 4.10: mRNA expression of the organic cation transporters of the *SLC22* family and MATE-1(*SLC47A1*) in human brain microvascular endothelial cells (HBMECs). Shown are the mean RNA expression levels in HBMECs obtained from three independent donors. At least two independent measurements were performed for each sample. The expression is normalised to the arithmetic mean of the expression of 6 housekeeping genes (GADPH, ACTB, HPRT1, MVP, TBP, UBC).

The large neutral amino-acid transporter (LAT-1, sub unit *SLC7A5*) is one of the most expressed membrane transporter genes in human brain microvascular endothelial cells (Figure 4.9). This amino-acid transporter has been recently shown to be able to transport psychotropic drugs (Geier *et al.* (2013b)). The efflux transporters MDR-1 (*ABCB1*) and BCRP (*ABCG2*) are also major drug transporters at the blood-brain barrier. The variability on the expression of LAT-1, MDR-1 and BCRP is shown on Figure 4.11 for the 3 samples analysed in this study. LAT-1 (*SLC7A5*) showed substantially higher expression in donor number 2 in comparison to donors number 1 and 3. The LAT-1 sub unit *SLC3A2*, which acts as a chaperone and does not have substrate binding properties, did not show inter-donor variability. The expression of MDR-1 and BCRP

also varied in the samples obtained from different donors. Donor number 2 showed very low expression of the efflux transporters MDR-1 (*ABCB1*) and BCRP (*ABCG2*).

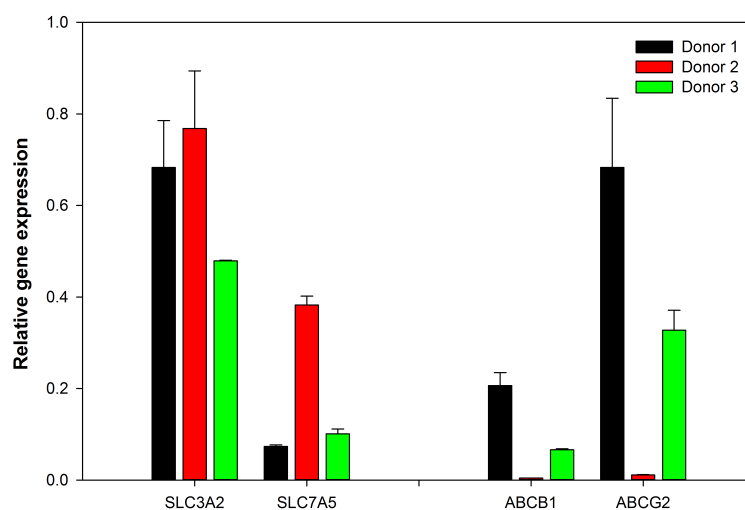


FIGURE 4.11: mRNA expression of the LAT-1 subunits(*SLC3A2* and *SLC7A5*), MDR-1(*ABCB1*) and BCRP (*ABCG2*) in human brain microvascular endothelial cells (HBMECs). Shown are the mean RNA expression levels in HBMECs obtained from 3 independent donors. At least two independent measurements were performed for each sample. The expression is normalised to the expression of 6 housekeeping genes (GADPH, ACTB, HPRT1, MVP, TBP, UBC).

The correlation between the transporter gene expression in HBMECs for the mRNA obtained from different donors was analysed for all the transporter genes studied. A good correlation for transporter gene expression between donor 1 and donor 3 was observed ($r=0.95$). The correlation between donors 1 and 2, and 2 and 3 was lower ($r=0.52$ and $r=0.57$, respectively). This shows the big similarities in transporter gene expression in the RNAs obtained from Donors 1 and 3, in contrast to donor 2 (Figure 4.12).

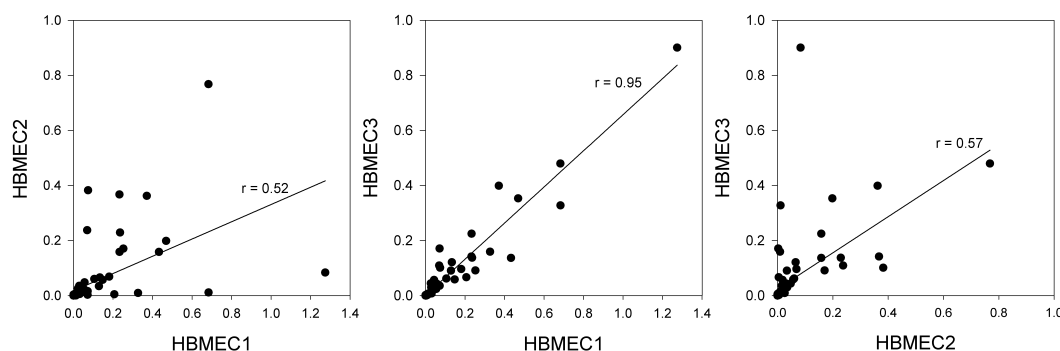


FIGURE 4.12: Comparison of the gene expression analysis in primary HBMECs (human brain microvascular endothelial cells) RNA obtained from different donors. The data represented in this figure is shown in tables C.1 and C.2 in Appendix C.

4.2.5 Gene expression analysis in the HEK293-pcDNA5, HEK-OCT1 and hCMEC/D3 cell lines

Here it was evaluated whether the over-expression of one membrane transporter affects the expression of other transporters in the *in vitro* model used in this study. The expression of drug transporters in the HEK293 cell line over expressing OCT1 was compared to the expression in the control cell line containing only the empty vector pcDNA5. This analysis showed that over-expressing the OCT1 gene does not alter the expression of other membrane transporter genes (Figure 4.13).

The expression of membrane transporters was also analysed in the human brain microvascular endothelial cell line hCMEC/D3. The expression of drug transporters in the hCMEC/D3 cell line is similar to primary HBMECs, with some notable exceptions (Figure 4.14). In hCMEC/D3 cells, the expression of LAT-1 (*SLC7A5*), and BCRP (*ABCG2*) were reduced by 3.8 and 4.6 -fold, respectively, in comparison to primary HBMECs. On the other hand, the expression of MDR1 (*ABCB1*), was 2-fold higher in the hCMEC/D3 cell line. The expression of the glucose transporter GLUT1 (*SLC2A1*) was also higher in hCMEC/D3 cells, as expected in an immortalised cell line.

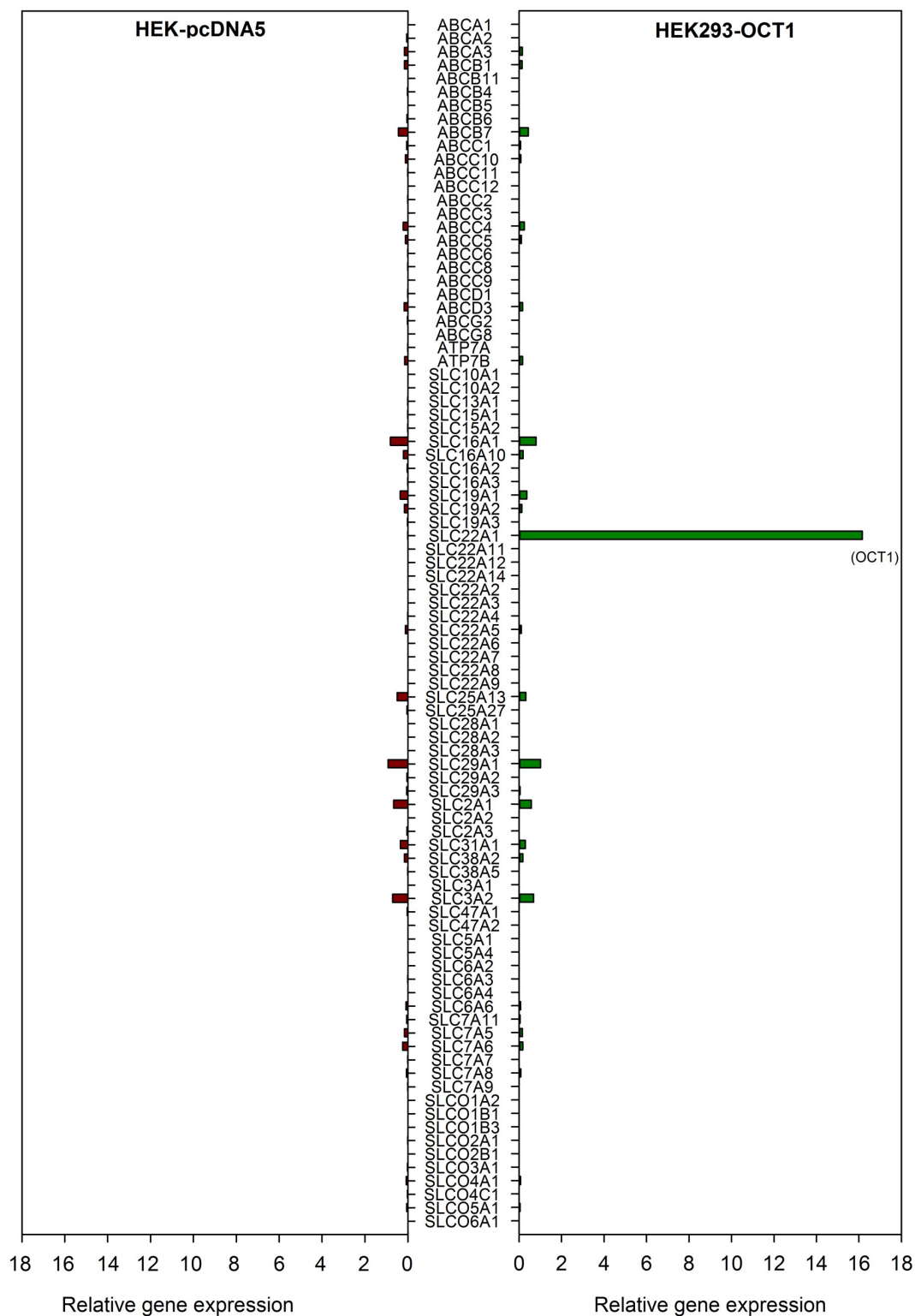


FIGURE 4.13: Gene expression analysis of membrane transporters in the HEK-pcDNA5 and HEK-OCT1 cell lines using TaqMan® Low density Array microfluidic cards. The data represented in this figure provides from table C.7 in Appendix C.

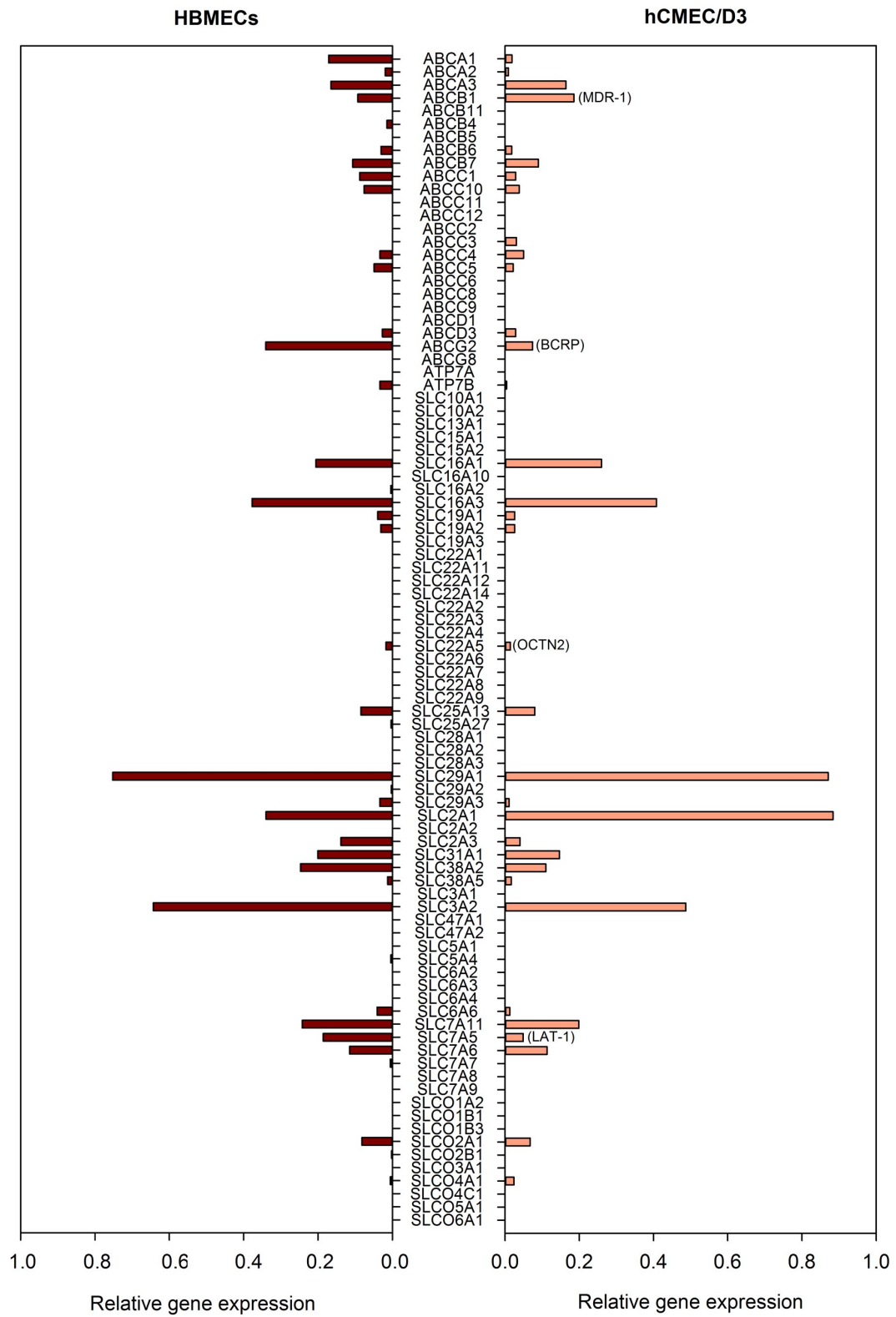


FIGURE 4.14: Gene expression analysis of membrane transporters in the hCMEC/D3 cell line using TaqMan[®] Low density Array microfluidic cards. The data represented in this figure is shown in tables C.1, C.2 and C.6 in Appendix C.

4.3 Immunohistochemistry of brain tissue

An experiment was performed to stain human membrane transporters in paraffin fixed brain tissue slides. The goal was to validate the expression and analyse the localisation of transporters, which were suggested to be expressed in brain microvascular endothelial cell lines at the mRNA level. BCRP (*ABCG2*) and MDR-1 (*ABCB1*) were highly expressed at the blood-brain barrier (Figure 4.9). The immunostaining of BCRP showed to be very specific for blood vessels in the brain (Figure 4.15), which is not surprising as this transporter has a very specific expression in brain microvascular endothelial cells (Figure 4.9 *vs* 4.8 and Geier *et al.* (2013a)). The staining of MDR-1 was not as strong as the staining of BCRP, but its expression on the microvascular blood vessels in the brain was still detected (Figure 4.16).

OCT1 (*SLC22A1*) and OCTN2 (*SLC22A2*) have been previously suggested to be expressed at the human blood-brain barrier by immunostaining (Lin *et al.* (2010) and Kido *et al.* (2001)). However, in the samples analysed in this study, OCTN2 was the only transporter which was detected at average levels at the mRNA level. The mRNA levels of OCT1 in human brain microvascular endothelial cells, were comparatively low (Figure 4.9). By means of immunostaining, it was not possible to detect either the presence of OCT1 nor of OCTN2 in the brain (Figure 4.17).

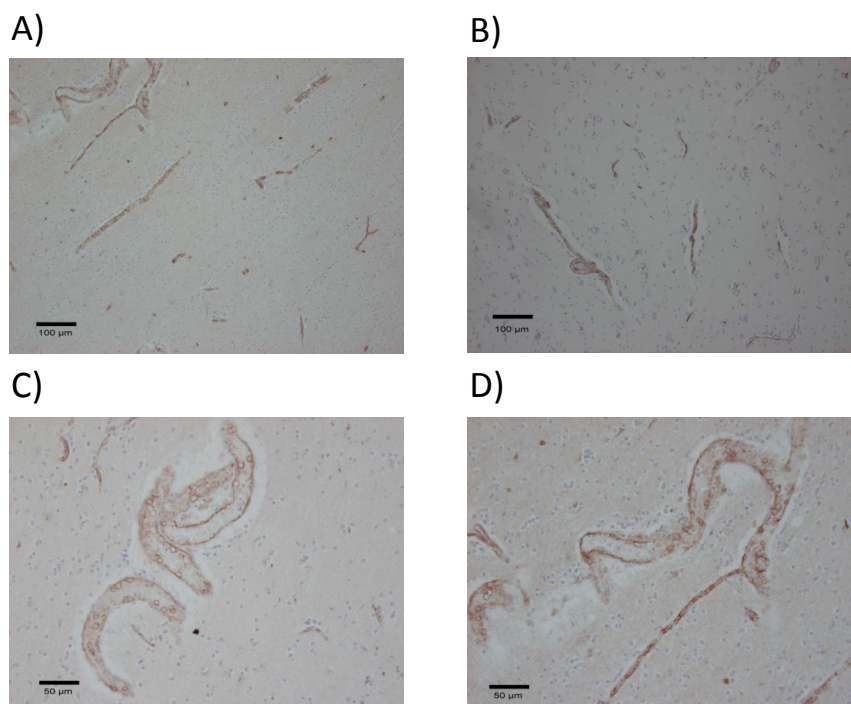


FIGURE 4.15: Immunostaining of BCRP in paraffin-fixed brain tissue slides. A) and B) show two regions of the same brain tissue slide at a magnification of 100 \times . C) and D) show two regions of the same brain tissue slide at a magnification of 200 \times .

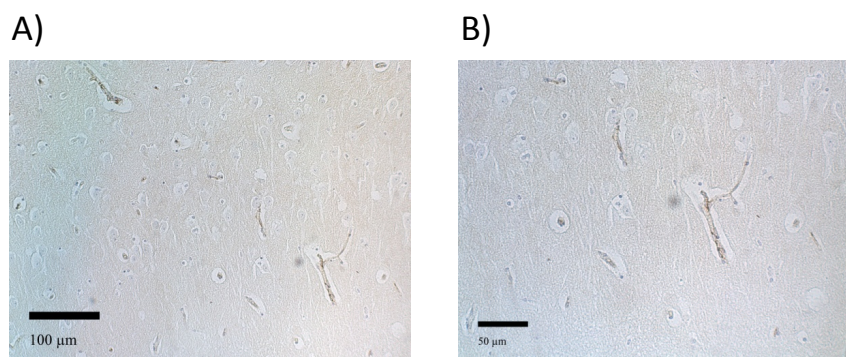


FIGURE 4.16: Immunostaining of MDR-1 in paraffin-fixed brain tissue slides. The magnification used was 100×(A) and 200×(B).

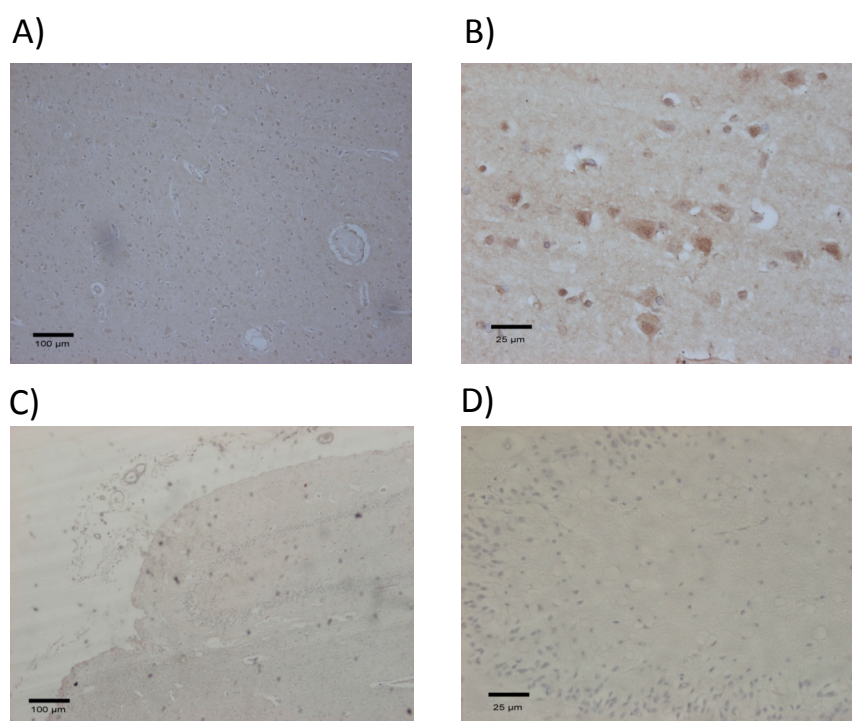


FIGURE 4.17: Lack of Immunostaining of OCTN2 (A and B) and OCT1 (C and D) in brain blood vessels. The magnification used was 100×for A) and C) and 400×for B) and D).

4.4 Validation of the HEK293 cell lines expressing OCT1, OCT2, OCT3, OCTN1 and OCTN2 with typical substrates

In this work, HEK293 cell lines over expressing the organic cation transporters of the SLC22 family, OCT1, OCT2, OCT3, OCTN1 and OCTN2, were used to study drug uptake. In order to validate these cell lines, they were incubated with the typical substrates for organic cation transporters, TEA⁺ (OCT1, OCT2, OCTN1 and OCTN2) and MPP⁺ (OCT1 and OCT3)(Koepsell (2013)). As expected, OCT1 and OCT3 transported MPP⁺, and OCT1, OCT2, OCTN1 and OCTN2 transported TEA⁺ (Figures 4.18 and 4.19). The K_M and V_{Max} were determined as explained on section 3.10.1. Differences in comparison to the literature were observed in the K_M values determined, which may be due to methodological differences in the determination of the kinetic parameters (Table 4.2).

The K_M for the uptake of MPP⁺ by OCT1 was 12-fold higher than reported in the literature. The differences could derive from the fact that Zhang *et al.* (1997) used oocytes as a transport system, and performed the uptake for 90 *min*, resulting in very different experimental conditions. The K_M for the OCT3 mediated MPP⁺ uptake was similar to what is reported in the literature.

The K_M for the uptake of TEA⁺ by OCT1 was on the same order of magnitude (2-fold higher) than what was previously reported in the literature and the K_M for the uptake of TEA⁺ by OCT2 was 4-fold higher than previously reported. In both cases, an indirect method for determining K_M was used, which may have resulted in these differences (Bednarczyk *et al.* (2003) and Suhre *et al.* (2005)). No kinetic parameters are known for the uptake of TEA⁺ by OCTN1 and OCTN2, but the uptake was comparable to what is described in the literature (Kawasaki *et al.* (2004) and Ohashi *et al.* (2002)).

TABLE 4.2: Kinetics of the uptake of TEA⁺ and MPP⁺ by organic cation transporters of the *SLC22* family

	V_{Max} $pmol\ min^{-1}\ mgprotein^{-1}$	K_M μM	K_M Literature μM
MPP ⁺			
OCT1	1591.0 ± 361.9	183.7 ± 42.7	15 (Zhang <i>et al.</i> (1997))
OCT3	1236.0 ± 118.6	29.3 ± 7.5	47 (Wu <i>et al.</i> (2000))
TEA ⁺			
OCT1	2521.0 ± 535.9	341.7 ± 46.2	168 (Bednarczyk <i>et al.</i> (2003))
OCT2	7685.7 ± 382.3	183.0 ± 5.7	46 (Suhre <i>et al.</i> (2005))
OCTN1	435.0 ± 66.0	570.0 ± 115.8	No Indication of K_M
OCTN2	533.0 ± 154.7	535.3 ± 140.5	No Indication of K_M

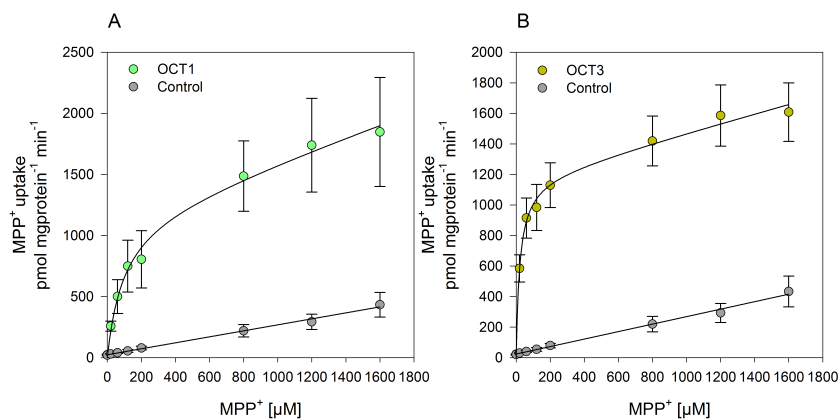


FIGURE 4.18: Validation of the HEK-OCT1(A) and HEK-OCT3 (B) cell lines with the substrate MPP⁺. The concentration dependent uptake was measured in comparison to the control cell line expressing the empty vector.

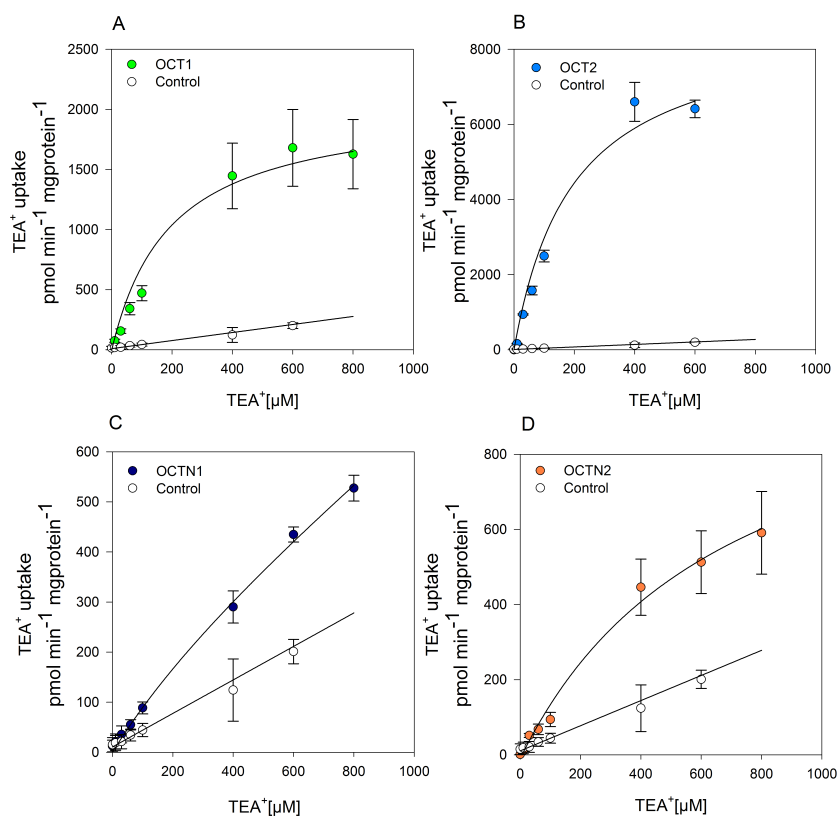


FIGURE 4.19: Validation of the HEK-OCT1, HEK-OCT2, HEK-OCTN1 and HEK-OCTN2 cell lines with the substrate TEA⁺. The concentration dependent uptake was measured for 2 min in cell lines over expressing OCT1(A) and OCT2(B), OCTN1(C) and OCTN2(D) in comparison to the control cell line expressing the empty vector.

4.5 Transport of the poorly membrane permeable antipsychotics amisulpride, sulpiride, sultopride and tiapride by organic cation transporters

As shown on section 4.1.2, the drugs amisulpride, sulpiride, sultopride and tiapride are very hydrophilic and have low membrane permeability. Furthermore, they are weak bases and are more than 96% positively charged at the physiological pH of 7.4 (Table 4.1), making them good candidates to be substrates of organic cation transporters. In this section, the ability of organic cation transporters to mediate the cellular uptake of amisulpride, sulpiride, sultopride and tiapride, was studied.

4.5.1 Uptake of amisulpride by the organic cation transporters of the *SLC22* family

Amisulpride is a weak base, with a pK_a of 9.0 (Figure 4.20). The ability of the organic cation transporters of the *SLC22* family to mediate the cellular uptake of amisulpride was studied. Amisulpride was incubated at concentration of $5 \mu\text{M}$ with HEK293 cells overexpressing the transporters OCT1(*SLC22A1*), OCT2(*SLC22A2*), OCT3(*SLC22A3*), OCTN1(*SLC22A4*) and OCTN2(*SLC22A5*) (Figure 4.21). The experiment was also performed in the presence of known OCT inhibitors. Tetrabutylammonium (TBA^+) was used to inhibit the uptake by OCT1 and OCT2 (Nies *et al.* (2011)), irinotecan was used to inhibit the uptake by OCT3 (Shnitsar *et al.* (2009)) and L-carnitine was used to inhibit the uptake by OCTN1 and OCTN2 (Stocker *et al.* (2013b)).

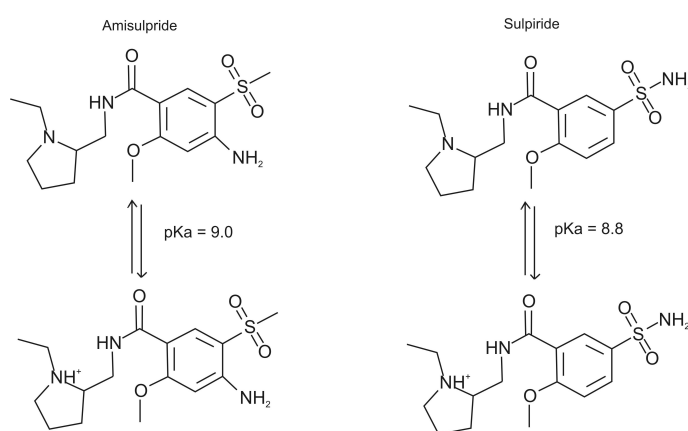


FIGURE 4.20: Chemical structures of amisulpride and sulpiride. The pK_a values were obtained using ADMET Predictor 5.5 (Table 4.1)

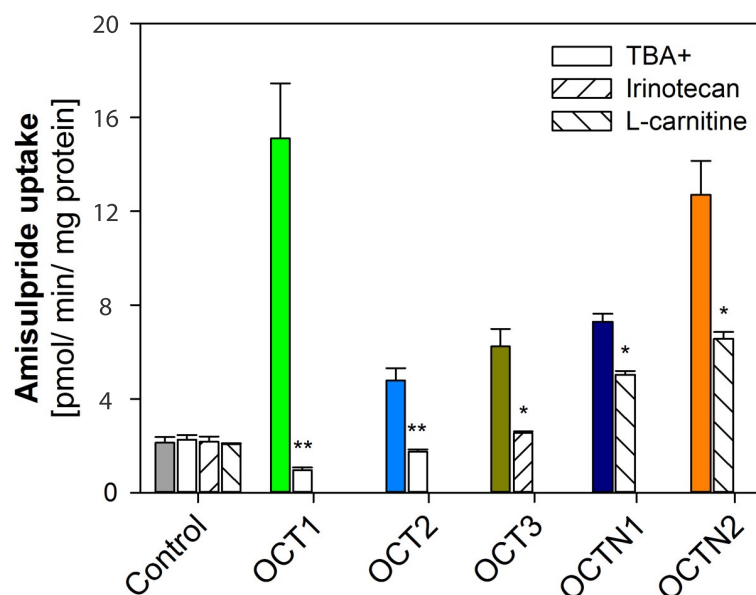


FIGURE 4.21: Cellular uptake of amisulpride at concentration of $5 \mu M$ in cells overexpressing OCT1, OCT2, OCT3, OCTN1, OCTN2, and the control cell line (transfected with the empty expression vector). The uptake was inhibited either by 1 mM TBA⁺ (OCT1 and OCT2), $250 \mu M$ irinotecan (OCT3), or $500 \mu M$ L-carnitine (OCTN1 and OCTN2). Shown are the means and standard error of the means of three independent experiments (* $p < 0,05$ and ** $p < 0,01$, Student's t-test).

Amisulpride was transported by all the organic cation transporters from the *SLC22* family studied (Figure 4.21). Cells over-expressing OCT1 and OCTN2 have shown the strongest transport (7.1-fold and 5.9-fold increase, respectively, compared to cells transfected with the empty vector, pcDNA5). The increase was 3.2-fold, 2.9-fold and 2.2-fold, in cells expressing OCTN1, OCT3 and OCT2, respectively. The uptake of amisulpride by OCT1 and OCT2 was completely inhibited by TBA⁺ ($p < 0,01$, Student's t-test) and the transport of amisulpride by OCT3 was completely inhibited by irinotecan ($p < 0.05$, Student's t-test). The uptake of amisulpride by OCTN1 and OCTN2 was significantly inhibited by L-carnitine ($p < 0.05$, Student's t-test)(Figure 4.21).

The concentration dependence of the amisulpride uptake by OCT1, OCT2, OCT3, OCTN1 and OCTN2, was investigated using concentrations ranging from 5 to $200 \mu M$. All cell lines expressing a drug transporter showed higher uptake of amisulpride than the control cell lines(Figure 4.22 A and B). In order to measure only the transporter-mediated amisulpride uptake, the uptake in the control cells was subtracted from the uptake in the cells over expressing a membrane transporter. The transporter-mediated uptake of amisulpride followed Michaelis-Menten kinetics (Figure 4.22 C and D). All the membrane transporters studied, showed moderate affinities for the uptake of amisulpride ($K_M > 150 \mu M$), with the exception of OCT1, which showed the highest affinity for amisulpride ($K_M = 31.3 \pm 5.4 \mu M$)(Table 4.3). With an intrinsic clearance of 1.9

$mL\ min^{-1}\ mg\ protein^{-1}$, OCT1 was the best transporter for amisulpride, within the cation transporters of the *SLC22* family (Table 4.3).

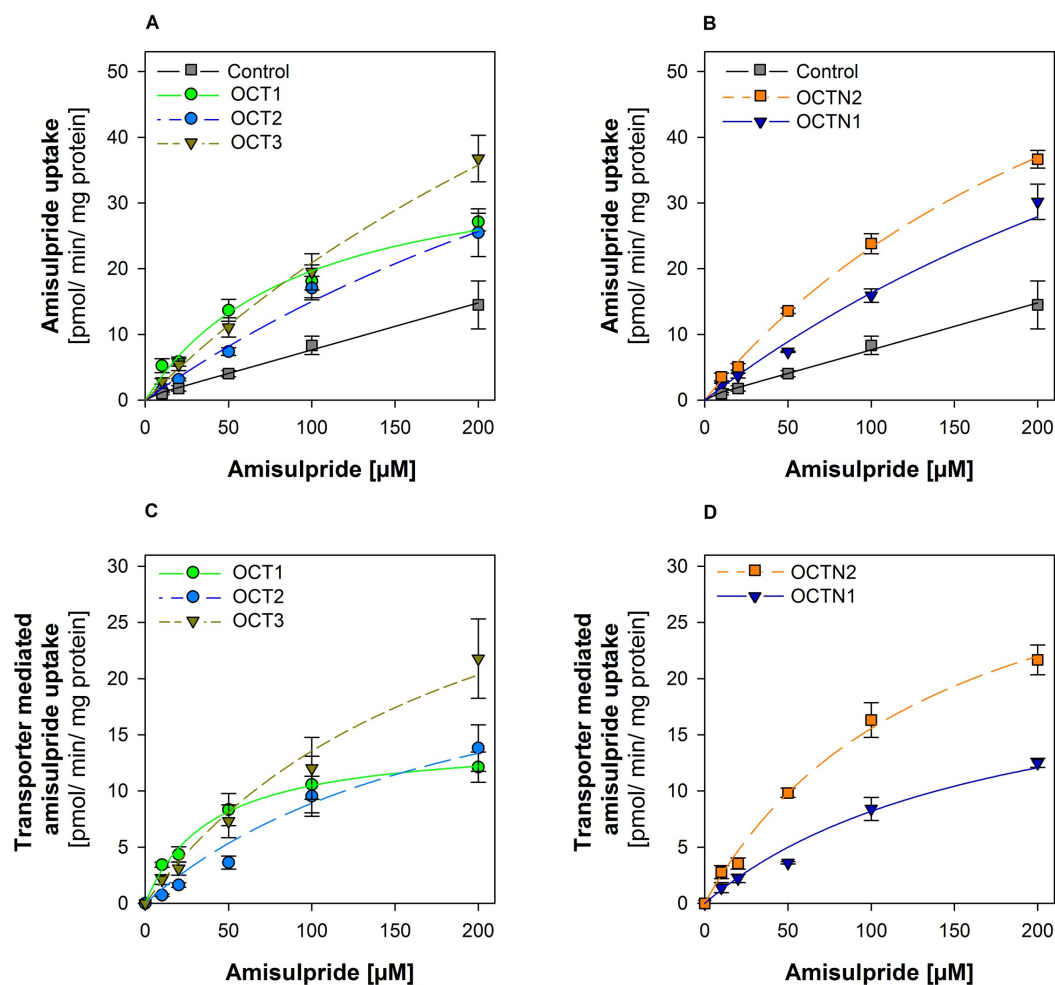


FIGURE 4.22: Concentration dependence of amisulpride uptake by OCT1, OCT2, and OCT3 (A) and by OCTN1 and OCTN2 (B). Transporter mediated uptake of amisulpride by OCT1, OCT2, OCT3 (C) and by OCTN1 and OCTN2 (D). The transporter mediated uptake was calculated by subtracting the uptake in the cell lines expressing the empty vector (control), from the transporter over-expressing cell lines) Show and the means and standard error of the means of three independent experiments.

4.5.2 Uptake of sulpiride by the organic cation transporters of the *SLC22* family

Sulpiride is a weak base, with a pK_a of 8.8 (Figure 4.20). The uptake of sulpiride by the organic cation transporters of the *SLC22* family was investigated. Sulpiride uptake was increased 2.5-fold in cells overexpressing OCT1 and 1.8-fold in cells over expressing OCT2, compared to the cells transfected with the empty vector. Co-incubation with the OCT1 and OCT2 inhibitor TBA⁺ completely inhibited the uptake of sulpiride by these transporters ($p < 0,01$, Student's t-test) (Figure 4.23). In contrary to amisulpride, no uptake was observed in cells over expressing OCT3, OCTN1 and OCTN2.

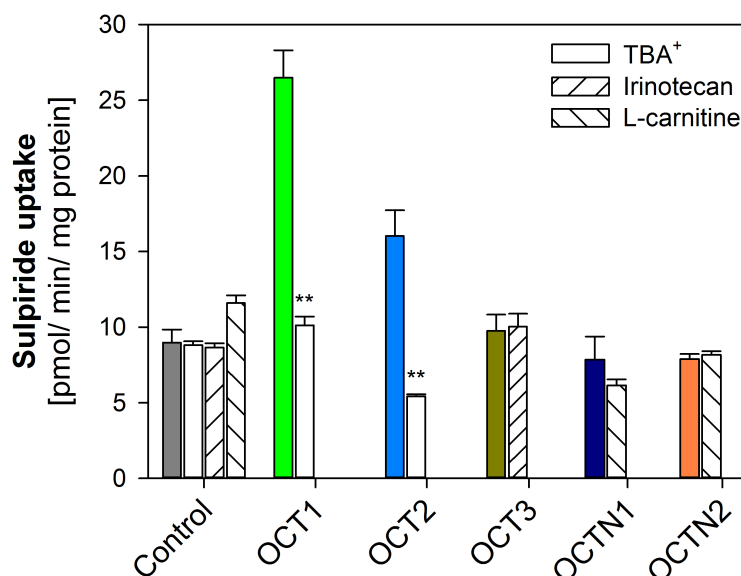


FIGURE 4.23: Cellular uptake of sulpiride at a concentration of $5 \mu M$ in cells overexpressing OCT1, OCT2, OCT3, OCTN1, OCTN2, and in the control cell line (transfected with the empty expression vector). The uptake was inhibited either by $1 mM$ TBA⁺ (OCT1 and OCT2), $250 \mu M$ irinotecan (OCT3), or $500 \mu M$ L-carnitine (OCTN1 and OCTN2). Shown are the means and standard error of the means of three independent experiments (** $p < 0,01$, Student's t-test).

A concentration dependent uptake of sulpiride was also observed in the OCT1 and OCT2 over-expressing cell lines which followed Michaelis-Menten kinetics (Figure 4.24 A and B). Both OCT1 and OCT2 showed low affinity for the transport of sulpiride. Similar to amisulpride, OCT1 was also the best transporter for sulpiride, among the transporters of the *SLC22* family, with an intrinsic clearance of $4,3 mL min^{-1} mgprotein^{-1}$ (Table 4.3).

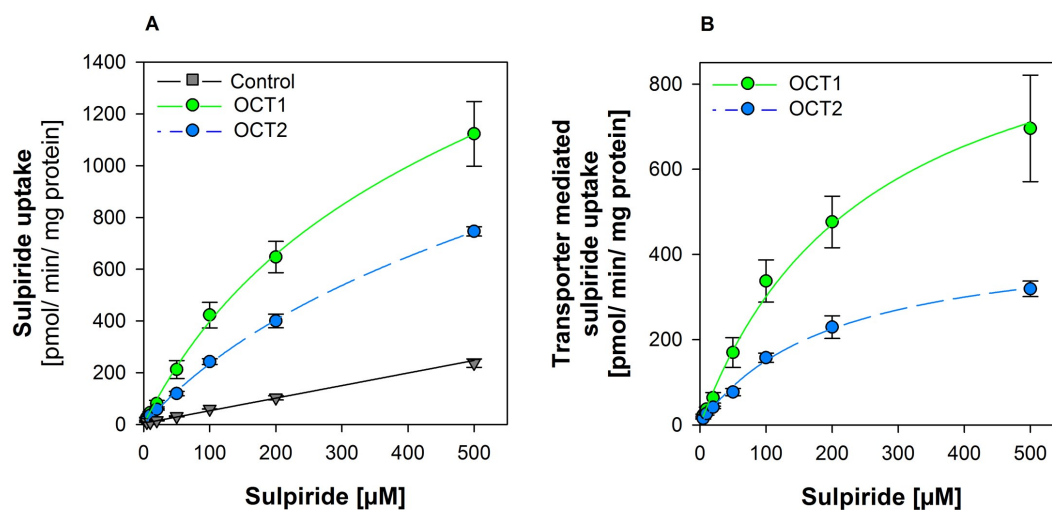


FIGURE 4.24: Concentration dependence of sulpiride uptake by OCT1, OCT2, and OCT3 (A) and by OCTN1 and OCTN2 (B). Transporter mediated uptake of sulpiride by OCT1, OCT2, OCT3 (C), OCTN1 and OCTN2 (D). The transporter mediated uptake was calculated by subtracting the uptake in the cell lines expressing the empty vector (Control), from the transporter over-expressing cell lines). Shown are the means and standard error of the means of three independent experiments.

TABLE 4.3: Kinetics of amisulpride and sulpiride transport by organic cation transporters of the *SLC22* family

	K_M μM	V_{Max} $pmol\ min^{-1}\ mgprotein^{-1}$	$CL_{int} (V_{Max}/K_M)$ $mL\ min^{-1}\ mgprotein^{-1}$
Amisulpride			
OCT1	31.3 ± 5.4	59.6 ± 6.4	1.9
OCT2	167.9 ± 32.1	99.2 ± 18.8	0.6
OCT3	191.9 ± 6.1	162.4 ± 28.6	0.8
OCTN1	179.9 ± 20.1	78.8 ± 13.6	0.4
OCTN2	185.3 ± 68.0	168.8 ± 34.8	0.9
Sulpiride			
OCT1	259.7 ± 5.4	1081.4 ± 188	4.2
OCT2	187.2 ± 21.6	439 ± 4.7	2.3

4.5.3 Uptake of sultopride and tiapride by the organic cation transporters of the *SLC22* family

Sultopride and tiapride are two psychotropic drugs which are structurally similar to amisulpride and sulpiride and also showed low membrane permeability on the PAMPA

assays ($P_e < 2,5 \times 10^{-6}$, Figure 4.1). Although they are not as broadly used as amisulpride in the clinics, the ability of the organic cation transporters of *SLC22* family to transport sultopride and tiapride was also studied. In contrast to amisulpride and sulpiride, the uptake of sultopride and tiapride was not increased in any of the cell lines over-expressing the organic cation transporters of the SLC22 family. In addition, the uptake did not decrease in the presence of specific OCT inhibitors. Therefore, it is concluded that tiapride and sultopride are not substrates of the organic cation transporters of the *SLC22* family.

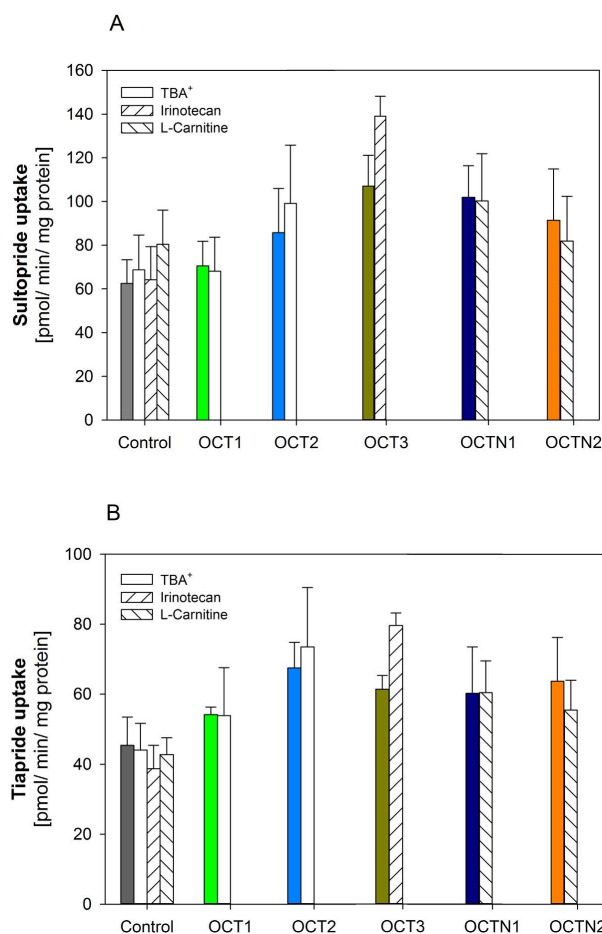


FIGURE 4.25: Lack of transport of sultopride and tiapride by the organic cation transporters of the *SLC22* family. The uptake of $5 \mu\text{M}$ of sultopride (A) and tiapride (B) was measured in HEK293 cell lines over-expressing the transporters OCT1, OCT2, OCT3, OCTN1, OCNT2 and the empty vector (control). The uptake was inhibited by either 1 mM TBA^+ (OCT1 and OCT2), $250 \mu\text{M}$ or $500 \mu\text{M}$ of L-carnitine. Shown are the means and standard error of the means of 3 independent experiments.

OCT1 can mediate the uptake of amisulpride and sulpiride and was the most efficient transporter for these two drugs (Figures 4.21 and 4.22). It is therefore surprising that OCT1 cannot mediate the uptake of sultopride or tiapride. In order to assess the ability

of these drugs to bind to the OCT1 transporter, an experiment was performed where amisulpride, sulpiride, sultopride and tiapride were used to inhibit MPP⁺, a typical OCT1 substrate. The results are presented on Figure 4.26 and Table 4.4.

As expected, amisulpride, the best OCT1 substrate within all the drugs tested (Table 4.3), was also the drug with the highest affinity to OCT1 ($IC_{50} = 104 \mu M$). Sultopride, tiapride and sulpiride had low affinity for the OCT1 transporter ($IC_{50} = 697 \mu M$, $IC_{50} > 1000 \mu M$ and $IC_{50} > 1000 \mu M$, respectively)(Table 4.4).

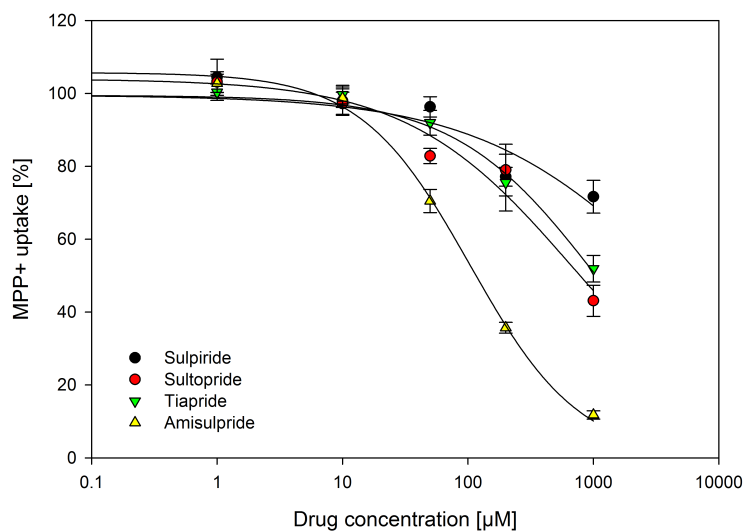


FIGURE 4.26: Inhibition of the OCT1 mediated MPP⁺ uptake by amisulpride, sulpiride, sultopride and tiapride. The uptake was measured for 2 min with $5 nM$ of MPP⁺ co incubated with drug concentrations ranging from 1 to $1000 \mu M$. Shown are the means and standard error of the means of 3 independent experiments.

TABLE 4.4: Inhibition of the OCT1-mediated MPP⁺ uptake by amisulpride, sulpiride, sultopride and tiapride: Half-maximal inhibition constants, IC_{50}

Drug	IC_{50} (μM)
Amisulpride	104
Sultopride	697
Tiapride	>1000
Sulpiride	>1000

4.5.4 Effect of polymorphisms on the OCT1 (*SLC22A1*) gene on the uptake of amisulpride by OCT1

The OCT1 gene (*SLC22A1*) is highly genetically polymorphic. Because OCT1 is the transporter with the highest intrinsic clearance for amisulpride and sulpiride, it is important to study how genetic variants in OCT1 may affect the uptake of amisulpride and sulpiride (Table 4.3). The uptake of amisulpride and sulpiride was measured in cells over-expressing the *wild-type* OCT1* allele and the OCT*2 to *6 variant alleles, which are the most common OCT1 variants in the Caucasian population. The uptake of both amisulpride and sulpiride was reduced in cells over-expressing the genetic variants, in comparison to the wild-type OCT1*1 variant (post hoc Tukey-HSD test $p < 0,001$; Figure 4.27). These results indicate that individuals which carry the loss of function OCT1 variants may have a reduced uptake of amisulpride and sulpiride in organs where OCT1 is expressed and plays a role in drug transport across the cell membrane.

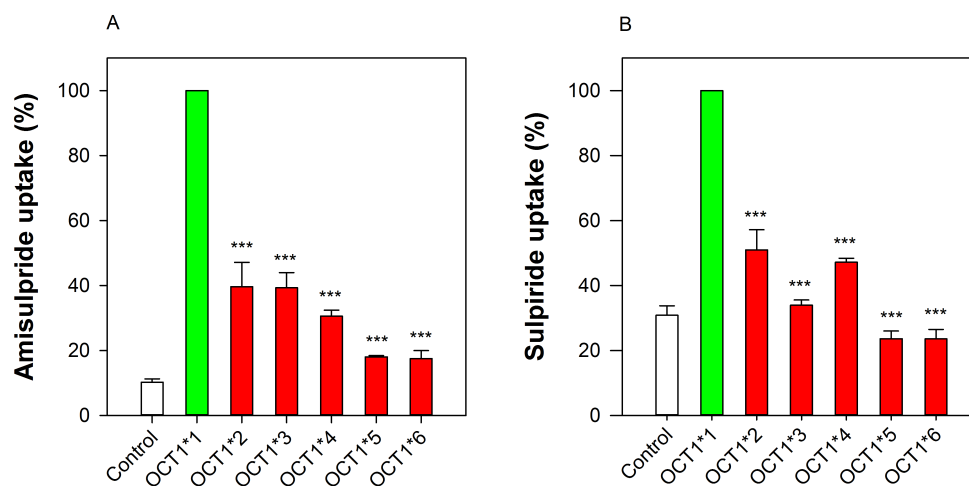


FIGURE 4.27: Uptake of $5\mu\text{M}$ of amisulpride (A) and sulpiride (B) by HEK293 cells expressing the wild-type OCT1*1 variant (*green bars*), the loss of function variants OCT1*2 to *6 (*red bars*), and the empty vector (*white bar*). Show are the means and standard error of the means of three independent experiments. * * * $p < 0,001$ for comparing the OCT1*2 to *6 alleles with the OCT1*1 allele (post-hoc Tukey-HSD after significant ANOVA test for differences among the groups).

4.5.5 Uptake of amisulpride by the MATE1 and MATE2-K transporters

A special focus was put on amisulpride, the most important neuroleptic of the benzamide class (Pani & Gessa (2002)) which has a high renal clearance (330 mL/min) (Rosenzweig *et al.* (2002)). The MATE1 and MATE2-K transporters (*SLC47A1* and *SLC47A2*, respectively) are expressed on the luminal membrane of the renal epithelium (Nies *et al.*

(2011)), and may be relevant for the elimination of amisulpride into the urine. Therefore, the ability of MATE1 and MATE2-K to transport amisulpride was evaluated. Both MATE1 (*SLC47A1*) and MATE2-K (*SLC47A2*) showed concentration dependent uptake of amisulpride (Figure 4.28). The transport-dependent uptake of amisulpride by MATE1 and MATE2-K was also calculated (Figure 4.28 B and C), and the Michaelis-Menten constants (K_M and V_{Max}) as well as the transporter intrinsic clearance (CL_{int} (V_{Max}/K_M)) were determined (Table 4.5). MATE1 showed the highest affinity for amisulpride ($K_M = 12.0$) which was higher than the affinity of MATE2-K ($K_M = 36.7$).

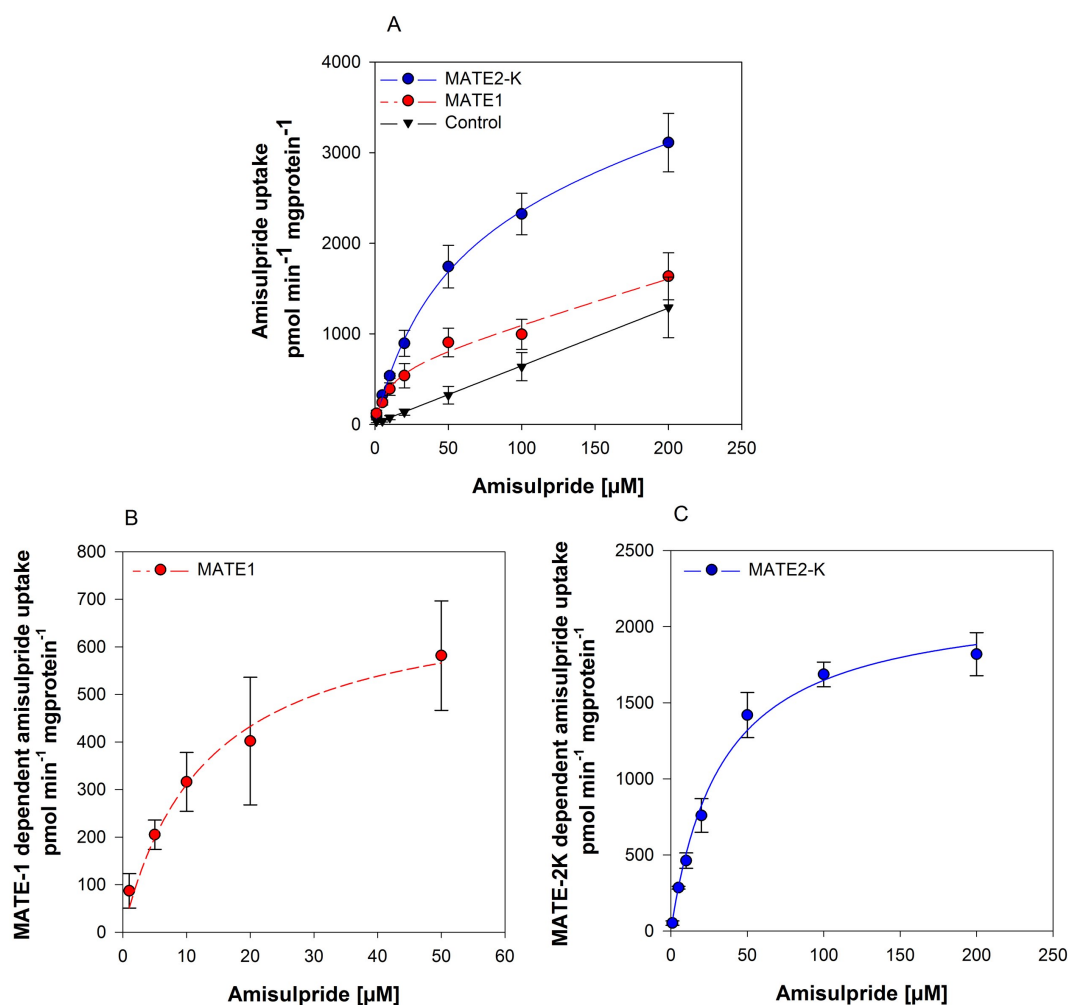


FIGURE 4.28: Uptake of amisulpride in cell lines expressing MATE-1 and MATE2-K in comparison to the control cell line expressing the empty vector (A). The transporter dependent uptake of amisulpride by MATE-1 (B) and MATE2-K (C) was calculated by subtracting the uptake in the cells expressing the empty vector from the uptake in the cell lines expressing the transporter. Shown are the means and standard error of the means of three independent experiments.

TABLE 4.5: Kinetics of amisulpride and sulpiride transport by the MATE-1 and MATE2-K transporters

	K_M μM	V_{Max} $pmol\ min^{-1}\ mgprotein^{-1}$	$CL_{int}\ (V_{Max}/K_M)$ $mL\ min^{-1}\ mgprotein^{-1}$
MATE-1	12.0 ± 1.5	704.3 ± 178.9	58.6
MATE2-K	36.7 ± 6.6	2247.3 ± 130.3	62.4

4.6 Uptake of amisulpride and sulpiride in the human brain endothelial cell line hCMEC/D3

The uptake of amisulpride and sulpiride was studied in human brain microvascular endothelial cells. The hCMEC/D3 cell line was used as a model, as it is a well characterised human brain microvascular endothelial cell line (Weksler *et al.* (2005)). The uptake of amisulpride and sulpiride was studied at the concentrations of 1, 5 and 25 μM at 37°C and 4°C. Both concentration dependent uptake and temperature dependent uptake was observed for amisulpride and sulpiride. This indicates the presence of a carrier-mediated transport mechanism in the hCMEC/D3 cell line, which is able to transport these two drugs.

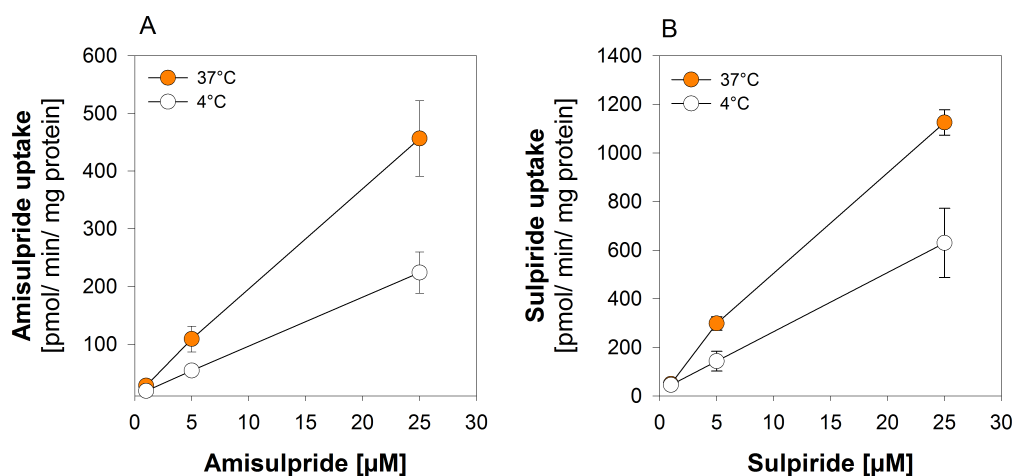


FIGURE 4.29: Concentration and temperature dependant uptake of amisulpride and sulpiride in the human brain microvascular endothelial cell line hCMEC/D3. The figures show the uptake of 1, 5 and 25 μM of amisulpride (A) and sulpiride (B) at 37°C (closed circles) and 4°C (open circles) for 2 min.

The uptake of amisulpride and sulpiride in the hCMEC/D3 cell line was inhibitable by MPP^+ (Figure 4.30), a model organic cation and known inhibitor of OCT1, OCT2 and OCT3 (Nies *et al.* (2011)). MPP^+ inhibited 45% of the temperature dependent fraction of the amisulpride uptake (difference between uptake at 37°C and uptake at 4°C), and 71% of the temperature dependent fraction of the sulpiride uptake.

In addition, 1 mM of non-radiolabeled MPP^+ also inhibited the uptake of radiolabeled 3H - MPP^+ itself, showing that a mechanism for the uptake of organic cation transporters is present in this cell line (Figure 4.31).

Verapamil and L-carnitine inhibited the uptake of sulpiride (Figure 4.30 A), but not amisulpride (Figure 4.30 B). Verapamil and L-carnitine are inhibitors of OCTN2 (Stocker *et al.* (2013b)), which is expressed in this cell line (Figure 4.14). Therefore, the opposite result was expected, because amisulpride, and not sulpiride, is an OCTN2 substrate (Figure 4.21). This could indicate the presence of an unknown transport mechanism and will be discussed in section 5.4.

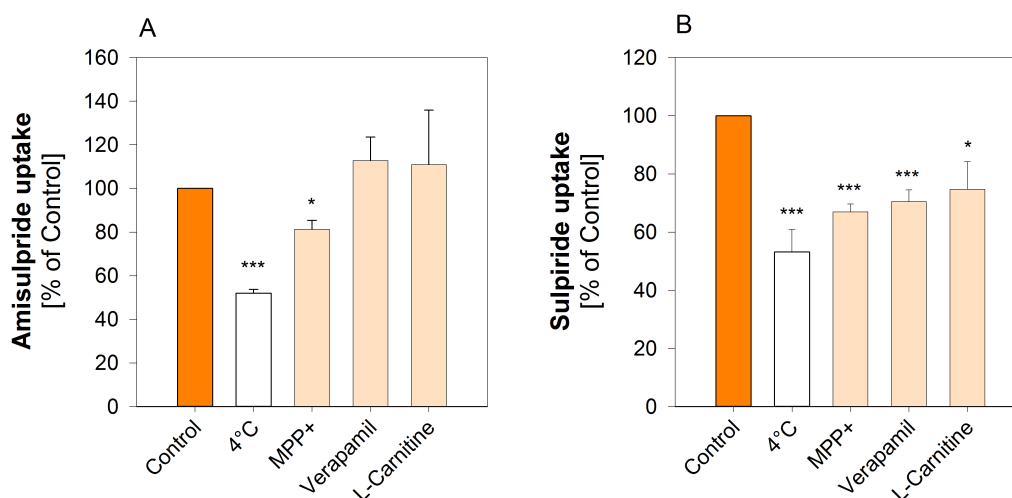


FIGURE 4.30: Inhibition of the uptake of amisulpride and sulpiride in the human brain microvascular endothelial cell line hCMEC/D3. The uptake of 5 μM of amisulpride (A) and sulpiride (B) was inhibited with medium at 4°C, with 1mM of MPP^+ , verapamil or L-carnitine. Shown are the means and standard error of the means of two or more independent experiments. * $p < 0,05$ and ** $p < 0,001$ for comparison with the uptake without inhibitors at 37°C (post hoc Turkey-HSD after significant ANOVA test for differences among the groups).

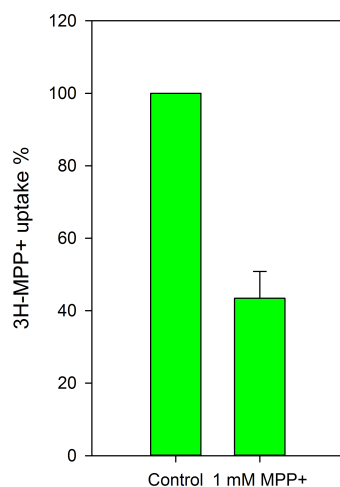


FIGURE 4.31: Inhibition of the uptake of $^3\text{H-MPP}^+$ on the hCMEC/D3 cell line by 1 mM of non-labeled MPP $^+$. The uptake of 10 nM of $^3\text{H-MPP}^+$ was performed for 2 min in the absence (Control) and in the presence of 1 mM of non-labeled MPP $^+$. Shown are the means and standard error of the means of two or more independent experiments (** $p < 0,01$, Student's t-test).

4.7 Interaction between psychotropic drugs with high membrane permeability and OCT1

It has been shown that several psychotropic drugs, including antidepressants, can strongly inhibit the organic cation transporter OCT1 (Zhang *et al.* (1998), Ahlin *et al.* (2008), Nies *et al.* (2011) and Haenisch *et al.* (2012)). These include clozapine, citalopram and amitriptyline. It was then speculated that these drugs may also be substrates for OCT1 and may depend on OCT1 to enter the liver and be further metabolized. In this work, clozapine, citalopram and amitriptyline were studied as possible OCT1 substrates. Lamotrigine and amantadine, two psychotropic drugs which are proposed in the literature as OCT1 substrates, were additionally studied (Dickens *et al.* (2012), Lozano *et al.* (2013) and Becker *et al.* (2011)).

4.7.1 Lack of uptake of clozapine, lamotrigine, amantadine and citalopram by OCT1

Clozapine, citalopram, lamotrigine and amantadine are psychotropic drugs prescribed for several different indications and are known to interact with OCT1 (Table 4.6).

Clozapine and citalopram are known to inhibit OCT1 (Nies *et al.* (2011) and Haenisch *et al.* (2012)) but it is not known whether they also are OCT1 substrates.

Lamotrigine has been suggested to be OCT1 substrate (Dickens *et al.* (2012)), although the evidence is very weak, as the experiments were performed in KCL22 cells, a leukaemia cell line. This approach to measure OCT1-mediated uptake has been heavily criticised in recent literature (Burger *et al.* (2013)).

Amantadine has also been proposed in the literature to be a substrate of the human OCT1, although without evidence (Lozano *et al.* (2013)) and Becker *et al.* (2011)). The only evidence for the uptake of amantadine by the organic cation transporter 1 is a publication which shows that amantadine is a substrate of the rat Oct1 (Goralski *et al.* (2002)).

In this work, the ability of OCT1 to mediate the uptake of clozapine, lamotrigine, amantadine and citalopram was investigated in a well validated HEK293 cell line over-expressing the human OCT1 (Saadatmand *et al.* (2012)). No increase in the uptake of these drugs was observed in HEK293 cell over-expressing the human OCT1 in relation to the control cells (Figure 4.32).

TABLE 4.6: Previous evidence for the interaction of the psychotropic drugs analyzed in this study, with OCT1

Drug	Indication	Literature	$IC_{50}\mu M$
Citalopram	Depression	OCT1 inhibitor	3,1; 19 (Nies <i>et al.</i> (2011))
Clozapine	Schizophrenia	OCT1 inhibitor	6.65 (Haenisch <i>et al.</i> (2012))
Lamotrigine	Epilepsy	OCT1 substrate (Dickens <i>et al.</i> (2012))	-
Amantadine	Parkinson	OCT1 substrate (Lozano <i>et al.</i> (2013))	18 (Nies <i>et al.</i> (2011))

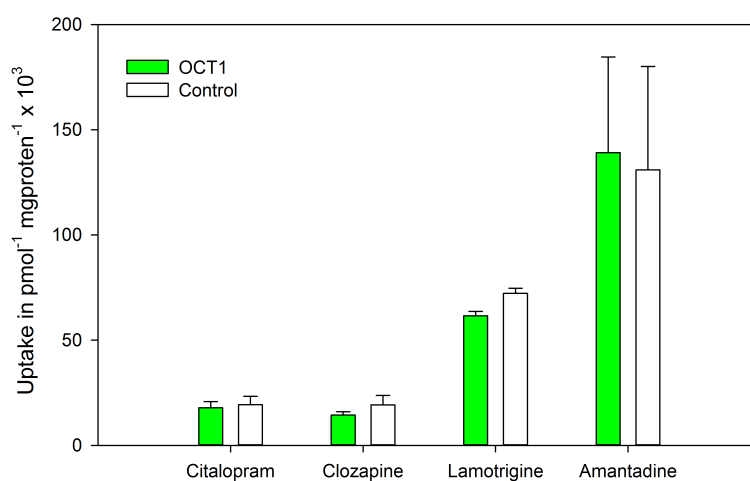


FIGURE 4.32: Lack of uptake of clozapine, citalopram, lamotrigine and amantadine by the human OCT1. The uptake was measured for 2 min. Drug concentrations used were 13nM for clozapine, 12 nM for citalopram, 200nM for lamotrigine and 2.2μM for amantadine. Show are the means and standard error of the means of 2-4 independent experiments.

4.7.2 Characterization of the interactions between amitriptyline and OCT1

Amitriptyline is a tricyclic antidepressant, which is known to inhibit OCT1 (Ahlin *et al.* (2008)) and has very high membrane permeability (Figure 4.1 and Table 4.1). Amitriptyline is an organic cation, protonated at pH 7.4, and is eliminated by metabolism in the liver. The pharmacokinetics of amitriptyline have been investigated in relation to polymorphisms in liver metabolising enzymes of the CYP450 family (Kirchheiner *et al.* (2004)). OCT1 is the major liver transporter for organic cations (Figure 4.5 and Koepsell (2013)) and an additional study is being currently conducted, at the Institute for Clinical Pharmacology in Göttingen, to study the influence of polymorphisms on the OCT1 gene on the pharmacokinetics of amitriptyline in healthy human volunteers. This section studies how amitriptyline interacts with the organic cation transporter 1, and whether amitriptyline is a substrate for this transporter.

First, the interaction of amitriptyline with OCT1 was confirmed by showing that amitriptyline inhibits the uptake of the typical OCT1 substrate MPP⁺ (Figure 4.33). Amitriptyline showed a high affinity to OCT1 ($IC_{50} = 4.3 \pm 1.3 \mu M$).

After showing that amitriptyline binds to OCT1 with high affinity, the uptake of amitriptyline was studied with different incubation times at the concentration of 15 nM. The uptake of amitriptyline was in average higher on cells over-expressing OCT1, as in the control cells (Figure 4.34). However, the absolute uptake on both the OCT1 over-expressing cell line and the control cell line was very variable in the three independent experiments performed (Figure 4.34 A). When comparing the uptake in the OCT1 over-expressing cells to the uptake in the control cell lines for each individual experiment, the uptake was significantly increased ($p < 0.05$) and was between 18% and 31% higher in cells over-expressing OCT1 for the incubation times between 10 s and 2 min (Figure (4.34 B)). For the incubation time of 2 s no uptake was observed, and for an incubation time of 5 s, the uptake of amitriptyline was 54% higher when comparing each individual experiment.

Amitriptyline has a high protein binding (Brunton & Knollman (2011)). Addition of serum may substantially decrease the fraction of drug which is unbound, and therefore, the amount of free drug which is available for the membrane transporter. Furthermore, it is not known whether the presence of serum proteins (or other substances present in serum) directly affects the activity of the membrane transporter. *In vivo*, when drugs are in the blood stream, they are bound to serum proteins. Therefore, the effect of serum on the uptake of amitriptyline was also experimentally studied. The average uptake on the cell lines expressing OCT1 was higher than in the control cells. However, the absolute

values were also very variable, probably due to the high passive diffusion component of the uptake (Figure 4.35). The net cellular uptake in both OCT and control cells in the presence of serum was lower.

Finally, the inhibition of amitriptyline uptake by specific OCT1 inhibitors was analysed. If a substance is substrate for a membrane transporter, its uptake should be reduced in the presence of specific inhibitors. The presence of MPP⁺ had no effect on the uptake of amitriptyline both on OCT1 over expressing and in the control cells. In contrast, the presence of desipramine reduced the uptake of amitriptyline in OCT1 over expressing cells by 66% (Figure 4.36 A). However, a similar reduction of the uptake of amitriptyline (60%), in the presence of desipramine, was also observed in the control cell line, which does not express OCT1 (Figure 4.36 B). Therefore, it could not be shown whether there is specific uptake of amitriptyline by OCT1.

Weak bases which are very lipophilic (like amitriptyline) can accumulate in a cell by a process called lysosomal trapping (Funk & Krise (2012), citeKazmi2013, and Logan *et al.* (2014)). Desipramine is known to reduce lysosomal trapping (Daniel *et al.* (1995)). High concentrations of NH₄Cl in the medium are also known to have the same effect. In order to confirm that the reduced uptake in the presence of desipramine is due to lysosomal trapping and not due to the inhibition of an unknown transporter present in HEK293 cells, the uptake was also measured in the presence of NH₄Cl. Co-incubation with NH₄Cl also reduced the uptake of amitriptyline in both the cells over expressing OCT1 and in the control cells carrying the empty vector (Figure 4.36).

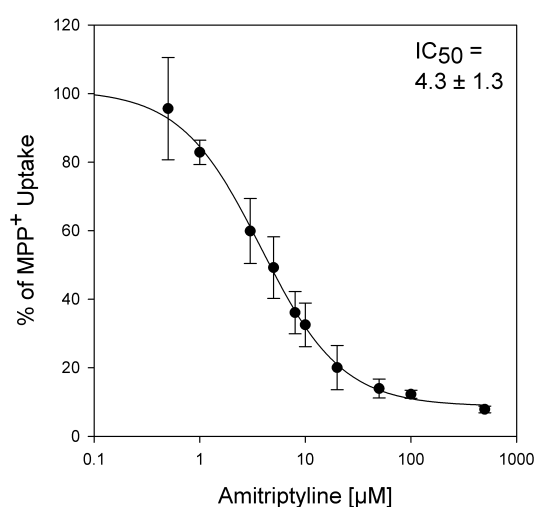


FIGURE 4.33: Inhibition of the OCT1 mediated MPP⁺ uptake by amitriptyline. OCT1-overexpressing cells were incubated for 2 min with 5 nM ³H-MPP⁺ in the presence of increasing concentrations of amitriptyline. Shown are the means and the standard error of the means of three independent experiments.

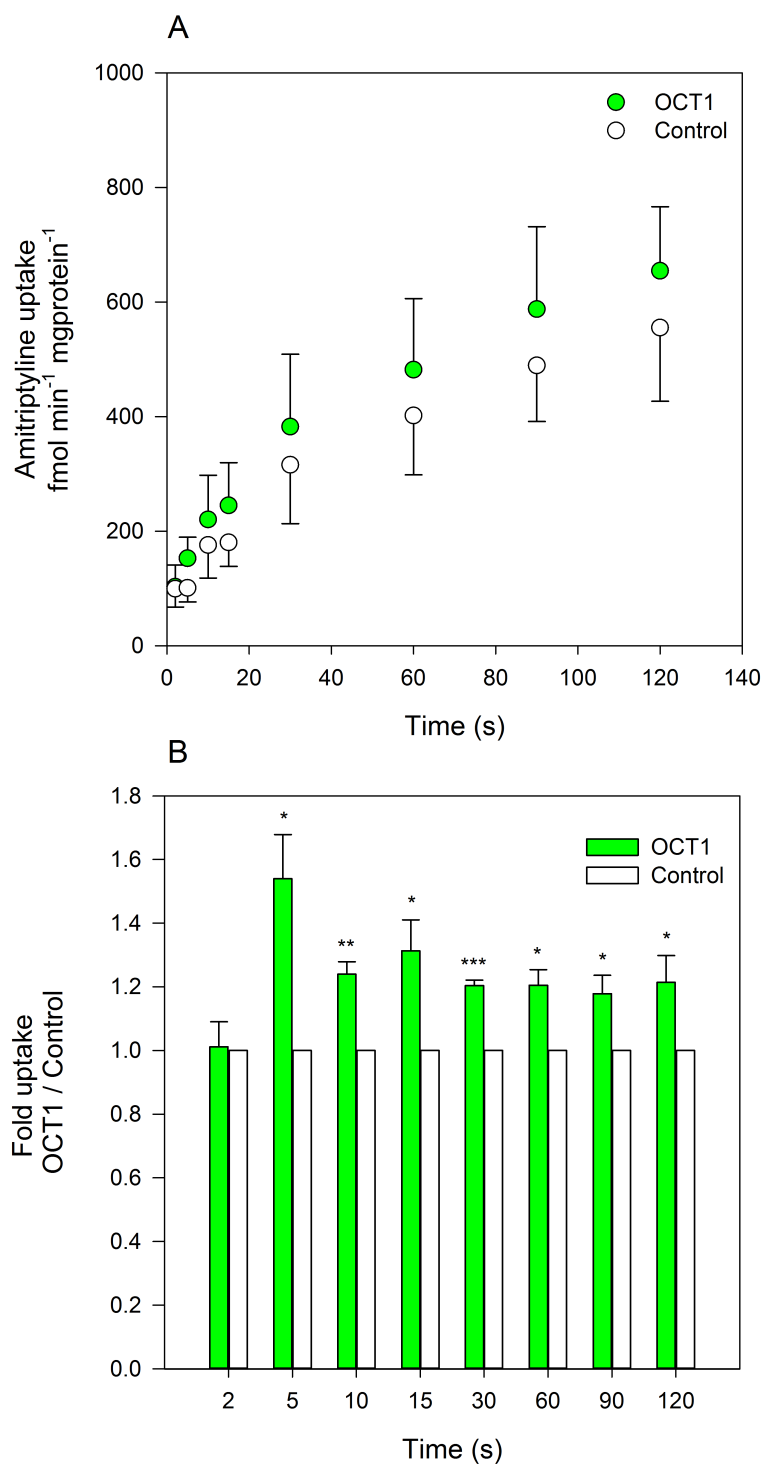


FIGURE 4.34: Time dependent uptake of amitriptyline by OCT1. The time dependence of the uptake of amitriptyline by OCT1 was studied by incubating 15 nM of ³H-labeled amitriptyline with HEK cells over expressing OCT1 and the control cells expressing the empty vector, with the uptake time varying between 2 and 120 s. (A) represents the absolute uptake in $pmol\ mg^{-1}\ mgprotein^{-1}$ in three independent experiments and (B) the relative uptake of amitriptyline by OCT1, calculated for each individual experiment by dividing the uptake in cells over-expressing OCT1 by the uptake in cells expressing the empty vector. Shown are the means and the standard error of the means of three independent experiments. (* $p < 0,05$, ** $p < 0,01$, *** $p < 0,001$ Student's t-test).

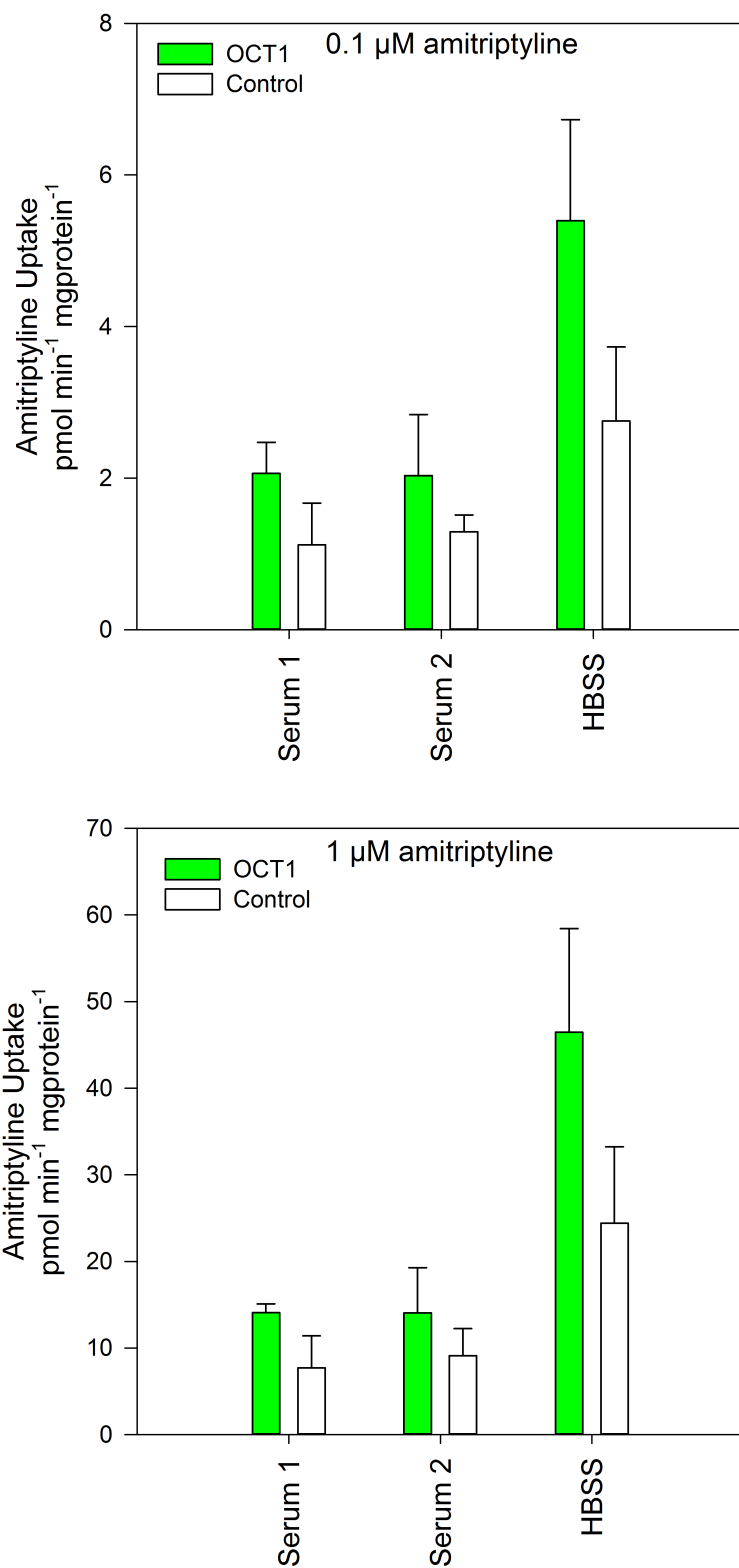


FIGURE 4.35: The role of human serum on the uptake of amiriptryline by OCT1. The uptake of 0.1 and 1 μM of amiriptryline was measured for 2 min in cell lines over-expressing OCT1 or the empty vector. The uptake was measured using as transport medium, HBSS, or serum obtained from the blood of 2 unrelated individuals. Shown are the means and the standard error of the means of two independent experiments. $p > 0.2$ for all the results shown (Student's t-test).

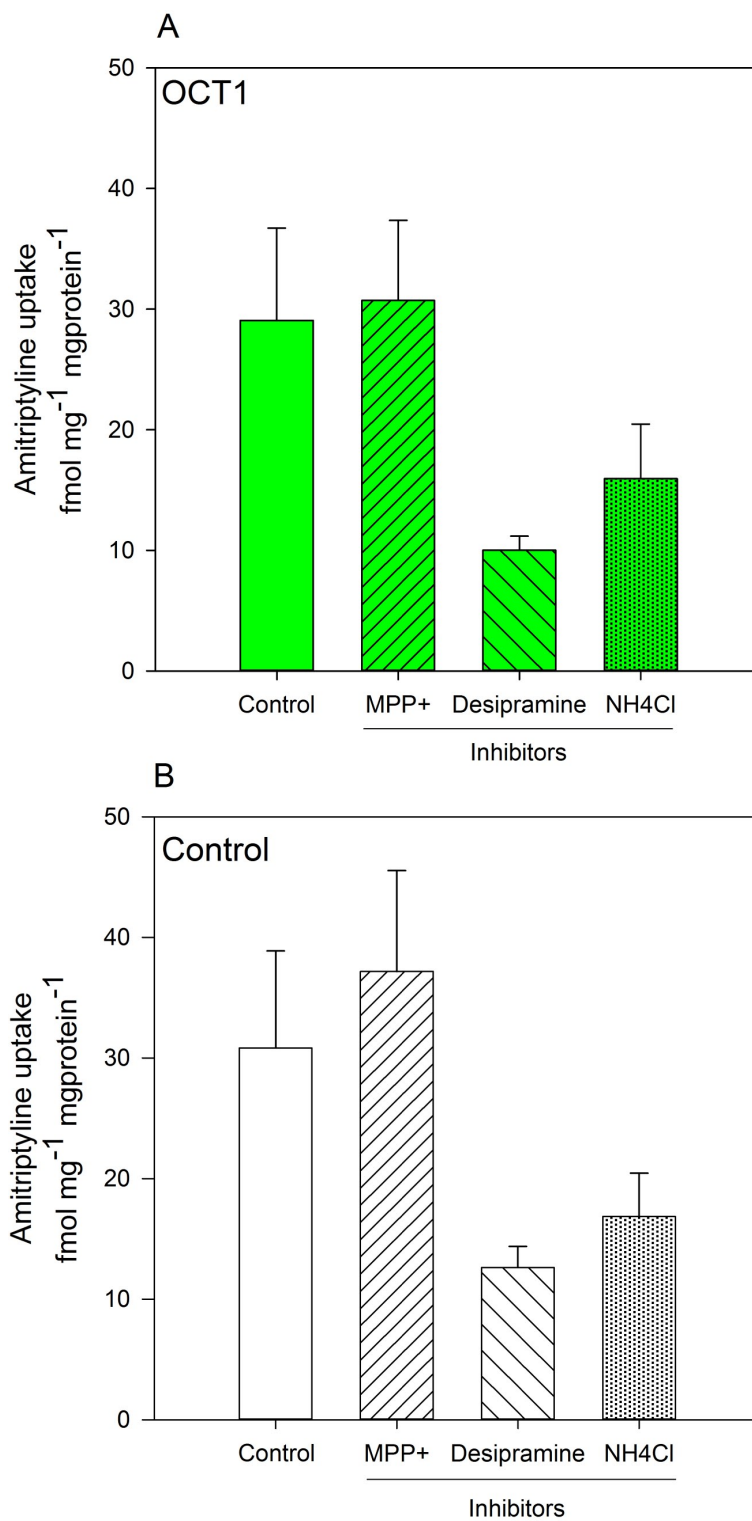


FIGURE 4.36: Inhibition of amitriptyline uptake by MPP⁺, desipramine and NH₄Cl. The uptake of 2 nM of amitriptyline was measured for 2 min in cell lines over-expressing OCT1 or the empty vector. The uptake was inhibited with either 1 mM of MPP⁺, 200 μM of desipramine or 20 μM of NH₄Cl. Shown are the means and the standard error of the means of three independent experiments.

4.7.3 Drug-drug interactions involving psychiatric drugs which affect the OCT1-mediated uptake of morphine

Morphine was recently described as a substrate of the organic cation transporter 1, OCT1. Morphine is mainly eliminated in the liver, where OCT1 plays a major role in its uptake (Tzvetkov *et al.* (2013)). Therefore, drugs which inhibit OCT1 may inhibit the uptake of morphine in the liver therefore affecting the elimination of morphine and leading to higher blood concentrations. Indeed, some antidepressants are used as adjuvants in pain treatment in order to potentiate the effects of morphine. Typically used antidepressants are amitriptyline, fluoxetine, imipramine and clomipramine. Also antiemetics, like topisetron and ondansetron, are prescribed together with morphine during cancer treatment or during or following surgical interventions. The chemotherapeutic agent irinotecan, may also be given together with morphine during cancer treatment, as well as the calcium channel blocker verapamil, which is known to potentiate the effects of morphine. These drugs were studied for drug-drug interactions with OCT1 (Vaupel *et al.* (1993)).

All the analysed drugs inhibited the uptake of morphine by OCT1. The strongest inhibitor was ondansetron ($IC_{50} = 1.2 \pm 0.2 \mu M$), and the weakest inhibitor was codeine ($IC_{50} = 10.9 \pm 0.8 \mu M$). All the drugs tested had an IC_{50} value lower than MPP⁺, a typical OCT1 substrate and inhibitor (Figures 4.37 and 4.38). It is interesting to observe that codeine, the pro-drug of morphine, also had a low IC_{50} .

When a drug is taken orally, its concentration in the portal vein is higher than in the peripheral circulation, because drugs have not yet suffered the first pass effect in the liver. The maximal unbound drug concentration in the portal vein ($C_{Max,Port,Unb.}$) and the maximal unbound plasma drug concentration $C_{Max,Unb.}$ can be calculated from the maximal plasma concentration (C_{Max}) as explained on section 3.10.2. This is specially important for drugs which are mainly liver metabolised and suffer from a very strong first pass effect (Table 4.7, $C_{Max,Unb.}$ vs $C_{Max,Port,Unb.}$). The IC_{50} values for the inhibition of morphine uptake by several drugs were compared with the estimated unbound maximal portal vein concentrations for each inhibitor (Table 4.7). At clinically relevant concentrations of the drugs in the portal vein, irinotecan, verapamil and ondansetron are able to inhibit more than 50% of the OCT1 mediated morphine uptake. On the other hand, only ondansetron and irinotecan had a $C_{Max,Unb.}/IC_{50}$ ratio equal or higher than 0,1.

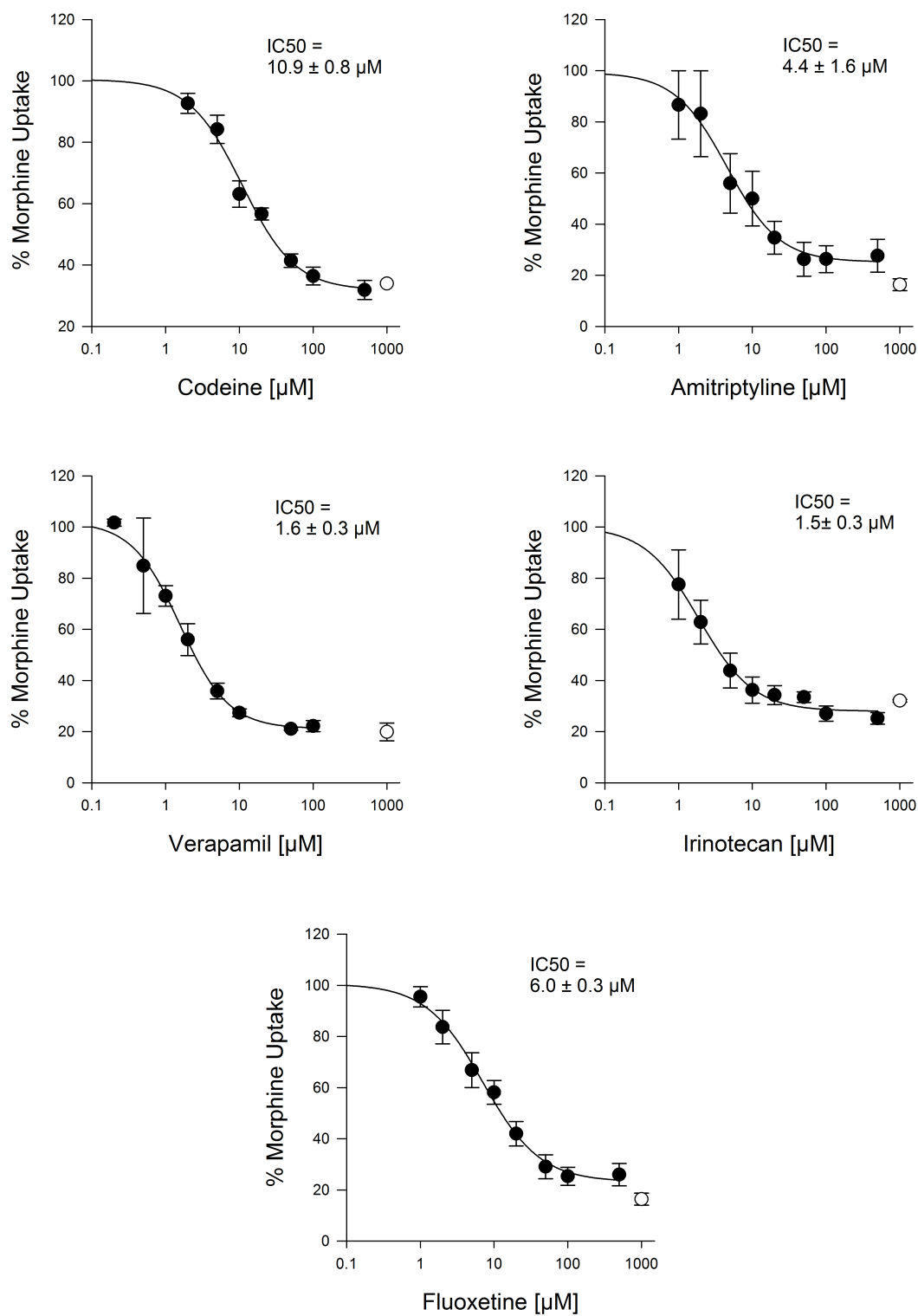


FIGURE 4.37: Inhibition of the OCT1 mediated morphine uptake by commonly co-administrated drugs: Codeine, amitriptyline, verapamil, irinotecan, fluoxetine. OCT1-overexpressing cells were incubated for 2 min with 5 nM ^3H -morphine in the presence of increasing concentrations of the inhibitor. The white circles show the uptake in the non-inhibited control cells transfected with the empty vector.

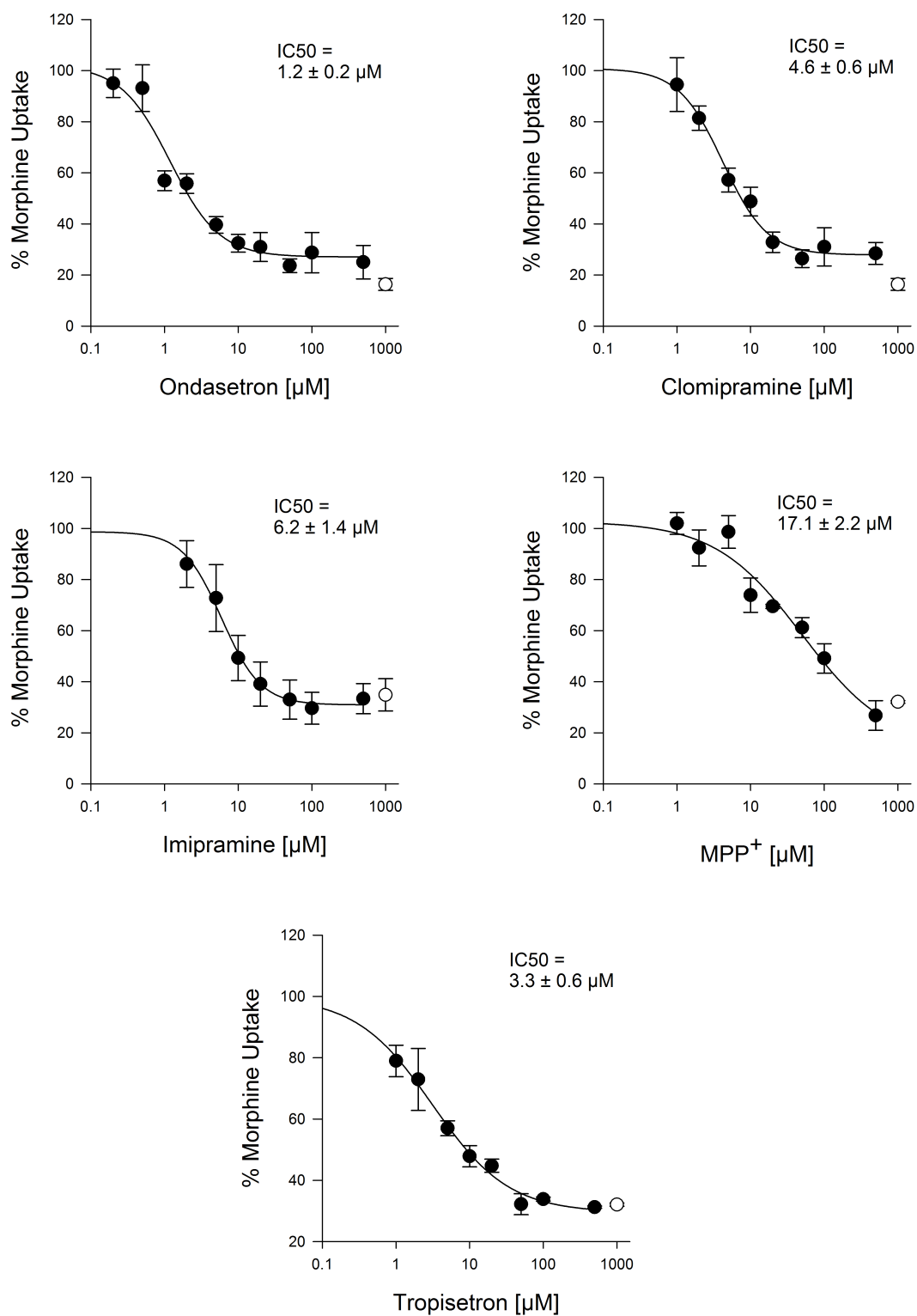


FIGURE 4.38: Inhibition of the OCT1 mediated morphine uptake by commonly co-administrated drugs: Ondasetron, clomipramine, tropisetron. OCT1-overexpressing cells were incubated for 2 min with 5 nM ^3H -morphine in the presence of increasing concentrations of the inhibitor. The white circles show the uptake in the non-inhibited control cells transfected with the empty vector.

TABLE 4.7: Inhibition of OCT1-mediated morphine uptake by drugs commonly co-administered with morphine.

	IC_{50} μM	Dose μM	$C_{Max,Unb.}$ μM	$C_{Max,Unb.}/IC_{50}$	$C_{Max,Port,Unb.}$	Inhibition of OCT1 mediated morphine uptake at $C_{MaxPort,Unb.}$
Irinotecan (i.v.)	1.5 \pm 0.3	240 mg/m ²	3.89	2.6	3.9	76%
Verapamil	1.6 \pm 0.3	120 mg	0.06	0.04	1.7	54%
Ondansetron (oral)	1.2 \pm 0.2	24 mg	0.12	0.1	1.2	52%
Ondansetron (i.v.)	1.2 \pm 0.2	0.15 mg/kg	0.08	0.06	0.08	3%
Imipramine	6.2 \pm 1.4	200 mg	0.07	0.01	4.5	34%
Codeine	10.9 \pm 0.8	30 mg	0.11	0.01	4.3	24%
Amitriptyline	4.4 \pm 1.6	100 mg	0.01	0.002	1	19%
Tropisetron	3.3 \pm 0.6	5 mg	0.04	0.01	0.3	17%
Fluoxetine	6.0 \pm 0.3	60 mg	0.01	0.002	0.7	6%
Clomipramine	4.6 \pm 0.6	50 mg	0.005	0.001	0.4	3%

$C_{MAX,Port,Unb.}$ represents the maximal unbound plasma concentration in the portal vein and is calculated with equation 3.9 described on section 3.10.2. The maximal plasma concentrations $C_{Max,Unb.}$ and the fraction of unbound drug in plasma (f_u), which are required for the calculations, were obtained from Goodman and Gilman's The Pharmacological Basis of Therapeutics (Brunton & Knollman (2011)) except for the C_{Max} of ondansetron (Zofran[®], information for prescribers), tropisetron (Kutz (1993)), codeine (Tzvetkov *et al.* (2013)), fluoxetine (Moraes *et al.* (1999)) and clomipramine (Herrera *et al.* (2000)) and the f_u of tropisetron (Navoban[®], information for prescribers) and clomipramine (Kelly & Myers (1990)). In the case of i.v. administration, the $C_{MAX,Port,Unb.}$ was assumed equal to $C_{Max,Unb.}$

4.8 The cellular uptake of tyramine is affected by genetic polymorphisms in OCT1

OCT1 is a highly polymorphic gene, whose polymorphisms show different patterns of distribution worldwide (Stalman *et al.* (2014)). OCT1 is an important transporter which may help to detoxify exogenous substances in the liver. The reasons for the occurrence of common polymorphisms in the OCT1 gene are unknown and one may speculate that diet is one of the responsible factors. Tyramine is a biogenic amine present in food, and it is been proposed to be a substrate for the human OCT1 (Schömig *et al.* (2006)). However, detailed characterisation of the uptake of tyramine by OCT1 is lacking. The interactions of tyramine with OCT1 and the effects of OCT1 polymorphisms on tyramine uptake were analysed in details in this work.

First, the ability of tyramine to inhibit the typical OCT1 substrate MPP⁺ was investigated (Figure 4.39). Tyramine showed only a moderate affinity for OCT1 ($IC_{50} =$

76.5 ± 12.9). Secondly, the uptake of tyramine by OCT1 has $K_M = 94.7 \pm 28.2$ and $V_{Max} = 380.9 \pm 19.6$ (Figure 4.40), corresponding to a $CL_{Int} 4 \text{ mL/min mgprotein}^{-1}$.

The influence of genetic polymorphisms in OCT1 on tyramine uptake was investigated (Figure 4.41). All the OCT1 genetic variants abolished the uptake of tyramine ($p < 0,001$), with the exceptions of alleles *8 *10 and *13. Allele *8 showed an uptake similar to the *wild-type* variant *1. Alleles *10 ($p < 0,01$) and *13 ($p < 0,001$) showed a decrease in uptake of 30% and 44% compared to the *1 allele, respectively.

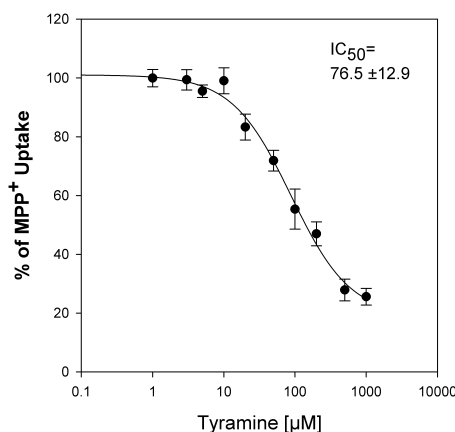


FIGURE 4.39: Inhibition of the OCT1 mediated MPP⁺ uptake by tyramine. OCT1-overexpressing cells were incubated for 2 min with $5 \text{ nM } ^3\text{H-MPP}^+$ in the presence of increasing concentrations of tyramine. Shown are the means and the standard error of the means of three independent experiments.

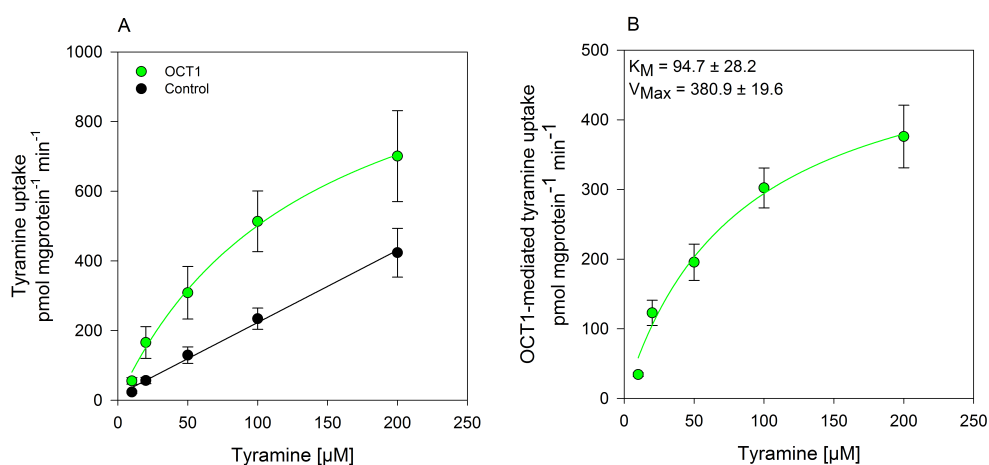


FIGURE 4.40: Kinetics of the OCT1 mediated tyramine uptake. Uptake of tyramine in HEK-293 cells expressing OCT1 in comparison to the control cell line expressing the empty vector (A). The transporter dependent uptake of tyramine by OCT1 (B) was calculated by subtracting the uptake in the cells expressing the empty vector from the uptake in the cell lines expressing the transporter. Shown are the means and standard error of the means of three independent experiments.

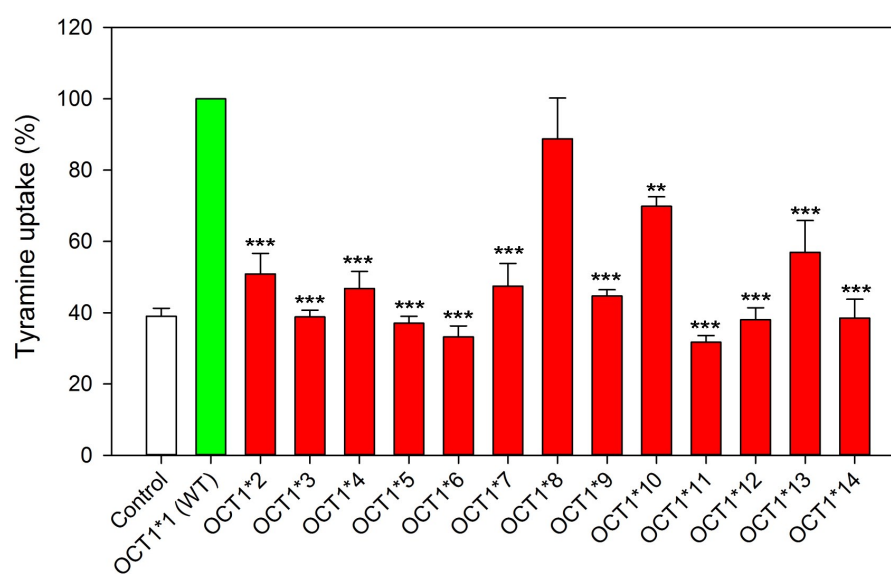


FIGURE 4.41: Uptake of $10 \mu\text{M}$ of tyramine by HEK293 cells expressing the wild-type OCT1*1 variant (green bars), the loss of function variants OCT1*2 to *14 (red bars), and the empty vector (white bar). Show are the means and standard error of the means of three independent experiments. *** $p < 0,001$ and ** $p < 0,01$ for comparing the OCT1*2 to *14 alleles with the OCT1*1 allele (post-hoc Tukey-HSD after significant ANOVA test for differences among the groups).

4.9 Establishment of a MDCK II cell line for targeted chromosomal gene integration

In this work, influx transport was measured in HEK293 cell lines which were established through targeted chromosomal integration (Saadatmand *et al.* (2012)). This is specially advantageous when studying genetic variants in proteins (for example, genetic variants in the OCT1 gene), as all the genes will be expressed at the same level and the different genetic variants cloned in different cell lines can be easily compared.

At the blood-brain barrier, efflux transport may play a more important role than influx transport. Whereas influx transport can be studied by measuring drug accumulation in normal cell cultures (for example, with HEK293 cells), in order to study membrane transport by efflux transporters, a cell line capable of forming a tight monolayer is needed. The substrate is placed on the bottom well of a Transwell[®] plate, and the permeability through the monolayer can be measured (similar to what is depicted on figure 1.6 B of the introduction). MDCK II cells can form tight polarised cell monolayers and allow for these types of measurements (Dukes *et al.* (2011)). When an efflux transporter is cloned into MDCK II cells, a difference in the membrane permeability of a drug can be measured if the drug is a substrate for the transporter.

Whereas HEK293 cell lines for targeted chromosomal integration, like the ones used in this study, are available commercially (Life Technologies), this is not the case for MDCK cells. The only MDCK cell line for target chromosomal integration which is described in the literature is a MDCK type I strain (Fröhlich *et al.* (2004)), which is known to have an unstable phenotype (Dukes *et al.* (2011)). Therefore, an MDCK II cell line which allows for targeted chromosomal gene integration was established. In this section three clones of a MDCK II cell line transfected with the pFRT/LacZeo plasmid were isolated and analysed.

In order to study whether the cloning procedure had an effect on the formation of polarised cell monolayers, the TEER (transepithelial electrical resistance) in the cell line stably expressing the plasmid was compared to the control, non-transfected, MDCK II cell line. There were no significant differences between the TEER on the MDCK II clones generated and the original cell line (Figure 4.42). The only exception was the higher TEER of Clone 2 at passage +4, on day 3, which was higher than the other cell lines. This may have due with differences on cell seeding. On day 4 the differences were not present any more.

In order to confirm the stable integration of this plasmid (which includes a gene for the β -Galactosidase enzyme), an ONPG hydrolysis assay was performed at two different passages (ONPG, o-Nitrophenyl- β -D-galactopyranosid, a synthetic substrate of the enzyme β -Galactosidase, section 3.9.5). All the clones showed β -Galactosidase activity, whereas the original MDCK II cell line did not show any activity (Figure 4.43). On both passages, +4 and +5, Clone 3 showed the highest amount of β -Galactosidase activity, followed by Clone 1 and Clone 2, respectively.

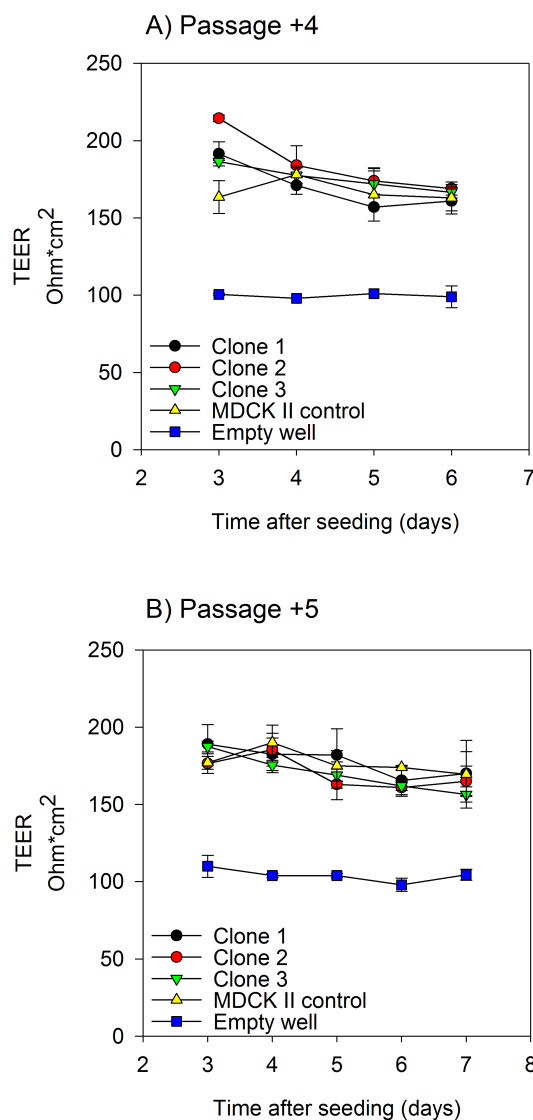


FIGURE 4.42: Characterization of the MDCK II cell lines cloned with the pFRT/LacZeo plasmid at two different passages. Measurements of the transepithelial electrical resistance (TEER) in transwell[®] plates. Panels A and B show the same analysis, performed in different clones at passage +4 and +5, respectively, compared to the untransfected control MDCK II cell line. Show and the means and standard deviations of two replicates for each data point.

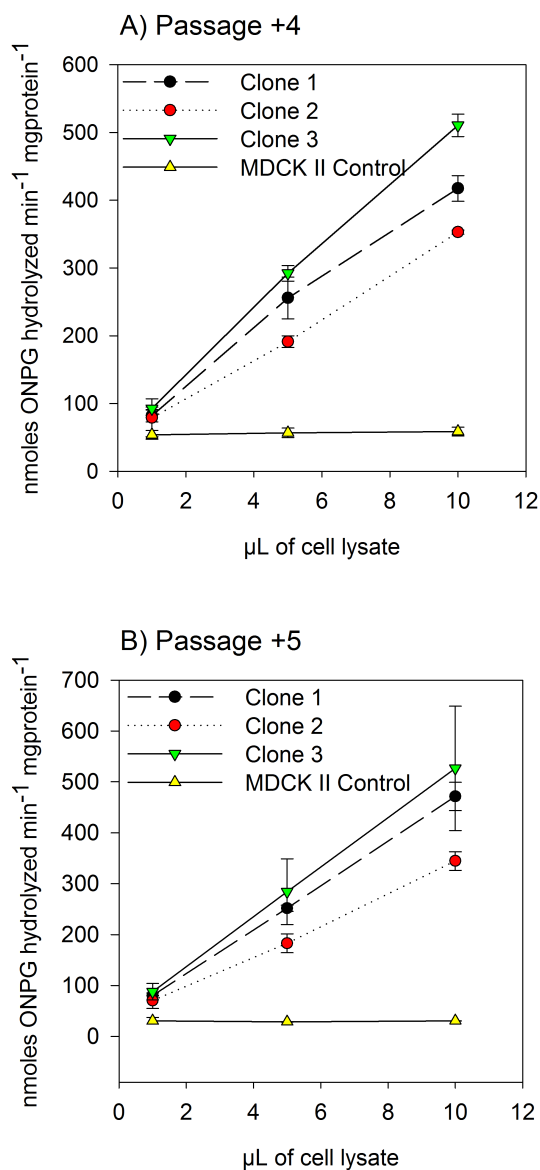


FIGURE 4.43: Characterization of the MDCKII cell lines cloned with the pFRT/LacZeo plasmid at two different passages. Activity of the enzyme β -Galactosidase, measured by hydrolysis of ONPG, which indicates expression of the pFRT/LacZeo plasmid. Panels A and B show the same analysis, performed in different clones at passage +4 and +5, respectively, compared to the untransfected control MDCK II cell line. Shown are the means and standard deviations of two replicates for each data point.

5

Discussion

5.1 Membrane permeability of psychotropic drugs

This work showed the potential of the PAMPA assay to identify substrates which may depend on membrane transport to penetrate cell membranes, within a pool of substances. Amisulpride, sulpiride, tiapride and sultopride were identified in the PAMPA assay as substances with low membrane permeability which may depend on membrane transporters to enter the cells. These are weak bases, more than 96% protonated at pH 7.4 (Table 4.1). Amisulpride and sulpiride were later identified as substrates of the organic cation transporters of the SLC22 family, and amisulpride as a substrate for the MATE1 and MATE2-K transporters.

Most of the psychiatric drugs studied in this work were weak bases and protonated at physiological pH (7,4) (Table 4.1). The most hydrophilic drugs, with the lowest $LogD_{7.4}$, were tranlycypromine, sulpiride, clozapine and amisulpride.

Substantial discrepancies were observed between the *in silico* predicted permeability, and the permeability measured experimentally with the PAMPA assay. Drugs which are more hydrophilic, should have lower membrane permeability. However, tranlycypromine, the drug with the lowest $LogD_{7.4}$ at pH 7.4 ($LogD_{7.4} = -0.53$, Table 4.1), showed a high membrane permeability on the PAMPA assay ($P_e = 9.5 \times 10^{-6} cm/s$, Figure 4.1). Tranlycypromine has a highly exposed amine group (Figure 5.1), which explains the high pKa and low $logD$ (Table 4.1), but the rest of the molecule is very hydrophobic, explaining the high $LogP$ (Table 4.1) and high permeability in the PAMPA assay (Figure 4.1).

The correlation of the $LogP$ with the membrane permeability was better than the correlation of the $LogD$ value (Figure 4.2). This may indicate that the permeability through

the PAMPA membrane depends more on the lipophilicity (measured by the $LogP$) than on the pK_a of the substance (which influences the $LogD$ value).

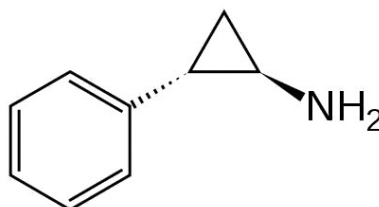


FIGURE 5.1: Tranylcypromine - a drug with low $LogD$ and high permeability in the PAMPA assay

Here, the PAMPA assay was successfully used to screen for drugs which are substrates of membrane transporters. This was possible due to the use of UV as a detection method which allowed the comparison of the membrane permeabilities of many different compounds in a short time frame. The development of a HPLC based method for each substance to be tested would be a work-intensive procedure.

The PAMPA assay also used for the early identification of other weak basic substances, like atropine and sumatriptan, which have limited drug permeability and benefit from carrier-mediated transport to enter the liver (not part of this dissertation). These drugs were later shown, in the working group, to be substrates of OCT1 and the pharmacokinetics of sumatriptan were in addition shown to be dependent on OCT1 genetic polymorphisms in healthy volunteers.

5.2 Amisulpride and sulpiride are substrates of the organic cation transporters of the SLC22 family and MATEs

This work identified amisulpride and sulpiride as substrates of the organic cation transporters of the SLC22 family. Amisulpride and sulpiride are psychotropic drugs in the class of the substituted benzamides, and are used to treat schizophrenia (Rao *et al.* (1981), Pani & Gessa (2002) and Komossa *et al.* (2010)). The chemical structures of amisulpride and sulpiride are very similar (Figure 4.20), however, small structural differences seem to account for different substrate specificities.

It was shown that amisulpride is a substrate for the transporters OCT1, OCT2, OCT3, OCTN1 and OCTN2 and that sulpiride is a substrate for the transporters OCT1 and OCT2 (Figures 4.21 and 4.23). This was the first time that an interaction between amisulpride and the organic cation transporters of the SLC22 family was reported.

The finding that sulpiride is a substrate of OCT1 and OCT2 (Figures 4.23 and 4.24) is in line with the previously reported ability of sulpiride to inhibit OCT2 (Kido *et al.* (2011)), and the suggested involvement of OCTs in the uptake of sulpiride in Caco-2 cells (Watanabe *et al.* (2002)).

This study shown that OCTN1 and OCTN2 do not transport sulpiride (Figure 4.23), in contrast to what was suggested by Watanabe *et al.* (2002). Watanabe *et al.* showed that 20% of the uptake of sulpiride in Caco-2 cells was inhibited by adding 3 mM L-Carnitine and suggested that OCTN1 and OCTN2 may transport sulpiride in Caco-2 cells. However, the authors also acknowledged that there may be another not-yet identified transporter transporting sulpiride from the apical side in Caco-2 cells. The present study showed that OCTN1 and OCTN2 do not transport sulpiride, supporting the hypothesis for the involvement of another apical transporter for sulpiride in Caco-2 cells. The involvement of another transporter is in line with the observed inhibition of the uptake of sulpiride by L-carnitine in hCMEC/D3 cells (Figure 4.30 B), which will be discussed in section 5.4.

The MATE1 and MATE2-K transporters, which are expressed in the liver (MATE1) and kidney (MATE1, MATE2-K) may be important for the elimination of amisulpride, which has been shown to be a substrate for both these transporters (Figure 4.28). The role of MATE1 and MATE2-K on the uptake of sulpiride is not known and it was not studied in this work, as sulpiride is not clinically as relevant as amisulpride.

5.3 The role of carrier-mediated transport of amisulpride and sulpiride at the blood-brain barrier

Amisulpride and sulpiride have a low membrane permeability and it is not known how they cross the blood-brain barrier. Both drugs are dopamine receptor D2 blockers and need to pass the blood-brain barrier in order to reach their site of action. Transporters from the SLC22 family have been suggested to be expressed at the blood-brain barrier (Dickens *et al.* (2012), Lin *et al.* (2010) and Geier *et al.* (2013a)). Furthermore, OCT1 and OCT2 have been shown to mediate the uptake of MPTP, and MPP⁺ in brain microvascular endothelial cells (Lin *et al.* (2010)). Taken together with the ability of OCT1 and OCT2 to transport amisulpride and sulpiride, it can be suggested that OCT1, OCT2 and other OCTs from the same family may mediate the uptake of amisulpride and sulpiride at the blood-brain barrier. Additionally, MATE1 has been recently proposed to be expressed in microvascular endothelial cells which form the blood-brain barrier and may be relevant for the uptake of amisulpride into the brain (Geier *et al.* (2013a)). Sulpiride has been previously indicated as a substrate of PEPT-1 (Watanabe *et al.* (2002)) which is, however, not expressed at the blood-brain barrier (Figure 4.9 and Geier *et al.* (2013a)).

The brain-to-blood ratios ($\frac{\text{concentration}_{\text{unbound,brain}}}{\text{concentration}_{\text{unbound,plasma}}}$) of amisulpride and sulpiride in rats, are lower than one (Dufour & De Santi (1988) and Culot *et al.* (2013)). When the ratio is lower than one, it may mean that drug uptake is a combination of the processes of passive diffusion, influx transport and efflux transport, and that efflux processes are the major part of the equation. However, this does not rule out that a small change in the influx transport alters the concentration of the drug at the site of action. On the other hand, the above mentioned studies were performed in rats, and the pattern of transporter expression in the brain may be different between rodents and humans. In contrast, Okura *et al.* (2014a) have shown in rats that tramadol has a brain-to-blood ratio greater than one, indicating the presence of a mechanism for the influx transport of cationic drugs at the blood-brain barrier in rats.

5.4 Transport of amisulpride and sulpiride in hCMEC/D3 cells

The hCMEC/D3 cell line is a well characterized immortalised brain microvascular endothelial cell line, used as a model of the blood-brain barrier (Weksler *et al.* (2005)). Several studies have already been performed where the expression of membrane transporters and their functionality were analysed in this cell line (Dauchy *et al.* (2009), Dickens *et al.* (2012), Ohtsuki *et al.* (2013) and Okura *et al.* (2014a)).

A carrier-mediated influx uptake mechanism for amisulpride and sulpiride was identified in the hCMEC/D3 cell line. Both concentration- and temperature dependent uptake were observed for amisulpride and sulpiride, which suggests carrier-mediated transport (Figure 4.29). Furthermore, the uptake of amisulpride and sulpiride was inhibited by MPP⁺ (Figure 4.30), a typical substrate and inhibitor of organic cation transporters (Nies *et al.* (2011)).

OCT1 and OCT2 can transporter amisulpride and sulpiride, as it was shown in this study (Figures 4.21 and 4.23). However, their expression in hCMEC/D3 cells is either low, or non-existent, as shown in this study, and by others (Figure 4.14 and C.6, Ohtsuki *et al.* (2013) and Okura *et al.* (2014a)). Dickens *et al.* (2012) have reported functionality of OCT1 in hCMEC/D3 cells, however, the mRNA levels of OCT1 in the hCMEC/D3 cells reported in their study were similar to the OCT1 expression in the kidney, which shows that OCT1 is not highly expressed in the hCMEC/D3 cells. The presence of OCNT2 on the other hand, was detected in this study, and corresponds to what is described in the literature (Ohtsuki *et al.* (2013)).

Regarding the evidence for the low expression of organic cation transporters in hCMEC/D3 cells (this work, Ohtsuki *et al.* (2013) and Okura *et al.* (2014a)), it is plausible to assume that, not OCTs, but another transport mechanism, which has not been yet identified, is present in hCMEC/D3 cells and can transport amisulpride and sulpiride. This transport mechanism seems to transport organic cations, and be inhibitable by "organic cation"-like substances. The existence of an unknown transport mechanism in hCMEC/D3 was suggested by publications of other authors which have shown that "organic cation"-like substances, as tramadol and apomorphine (Kitamura *et al.* (2014), Okura *et al.* (2014b) and Shimomura *et al.* (2013)), are transported into hCMEC/D3 cells by a not yet identified carrier-mediated transport mechanism. Tramadol and morphine (similar to apomorphine) have been both shown to be a substrate for OCT1 in humans (Tzvetkov *et al.* (2011) and Tzvetkov *et al.* (2013)).

Another piece of evidence supporting the existence and involvement of another organic cation transporter in the amisulpride and sulpiride uptake in hCMEC/D3 cells is the inhibition of sulpiride uptake by L-carnitine (Figure 4.30 B). L-carnitine is an inhibitor of OCTN2 (Stocker *et al.* (2013b)) and it was shown that sulpiride is not a substrate for OCTN2 (Figure 4.23). Therefore, the inhibition of sulpiride uptake in hCMEC/D3 cells cannot be due to inhibition of OCTN2. Watanabe *et al.* (2002) have also reported the inhibition of the uptake of sulpiride in Caco-2 cells by L-carnitine. This suggests that sulpiride may be taken up in Caco-2 and hCMEC/D3 cells, not by OCTN2, but by another kind of transport mechanism, which is inhibitable by L-carnitine. Watanabe *et al.* (2002) also proposed the existence of this mechanism in Caco-2 cells.

The influx of amisulpride may also be mediated by an unknown transport mechanism. In contrast to sulpiride, L-carnitine does not inhibit the uptake of amisulpride in hCMEC/D3 cells, although amisulpride is transported by OCTN2 (Figures 4.21 and 4.22). OCTN2 can transport in both directions (influx and efflux, Koepsell (2013)). This means that the influx of amisulpride may be mediated by the already mentioned unknown transport mechanism and the efflux may be mediated by OCTN2. In this scenario, when both the influx and efflux are inhibited, the net uptake will be equal to the non-inhibited control (Figure 4.30 A).

A possible interaction between influx transport and efflux transport in the uptake of amisulpride was identified in hCMEC/D3 cells. Verapamil did not change the rate of amisulpride uptake into the hCMEC/D3 cell line (Figure 4.30). Verapamil is known to inhibit both organic cation transporters and MDR1 (Nies *et al.* (2011) and Pauli-Magnus *et al.* (2000)). MDR1 is known to transport amisulpride (Schmitt *et al.* (2006)) and is expressed and functional in the hCMEC/D3 cell line (Figure 4.14, Poller *et al.* (2008), Dauchy *et al.* (2009) and Ohtsuki *et al.* (2013)). Therefore, the net uptake equal to the control may be the result of simultaneous inhibition of OCT-mediated influx and MDR1-mediated efflux of amisulpride by verapamil (Figure 4.30 A). On the other hand, sulpiride is not a substrate for MDR1 (Feng *et al.* (2008)), and therefore, verapamil only inhibits the influx transport, resulting in an uptake lower than the uptake in the non-inhibited control (Figure 4.30 B).

Currently, there have been 1022 transporter genes identified in the human genome (section 1.3.2, Introduction) from which 395 are solute carriers (SLC family, Hediger *et al.* (2013)). Therefore, the analysis of amisulpride and sulpiride uptake by the organic cation transporters of the SLC22 family may have just scratched the surface of the possible number of transporters which are relevant for the blood-brain barrier uptake of amisulpride and sulpiride and other drugs.

5.5 Organic cation transporters may influence the pharmacokinetics of amisulpride and sulpiride

Besides the penetration of the blood-brain barrier, carrier-mediated transport of amisulpride and sulpiride may allow these drugs to cross several cellular barriers important for drug absorption and elimination (Figure 5.2).

The transporters relevant for the pharmacokinetics of sulpiride are the same as for amisulpride, with the exception of OCTN2, OCTN1 (Figure 4.23) and MDR1. Amisulpride is a substrate for MDR1 (Schmitt *et al.* (2006)), whereas sulpiride is not (Feng *et al.* (2008)). A summary of the membrane transporters important for the absorption, metabolism, distribution and elimination of amisulpride is depicted on figure 5.2.

The renal clearances of amisulpride and sulpiride are 330 and 223 ml/min , respectively, (Rosenzweig *et al.* (2002) and Wiesel *et al.* (1980)), indicating that tubular secretion plays a substantial role in drug elimination (Introduction, section 1.2.3). For amisulpride, $f_u \times GFR = 104 mL min^{-1}$, which means that more than two thirds of the renal clearance of amisulpride are due to tubular secretion. It is likely that OCT2 is the basolateral (blood) transporter responsible for the high renal secretion of both drugs. On the other hand, MATE1 and MATE2-K are known to be expressed on the luminal membrane (urine) of kidney proximal tubule cells and may be mediate the secretion of amisulpride into the urine. MATE1 and MATE2-K have a higher intrinsic clearance for transporting amisulpride, and higher affinity for amisulpride, than OCT2 (Tables 4.3 and 4.5). This could mean that the basolateral (blood) uptake of amisulpride in the kidney is the rate-limiting step for its elimination in the kidney. However, the analysis of drug-drug interactions, has to be done on a case-to-case basis, taking into account the affinity of the inhibiting drug for OCT2 and MATE1 and MATE2-K. Ito *et al.* (2012) have elegantly shown that inhibition of the MATE transporters on the luminal membrane, and not of the OCT2 transporters on the basolateral membrane of kidney proximal tubules is the mechanisms responsible for the inhibition of the renal clearance of organic cations by cimetidine.

A drug-drug interaction study of amisulpride with cimetidine has never been performed. Interestingly, the prescribing information of both amisulpride and sulpiride cites several known drug-drug interactions which drugs which are also known to inhibit organic cation transporters like quinidine, verapamil and imipramine (Nies *et al.* (2011)).

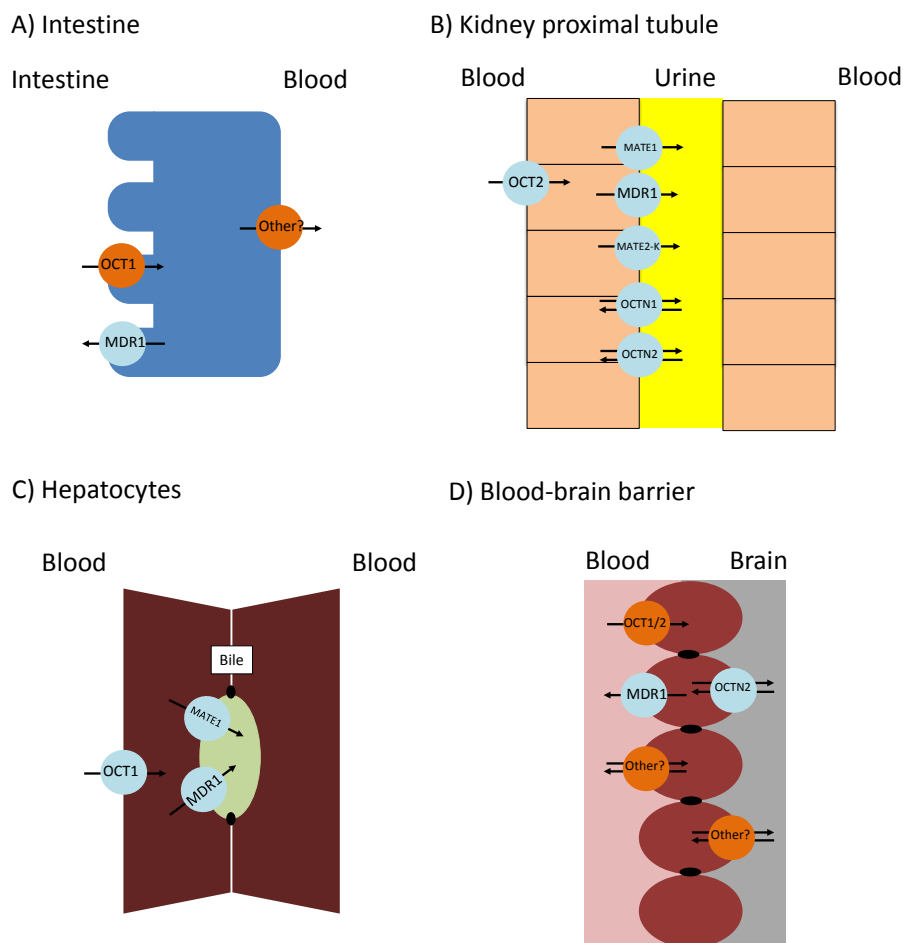


FIGURE 5.2: Localization of the membrane transporters which may play a role on the pharmacokinetics of amisulpride. The difference between this figure and figure 1.9 from the introduction is inclusion of only the organic cation transporters which may be relevant for the pharmacokinetics of amisulpride (blue), as well as the inclusion of transporters where their localisation and role is still debatable (orange). These include the presence of OCT1 in the apical membrane in the intestine (Han *et al.* (2013)) and a transporter responsible for the basolateral intestinal transport of amisulpride into the blood. The role of OCT1 and OCT2 at the blood-brain barrier is still debatable, as discussed on section 5.8 (Lin *et al.* (2010)). OCTN2 has been proposed to be localised on the basolateral in bovine BMECs (Miecz *et al.* (2008)) and is expressed at the human blood-brain barrier (Figure 4.9). As discussed in section 5.4, another transporter may be involved on the transport of amisulpride at the blood-brain barrier.

Amisulpride and sulpiride are not metabolized in the liver, but biliary excretion may account for up to 20% of their total clearance (Rosenzweig *et al.* (2002) and Wiesel *et al.* (1980)). OCT1 is a transporter of both amisulpride and sulpiride and it is likely that it plays a role on the hepatic uptake and further biliary clearance of these two drugs. As shown on figure 5.2, OCT1 is the sinusoidal (blood) uptake transporter for amisulpride in the liver, and MDR1 and MATE-1 are the canicular (bile) efflux transporters for amisulpride. MATE-1 has a higher affinity (lower K_M , and a higher

CL_{int} for amisulpride than OCT1 (Tables 4.3 and 4.5). This may mean that MATE1, together with MDR1 clear amisulpride from the hepatocytes, at a rate which is higher than its OCT1 mediated uptake. This suggests that OCT1 mediated uptake is the limiting step on the biliary clearance of amisulpride.

PEPT-1 is highly expressed in the intestine and is likely to be responsible for the absorption of sulpiride (Figure 1.9 and Figure 4.6). In addition, OCT1 has also been identified in the intestinal epithelium (Han *et al.* (2013)) and may play a role on the absorption of amisulpride and sulpiride.

5.6 Role of polymorphisms in organic cation transporters on the pharmacokinetics of amisulpride and sulpiride

In this study it was shown that the uptake of amisulpride and sulpiride is affected by genetic variants in OCT1. OCT1 is highly polymorphic, and five of the common OCT1 alleles are known to lead to reduced OCT1 activity in 9% of the caucasian population (Brockmöller & Tzvetkov (2013)). This adds amisulpride and sulpiride to the limited list of clinically relevant drugs which were shown to be dependent on OCT1 to cross cellular barriers (Table 5.1). As stated previously, 20% of the amisulpride present in the blood stream is eliminated through the bile and OCT1 is likely the limiting step in the biliary elimination of amisulpride. The role of OCT1 on the distribution of amisulpride and sulpiride to the brain still needs confirmation *in vivo*, before concluding about the possible role of OCT1 polymorphisms on the therapy with these two drugs. Likewise, the role of OCT1 in intestinal absorption also needs further investigations (Han *et al.* (2013)). In addition to OCT1, genetic polymorphisms in OCT2, MATE1 and MATE2 are also known and should be considered for further studies (Tzvetkov *et al.* (2009) and Stocker *et al.* (2013a)).

TABLE 5.1: Clinically relevant drugs shown to be OCT1 substrates

Drug	Reference	Drug	Reference
Metformin	Shu <i>et al.</i> (2007)	Lamivudine	Jung <i>et al.</i> (2008)
Morphine	Tzvetkov <i>et al.</i> (2013)	Zalcitabine	Jung <i>et al.</i> (2008)
Tramadol	Tzvetkov <i>et al.</i> (2011)	Amisulpride	This work
Tropisetron	Tzvetkov <i>et al.</i> (2012)	Sulpiride	This work
Sorafenib	Swift <i>et al.</i> (2013)		

5.7 Sultopride and Tiapride are not substrates of the organic cation transporters of the SLC22 family

Although organic cation transporters of the SLC22 family can transport amisulpride and sulpiride, they cannot transport sultopride and tiapride, two drugs which are structurally very similar (Figure 4.25). These results suggest that structural differences between these drugs account for substrate specificity. One of such differences may be the amine moiety, near the aromatic ring, which is present in amisulpride and sulpiride, but missing in sultopride and tiapride (Figure 5.3).

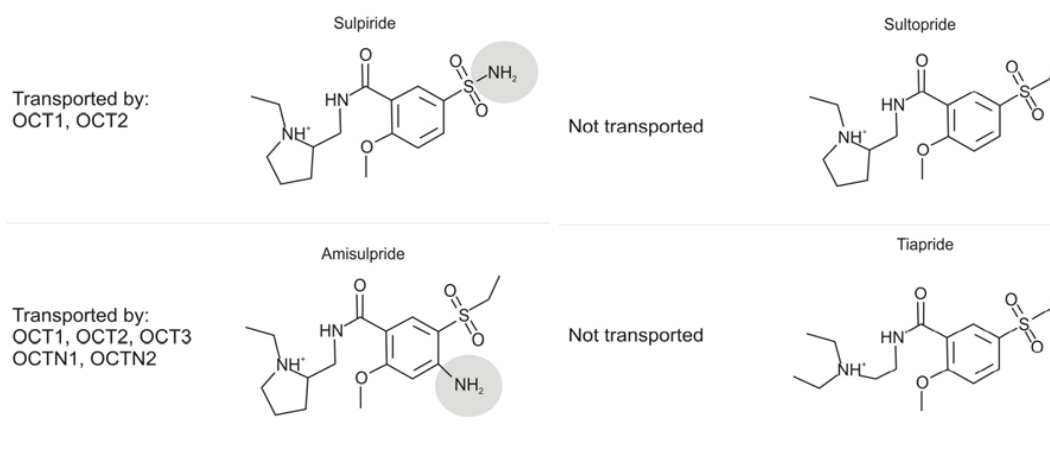


FIGURE 5.3: Comparison of the chemical structures of sulpiride, amisulpride, sultopride and tiapride. Shown in grey is the amine group which is present in amisulpride and sulpiride but not in sultopride and tiapride.

The amine group in amisulpride and sultopride could form hydrogen bonds with the OCT1 transporter. Amine groups which are connected to a benzene ring (like amisulpride, Figure 5.3) may also form hydrogen bonds (Szatyłowicz (2008)). It has been suggested by Moaddel *et al.* (2005) that an electron donor pair is important for binding to OCT1 (Figure 1.10). An interesting experiment to confirm this hypothesis, would be testing whether amisulpride and sulpiride are still substrates of organic cation transporters after substituting the amino group in amisulpride and sulpiride by a methyl group (-CH₃).

Although sultopride and tiapride are not transported by OCT1, they also inhibited the OCT1-mediated uptake of MPP⁺ with different affinities. Amisulpride showed the highest affinity for OCT1, whereas sultopride, tiapride and sulpiride showed lower affinity (Figure 4.26 and Table 4.4). Because sultopride and tiapride showed low affinity to OCT1, it is not surprising that they are not substrates of this transporter (Figure 4.25). On the other hand, sulpiride, which was shown to be an OCT1 substrate (Table 4.3 and

Figures 4.23 and 4.24), had the lowest affinity from all the drugs tested ($>1000 \mu M$, Figure 4.26). The fact that the K_M of sulpiride ($259.7 \mu M$, Table 4.3) is lower than its IC_{50} for inhibiting MPP^+ may reflect the polyspecificity of the OCT1 transporter. The binding sites for MPP^+ may be different than the binding sites for sulpiride, therefore sulpiride may not be efficient in inhibiting the transport of MPP^+ .

5.8 Gene expression analysis of drug membrane transporters in tissues relevant for drug distribution and primary brain cells

The gene expression of membrane transporters was studied at the mRNA level on liver, kidney, intestine and brain tissues. The major transporters which are known to be expressed in these organs, were also found in the samples analysed in this study (Figures 4.5, 4.6, 4.8 and 4.9, Section 4.2). In the liver, the uptake transporters OCT1 (SLC22A1) and OATP1B1 (SLCO1B1) were found to be highly expressed. Within all the transporters analysed, OCT1 was the major membrane transporter in the liver, which reinforces the likely important role that it plays in the removal of xenobiotics from the blood flow. In the kidney, the transporters OCT2 (SLC22A2) and OAT1 (SLC22A6) and OAT3 (SLC22A8) were highly expressed. In the intestine, high expression of the efflux transporter MDR1 (ABC1B1) could be shown, as well as of the PEPT1 transporters (SLC15A1). In the brain, high expression of MDR1 (ABCB1) was detected.

Within the primary cells from the brain which were analysed, the transporter expression was the highest in HBMECs (human brain microvascular endothelial cells)(Figure 4.7). This was expected, as these cells form the major barrier between the blood and the brain, and are also important for the transport of for example nutrients from the blood into the brain. The transporter expression was also analysed in mRNA from primary human choroid plexus epithelial cells and astrocytes. The expression of membrane transporters was the lowest in astrocytes, reflecting the non-barrier properties of these cells. On the other hand, astrocytes which are close to blood vessels in the brain may have different transporter-expressing patterns, however this was not studied in this work (Figures 4.7, 4.8 and 4.9).

A principle component analysis of the gene expression of membrane transporters in the several different tissues analysed, grouped the HBMECs close to the choroid plexus epithelial cells. This shows that the pattern of transporter expression is similar in these two cell types which have barrier functions (Figure 5.4). Nonetheless, the relative

gene expression of membrane transporters is higher in HBMECs than in choroid plexus epithelial cells. This is shown on figure 4.7 and can be observed by comparing the figures 4.8 and 4.9.

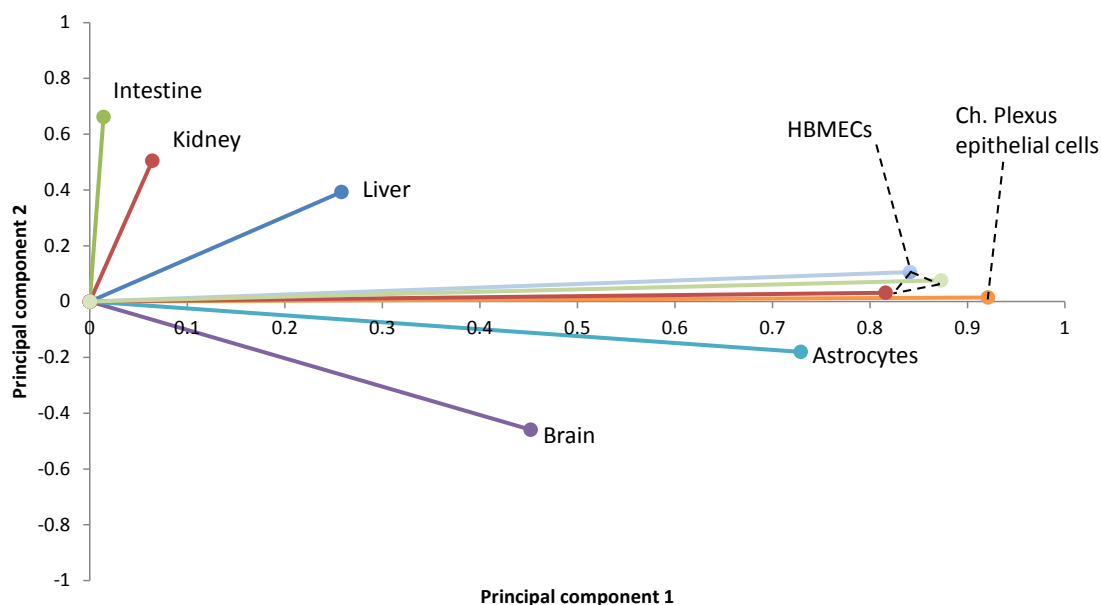


FIGURE 5.4: Principal component analysis of gene expression in tissues and primary cells. The analysis was performed on SPSS 21.0, by extracting two factors, which are shown on the figure. *Note: The KMO test of sample adequacy = 0.718 and Bartlett's test of sphericity (significance < 0.05) show that the analysis can be performed (SPSS user manual).*

The mRNA expression analyses showed that OCTN2 (*SLC22A5*), OCT1(*SLC22A1*), OCT3(*SLC22A3*) and OCTN1(*SLC22A4*) are expressed in human brain microvascular endothelial cells and may play a role in drug uptake at the blood-brain barrier (Figure 4.10). These findings are consistent with previous studies reporting mRNA (Lin *et al.* (2010), Dickens *et al.* (2012), Kido *et al.* (2001) and Geier *et al.* (2013a)) and protein expression (Lin *et al.* (2010) and Geier *et al.* (2013a)) of these transporters at blood-brain barrier.

It is debatable whether OCT1 is really expressed at the blood-brain barrier. This work (Figure 4.9 and Figure 4.10) and others (Shawahna *et al.* (2011) and Geier *et al.* (2013a)) show that the expression of OCT1 in the brain is very low, in contrast to Dickens *et al.* (2012) and Lin *et al.* (2010), who proposed that OCT1 is functional and highly expressed at the blood-brain barrier. The presence of OCT1 in the brain could not be confirmed in this study by immunostaining (Figure 4.17).

OCTN2, on the other hand, has been shown to be present at the blood-brain barrier (Kido *et al.* (2001)) and its gene expression was also detectable both in this work, as in

the rest of the literature (Figure 4.9 and Geier *et al.* (2013a)). Like OCT1, the presence of OCTN2 at the blood-brain barrier could not be confirmed by immunostaining (Figure 4.17). Other antibodies and staining procedures may help to detect OCT1 and OCTN2 at the blood-brain barrier.

The previously suggested expression of OCT2 (Lin *et al.* (2010)) in human brain endothelial cells was not confirmed by this work (Figures 4.9 and table C.2). Lin *et al.* (2010) have obtained the primary human brain endothelial cells (HBMECs) from the same provider where the RNA for this work was obtained (Sciencell, Table 2.2). However, whereas this work studied RNA expression in HBMECs, Lin *et al.* have only studied protein expression, using antibodies. The antibodies used by Lin *et al.* have yet to be validated. Antibodies can be non-specific and also stain other proteins which are not OCT2. Furthermore, Lin *et al.* have shown reduced uptake of MPP⁺ in BMECs after transfection with an siRNA against OCT2. Again, no validation of the siRNAs is shown on the work of Lin *et al.*, and siRNAs may also have off-target effects. On the other hand, Lin *et al.* have cultured the HBMECs *ex vivo* and it cannot be excluded that the cell culture conditions may affect the gene expression of membrane transporters.

The already known presence of MDR1 (*ABCB1*) and BCRP (*ABCG2*) at the blood-brain barrier was confirmed in this study both at the RNA expression level (Figure 4.9) as well as at the protein level (Figures 4.15 and 4.16). It was shown that this staining procedure can be used to detect membrane transporters in brain microvascular endothelial cells. Furthermore, the expression of BCRP at the blood-brain barrier was stronger than the expression of MDR1. This may suggest that BCRP is the main efflux transporter at the blood-brain barrier, and it requires further investigation in order to identify the role that BCRP plays on preventing the entrance of drugs into the brain, also in relation to its genetics polymorphisms (Ieiri *et al.* (2009)).

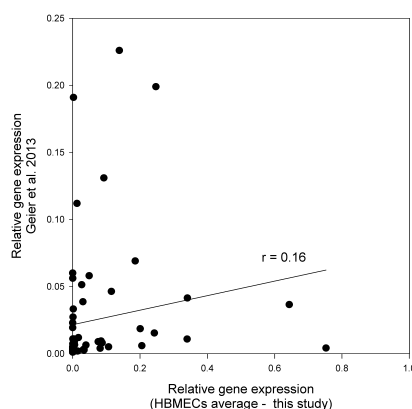


FIGURE 5.5: Comparison of the gene expression analysis in primary HBMECs (human brain microvascular endothelial cells) with the study of Geier *et al.* (2013a). The correlated data was obtained from tables C.1 and C.2.

The expression of drug transporters in HBMECs determined in this study correlated poorly with recently published data by Geier *et al.* (2013a) ($r=0.17$, Figure 5.5). Geier *et al.* detected, for example, high expression of OCT3 and MATE1 and the blood-brain barrier, which could not be confirmed in this study. The correlation between donor 2 alone and the data from Geier *et al.* was better than the correlation for the average of donors 1 and 3, but still low ($r=0.33$, Figure 5.6). The correlation was better for comparing the mRNA samples from the three donors used in this study (Figure 4.12, results).

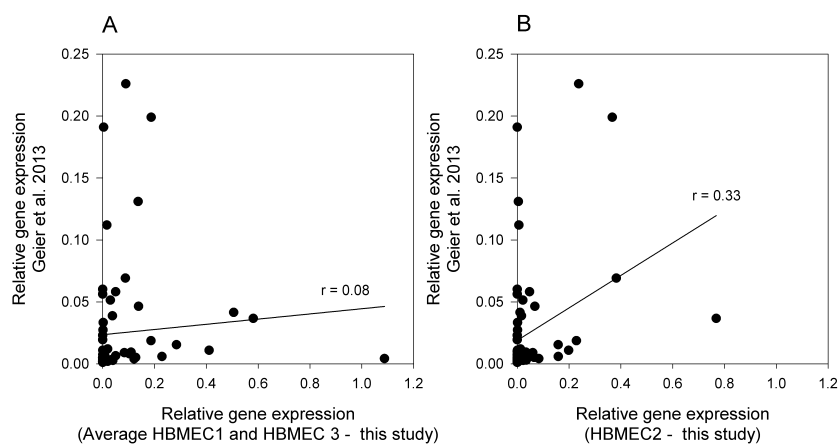


FIGURE 5.6: Comparison of the gene expression analysis in primary HBMECs (human brain microvascular endothelial cells) with the study of Geier *et al.* (2013a) - Part 2. The average of transporter gene expression in mRNA from donors 1 and 3 (A) and transporter gene expression in mRNA from donor 2 were compared with the study of Geier *et al.*. The correlated data was obtained from tables C.3, C.4 and C.5.

The discrepancies between this study and the study from Geier *et al.* may be due to variations in the procedure used to obtain the RNA. The RNA used by Geier *et al.* was obtained directly from freshly isolated HBMECs, whereas the samples analyzed in this study were obtained from HBMECs cultured *ex vivo*. Both approaches have advantages and disadvantages. Using freshly isolated HBMECs has the advantage of avoiding the changes in transporter gene expression which may occur by culturing the cells *ex vivo*. It has been reported that the expression of transporter genes in primary hepatocytes decreases with culture time (Tchaparian *et al.* (2011)). On the other hand, the direct analysis of the mRNA after cell isolation increases the risk of contamination with other cell types (for example, astrocytes). The *ex vivo* approach, as used in this work, guarantees a more homogeneous endothelial cell culture, as the cells are grown for one passage on specific endothelial cell medium, before the isolation of the mRNA.

Differences in the procedure used to analyse gene expression may also lead to the discrepant results between this study and the study from Geier *et al.* (2013a). In this work

TaqMan® qPCR assays for gene expression analysis were used, whereas Geier *et al.* (2013a) used an OpenArray® system, which in their hands, showed a poor correlation with the TaqMan® assay (Geier *et al.* (2013a), Supplementary figure S2). In contrast, the TaqMan® low density arrays used in this study use the same principle of detection as the gold standard TaqMan® single assay. As expected, the *Ct* values obtained in the microfluidic cards correlated very well to the *Ct* values obtained with single gene expression assays, for the genes analysed (Figure 4.4).

In the study of Geier *et al.* (2013a) no reproducibility studies for validating the cDNA synthesis or inter-array variability were performed. In contrast, the cDNA synthesis and the TaqMan® arrays used in this study proved to be very robust (Figure 4.3).

Inter-donor variability in transporter expression in HBMECs was observed in this study. The correlation between the gene expression in donors 1 and 3 is 95%, whereas the correlation between donors 1 and 2 and 2 and 3 were 52% and 57%, respectively (Figure 4.12). Regarding the expression of organic cation transporters, strong inter-individual variability in the expression of OCT1 and OCT3 was observed (Figure 4.10). Strong variations in OCT transporters in other organs are well known. More than 100-fold variation has been observed in the expression of OCT1 in the liver (Nies *et al.* (2009) and O'Brien *et al.* (2013)). One explanation of this may be differences in methylation status (Schaeffeler *et al.* (2011)). Also the LAT-1 transporter (subunit SLC7A5), a well defined hallmark transporter in HBMECs showed, showed much higher expression in donor number 2 as in donors number 1 and 3. The same donor number 2, showed very low expression of MDR1 and ABCG2 (Figure 4.11). Differences in the expression of MDR1 have been attributed to genetic polymorphisms (Johne *et al.* (2002)), however, the three donors of the mRNA analysed in this work, were not genotyped.

5.9 Interaction between psychotropic drugs with high membrane permeability and OCT1

Neither citalopram, clozapine, amantadine nor lamotrigine benefited from the over expression of OCT1 to cross the cell membrane. All these drugs showed the same uptake in cells over-expressing OCT1 compared to control cells (Figure 4.32).

Citalopram and clozapine can inhibit OCT1 (Table 4.6). However they have high membrane permeability (Figure 4.1) and may simply diffuse through the cell membrane, making its interaction with OCT irrelevant for their *in vitro* uptake.

Although amantadine is a substrate of the rat Oct1 (Goralski *et al.* (2002)), this study shows that it is not a substrate of the human OCT1, as it has been stated by (Lozano

et al. (2013) and Becker *et al.* (2011)). These authors incorrectly cite a paper from Jonker & Schinkel (2004), where it is stated that amantadine is a substrate for the rat Oct1. Jonker & Schinkel (2004) correctly cite the paper of Goralski *et al.* (2002) where it is shown that amantadine is transported by the rat Oct1. It is known for other substrates that the mouse, rat and human OCT1 differ in their substrate specificity (Dresser *et al.* (2000)).

This study suggests also that lamotrigine does not depend on OCT1 to penetrate cell membranes. Lamotrigine (Dickens *et al.* (2012)) has been proposed to be a substrate for OCT1 in KCL22 cells. Measurements of OCT1-mediated drug uptake in this cells has been heavily criticised. KCL22 cells have been used to show *in vitro* uptake of imatinib by OCT1, which has been refuted by recent publications (Burger *et al.* (2013) and Nies *et al.* (2014)).

In this work it is shown that there is no increase in the uptake of lamotrigine in OCT1 over expressing HEK293 cells in comparison to the control cells. The HEK293 cell lines used in the present study have been established by targeted chromosomal gene integration and extensively validated (Saadatmand *et al.* (2012)), and present a much better model to study the uptake of lamotrigine by OCT1. Further evidence which supports the finding that lamotrigine is not a substrate for OCT1 is the fact that lamotrigine is very lipophilic and not protonated at the physiological pH of 7.4 ($pK_a = 3.41$, $\text{Log}D_{7.4} = 1.99$ and 0% protonated at pH 7.4, Table 4.1).

5.9.1 The interaction of amitriptyline with OCT1

Amitriptyline is an interesting drug to be analyzed from the point of view of personalized medicine guided by pharmacogenomics, as it is extensively metabolized in the liver. The influence of polymorphisms on liver metabolising enzymes on amitriptyline pharmacokinetics has already been studied in detail (Kirchheiner *et al.* (2004) and Steimer *et al.* (2004)), however, nothing is known about drug influx transporters. OCT1 is the major organic cation transporter in the liver, and amitriptyline has been already shown to interact with OCT1 by inhibiting the uptake of the OCT1 model substrate ASP^+ (Ahlin *et al.* (2008)). This finding was confirmed in this study by showing that amitriptyline inhibits the OCT1-mediated uptake of MPP^+ and morphine (Figures 4.33 and 4.37).

The measurements of amitriptyline uptake in OCT1 over-expressing cells in comparison to the control cells showed a big variation, as seen on figure 4.34 A. Despite the big variation, the average uptake in OCT1 over-expressing cells was higher than in the control cells. However, the standard error of the mean in the control cells was higher

than the increase in the uptake observed in the OCT1 over-expressing cells. This may be related to the fact that amitriptyline is a very lipophilic drug with high membrane permeability (Figure 4.1 and Table 4.1). However, when analysing each independent experiment, the uptake of amitriptyline was between 18% and 31% higher in the cells over-expressing OCT1 in comparison the control cells (Figure (4.34 B)).

The presence of serum did not affect the uptake of amitriptyline by OCT1. As expected, the net cellular uptake in the presence of serum was lower, as serum reduces the amount of drug which free to cross the cell membrane (Figure 4.35). *In vivo*, the fraction of amitriptyline which is bound to serum is 92.7% (Brunton & Knollman (2011)). However, as observed on figure 4.35, the reduction in the uptake of amitriptyline in the presence of serum was only between 40%-74%. In the *in vitro* system used in this work, other factors like drug binding to the plastic in the cell culture plates may contribute to the final amitriptyline amounts determined after cell lysis and could explain why in the presence of serum the reduction was not equal to the fraction bound to plasma proteins.

The inhibition of amitriptyline uptake in OCT1-overexpressing cells and control cells in the presence of inhibitors could not shown that amitriptyline is a substrate for OCT1. The typical OCT1 inhibitor MPP⁺ did not reduced the uptake of amitriptyline in cells over-expressing OCT1 and in the control cell lines. Incubation with desipramine reduced the uptake of amitriptyline in cells over-expressing OCT1, but also in the control cells (Figure 4.36), showing that this reduction of the uptake does not depend on OCT1.

The inhibition of amitriptyline uptake by desipramine in the control cell lines, as well as in the OCT1-overexpressing cells, can also be due a phenomena called "lysosomal trapping" (Ohkuma & Poole (1978), de Duve *et al.* (1974), Daniel *et al.* (2001) and Kazmi *et al.* (2013)). Lysosomal trapping is typical for lipophilic drugs (LogP >1) with a pKa above 6. This is the case for both amitriptyline and desipramine (Table 4.1). Such drugs can easily diffuse through the cell membrane, and when they diffuses into the lysosomes, they become protonated (lysosomes have a pH of 4-5) and do not diffuse back into the cell, resulting in an accumulation of drug in the lysosome (Kazmi *et al.* (2013)). The accumulation ratio in lysosomes for mono- and dibasic drugs are about 3 and 1000 times the total volume of the cell (Kazmi *et al.* (2013)). Lysosomal trapping is a saturable process (Daniel *et al.* (2001)) and one hypothesis is that desipramine may compete for the lysosomal trapping of amitriptyline and therefore, reduce the drug uptake. The hypothesis of lysosomal trapping was confirmed, because NH₄Cl also inhibited the uptake of amitriptyline in both cell lines. NH₄Cl is a competitor for the lysosomal trapping of drugs (Kazmi *et al.* (2013)). Lysosomal trapping does not depend on the expression of membrane transporters and therefore, it is observed in both the OCT1 over-expressing cells and in the control cells.

Although OCT1 mediated amitriptyline uptake could not be shown in the *in vivo* model used in this study, it cannot be ruled out that OCT1 has a role in amitriptyline pharmacokinetics as amitriptyline has a big affinity for OCT1 (Ahlin *et al.* (2008) and Figures 4.37 and 4.33). OCT1 polymorphisms have been shown in humans to be important in the pharmacokinetics (ondansetron) and pharmacodynamics (ondansetron and imatinib) of drugs, which could not be shown *in vitro* to be OCT1 substrates (Tzvetkov *et al.* (2012), White *et al.* (2007), White *et al.* (2010) and Burger *et al.* (2013) and Nies *et al.* (2014)). Studies in patients and healthy volunteers may be required in order to fully understand whether OCT1 has a role on the pharmacokinetics of amitriptyline.

5.9.2 Inhibition of OCT1-mediated morphine uptake by antidepressants and other drugs

Although the antidepressants analysed in this study did not benefit from OCT1 to penetrate cell membranes, they can still interact with OCT1. Here it was shown that antidepressants (amitriptyline, clomipramine, fluoxetine and imipramine), and other drugs can inhibit the OCT1-mediated uptake of morphine (Figures 4.37 and 4.38). Morphine is eliminated through glucuronidation in the liver, and has been identified as a substrate for OCT1. Furthermore, the pharmacokinetics of morphine have been shown to depend on OCT1-mediated liver uptake Tzvetkov *et al.* (2013).

Co-medication with irinotecan, a cancer drug which may be administered together with morphine, may result in higher morphine plasma concentrations. At clinically relevant concentrations, irinotecan inhibited 76% of the OCT1-mediated morphine uptake (Table 4.7).

The concentration of drugs on the portal vein is transiently higher than on the peripheral circulation because drugs have not yet been subjected to first pass metabolism in the liver. When considering the maximal unbound concentration in the portal vein, irinotecan, ondansetron and verapamil are able to inhibit more than 50% of the OCT1-mediated morphine uptake (Table 4.7).

New molecular entities may be tested for OCT1 inhibition during drug development if they are expected to be given together with morphine. In addition, other opioids should also be tested for these interactions. The International transporter consortium recommends that a clinical drug-drug interaction study is performed in case a relevant drug-drug interaction is identified. When the ratio $C_{Max,Unb}/IC_{50}$ is equal or greater than 0.1 a relevant drug-drug interaction may occur (Giacomini *et al.* (2010)). This was the case for irinotecan (i.v) and ondansetron (oral) (Table 4.7). The pharmacokinetics of ondansetron, may depend on the CYP2D6 genotype (Kaiser *et al.* (2002)), making

its plasma concentrations, and OCT1 inhibition potential, genotype-dependent. This is an example of a possibly complex drug-gene-drug interaction.

The OCT1 variants *2 and *3 have a residual morphine transport activity, meaning that they are still able to transport small amounts of morphine.(Tzvetkov *et al.* (2013)). It is known that different OCT1 variants react differently to OCT1 inhibitors (Ahlin *et al.* (2011)). The study of the inhibition of morphine-mediated OCT1 uptake in OCT1 variants *2 and *3 also needs to be considered.

5.10 Genetic variants in OCT1 affect the uptake of the biogenic amine tyramine

Polymorphisms in the OCT1 gene reduced tyramine uptake (Figure 4.41). Tyramine is a biogenic amine that is produced as a by-product of bacterial fermentation. It is produced by bacteria like *Carnobacterium sp.* and *Lactobacillus sp.* (Masson *et al.* (1996)). As a product of bacterial fermentation, tyramine is present in food products like smoked meat, cheese and wine (Pechanek *et al.* (1983)). High amounts of tyramine in the blood may lead to high blood pressure, migraine and nausea. Tyramine is metabolised by mono-amine oxidases (MAO), which are present in the liver (Grimsby *et al.* (1990)). The ability of tyramine to interact with OCT1, and the kinetic parameters of tyramine uptake by OCT1 were analysed in this study (Section 4.8). The intrinsic clearance of tyramine by OCT1 was in the same order of magnitude as previously reported (Schömig *et al.* (2006)). Tyramine represents therefore a good example of how genetics may be related to food and natural compounds. It is ,however, unlikely that tyramine represented a selection process for the loss of OCT1 activity, as nausea, migraine and high blood pressure are not directly life-threatening conditions. Still, according to the *in vitro* evidence presented in this study, carriers of decreased function OCT1 alleles may experience increases blood pressure and unpleasant feelings when eating food containing tyramine. This hypothesis needs confirmation *in vivo*.

5.11 Establishment of a MDCK II cell line for targeted chromosomal integration

One of the aims of this work was to develop models to study drug transport at the blood-brain barrier. One approach was to use the hCMEC/D3 cell line to study influx transport of psychotropic drugs. The other approach was to develop a cell line which may be used in the future to study the transport of drugs by efflux transporters .

In this work, a MDCK II cell line, including a site for target chromosomal integration in its genome, was established. To achieve this goal, the pFRT/LacZeo plasmid was transfected into the cell line, and after successfully picking of the clones, the cell line demonstrated TEER measurements between 150-200 $\text{Ohm} * \text{cm}^2$ (Figure 4.42), which were similar to the untransfected control cell line, and in accordance with values reported in the literature for the MDCK II cell line (Soldner *et al.* (2000)). The successful integration of the plasmid was confirmed by measuring the functionality of the β -Galactosidase marker gene by means of an ONPG hydrolysis assay (Figure 4.43). This does not, however, show how many copies of the plasmid are integrated in the genome of the MDCKII-pFRT/LacZeo cell lines. Quantitative real-time PCR may be used to quantify the number of copies of the plasmid which were integrated in the genome of the parental MDCK II cell line (Abad *et al.* (2010) and Huang *et al.* (2013)).

The MDCK II cell line is a strain isolated from the parental MDCK cell line, and is the most commonly used MDCK strain (Dukes *et al.* (2011)). The parental MDCK cell line and the MDCK I strain, have unstable phenotypes (Dukes *et al.* (2011)), and therefore may not be as suitable as the MDCK II cell line for the establishment of transporter models. The MDCK II cell line has been widely used to study vectorial transport with efflux transporters by research groups which are well established in the field (example: Jonker *et al.* (2000) and Poller *et al.* (2011)).

This MDCK II cell line can in the future be used as a model to study efflux transport, by allowing the stable expression of transporter genes. In particular, the targeted chromosomal integration approach is interesting for studying transporter pharmacogenetics. This approach guarantees that after stable integration of the genes, the membrane transporters carrying different genetic variants, will be expressed at the same level, allowing the comparison between different genetic variants.

6

Conclusion

This study has shown that most psychiatric drugs have high membrane permeability, and may not require carrier-mediated efflux transport to enter cells. The potential of the PAMPA assay (Parallel Artificial Membrane Permeability Assay) to quickly screen drugs with high and low membrane permeability was also shown. Using the PAMPA assay, the psychotropic drugs amisulpride and sulpiride were identified as drugs with limited membrane permeability which benefit from carrier-mediated transport to cross cellular barriers.

Amisulpride is a substrate for all the organic cation transporters of the SLC22 family, OCT1, OCT2, OCT3, OCTN1 and OCTN2. On the other hand, sulpiride is only a substrate for OCT1 and OCT2. The OCTs of the SLC22 family may contribute to the penetration of amisulpride and sulpiride through the blood-brain barrier, but further work is required in order to clarify the clinical implications of these findings, with respect to therapy efficacy, genetic variation in drug transporters and potential drug-drug interactions. Although amisulpride and sulpiride are not metabolized in the liver, OCT1 may still be relevant for their biliary clearance, which accounts for ca. 20% of the total clearance of amisulpride and sulpiride. Amisulpride and sulpiride are slowly absorbed, and it remains unknown whether OCT1 plays a role on the enterohepatic circulation of amisulpride and sulpiride, and whether it contributes to a longer permanence of these drugs in the body. On the other hand, amisulpride and sulpiride are predominantly eliminated in the kidney and have a high renal clearance, suggesting a secretion mechanism in the kidney proximal tubules. In this context, OCT2 was identified as the transporter which is likely responsible for the removal of amisulpride and sulpiride from the blood on the renal proximal tubule. Furthermore, amisulpride, the most important psychotropic drug within the benzodiazepine class, was also identified as a substrate for MATE1 and MATE2-K transporters, which may also contribute to its renal secretion

and blood-brain barrier transport (in case of MATE1). However, OCT2, and not the MATEs, is likely the limiting step in the secretion of amisulpride in the kidney.

Extensive gene expression analysis were carried out in primary cells from the brain and in tissues relevant for drug distribution. It was shown that the expression of organic cation transporter in brain tissues is much lower compared to the expression in, for example, liver or kidney. According to this study, the organic cation transporters OCT1, OCT3, OCTN1, OCTN2 and MATE1 are expressed at the blood-brain barrier. However, OCT1, OCT3, OCTN1 and MATE1 are expressed at low levels. In contrast, the expression of efflux transporters like MDR1 and BCRP was, as expected, very high at the blood-brain barrier. Considering the evidence presented in this study, and available the literature, leads to the conclusion that the study of the expression of membrane transporters at the blood-brain barrier is not a simple question. The presence of organic cation transporters in brain microvascular endothelial cells is still in debate, with different authors, reporting contradictory results. This also reflects the difficulties in studying the brain, and in obtaining brain material from humans. Still, it becomes clear that even if organic cation transporters are expressed in the blood-brain barrier, they are not expressed at high levels. Likely, there is a not yet identified transporter which can transport organic cations through the blood-brain barrier. On the other hand, some drugs may also take advantage of nutrient transporters which are highly expressed at the blood-brain barrier, like LAT-1 (amino-acid transporter) in order to penetrate the brain.

It was shown that some psychotropic drugs with high membrane permeability interact strongly with OCT1, and are capable of inhibiting the OCT1 mediated uptake of drugs which depend on OCT1 to be metabolized in the liver, as morphine. Potentially relevant drug-drug interactions involving morphine and OCT1 were identified. Irinotecan, ondansetron and verapamil are able to inhibit the OCT1 mediated uptake of morphine by more than 50% at concentrations which are clinically relevant.

Several drugs which are known to interact with OCT1, such as amitriptyline, citalopramin, clozapine, lamotrigine and amantadine were tested as OCT1 substrates. It is concluded that OCT1 does not mediate the *in vitro* uptake of any of these drugs in the models used. However, other examples, like imatinib and ondansetron, exist, where OCT1 polymorphisms were suggested to affect the pharmacokinetics and efficacy in humans, although the affected drugs were not shown to be OCT1 substrates in the *in vitro* models used. Therefore, studies in patient cohorts or healthy volunteers are required in order to conclude on the influence of OCT1 polymorphisms on the pharmacokinetics of psychotropic drugs with high membrane permeability, like amitriptyline.

Tyramine, previously suggested as a substrate of OCT1, was identified in this work in relation to polymorphisms in the OCT1 gene. It was shown that tyramine uptake is lower

in cells over-expressing OCT1 genetic variants in comparison to cells over-expressing the *wild type* OCT1. Tyramine was studied in the context of finding naturally occurring substances (not synthetic drugs) which may depend on OCT1 to be eliminated in the liver, in order to find substances that may have been responsible during evolution for the appearance of very common genetic mutations in OCT1. Although it is likely that tyramine is not the substance responsible for establishing the selection pressure leading to OCT1 deficiency, it is a good example of how genetic variation may interact with food and nutrition.

In the context of establishing a model of the blood-brain barrier, the hCMEC/D3 cell line was used at the Institute of Clinical Pharmacology to show carrier-mediated transport of amisulpride and sulpiride in a relevant blood-brain barrier model. This work also showed that the hCMEC/D3 cell line does not express either OCT1 or OCT2. Comparing this work, and work from other authors, it can be concluded that there is a not yet identified carrier-mediated transport mechanism in the hCMEC/D3 cell line which has some substrate overlap with OCT1 (amisulpride, sulpiride, tramadol). The identification of this transporter could in the future be achieved through methods like high-throughput RNA-sequencing and searching for gene homology, as well as by studying the uptake of these drugs in the presence of different inhibitors. Identifying this influx transport mechanism would bring the field of membrane transport at the blood-brain barrier a step further. As efflux transport may play a bigger role than influx transport at the blood-brain barrier, an MDCK II cell line ready for targeted chromosomal integration of transporter genes was successfully established and may be used in further studies analysing membrane drug permeability in cellular monolayers expressing several different efflux transporters and their genetic variants.

Ultimately, the identification of drugs which require membrane transport to cross cellular barriers, and the corresponding membrane transporters, is an important step in understanding the complexity of drug pharmacokinetics and variability in drug response. This may be especially true for psychotropic drugs acting in the central nervous system, which need to penetrate the blood-brain barrier to reach their site of action. This work can serve as basis for further, more complex and detailed studies analysing not only drug transport at the blood-brain barrier using the established models, but also to dissect the factors which may affect the pharmacokinetics of drugs like amisulpride and sulpiride, for which the relevant cation transporters are now known.

Appendix A

Assays used on the custom-made TaqMan[®] low density arrays

TABLE A.1: Reference numbers of the assays used on the custom made TaqMan[®] low density arrays. The assays signed with a * were also used as TaqMan[®] single assays for validating the low density arrays.

Gene	Assay Number	Gene	Assay number
ABCA1	Hs01059118_m1	SLC22A4	Hs00268200_m1
ABCA2	Hs00242232_m1	SLC22A5*	Hs00929869_m1
ABCA3	Hs00975530_m1	SLC22A6	Hs00537914_m1
ABCB1	Hs00184500_m1	SLC22A7	Hs00198527_m1
ABCB11	Hs00184824_m1	SLC22A8	Hs01056647_m1
ABCB4	Hs00240956_m1	SLC22A9	Hs00971064_m1
ABCB5	Hs00698751_m1	SLC25A13	Hs00185185_m1
ABCB6	Hs01039213_m1	SLC25A27	Hs00188687_m1
ABCB7	Hs00188776_m1	SLC28A1	Hs00984403_m1
ABCC1	Hs00219905_m1	SLC28A2	Hs00188407_m1
ABCC10	Hs00375701_m1	SLC28A3	Hs00910439_m1
ABCC11	Hs01090768_m1	SLC29A1	Hs01085706_m1
ABCC12	Hs00264354_m1	SLC29A2	Hs00155426_m1
ABCC2	Hs00166123_m1	SLC29A3	Hs00983219_m1
ABCC3	Hs00358656_m1	SLC2A1	Hs00892681_m1
ABCC4	Hs00988734_m1	SLC2A2	Hs01096904_m1
ABCC5	Hs00981087_m1	SLC2A3	Hs00359840_m1
ABCC6	Hs01081201_m1	SLC31A1	Hs00977268_g1
ABCC8	Hs01093761_m1	SLC38A2	Hs01089954_m1
ABCC9	Hs00245832_m1	SLC38A5	Hs01012028_m1
ABCD1	Hs00163610_m1	SLC3A1	Hs00165789_m1
ABCD3	Hs00161065_m1	SLC3A2	Hs00374243_m1
ABCG2	Hs01053790_m1	SLC47A1	Hs00217320_m1
ABCG8	Hs00223690_m1	SLC47A2	Hs00398719_m1
ACTB	Hs99999903_m1	SLC5A1	Hs01573790_m1
ATP7A	Hs00163707_m1	SLC5A4	Hs00429526_m1
ATP7B	Hs00163739_m1	SLC6A2	Hs01567442_m1
GAPDH	Hs99999905_m1	SLC6A3	Hs00997364_m1
HPRT1	Hs99999909_m1	SLC6A4	Hs00984355_g1
MVP	Hs00245438_m1	SLC6A6	Hs00161778_m1
SLC10A1	Hs00161820_m1	SLC7A11	Hs00204928_m1
SLC10A2	Hs01001557_m1	SLC7A5	Hs00185826_m1
SLC13A1	Hs00223704_m1	SLC7A6	Hs00938056_m1
SLC15A1	Hs00953898_m1	SLC7A7	Hs00909952_m1
SLC15A2	Hs00221539_m1	SLC7A8	Hs00794796_m1
SLC16A1	Hs00161826_m1	SLC7A9	Hs00943195_m1
SLC16A10	Hs01039921_m1	SLCO1A2	Hs00366488_m1
SLC16A2	Hs00185140_m1	SLCO1B1	Hs00272374_m1
SLC16A3	Hs00358829_m1	SLCO1B3	Hs00251986_m1
SLC19A1	Hs00953342_m1	SLCO2A1	Hs00194554_m1
SLC19A2	Hs00949693_m1	SLCO2B1	Hs00200670_m1
SLC19A3	Hs00228858_m1	SLCO3A1	Hs00203184_m1
SLC22A1*	Hs00427552_m1	SLCO4A1	Hs00249583_m1
SLC22A11	Hs00218486_m1	SLCO4C1	Hs00698884_m1
SLC22A12	Hs00375985_m1	SLCO5A1	Hs00229597_m1
SLC22A14	Hs00899722_m1	SLCO6A1	Hs00542846_m1
SLC22A2*	Hs01010723_m1	TBP*	Hs99999910_m1
SLC22A3	Hs01009568_m1	UBC	Hs00824723_m1

Appendix B

Step-by-step protocol for DAB-immunostaining of paraffin-embedded sections on glass

Protocol for the DAB-Immunostaining of paraffin-embedded sections on glass:

- Deparaffinization
 - 2 × 5 min Xylene
- Hydration
 - 10 min 100% Ethanol
 - 5 min 95% Ethanol
 - 5 min 70% Ethanol
 - 1 min ddH₂O
- Peroxidase block
 - 30 min 0,01 M PBS + 2 mL 30% H₂O₂
 - 1 min ddH₂O
- Antigen retrieval
 - 10 mM citrate buffer
 - 10 min microwave: 800 W until boiling, then 80 W
 - 15 min cool down
- Washing
 - 1 min ddH₂O
 - 15 min 0,01 M PBS + 0,1% Triton (permeabilisation of membranes)
 - 5 min 0,01 M PBS
- Unspecific block
 - 1h: 0,01 M PBS + 10% FCS + 4% milk powder
 - incubate by circle sections with a lipid pen
- Incubation with the primary antibody
 - Dilute primary antibody at specific concentration in 0,01 M PBS + 10% FCS
 - Overnight incubation
- Washing
 - 3x5 min 0,01 M PBS + 0,1% Triton
 - 1 min 0,01 M PBS

- Incubation with the secondary antibody
 - Dilute antibody (1:200) in 0,01 M PBS + 10% FCS
 - Incubate 1h at 37°C and during the waiting time prepare the ABC solution
- Washing
 - 3x5 min 0,01 M PBS
- ABC incubation (VECTASTAIN[®] Elite ABC system - Avidin/Biotin Complex)
 - 0,01 M PBS + 10% FCS + solution A 1:100 + solution B:100 (prepared at least 30 min before use and stored at 4°C)
 - Incubate 1,5h at 37°C
- Washing
 - 3x5 min 0,01 M PBS
- DAB staining
 - 5 mL 50mM Tris/HCl pH 7,5 + 100 μ L DAB stock solution (Toxic) + 2,5 μ L 30% H₂O₂ (added just before use)
 - DAB stock solution: 25 mg/mL in 50 mM Tris/HCl pH 7,5
- Washing
 - 3x5 min 0,01 M PBS
- Counterstaining
 - 40 s filtered hematoxylin
 - dip in ddH₂O
 - 5 min under running tap water
- Dehydration
 - 1 min 70% Ethanol
 - 5 min 95% Ethanol
 - 10 min 100% Ethanol
 - 2x5 min Xylene
- Embedding
 - Eukitt Quick hardening mounting medium

Appendix C

Gene expression of membrane transporters - Tables

TABLE C.1: Gene expression analysis in tissues and primary cells - Part 1. Liver and kidney show the average of one sample measured two independent times. Intestine, Brain, Astrocytes and CP. Epi. Cells (choroid plexus epithelial cells) were determined one time. HBMECs (human brain microvascular endothelial cells) represent the average of three samples obtained from three different donors, measured more than 2 times each (the results for each donor are shown on tables C.3, C.4 and C.5).

Gene	Liver	Kidney	Intestine	Brain	Astrocytes	CP. Epi. Cells	HBMECs
ABCA1	1.080	0.071	0.195	0.058	0.039	0.063	0.171
ABCA2	0.022	0.073	0.065	1.175	0.062	0.031	0.019
ABCA3	0.016	0.079	0.021	0.445	0.003	0.027	0.165
ABCB1	0.336	0.474	1.050	0.085	0.008	0.012	0.092
ABCB11	0.026	0.000	0.000	0.000	0.001	0.000	0.000
ABCB4	0.998	0.011	0.004	0.003	0.007	0.005	0.015
ABCB5	0.000	0.000	0.000	0.000	0.000	0.000	0.000
ABCB6	0.034	0.050	0.031	0.045	0.023	0.026	0.030
ABCB7	0.188	0.308	0.307	0.179	0.142	0.126	0.106
ABCC1	0.012	0.021	0.028	0.011	0.043	0.055	0.088
ABCC10	0.045	0.042	0.094	0.079	0.064	0.047	0.076
ABCC11	0.013	0.001	0.000	0.002	0.000	0.000	0.000
ABCC12	0.000	0.000	0.000	0.000	0.000	0.000	0.000
ABCC2	0.047	0.158	0.167	0.001	0.001	0.000	0.001
ABCC3	0.200	0.087	0.128	0.001	0.051	0.013	0.000
ABCC4	0.019	0.240	0.050	0.023	0.024	0.096	0.034
ABCC5	0.035	0.148	0.100	0.393	0.066	0.054	0.049
ABCC6	0.031	0.023	0.021	0.000	0.000	0.000	0.000
ABCC8	0.000	0.001	0.002	0.126	0.000	0.000	0.000
ABCC9	0.016	0.014	0.020	0.010	0.000	0.001	0.000
ABCD1	0.003	0.002	0.014	0.000	0.004	0.002	0.002
ABCD3	0.108	0.178	0.103	0.059	0.036	0.044	0.027
ABCG2	0.063	0.020	0.604	0.094	0.000	0.001	0.341
ABCG8	0.152	0.000	0.409	0.003	0.000	0.000	0.000
ATP7A	0.000	0.000	0.000	0.000	0.000	0.000	0.000
ATP7B	0.067	0.044	0.117	0.042	0.019	0.025	0.033
SLC10A1	0.048	0.000	0.000	0.000	0.000	0.000	0.000
SLC10A2	0.000	0.082	0.314	0.000	0.000	0.000	0.000
SLC13A1	0.000	1.382	0.067	0.000	0.000	0.000	0.000
SLC15A1	0.016	0.281	2.046	0.000	0.001	0.002	0.000
SLC15A2	0.002	0.078	0.007	0.079	0.001	0.001	0.000
SLC16A1	0.227	0.188	0.131	0.111	0.164	0.275	0.205
SLC16A10	0.169	0.067	0.074	0.042	0.000	0.011	0.000
SLC16A2	0.022	0.022	0.002	0.022	0.010	0.032	0.005
SLC16A3	0.021	0.054	0.035	0.015	0.084	0.144	0.377
SLC19A1	0.025	0.012	0.081	0.023	0.025	0.049	0.039
SLC19A2	0.064	0.132	0.081	0.101	0.037	0.139	0.031
SLC19A3	0.432	0.032	0.090	0.015	0.001	0.001	0.001
SLC22A1	1.697	0.003	0.001	0.001	0.001	0.001	0.001
SLC22A11	0.002	0.399	0.000	0.000	0.000	0.000	0.000
SLC22A12	0.000	0.534	0.000	0.000	0.000	0.000	0.000
SLC22A14	0.000	0.002	0.001	0.003	0.001	0.001	0.000
SLC22A2	0.000	0.870	0.001	0.002	0.000	0.000	0.000
SLC22A3	0.144	0.061	0.054	0.013	0.001	0.000	0.002
SLC22A4	0.001	0.007	0.006	0.001	0.000	0.001	0.001

TABLE C.3: Gene expression analysis in human brain microvascular endothelial cells - **Donor 1**. Samples 1 and 2 represent the same cDNA run on two different microfluidic cards. Samples 3 and 4 represent independent measurements (RNA synthesis and real-time qPCR) of this sample. Figure 4.3 A shows the graphical representation of the correlation between samples 2 and 3 (independent cDNA synthesis) and Figure 4.3 B shows the graphical representation of the correlation between samples 1 and 2 (same cDNA synthesis, independent microfluidic cards).

Drug membrane transporter expression in HBMECs - Donor 1											
Detector	Measurement					Detector	Measurement				
	1	2	3	4	Average		1	2	3	4	Average
ABCA1	0.206	0.237	0.228	0.338	0.252	SLC22A5	0.020	0.023	0.017	0.044	0.026
ABCA2	0.017	0.022	0.012	0.039	0.022	SLC22A6	0.000	0.000	0.000	0.000	0.000
ABCA3	0.299	0.308	0.275	0.424	0.327	SLC22A7	0.000	0.000	0.000	0.000	0.000
ABCB1	0.169	0.223	0.156	0.278	0.207	SLC22A8	0.000	0.000	0.000	0.000	0.000
ABCB11	0.000	0.000	0.000	0.000	0.000	SLC22A9	0.000	0.000	0.000	0.000	0.000
ABCB4	0.021	0.029	0.029	0.044	0.031	SLC25A13	0.104	0.125	0.090	0.195	0.128
ABCB5	0.000	0.000	0.000	0.000	0.000	SLC25A27	0.004	0.006	0.004	0.011	0.007
ABCB6	0.032	0.024	0.024	0.071	0.038	SLC28A1	0.000	0.000	0.000	0.000	0.000
ABCB7	0.089	0.100	0.095	0.247	0.133	SLC28A2	0.000	0.000	0.000	0.000	0.000
ABCC1	0.098	0.100	0.096	0.296	0.147	SLC28A3	0.001	0.000	0.000	0.000	0.000
ABCC10	0.090	0.079	0.096	0.154	0.105	SLC29A1	0.765	0.939	0.792	2.599	1.274
ABCC11	0.000	0.000	0.000	0.000	0.000	SLC29A2	0.004	0.002	0.003	0.008	0.004
ABCC12	0.000	0.000	0.000	0.000	0.000	SLC29A3	0.027	0.049	0.025	0.099	0.050
ABCC2	0.001	0.003	0.001	0.002	0.002	SLC2A1	0.406	0.339	0.450	0.680	0.468
ABCC3	0.000	0.000	0.000	0.000	0.000	SLC2A2	0.000	0.000	0.000	0.000	0.000
ABCC4	0.025	0.018	0.018	0.046	0.027	SLC2A3	0.068	0.052	0.061	0.096	0.069
ABCC5	0.052	0.034	0.041	0.096	0.056	SLC31A1	0.152	0.221	0.130	0.437	0.235
ABCC6	0.000	0.000	0.000	0.000	0.000	SLC38A2	0.197	0.258	0.169	0.306	0.233
ABCC8	0.000	0.000	0.000	0.000	0.000	SLC38A5	0.015	0.013	0.010	0.049	0.022
ABCC9	0.000	0.000	0.000	0.000	0.000	SLC3A1	0.000	0.000	0.000	0.000	0.000
ABCD1	0.003	0.002	0.003	0.002	0.003	SLC3A2	0.675	0.429	0.699	0.930	0.683
ABCD3	0.036	0.031	0.027	0.042	0.034	SLC47A1	0.000	0.000	0.000	0.000	0.000
ABCG2	0.520	0.539	0.538	1.136	0.683	SLC47A2	0.000	0.000	0.000	0.000	0.000
ABCG8	0.000	0.000	0.000	0.000	0.000	SLC5A1	0.000	0.000	0.001	0.000	0.000
ATP7A	0.000	0.000	0.000	0.000	0.000	SLC5A4	0.009	0.011	0.008	0.013	0.010
ATP7B	0.043	0.056	0.047	0.070	0.054	SLC6A2	0.000	0.000	0.000	0.000	0.000
SLC10A1	0.000	0.000	0.000	0.000	0.000	SLC6A3	0.000	0.000	0.000	0.000	0.000
SLC10A2	0.000	0.000	0.000	0.000	0.000	SLC6A4	0.000	0.000	0.000	0.000	0.000
SLC13A1	0.000	0.000	0.000	0.000	0.000	SLC6A6	0.052	0.061	0.065	0.109	0.072
SLC15A1	0.000	0.000	0.000	0.000	0.000	SLC7A11	0.374	0.427	0.375	0.555	0.433
SLC15A2	0.000	0.000	0.000	0.000	0.000	SLC7A5	0.077	0.079	0.064	0.074	0.073
SLC16A1	0.147	0.200	0.150	0.435	0.233	SLC7A6	0.161	0.149	0.142	0.270	0.180
SLC16A10	0.000	0.000	0.002	0.001	0.001	SLC7A7	0.010	0.010	0.008	0.011	0.010
SLC16A2	0.004	0.006	0.005	0.010	0.006	SLC7A8	0.001	0.002	0.003	0.006	0.003
SLC16A3	0.369	0.238	0.403	0.474	0.371	SLC7A9	0.000	0.000	0.001	0.000	0.000
SLC19A1	0.034	0.038	0.043	0.056	0.043	SLCO1A2	0.000	0.000	0.000	0.000	0.000
SLC19A2	0.022	0.032	0.028	0.034	0.029	SLCO1B1	0.000	0.000	0.000	0.000	0.000
SLC19A3	0.001	0.002	0.000	0.001	0.001	SLCO1B3	0.000	0.000	0.000	0.000	0.000
SLC22A1	0.000	0.005	0.001	0.001	0.002	SLCO2A1	0.053	0.040	0.044	0.148	0.071
SLC22A11	0.000	0.000	0.000	0.000	0.000	SLCO2B1	0.010	0.002	0.001	0.011	0.006
SLC22A12	0.000	0.000	0.000	0.000	0.000	SLCO3A1	0.002	0.002	0.002	0.003	0.002
SLC22A14	0.000	0.000	0.000	0.000	0.000	SLCO4A1	0.010	0.008	0.007	0.022	0.012
SLC22A2	0.000	0.000	0.000	0.000	0.000	SLCO4C1	0.003	0.005	0.002	0.004	0.003
SLC22A3	0.000	0.000	0.000	0.001	0.000	SLCO5A1	0.000	0.000	0.000	0.001	0.000
SLC22A4	0.003	0.002	0.001	0.001	0.002	SLCO6A1	0.000	0.000	0.000	0.000	0.000

TABLE C.4: Gene expression analysis in human brain microvascular endothelial cells - **Donor 2**. Samples 1 and 2 represent independent measurements (RNA synthesis and real-time qPCR) of this sample. Figure 4.3 A shows the graphical representation of the correlation between samples 1 and 2.

Drug membrane transporter expression in HBMECs - Donor 2							
Gene	Measurement			Gene	Measurement		
	1	2	Average		1	1	Average
ABCA1	0.192	0.149	0.170	SLC22A5	0.011	0.014	0.013
ABCA2	0.030	0.022	0.026	SLC22A6	0.000	0.000	0.000
ABCA3	0.009	0.010	0.009	SLC22A7	0.000	0.000	0.000
ABCB1	0.005	0.004	0.004	SLC22A8	0.000	0.000	0.000
ABCB11	0.000	0.000	0.000	SLC22A9	0.000	0.000	0.000
ABCB4	0.007	0.004	0.005	SLC25A13	0.035	0.033	0.034
ABCB5	0.000	0.000	0.000	SLC25A27	0.002	0.002	0.002
ABCB6	0.016	0.016	0.016	SLC28A1	0.000	0.000	0.000
ABCB7	0.055	0.076	0.066	SLC28A2	0.000	0.000	0.000
ABCC1	0.046	0.068	0.057	SLC28A3	0.001	0.002	0.001
ABCC10	0.054	0.066	0.060	SLC29A1	0.057	0.110	0.083
ABCC11	0.000	0.000	0.000	SLC29A2	0.004	0.002	0.003
ABCC12	0.000	0.000	0.000	SLC29A3	0.015	0.031	0.023
ABCC2	0.001	0.001	0.001	SLC2A1	0.192	0.205	0.199
ABCC3	0.000	0.000	0.000	SLC2A2	0.000	0.000	0.000
ABCC4	0.026	0.034	0.030	SLC2A3	0.236	0.239	0.237
ABCC5	0.044	0.051	0.048	SLC31A1	0.168	0.290	0.229
ABCC6	0.000	0.000	0.000	SLC38A2	0.403	0.331	0.367
ABCC8	0.000	0.000	0.000	SLC38A5	0.006	0.006	0.006
ABCC9	0.001	0.001	0.001	SLC3A1	0.000	0.000	0.000
ABCD1	0.001	0.001	0.001	SLC3A2	0.946	0.590	0.768
ABCD3	0.024	0.019	0.022	SLC47A1	0.001	0.000	0.000
ABCG2	0.012	0.010	0.011	SLC47A2	0.000	0.000	0.000
ABCG8	0.000	0.000	0.000	SLC5A1	0.000	0.000	0.000
ATP7A	0.000	0.000	0.000	SLC5A4	0.000	0.001	0.001
ATP7B	0.017	0.028	0.022	SLC6A2	0.000	0.000	0.000
SLC10A1	0.000	0.000	0.000	SLC6A3	0.000	0.000	0.000
SLC10A2	0.000	0.000	0.000	SLC6A4	0.000	0.000	0.000
SLC13A1	0.000	0.000	0.000	SLC6A6	0.017	0.014	0.016
SLC15A1	0.000	0.000	0.000	SLC7A11	0.161	0.156	0.158
SLC15A2	0.000	0.000	0.000	SLC7A5	0.410	0.355	0.382
SLC16A1	0.115	0.202	0.158	SLC7A6	0.074	0.063	0.068
SLC16A10	0.000	0.000	0.000	SLC7A7	0.001	0.000	0.001
SLC16A2	0.005	0.007	0.006	SLC7A8	0.001	0.002	0.001
SLC16A3	0.368	0.357	0.362	SLC7A9	0.000	0.000	0.000
SLC19A1	0.020	0.017	0.019	SLCO1A2	0.000	0.000	0.000
SLC19A2	0.031	0.039	0.035	SLCO1B1	0.000	0.000	0.000
SLC19A3	0.001	0.002	0.001	SLCO1B3	0.000	0.000	0.000
SLC22A1	0.000	0.001	0.001	SLCO2A1	0.003	0.003	0.003
SLC22A11	0.000	0.000	0.000	SLCO2B1	0.000	0.000	0.000
SLC22A12	0.000	0.000	0.000	SLCO3A1	0.001	0.000	0.001
SLC22A14	0.000	0.000	0.000	SLCO4A1	0.000	0.000	0.000
SLC22A2	0.000	0.000	0.000	SLCO4C1	0.000	0.001	0.000
SLC22A3	0.003	0.004	0.003	SLCO5A1	0.000	0.001	0.000
SLC22A4	0.001	0.000	0.001	SLCO6A1	0.000	0.000	0.000

TABLE C.5: Gene expression analysis in human brain microvascular endothelial cells (HBMECs) - **Donor 3**. Samples 1 and 2 represent independent measurements (RNA synthesis and real-time qPCR) of this sample. Figure 4.3 A shows the graphical representation of the correlation between samples 1 and 2.

Drug membrane transporter expression in HBMECs - Donor 3							
Gene	Measurement			Gene	Measurement		
	1	2	Average		1	2	Average
ABCA1	0.090	0.092	0.091	SLC22A5	0.011	0.013	0.012
ABCA2	0.009	0.009	0.009	SLC22A6	0.000	0.000	0.000
ABCA3	0.162	0.156	0.159	SLC22A7	0.000	0.000	0.000
ABCB1	0.070	0.063	0.066	SLC22A8	0.000	0.000	0.000
ABCB11	0.000	0.000	0.000	SLC22A9	0.000	0.000	0.000
ABCB4	0.007	0.009	0.008	SLC25A13	0.098	0.083	0.090
ABCB5	0.000	0.000	0.000	SLC25A27	0.001	0.001	0.001
ABCB6	0.030	0.044	0.037	SLC28A1	0.000	0.000	0.000
ABCB7	0.128	0.113	0.121	SLC28A2	0.000	0.000	0.000
ABCC1	0.063	0.054	0.058	SLC28A3	0.001	0.001	0.001
ABCC10	0.056	0.068	0.062	SLC29A1	0.831	0.970	0.901
ABCC11	0.000	0.000	0.000	SLC29A2	0.002	0.001	0.002
ABCC12	0.000	0.000	0.000	SLC29A3	0.028	0.029	0.028
ABCC2	0.001	0.000	0.000	SLC2A1	0.360	0.345	0.353
ABCC3	0.000	0.000	0.000	SLC2A2	0.000	0.000	0.000
ABCC4	0.037	0.051	0.044	SLC2A3	0.109	0.109	0.109
ABCC5	0.045	0.042	0.043	SLC31A1	0.147	0.128	0.137
ABCC6	0.000	0.000	0.000	SLC38A2	0.165	0.118	0.142
ABCC8	0.000	0.000	0.000	SLC38A5	0.014	0.007	0.010
ABCC9	0.000	0.000	0.000	SLC3A1	0.000	0.000	0.000
ABCD1	0.001	0.001	0.001	SLC3A2	0.478	0.481	0.479
ABCD3	0.028	0.021	0.025	SLC47A1	0.000	0.000	0.000
ABCG2	0.389	0.266	0.327	SLC47A2	0.000	0.000	0.000
ABCG8	0.000	0.000	0.000	SLC5A1	0.000	0.000	0.000
ATP7A	0.000	0.000	0.000	SLC5A4	0.002	0.003	0.003
ATP7B	0.024	0.024	0.024	SLC6A2	0.000	0.000	0.000
SLC10A1	0.000	0.000	0.000	SLC6A3	0.000	0.000	0.000
SLC10A2	0.000	0.000	0.000	SLC6A4	0.000	0.000	0.000
SLC13A1	0.000	0.000	0.000	SLC6A6	0.037	0.034	0.035
SLC15A1	0.000	0.000	0.000	SLC7A11	0.137	0.136	0.136
SLC15A2	0.001	0.000	0.000	SLC7A5	0.116	0.086	0.101
SLC16A1	0.227	0.222	0.225	SLC7A6	0.107	0.085	0.096
SLC16A10	0.000	0.000	0.000	SLC7A7	0.006	0.006	0.006
SLC16A2	0.002	0.002	0.002	SLC7A8	0.001	0.000	0.001
SLC16A3	0.379	0.419	0.399	SLC7A9	0.001	0.000	0.000
SLC19A1	0.064	0.050	0.057	SLCO1A2	0.000	0.000	0.000
SLC19A2	0.030	0.030	0.030	SLCO1B1	0.000	0.000	0.000
SLC19A3	0.001	0.001	0.001	SLCO1B3	0.000	0.000	0.000
SLC22A1	0.000	0.000	0.000	SLCO2A1	0.185	0.156	0.171
SLC22A11	0.000	0.000	0.000	SLCO2B1	0.002	0.000	0.001
SLC22A12	0.000	0.000	0.000	SLCO3A1	0.002	0.002	0.002
SLC22A14	0.000	0.000	0.000	SLCO4A1	0.003	0.006	0.004
SLC22A2	0.000	0.000	0.000	SLCO4C1	0.000	0.000	0.000
SLC22A3	0.002	0.001	0.002	SLCO5A1	0.000	0.002	0.001
SLC22A4	0.001	0.001	0.001	SLCO6A1	0.000	0.000	0.000

TABLE C.6: Gene expression analysis in the hCMEC/D3 cell line. Figure 4.14 shows the graphical representation of the data contained in this table.

Drug membrane transporter expression in the hCMEC/D3 cell line

Gene		Gene	
ABCA1	0.019	SLC22A5	0.014
ABCA2	0.009	SLC22A6	0.000
ABCA3	0.164	SLC22A7	0.000
ABCB1	0.185	SLC22A8	0.000
ABCB11	0.000	SLC22A9	0.000
ABCB4	0.000	SLC25A13	0.080
ABCB5	0.000	SLC25A27	0.000
ABCB6	0.018	SLC28A1	0.000
ABCB7	0.090	SLC28A2	0.000
ABCC1	0.029	SLC28A3	0.000
ABCC10	0.038	SLC29A1	0.870
ABCC11	0.000	SLC29A2	0.001
ABCC12	0.000	SLC29A3	0.011
ABCC2	0.001	SLC2A1	0.884
ABCC3	0.031	SLC2A2	0.000
ABCC4	0.050	SLC2A3	0.041
ABCC5	0.022	SLC31A1	0.147
ABCC6	0.000	SLC38A2	0.110
ABCC8	0.000	SLC38A5	0.016
ABCC9	0.000	SLC3A1	0.000
ABCD1	0.000	SLC3A2	0.487
ABCD3	0.029	SLC47A1	0.000
ABCG2	0.074	SLC47A2	0.000
ABCG8	0.000	SLC5A1	0.000
ATP7A	0.000	SLC5A4	0.002
ATP7B	0.004	SLC6A2	0.000
SLC10A1	0.000	SLC6A3	0.000
SLC10A2	0.000	SLC6A4	0.000
SLC13A1	0.000	SLC6A6	0.013
SLC15A1	0.000	SLC7A11	0.199
SLC15A2	0.001	SLC7A5	0.049
SLC16A1	0.260	SLC7A6	0.113
SLC16A10	0.000	SLC7A7	0.000
SLC16A2	0.000	SLC7A8	0.001
SLC16A3	0.408	SLC7A9	0.000
SLC19A1	0.026	SLCO1A2	0.000
SLC19A2	0.026	SLCO1B1	0.000
SLC19A3	0.000	SLCO1B3	0.000
SLC22A1	0.000	SLCO2A1	0.068
SLC22A11	0.000	SLCO2B1	0.000
SLC22A12	0.000	SLCO3A1	0.000
SLC22A14	0.000	SLCO4A1	0.024
SLC22A2	0.000	SLCO4C1	0.000
SLC22A3	0.000	SLCO5A1	0.000
SLC22A4	0.001	SLCO6A1	0.000

TABLE C.7: Gene expression analysis in the HEK-OCT1 and HEK-pcDNA5 cell lines.
Figure 4.13 shows the graphical representation of the data contained in this table.

Drug membrane transporter expression in the HEK-OCT1 and HEK-pcDNA5 cell lines

Gene	Sample		Gene	Sample	
	HEK-OCT1	HEK-pcDNA5		HEK-OCT1	HEK-pcDNA5
ABCA1	0.000	0.000	SLC22A5	0.112	0.110
ABCA2	0.042	0.044	SLC22A6	0.000	0.000
ABCA3	0.152	0.157	SLC22A7	0.000	0.000
ABCB1	0.136	0.157	SLC22A8	0.000	0.000
ABCB11	0.000	0.000	SLC22A9	0.000	0.000
ABCB4	0.003	0.009	SLC25A13	0.321	0.499
ABCB5	0.000	0.000	SLC25A27	0.028	0.039
ABCB6	0.031	0.041	SLC28A1	0.000	0.000
ABCB7	0.434	0.434	SLC28A2	0.000	0.000
ABCC1	0.065	0.055	SLC28A3	0.000	0.000
ABCC10	0.080	0.111	SLC29A1	1.011	0.922
ABCC11	0.000	0.000	SLC29A2	0.037	0.036
ABCC12	0.000	0.000	SLC29A3	0.044	0.044
ABCC2	0.001	0.001	SLC2A1	0.584	0.662
ABCC3	0.000	0.000	SLC2A2	0.000	0.000
ABCC4	0.240	0.211	SLC2A3	0.013	0.037
ABCC5	0.108	0.112	SLC31A1	0.303	0.342
ABCC6	0.000	0.000	SLC38A2	0.175	0.161
ABCC8	0.001	0.000	SLC38A5	0.000	0.000
ABCC9	0.000	0.000	SLC3A1	0.000	0.000
ABCD1	0.000	0.001	SLC3A2	0.688	0.710
ABCD3	0.167	0.166	SLC47A1	0.038	0.033
ABCG2	0.014	0.014	SLC47A2	0.000	0.000
ABCG8	0.000	0.000	SLC5A1	0.000	0.000
ATP7A	0.000	0.000	SLC5A4	0.000	0.000
ATP7B	0.167	0.146	SLC6A2	0.000	0.000
SLC10A1	0.000	0.000	SLC6A3	0.000	0.000
SLC10A2	0.000	0.000	SLC6A4	0.000	0.000
SLC13A1	0.000	0.000	SLC6A6	0.075	0.083
SLC15A1	0.005	0.001	SLC7A11	0.054	0.052
SLC15A2	0.001	0.001	SLC7A5	0.155	0.153
SLC16A1	0.802	0.810	SLC7A6	0.175	0.233
SLC16A10	0.187	0.201	SLC7A7	0.000	0.000
SLC16A2	0.032	0.023	SLC7A8	0.078	0.066
SLC16A3	0.000	0.001	SLC7A9	0.001	0.001
SLC19A1	0.363	0.351	SLCO1A2	0.000	0.000
SLC19A2	0.131	0.159	SLCO1B1	0.000	0.000
SLC19A3	0.012	0.010	SLCO1B3	0.000	0.000
SLC22A1	16.163	0.002	SLCO2A1	0.001	0.002
SLC22A11	0.000	0.000	SLCO2B1	0.000	0.000
SLC22A12	0.000	0.000	SLCO3A1	0.018	0.010
SLC22A14	0.000	0.000	SLCO4A1	0.076	0.076
SLC22A2	0.000	0.000	SLCO4C1	0.017	0.009
SLC22A3	0.000	0.000	SLCO5A1	0.049	0.047
SLC22A4	0.000	0.000	SLCO6A1	0.000	0.000

Bibliography

- Abad, Sandra, Kitz, Kerstin, Hörmann, Astrid, Schreiner, Ulrike, Hartner, Franz S., & Glieder, Anton. 2010. Real-time PCR-based determination of gene copy numbers in *Pichia pastoris*. *Biotechnology journal*, **5**(4), 413–420.
- About, A. Y., Chevanne, F., & Le Corre, P. 2009. Influence of efflux transporters on liver, bile and brain disposition of amitriptyline in mice. *International journal of pharmaceutics*, **378**(1-2), 80–85.
- Ahlin, G., Chen, L., Lazorova, L., Chen, Y., Ianculescu, A. G., Davis, R. L., Giacomini, K. M., & Artursson, P. 2011. Genotype-dependent effects of inhibitors of the organic cation transporter, OCT1: predictions of metformin interactions. *The pharmacogenomics journal*, **11**(6), 400–411.
- Ahlin, Gustav, Karlsson, Johan, Pedersen, Jenny M., Gustavsson, Lena, Larsson, Rolf, Matsson, Pär, Norinder, Ulf, Bergström, Christel A. S., & Artursson, Per. 2008. Structural requirements for drug inhibition of the liver specific human organic cation transport protein 1. *Journal of medicinal chemistry*, **51**(19), 5932–5942.
- Artursson, P. 1990. Epithelial transport of drugs in cell culture. I: A model for studying the passive diffusion of drugs over intestinal absorptive (Caco-2) cells. *Journal of pharmaceutical sciences*, **79**(6), 476–482.
- Becker, Matthijs L., Visser, Loes E., van Schaik, Ron H. N., Hofman, Albert, Uitterlinden, André G., & Stricker, Bruno H. Ch. 2011. OCT1 polymorphism is associated with response and survival time in anti-Parkinsonian drug users. *Neurogenetics*, **12**(1), 79–82.
- Bednarczyk, Dallas, Ekins, Sean, Wikel, James H., & Wright, Stephen H. 2003. Influence of molecular structure on substrate binding to the human organic cation transporter, hOCT1. *Molecular pharmacology*, **63**(3), 489–498.
- Boado, R. J., Li, J. Y., Nagaya, M., Zhang, C., & Pardridge, W. M. 1999. Selective expression of the large neutral amino acid transporter at the blood-brain barrier.

- Proceedings of the National Academy of Sciences of the United States of America*, **96**(21), 12079–12084.
- Brockmöller, Jürgen, & Tzvetkov, Mladen V. 2013. Polymorphic OCT1: a valid biomarker, but for which drugs? *Pharmacogenomics*, **14**(16), 1933–1936.
- Brunton, Laurence L, & Knollman, Björn C. 2011. *Goodman and Gilman's The Pharmacological Basis of Therapeutics*. McGraw-Hill.
- Budak, Murat T., Alpdogan, Onder S., Zhou, Mingyuan, Lavker, Robert M., Akinci, M. A. Murat, & Wolosin, J. Mario. 2005. Ocular surface epithelia contain ABCG2-dependent side population cells exhibiting features associated with stem cells. *Journal of cell science*, **118**(Pt 8), 1715–1724.
- Burger, Herman, Mathijssen, Ron H.J., Sparreboom, Alex, & Wiemer, Erik A.C. 2013. Can specific OCT1 inhibitors be used to determine OCT1 transporter activity towards imatinib? *Blood*, **121**(24).
- Cecchelli, Romeo, Berezowski, Vincent, Lundquist, Stefan, Culot, Maxime, Renftel, Mila, Dehouck, Marie-Pierre, & Fenart, Laurence. 2007. Modelling of the blood-brain barrier in drug discovery and development. *Nature reviews. Drug discovery*, **6**(8), 650–661.
- Chang, Ting-Ting, Shyu, Ming-Kwang, Huang, Min-Chuan, Hsu, Chen-Chi, Yeh, Szu-Yu, Chen, Mei-Ru, & Lin, Chun-Jung. 2011. Hypoxia-mediated down-regulation of OCTN2 and PPAR α expression in human placentas and in BeWo cells. *Molecular pharmaceutics*, **8**(1), 117–125.
- Culot, Maxime, Fabulas-da Costa, Anaëlle, Sevin, Emmanuel, Szorath, Erica, Martinsson, Stefan, Renftel, Mila, Hongmei, Yan, Cecchelli, Romeo, & Lundquist, Stefan. 2013. A simple method for assessing free brain/free plasma ratios using an in vitro model of the blood brain barrier. *PloS one*, **8**(12), e80634.
- Daniel, W. A., Bickel, M. H., & Honegger, U. E. 1995. The contribution of lysosomal trapping in the uptake of desipramine and chloroquine by different tissues. *Pharmacology & toxicology*, **77**(6), 402–406.
- Daniel, W. A., Wójcikowski, J., & Palucha, A. 2001. Intracellular distribution of psychotropic drugs in the grey and white matter of the brain: the role of lysosomal trapping. *British journal of pharmacology*, **134**(4), 807–814.
- Dauchy, Sandrine, Miller, Florence, Couraud, Pierre-Olivier, Weaver, Richard J., Weksler, Babette, Romero, Ignacio-Andres, Scherrmann, Jean-Michel, De Waziers, Isabelle, & Declèves, Xavier. 2009. Expression and transcriptional regulation of ABC

- transporters and cytochromes P450 in hCMEC/D3 human cerebral microvascular endothelial cells. *Biochemical pharmacology*, **77**(5), 897–909.
- de Duve, C., de Barse, T., Poole, B., Trouet, A., Tulkens, P., & Van Hoof, F. 1974. Commentary. Lysosomotropic agents. *Biochemical pharmacology*, **23**(18), 2495–2531.
- Dickens, David, Owen, Andrew, Alfirevic, Ana, Giannoudis, Athina, Davies, Andrea, Weksler, Babette, Romero, Ignacio A., Couraud, Pierre-Olivier, & Pirmohamed, Munir. 2012. Lamotrigine is a substrate for OCT1 in brain endothelial cells. *Biochemical pharmacology*, **83**(6), 805–814.
- Dobson, Paul D., & Kell, Douglas B. 2008. Carrier-mediated cellular uptake of pharmaceutical drugs: an exception or the rule? *Nature reviews. Drug discovery*, **7**(3), 205–220.
- Dos Santos Pereira, Joao N., Tadjerpisheh, Sina, Abed, Manar Abu, Saadatmand, Ali R., Weksler, Babette, Romero, Ignacio A., Couraud, Pierre-Olivier, Brockmüller, Jürgen, & Tzvetkov, Mladen V. 2014. The Poorly Membrane Permeable Antipsychotic Drugs Amisulpride and Sulpiride Are Substrates of the Organic Cation Transporters from the SLC22 Family. *The AAPS journal*, **16**(6), 1247–1258.
- Dost, Friedrich Hartmut. 1949. Die Clearance. *Klinische Wochenschrift*, **27**(15-16), 257–264.
- Dost, Friedrich Hartmut. 1953. *Der Blutspiegel. Kinetik der Konzentrationsabläufe in der Kreislauflüssigkeit*. Georg Thieme Verlag, Leipzig.
- Dresser, M. J., Gray, A. T., & Giacomini, K. M. 2000. Kinetic and selectivity differences between rodent, rabbit, and human organic cation transporters (OCT1). *The Journal of pharmacology and experimental therapeutics*, **292**(3), 1146–1152.
- Dufour, A, & De Santi, C. 1988. Pharmacokinetics and metabolism of amisulpride (In French). *Ann Psychiatr.*, **3**(7).
- Dukes, Joseph D., Whitley, Paul, & Chalmers, Andrew D. 2011. The MDCK variety pack: choosing the right strain. *BMC cell biology*, **12**(Oct), 43.
- Fan, Jianghong, & de Lannoy, Inés A. M. 2014. Pharmacokinetics. *Biochemical pharmacology*, **87**(1), 93–120.
- Fellner, Stephan, Bauer, Björn, Miller, David S., Schaffrik, Martina, Fankhänel, Martina, Spruss, Thilo, Bernhardt, Günther, Graeff, Claudia, Färber, Lothar, Gschaidmeier, Harald, Buschauer, Armin, & Fricker, Gert. 2002. Transport of paclitaxel (Taxol) across the blood-brain barrier in vitro and in vivo. *The Journal of clinical investigation*, **110**(9), 1309–1318.

- Feng, Bo, Mills, Jessica B., Davidson, Ralph E., Mireles, Rouchelle J., Janiszewski, John S., Troutman, Matthew D., & de Morais, Sonia M. 2008. In vitro P-glycoprotein assays to predict the in vivo interactions of P-glycoprotein with drugs in the central nervous system. *Drug metabolism and disposition: the biological fate of chemicals*, **36**(2), 268–275.
- Feng, Bo, LaPerle, Jennifer L., Chang, George, & Varma, Manthena V. S. 2010. Renal clearance in drug discovery and development: molecular descriptors, drug transporters and disease state. *Expert opinion on drug metabolism & toxicology*, **6**(8), 939–952.
- Fisher, Danielle S., Partridge, Suzanne J., Handley, Simon A., Couchman, Lewis, Morgan, Phillip E., & Flanagan, Robert J. 2013. LC-MS/MS of some atypical antipsychotics in human plasma, serum, oral fluid and haemolysed whole blood. *Forensic science international*, **229**(1-3), 145–150.
- Franks, N. P., & Lieb, W. R. 1978. Where do general anaesthetics act? *Nature*, **274**(5669), 339–342.
- Fröhlich, Otto, Klein, Janet D., Smith, Pauline M., Sands, Jeff M., & Gunn, Robert B. 2004. Urea transport in MDCK cells that are stably transfected with UT-A1. *American journal of physiology. Cell physiology*, **286**(6), C1264–C1270.
- Funk, Ryan S., & Krise, Jeffrey P. 2012. Cationic amphiphilic drugs cause a marked expansion of apparent lysosomal volume: implications for an intracellular distribution-based drug interaction. *Molecular pharmaceutics*, **9**(5), 1384–1395.
- Geier, E. G., Chen, E. C., Webb, A., Papp, A. C., Yee, S. W., Sadee, W., & Giacomini, K. M. 2013a. Profiling solute carrier transporters in the human blood-brain barrier. *Clinical pharmacology and therapeutics*, **94**(6), 636–639.
- Geier, Ethan G., Schlessinger, Avner, Fan, Hao, Gable, Jonathan E., Irwin, John J., Sali, Andrej, & Giacomini, Kathleen M. 2013b. Structure-based ligand discovery for the Large-neutral Amino Acid Transporter 1, LAT-1. *Proceedings of the National Academy of Sciences of the United States of America*, **110**(14), 5480–5485.
- Giacomini, Kathleen M., Huang, Shiew-Mei, Tweedie, Donald J., Benet, Leslie Z., Brouwer, Kim L. R., Chu, Xiaoyan, Dahlin, Amber, Evers, Raymond, Fischer, Volker, Hillgren, Kathleen M., Hoffmaster, Keith A., Ishikawa, Toshihisa, Keppler, Dietrich, Kim, Richard B., Lee, Caroline A., Niemi, Mikko, Polli, Joseph W., Sugiyama, Yuichi, Swaan, Peter W., Ware, Joseph A., Wright, Stephen H., Yee, Sook Wah, Zamek-Gliszczyński, Maciej J., & Zhang, Lei. 2010. Membrane transporters in drug development. *Nature reviews. Drug discovery*, **9**(3), 215–236.

- Goralski, Kerry B., Lou, Ganlu, Prowse, Matthew T., Gorboulev, Valentin, Volk, Christopher, Koepsell, Hermann, & Sitar, Daniel S. 2002. The cation transporters rOCT1 and rOCT2 interact with bicarbonate but play only a minor role for amantadine uptake into rat renal proximal tubules. *The Journal of pharmacology and experimental therapeutics*, **303**(3), 959–968.
- Grauer, Markus T., & Uhr, Manfred. 2004. P-glycoprotein reduces the ability of amitriptyline metabolites to cross the blood brain barrier in mice after a 10-day administration of amitriptyline. *Journal of psychopharmacology (Oxford, England)*, **18**(1), 66–74.
- Grimsby, J., Lan, N. C., Neve, R., Chen, K., & Shih, J. C. 1990. Tissue distribution of human monoamine oxidase A and B mRNA. *Journal of neurochemistry*, **55**(4), 1166–1169.
- Ha Choi, Ji, Wah Yee, Sook, Kim, Mee J., Nguyen, Loan, Ho Lee, Jeong, Kang, Ji-One, Hesselson, Stephanie, Castro, Richard A., Stryke, Doug, Johns, Susan J., Kwok, Pui-Yan, Ferrin, Thomas E., Goo Lee, Min, Black, Brain L., Ahituv, Nadav, & Giacomini, Kathleen M. 2009. Identification and characterization of novel polymorphisms in the basal promoter of the human transporter, MATE1. *Pharmacogenetics and genomics*, **19**(10), 770–780.
- Haenisch, Britta, Drescher, Eva, Thiemer, Lidia, Xin, Hu, Giros, Bruno, Gautron, Sophie, & Bönisch, Heinz. 2012. Interaction of antidepressant and antipsychotic drugs with the human organic cation transporters hOCT1, hOCT2 and hOCT3. *Naunyn-Schmiedeberg's archives of pharmacology*, **385**(10), 1017–1023.
- Hammarlund-Udenaes, Margareta, Fridén, Markus, Syvänen, Stina, & Gupta, Anubha. 2008. On the rate and extent of drug delivery to the brain. *Pharmaceutical research*, **25**(8), 1737–1750.
- Han, Tianxiang Kevin, Everett, Ruth S., Proctor, William R., Ng, Chee M., Costales, Chester L., Brouwer, Kim L. R., & Thakker, Dhiren R. 2013. Organic cation transporter 1 (OCT1/mOct1) is localized in the apical membrane of Caco-2 cell monolayers and enterocytes. *Molecular pharmacology*, **84**(2), 182–189.
- Hediger, Matthias A., Cléménçon, Benjamin, Burrier, Robert E., & Bruford, Elspeth A. 2013. The ABCs of membrane transporters in health and disease (SLC series): introduction. *Molecular aspects of medicine*, **34**(2-3), 95–107.
- Hendset, M., Haslemo, T., Rudberg, I., Refsum, H., & Molden, E. 2006. The complexity of active metabolites in therapeutic drug monitoring of psychotropic drugs. *Pharmacopsychiatry*, **39**(4), 121–127.

- Herrera, D., Mayet, L., Galindo, M. C., & Jung, H. 2000. Pharmacokinetics of a sustained-release dosage form of clomipramine. *Journal of clinical pharmacology*, **40**(12 Pt 2), 1488–1493.
- Hilgendorf, Constanze, Ahlin, Gustav, Seithel, Annick, Artursson, Per, Ungell, Anna-Lena, & Karlsson, Johan. 2007. Expression of thirty-six drug transporter genes in human intestine, liver, kidney, and organotypic cell lines. *Drug metabolism and disposition: the biological fate of chemicals*, **35**(8), 1333–1340.
- Hillgren, K. M., Keppler, D., Zur, A. A., Giacomini, K. M., Stieger, B., Cass, C. E., Zhang, L., & International Transporter Consortium. 2013. Emerging transporters of clinical importance: an update from the International Transporter Consortium. *Clinical pharmacology and therapeutics*, **94**(1), 52–63.
- Hodgson, J. 2001. ADMET—turning chemicals into drugs. *Nature biotechnology*, **19**(8), 722–726.
- Huang, Yuji, Yin, Xueren, Zhu, Changqing, Wang, Weiwei, Grierson, Donald, Xu, Changjie, & Chen, Kunsong. 2013. Standard addition quantitative real-time PCR (SAQPCR): a novel approach for determination of transgene copy number avoiding PCR efficiency estimation. *PloS one*, **8**(1), e53489.
- Ieiri, Ichiro, Higuchi, Shun, & Sugiyama, Yuichi. 2009. Genetic polymorphisms of uptake (OATP1B1, 1B3) and efflux (MRP2, BCRP) transporters: implications for inter-individual differences in the pharmacokinetics and pharmacodynamics of statins and other clinically relevant drugs. *Expert opinion on drug metabolism & toxicology*, **5**(7), 703–729.
- Ito, K., Iwatsubo, T., Kanamitsu, S., Ueda, K., Suzuki, H., & Sugiyama, Y. 1998. Prediction of pharmacokinetic alterations caused by drug-drug interactions: metabolic interaction in the liver. *Pharmacological reviews*, **50**(3), 387–412.
- Ito, Sumito, Kusahara, Hiroyuki, Yokochi, Miyu, Toyoshima, Junko, Inoue, Katsuhisa, Yuasa, Hiroaki, & Sugiyama, Yuichi. 2012. Competitive inhibition of the luminal efflux by multidrug and toxin extrusions, but not basolateral uptake by organic cation transporter 2, is the likely mechanism underlying the pharmacokinetic drug-drug interactions caused by cimetidine in the kidney. *The Journal of pharmacology and experimental therapeutics*, **340**(2), 393–403.
- Johne, Andreas, Köpke, Karla, Gerloff, Thomas, Mai, Ingrid, Rietbrock, Stephan, Meisel, Christian, Hoffmeyer, Sven, Kerb, Reinhold, Fromm, Martin F., Brinkmann, Ulrich, Eichelbaum, Michel, Brockmüller, Jürgen, Cascorbi, Ingolf, & Roots, Ivar.

2002. Modulation of steady-state kinetics of digoxin by haplotypes of the P-glycoprotein MDR1 gene. *Clinical pharmacology and therapeutics*, **72**(5), 584–594.
- Jonker, J. W., Smit, J. W., Brinkhuis, R. F., Maliepaard, M., Beijnen, J. H., Schellens, J. H., & Schinkel, A. H. 2000. Role of breast cancer resistance protein in the bioavailability and fetal penetration of topotecan. *Journal of the National Cancer Institute*, **92**(20), 1651–1656.
- Jonker, Johan W., & Schinkel, Alfred H. 2004. Pharmacological and physiological functions of the polyspecific organic cation transporters: OCT1, 2, and 3 (SLC22A1-3). *The Journal of pharmacology and experimental therapeutics*, **308**(1), 2–9.
- Jung, Norma, Lehmann, Clara, Rubbert, Andrea, Knispel, Meike, Hartmann, Pia, van Lunzen, Jan, Stellbrink, Hans-Juergen, Faetkenheuer, Gerd, & Taubert, Dirk. 2008. Relevance of the organic cation transporters 1 and 2 for antiretroviral drug therapy in human immunodeficiency virus infection. *Drug metabolism and disposition: the biological fate of chemicals*, **36**(8), 1616–1623.
- Kaiser, Rolf, Sezer, Orhan, Papiés, Anja, Bauer, Steffen, Schelenz, Claudia, Tremblay, Pierre-Benoit, Possinger, Kurt, Roots, Ivar, & Brockmüller, Jürgen. 2002. Patient-tailored antiemetic treatment with 5-hydroxytryptamine type 3 receptor antagonists according to cytochrome P-450 2D6 genotypes. *Journal of clinical oncology : official journal of the American Society of Clinical Oncology*, **20**(12), 2805–2811.
- Kansy, M., Senner, F., & Gubernator, K. 1998. Physicochemical high throughput screening: parallel artificial membrane permeation assay in the description of passive absorption processes. *Journal of medicinal chemistry*, **41**(7), 1007–1010.
- Kawasaki, Yuki, Kato, Yukio, Sai, Yoshimichi, & Tsuji, Akira. 2004. Functional characterization of human organic cation transporter OCTN1 single nucleotide polymorphisms in the Japanese population. *Journal of pharmaceutical sciences*, **93**(12), 2920–2926.
- Kazmi, Faraz, Hensley, Tiffini, Pope, Chad, Funk, Ryan S., Loewen, Greg J., Buckley, David B., & Parkinson, Andrew. 2013. Lysosomal sequestration (trapping) of lipophilic amine (cationic amphiphilic) drugs in immortalized human hepatocytes (Fa2N-4 cells). *Drug metabolism and disposition: the biological fate of chemicals*, **41**(4), 897–905.
- Kelly, M. W., & Myers, C. W. 1990. Clomipramine: a tricyclic antidepressant effective in obsessive compulsive disorder. *DICP : the annals of pharmacotherapy*, **24**(7-8), 739–744.

- Kerb, Reinhold. 2006. Implications of genetic polymorphisms in drug transporters for pharmacotherapy. *Cancer letters*, **234**(1), 4–33.
- Kido, Y., Tamai, I., Ohnari, A., Sai, Y., Kagami, T., Nezu, J., Nikaïdo, H., Hashimoto, N., Asano, M., & Tsuji, A. 2001. Functional relevance of carnitine transporter OCTN2 to brain distribution of L-carnitine and acetyl-L-carnitine across the blood-brain barrier. *Journal of neurochemistry*, **79**(5), 959–969.
- Kido, Yasuto, Matsson, Pär, & Giacomini, Kathleen M. 2011. Profiling of a prescription drug library for potential renal drug-drug interactions mediated by the organic cation transporter 2. *Journal of medicinal chemistry*, **54**(13), 4548–4558.
- Kirchheiner, J., Nickchen, K., Bauer, M., Wong, M-L, Licinio, J., Roots, I., & Brockmüller, J. 2004. Pharmacogenetics of antidepressants and antipsychotics: the contribution of allelic variations to the phenotype of drug response. *Molecular psychiatry*, **9**(5), 442–473.
- Kirsch, Irving, Deacon, Brett J., Huedo-Medina, Tania B., Scoboria, Alan, Moore, Thomas J., & Johnson, Blair T. 2008. Initial severity and antidepressant benefits: a meta-analysis of data submitted to the Food and Drug Administration. *PLoS medicine*, **5**(2), e45.
- Kitamura, Atsushi, Higuchi, Kei, Okura, Takashi, & Deguchi, Yoshiharu. 2014. Transport characteristics of tramadol in the blood-brain barrier. *Journal of pharmaceutical sciences*, **103**(10), 3335–3341.
- Koepsell, Hermann. 2013. The SLC22 family with transporters of organic cations, anions and zwitterions. *Molecular aspects of medicine*, **34**(2-3), 413–435.
- Koepsell, Hermann, Lips, Katrin, & Volk, Christopher. 2007. Polyspecific organic cation transporters: structure, function, physiological roles, and biopharmaceutical implications. *Pharmaceutical research*, **24**(7), 1227–1251.
- Komossa, Katja, Rummel-Kluge, Christine, Hunger, Heike, Schmid, Franziska, Schwarz, Sandra, Silveira da Mota Neto, Joaquim I., Kissling, Werner, & Leucht, Stefan. 2010. Amisulpride versus other atypical antipsychotics for schizophrenia. *The Cochrane database of systematic reviews*, Jan, CD006624.
- König, Jörg, Müller, Fabian, & Fromm, Martin F. 2013. Transporters and drug-drug interactions: important determinants of drug disposition and effects. *Pharmacological reviews*, **65**(3), 944–966.
- Kusuhara, Hiroyuki, & Sugiyama, Yuichi. 2009. In vitro-in vivo extrapolation of transporter-mediated clearance in the liver and kidney. *Drug metabolism and pharmacokinetics*, **24**(1), 37–52.

- Kutz, K. 1993. Pharmacology, toxicology and human pharmacokinetics of tropisetron. *Annals of oncology : official journal of the European Society for Medical Oncology / ESMO*, **4 Suppl 3**, 15–18.
- Kwon, Y. 2001. *Handbook of essential pharmacokinetics, pharmacodynamics and drug metabolism for industrial scientists*. Kluwer Academic/Plenum publishers.
- Lin, Chun-Jung, Tai, Ying, Huang, Miao-Tzu, Tsai, Yuan-Feen, Hsu, Hao-Jui, Tzen, Kai-Yuan, & Liou, Horng-Huei. 2010. Cellular localization of the organic cation transporters, OCT1 and OCT2, in brain microvessel endothelial cells and its implication for MPTP transport across the blood-brain barrier and MPTP-induced dopaminergic toxicity in rodents. *Journal of neurochemistry*, **114**(3), 717–727.
- Logan, Randall, Kong, Alex C., Axcell, Erick, & Krise, Jeffrey P. 2014. Amine-containing molecules and the induction of an expanded lysosomal volume phenotype: a structure-activity relationship study. *Journal of pharmaceutical sciences*, **103**(5), 1572–1580.
- Lozano, Elisa, Herraiez, Elisa, Briz, Oscar, Robledo, Virginia S., Hernandez-Iglesias, Jorge, Gonzalez-Hernandez, Ana, & Marin, Jose J. G. 2013. Role of the plasma membrane transporter of organic cations OCT1 and its genetic variants in modern liver pharmacology. *BioMed research international*, **2013**(Jul), 692071.
- Masson, F., Talon, R., & Montel, M. C. 1996. Histamine and tyramine production by bacteria from meat products. *International journal of food microbiology*, **32**(1-2), 199–207.
- Meyer, Hans. 1899. Zur Theorie der Alkoholnarkose. *Archiv für experimentelle Pathologie und Pharmakologie*, **42**(2-4), 109–118.
- Miecz, Dorota, Januszewicz, Elzbieta, Czeredys, Magdalena, Hinton, Barry T., Berzowski, Vincent, Cecchelli, Roméo, & Nalecz, Katarzyna A. 2008. Localization of organic cation/carnitine transporter (OCTN2) in cells forming the blood-brain barrier. *Journal of neurochemistry*, **104**(1), 113–123.
- Missner, Andreas, & Pohl, Peter. 2009. 110 years of the Meyer-Overton rule: predicting membrane permeability of gases and other small compounds. *Chemphyschem : a European journal of chemical physics and physical chemistry*, **10**(9-10), 1405–1414.
- Moaddel, R., Patel, S., Jozwiak, K., Yamaguchi, R., Ho, P. C., & Wainer, I. W. 2005. Enantioselective binding to the human organic cation transporter-1 (hOCT1) determined using an immobilized hOCT1 liquid chromatographic stationary phase. *Chirality*, **17**(8), 501–506.

- Moon, Ya, Paek, In Bok, Kim, Hui-Hyun, Ji, Hye Young, Lee, Hye Won, Park, Hyoung-Geun, & Lee, Hye Suk. 2004. Determination of tiapride in human plasma using hydrophilic interaction liquid chromatography-tandem mass spectrometry. *Archives of pharmacal research*, **27**(9), 901–905.
- Moraes, M. O., Lerner, F. E., Corso, G., Bezerra, F. A., Moraes, M. E., & De Nucci, G. 1999. Fluoxetine bioequivalence study: quantification of fluoxetine and norfluoxetine by liquid chromatography coupled to mass spectrometry. *Journal of clinical pharmacology*, **39**(10), 1053–1061.
- Nellans, Hugh N. 1991. Paracellular intestinal transport: modulation of absorption. *Advanced Drug Delivery Reviews*, **7**, 339–364.
- Niemi, Mikko, Pasanen, Marja K., & Neuvonen, Pertti J. 2011. Organic anion transporting polypeptide 1B1: a genetically polymorphic transporter of major importance for hepatic drug uptake. *Pharmacological reviews*, **63**(1), 157–181.
- Nies, Anne T., Koepsell, Hermann, Winter, Stefan, Burk, Oliver, Klein, Kathrin, Kerb, Reinhold, Zanger, Ulrich M., Keppler, Dietrich, Schwab, Matthias, & Schaeffeler, Elke. 2009. Expression of organic cation transporters OCT1 (SLC22A1) and OCT3 (SLC22A3) is affected by genetic factors and cholestasis in human liver. *Hepatology (Baltimore, Md.)*, **50**(4), 1227–1240.
- Nies, Anne T., Koepsell, Hermann, Damme, Katja, & Schwab, Matthias. 2011. Organic cation transporters (OCTs, MATEs), in vitro and in vivo evidence for the importance in drug therapy. *Handbook of experimental pharmacology*, 105–167.
- Nies, Anne T., Schaeffeler, Elke, van der Kuip, Heiko, Cascorbi, Ingolf, Bruhn, Oliver, Kneba, Michael, Pott, Christiane, Hofmann, Ute, Volk, Christopher, Hu, Shuiying, Baker, Sharyn D., Sparreboom, Alex, Ruth, Peter, Koepsell, Hermann, & Schwab, Matthias. 2014. Cellular uptake of imatinib into leukemic cells is independent of human organic cation transporter 1 (OCT1). *Clinical cancer research : an official journal of the American Association for Cancer Research*, **20**(4), 985–994.
- O'Brien, Valerie P., Bokelmann, Kristin, Ramírez, Jacqueline, Jobst, Karoline, Ratain, Mark J., Brockmüller, Jürgen, & Tzvetkov, Mladen V. 2013. Hepatocyte nuclear factor 1 regulates the expression of the organic cation transporter 1 via binding to an evolutionary conserved region in intron 1 of the OCT1 gene. *The Journal of pharmacology and experimental therapeutics*, **347**(1), 181–192.
- Ohashi, Rikiya, Tamai, Ikumi, Inano, Akihiro, Katsura, Masaki, Sai, Yoshimichi, Nezu, Jun-ichi, & Tsuji, Akira. 2002. Studies on functional sites of organic cation/carnitine

- transporter OCTN2 (SLC22A5) using a Ser467Cys mutant protein. *The Journal of pharmacology and experimental therapeutics*, **302**(3), 1286–1294.
- Ohkuma, S., & Poole, B. 1978. Fluorescence probe measurement of the intralysosomal pH in living cells and the perturbation of pH by various agents. *Proceedings of the National Academy of Sciences of the United States of America*, **75**(7), 3327–3331.
- Ohtsuki, Sumio, Ikeda, Chiemi, Uchida, Yasuo, Sakamoto, Yumi, Miller, Florence, Glacial, Fabienne, Decleves, Xavier, Scherrmann, Jean-Michel, Couraud, Pierre-Olivier, Kubo, Yoshiyuki, Tachikawa, Masanori, & Terasaki, Tetsuya. 2013. Quantitative targeted absolute proteomic analysis of transporters, receptors and junction proteins for validation of human cerebral microvascular endothelial cell line hCMEC/D3 as a human blood-brain barrier model.”. *Molecular pharmaceutics*, **10**(1), 289–296.
- Okura, Takashi, Kato, Sayaka, & Deguchi, Yoshiharu. 2014a. Functional expression of organic cation/carnitine transporter 2 (OCTN2/SLC22A5) in human brain capillary endothelial cell line hCMEC/D3, a human blood-brain barrier model. *Drug metabolism and pharmacokinetics*, **29**(1), 69–74.
- Okura, Takashi, Higuchi, Kei, Kitamura, Atsushi, & Deguchi, Yoshiharu. 2014b. Proton-coupled organic cation antiporter-mediated uptake of apomorphine enantiomers in human brain capillary endothelial cell line hCMEC/D3. *Biological & pharmaceutical bulletin*, **37**(2), 286–291.
- Overton, Charles Ernst. 1901. *Studien über die Narkose zugleich ein Beitrag zur allgemeinen Pharmakologie*. Jena, Gustav Fischer.
- Pandit, Nita K., & Soltis, Robert P. 2011. *Introduction to the Pharmaceutical Sciences: An Integrated Approach*. Lippincott Williams & Wilkins.
- Pani, L., & Gessa, G. L. 2002. The substituted benzamides and their clinical potential on dysthymia and on the negative symptoms of schizophrenia. *Molecular psychiatry*, **7**(3), 247–253.
- Pauli-Magnus, C., von Richter, O., Burk, O., Ziegler, A., Mettang, T., Eichelbaum, M., & Fromm, M. F. 2000. Characterization of the major metabolites of verapamil as substrates and inhibitors of P-glycoprotein. *The Journal of pharmacology and experimental therapeutics*, **293**(2), 376–382.
- Pechanek, U., Pfannhauser, W., & Woidich, H. 1983. [Content of biogenic amines in four food groups of the Austrian marketplace]. *Zeitschrift für Lebensmittel-Untersuchung und -Forschung*, **176**(5), 335–340.

- Poller, Birk, Gutmann, Heike, Krähenbühl, Stephan, Weksler, Babette, Romero, Ignacio, Couraud, Pierre-Olivier, Tuffin, Gerald, Drewe, Jürgen, & Huwyler, Jörg. 2008. The human brain endothelial cell line hCMEC/D3 as a human blood-brain barrier model for drug transport studies. *Journal of neurochemistry*, **107**(5), 1358–1368.
- Poller, Birk, Wagenaar, Els, Tang, Seng Chuan, & Schinkel, Alfred H. 2011. Double-transduced MDCKII cells to study human P-glycoprotein (ABCB1) and breast cancer resistance protein (ABCG2) interplay in drug transport across the blood-brain barrier. *Molecular pharmaceutics*, **8**(2), 571–582.
- Rao, V. A., Bailey, J., Bishop, M., & Coppen, A. 1981. A clinical and pharmacodynamic evaluation of sulpiride. *Psychopharmacology*, **73**(1), 77–80.
- Rau, Thomas, Wohlleben, Gerlinde, Wuttke, Henrike, Thuerauf, Norbert, Lunkenheimer, Jens, Lanczik, Mario, & Eschenhagen, Thomas. 2004. CYP2D6 genotype: impact on adverse effects and nonresponse during treatment with antidepressants—a pilot study. *Clinical pharmacology and therapeutics*, **75**(5), 386–393.
- Ren, Qinghu, Chen, Kaixi, & Paulsen, Ian T. 2007. TransportDB: a comprehensive database resource for cytoplasmic membrane transport systems and outer membrane channels. *Nucleic acids research*, **35**(Database issue), D274–D279.
- Rosenzweig, P., Canal, M., Patat, A., Bergougnan, L., Zieleniuk, I., & Bianchetti, G. 2002. A review of the pharmacokinetics, tolerability and pharmacodynamics of amisulpride in healthy volunteers. *Human psychopharmacology*, **17**(1), 1–13.
- Saadatmand, Ali R. 2012. OCT1-mediated cellular drug uptake and interactions between drug transport and drug metabolism (Doctoral Thesis). *Georg-August University, Göttingen*.
- Saadatmand, Ali R., Tadjerpisheh, Sina, Brockmöller, Jürgen, & Tzvetkov, Mladen V. 2012. The prototypic pharmacogenetic drug debrisoquine is a substrate of the genetically polymorphic organic cation transporter OCT1. *Biochemical pharmacology*, **83**(10), 1427–1434.
- Schaefer, Olaf, Ohtsuki, Sumio, Kawakami, Hirotaka, Inoue, Tae, Liehner, Stephanie, Saito, Asami, Sakamoto, Atsushi, Ishiguro, Naoki, Matsumaru, Takehisa, Terasaki, Tetsuya, & Ebner, Thomas. 2012. Absolute quantification and differential expression of drug transporters, cytochrome P450 enzymes, and UDP-glucuronosyltransferases in cultured primary human hepatocytes. *Drug metabolism and disposition: the biological fate of chemicals*, **40**(1), 93–103.
- Schaeffeler, Elke, Hellerbrand, Claus, Nies, Anne T., Winter, Stefan, Kruck, Stephan, Hofmann, Ute, van der Kuip, Heiko, Zanger, Ulrich M., Koepsell, Hermann, & Schwab,

- Matthias. 2011. DNA methylation is associated with downregulation of the organic cation transporter OCT1 (SLC22A1) in human hepatocellular carcinoma. *Genome medicine*, **3**(12), 82.
- Schmitt, U., Abou El-Ela, A., Guo, L. J., Glavinas, H., Krajcsi, P., Baron, J. M., Tillmann, C., Hiemke, C., Langguth, P., & Härtter, S. 2006. Cyclosporine A (CsA) affects the pharmacodynamics and pharmacokinetics of the atypical antipsychotic amisulpride probably via inhibition of P-glycoprotein (P-gp). *Journal of neural transmission (Vienna, Austria : 1996)*, **113**(7), 787–801.
- Schömig, E., Lazar, A., & Gründemann, D. 2006. Extraneuronal monoamine transporter and organic cation transporters 1 and 2: a review of transport efficiency. *Handbook of experimental pharmacology*, 151–180.
- Schwenk, M. 1987. Drug transport in intestine, liver and kidney. *Archives of toxicology*, **60**(1-3), 37–42.
- Shawahna, Ramzi, Uchida, Yasuo, Declèves, Xavier, Ohtsuki, Sumio, Yousif, Salah, Dauchy, Sandrine, Jacob, Aude, Chassoux, Francine, Daumas-Duport, Catherine, Couraud, Pierre-Olivier, Terasaki, Tetsuya, & Scherrmann, Jean-Michel. 2011. Transcriptomic and quantitative proteomic analysis of transporters and drug metabolizing enzymes in freshly isolated human brain microvessels. *Molecular pharmaceuticals*, **8**(4), 1332–1341.
- Shimomura, Keita, Okura, Takashi, Kato, Sayaka, Couraud, Pierre-Olivier, Scherrmann, Jean-Michel, Terasaki, Tetsuya, & Deguchi, Yoshiharu. 2013. Functional expression of a proton-coupled organic cation (H⁺/OC) antiporter in human brain capillary endothelial cell line hCMEC/D3, a human blood-brain barrier model. *Fluids and barriers of the CNS*, **10**(1), 8.
- Shnitsar, Volodymyr, Eckardt, Ronny, Gupta, Shivangi, Grottker, Julia, Müller, Gerhard A., Koepsell, Hermann, Burckhardt, Gerhard, & Hagos, Yohannes. 2009. Expression of human organic cation transporter 3 in kidney carcinoma cell lines increases chemosensitivity to melphalan, irinotecan, and vincristine. *Cancer research*, **69**(4), 1494–1501.
- Shu, Yan, Sheardown, Steven A., Brown, Chaline, Owen, Ryan P., Zhang, Shuzhong, Castro, Richard A., Ianculescu, Alexandra G., Yue, Lin, Lo, Joan C., Burchard, Esteban G., Brett, Claire M., & Giacomini, Kathleen M. 2007. Effect of genetic variation in the organic cation transporter 1 (OCT1) on metformin action. *The Journal of clinical investigation*, **117**(5), 1422–1431.

- Smith, P. K., Krohn, R. I., Hermanson, G. T., Mallia, A. K., Gartner, F. H., Provenzano, M. D., Fujimoto, E. K., Goeke, N. M., Olson, B. J., & Klenk, D. C. 1985. Measurement of protein using bicinchoninic acid. *Analytical biochemistry*, **150**(1), 76–85.
- Soldner, A., Benet, L. Z., Mutschler, E., & Christians, U. 2000. Active transport of the angiotensin-II antagonist losartan and its main metabolite EXP 3174 across MDCK-MDR1 and caco-2 cell monolayers. *British journal of pharmacology*, **129**(6), 1235–1243.
- Somogyi, A., Stockley, C., Keal, J., Rolan, P., & Bochner, F. 1987. Reduction of metformin renal tubular secretion by cimetidine in man. *British journal of clinical pharmacology*, **23**(5), 545–551.
- Stalman, Robert, Seitz, Tina, Brockmüller, Jürgen, & Tzvetkov, Mladen V. 2014. What can we learn about the reasons for losing OCT1 activity by exploring the worldwide genetic variability in the OCT1 gene? *Naunyn-Schmiedeberg's Archives of Pharmacology. Deutsche Gesellschaft für Experimentelle und Klinische Pharmakologie und Toxikologie e.V.: Abstracts of the 80th Annual Meeting April 1-3, 2014 Hannover, Germany*, **387 (Suppl 1)**, S21.
- Steimer, Werner, Zöpf, Konstanze, von Amelunxen, Silvia, Pfeiffer, Herbert, Bachofer, Julia, Popp, Johannes, Messner, Barbara, Kissling, Werner, & Leucht, Stefan. 2004. Allele-specific change of concentration and functional gene dose for the prediction of steady-state serum concentrations of amitriptyline and nortriptyline in CYP2C19 and CYP2D6 extensive and intermediate metabolizers. *Clinical chemistry*, **50**(9), 1623–1633.
- Stevens, Lesley A., Coresh, Josef, Greene, Tom, & Levey, Andrew S. 2006. Assessing kidney function—measured and estimated glomerular filtration rate. *The New England journal of medicine*, **354**(23), 2473–2483.
- Stocker, S. L., Morrissey, K. M., Yee, S. W., Castro, R. A., Xu, L., Dahlin, A., Ramirez, A. H., Roden, D. M., Wilke, R. A., McCarty, C. A., Davis, R. L., Brett, C. M., & Giacomini, K. M. 2013a. The effect of novel promoter variants in MATE1 and MATE2 on the pharmacokinetics and pharmacodynamics of metformin. *Clinical pharmacology and therapeutics*, **93**(2), 186–194.
- Stocker, SL, Emami Riedmaier, A, Schwab, Matthias, & Giacomini, K. M. 2013b. OCT (SLC22A) and OCTN family. *Pharmacogenomics of Human Drug Transporters: John Wiley & Sons, Inc*, 171–208.

- Strazielle, N., & Ghersi-Egea, J. F. 2013. Physiology of blood-brain interfaces in relation to brain disposition of small compounds and macromolecules. *Molecular pharmaceuticals*, **10**(5), 1473–1491.
- Sugano, Kiyohiko, Kansy, Manfred, Artursson, Per, Avdeef, Alex, Bendels, Stefanie, Di, Li, Ecker, Gerhard F., Faller, Bernard, Fischer, Holger, Gerebtzoff, Grégori, Lennernaes, Hans, & Senner, Frank. 2010. Coexistence of passive and carrier-mediated processes in drug transport. *Nature reviews. Drug discovery*, **9**(8), 597–614.
- Suhre, Wendy M., Ekins, Sean, Chang, Cheng, Swaan, Peter W., & Wright, Stephen H. 2005. Molecular determinants of substrate/inhibitor binding to the human and rabbit renal organic cation transporters hOCT2 and rbOCT2. *Molecular pharmacology*, **67**(4), 1067–1077.
- Swift, Brandon, Nebot, Noelia, Lee, Jin Kyung, Han, Tianxiang, Proctor, William R., Thakker, Dhiren R., Lang, Dieter, Radtke, Martin, Gnoth, Mark J., & Brouwer, Kim L. R. 2013. Sorafenib hepatobiliary disposition: mechanisms of hepatic uptake and disposition of generated metabolites. *Drug metabolism and disposition: the biological fate of chemicals*, **41**(6), 1179–1186.
- Szatyłowicz, Halina. 2008. Structural aspects of the intermolecular hydrogen bond strength: H-bonded complexes of aniline, phenol and pyridine derivatives. *Journal of Physical Organic Chemistry*, **21**(10), 897–914.
- Tarling, Elizabeth J., de Aguiar Vallim, Thomas Q., & Edwards, Peter A. 2013. Role of ABC transporters in lipid transport and human disease. *Trends in endocrinology and metabolism: TEM*, **24**(7), 342–350.
- Tchaparian, Eskouhie H., Houghton, Jessica S., Uyeda, Craig, Grillo, Mark P., & Jin, Lixia. 2011. Effect of culture time on the basal expression levels of drug transporters in sandwich-cultured primary rat hepatocytes. *Drug metabolism and disposition: the biological fate of chemicals*, **39**(12), 2387–2394.
- Tzvetkov, M. V., Vormfelde, S. V., Balen, D., Meineke, I., Schmidt, T., Sehart, D., Sabolić, I., Koepsell, H., & Brockmüller, J. 2009. The effects of genetic polymorphisms in the organic cation transporters OCT1, OCT2, and OCT3 on the renal clearance of metformin. *Clinical pharmacology and therapeutics*, **86**(3), 299–306.
- Tzvetkov, M. V., Saadatmand, A. R., Lötsch, J., Tegeder, I., Stingl, J. C., & Brockmüller, J. 2011. Genetically polymorphic OCT1: another piece in the puzzle of the variable pharmacokinetics and pharmacodynamics of the opioidergic drug tramadol. *Clinical pharmacology and therapeutics*, **90**(1), 143–150.

- Tzvetkov, M. V., Saadatmand, A. R., Bokelmann, K., Meineke, I., Kaiser, R., & Brockmüller, J. 2012. Effects of OCT1 polymorphisms on the cellular uptake, plasma concentrations and efficacy of the 5-HT(3) antagonists tropisetron and ondansetron. *The pharmacogenomics journal*, **12**(1), 22–29.
- Tzvetkov, Mladen V., dos Santos Pereira, Joao N., Meineke, Ingolf, Saadatmand, Ali R., Stingl, Julia C., & Brockmüller, Jürgen. 2013. Morphine is a substrate of the organic cation transporter OCT1 and polymorphisms in OCT1 gene affect morphine pharmacokinetics after codeine administration. *Biochemical pharmacology*, **86**(5), 666–678.
- Uhlen, Mathias, Oksvold, Per, Fagerberg, Linn, Lundberg, Emma, Jonasson, Kalle, Forsberg, Mattias, Zwahlen, Martin, Kampf, Caroline, Wester, Kenneth, Hober, Sophia, Wernerus, Henrik, Björling, Lisa, & Ponten, Fredrik. 2010. Towards a knowledge-based Human Protein Atlas. *Nature biotechnology*, **28**(12), 1248–1250.
- Uhr, Manfred, Tontsch, Alina, Namendorf, Christian, Ripke, Stephan, Lucae, Susanne, Ising, Marcus, Dose, Tatjana, Ebinger, Martin, Rosenhagen, Marcus, Kohli, Martin, Kloiber, Stefan, Salyakina, Daria, Bettecken, Thomas, Specht, Michael, Pütz, Benno, Binder, Elisabeth B., Müller-Myhsok, Bertram, & Holsboer, Florian. 2008. Polymorphisms in the drug transporter gene ABCB1 predict antidepressant treatment response in depression. *Neuron*, **57**(2), 203–209.
- Ullrich, K. J. 1997. Renal transporters for organic anions and organic cations. Structural requirements for substrates. *The Journal of membrane biology*, **158**(2), 95–107.
- Vaupel, D. B., Lange, W. R., & London, E. D. 1993. Effects of verapamil on morphine-induced euphoria, analgesia and respiratory depression in humans. *The Journal of pharmacology and experimental therapeutics*, **267**(3), 1386–1394.
- Watanabe, Kazuhiro, Sawano, Tetsuya, Endo, Tetsuya, Sakata, Masakatsu, & Sato, Juichi. 2002. Studies on intestinal absorption of sulpiride (2): transepithelial transport of sulpiride across the human intestinal cell line Caco-2. *Biological & pharmaceutical bulletin*, **25**(10), 1345–1350.
- Weksler, B. B., Subileau, E. A., Perrière, N., Charneau, P., Holloway, K., Leveque, M., Tricoire-Leignel, H., Nicotra, A., Bourdoulous, S., Turowski, P., Male, D. K., Roux, F., Greenwood, J., Romero, I. A., & Couraud, P. O. 2005. Blood-brain barrier-specific properties of a human adult brain endothelial cell line. *FASEB journal : official publication of the Federation of American Societies for Experimental Biology*, **19**(13), 1872–1874.
- White, Deborah L., Sauders, Verity A., Dang, Phuong, Engler, Jane, Venables, Amity, Zrim, Stephanie, Zannettino, Andrew, Lynch, Kevin, Manley, Paul W., & Hughes,

- Timothy. 2007. Most CML patients who have a suboptimal response to imatinib have low OCT-1 activity: higher doses of imatinib may overcome the negative impact of low OCT-1 activity. *Blood*, **110**(12).
- White, Deborah L., Dang, Phuong, Engler, Jane, Frede, Amity, Zrim, Stephanie, Osborn, Michael, Sauders, Verity A., Manley, Paul W., & Hughes, Timothy. 2010. Functional activity of the OCT-1 Protein is Predictive of Long-Term Outcome in Patients With Chronic-Phase Chronic Myeloid Leukemia Treated With Imatinib. *Journal of Clinical Oncology*, **28**(16), 2761–2767.
- Wienkers, Larry C., & Heath, Timothy G. 2005. Predicting in vivo drug interactions from in vitro drug discovery data. *Nature reviews. Drug discovery*, **4**(10), 825–833.
- Wiesel, F. A., Alfredsson, G., Ehrnebo, M., & Sedvall, G. 1980. The pharmacokinetics of intravenous and oral sulpiride in healthy human subjects. *European journal of clinical pharmacology*, **17**(5), 385–391.
- Wirhth, Oliver, Multhaup, Gerd, Czech, Christian, Feldmann, Nicole, Blanchard, Véronique, Treppe, Günter, Beyreuther, Konrad, Pradier, Laurent, & Bayer, Thomas A. 2002. Intraneuronal APP/A beta trafficking and plaque formation in beta-amyloid precursor protein and presenilin-1 transgenic mice. *Brain pathology (Zurich, Switzerland)*, **12**(3), 275–286.
- Wu, X., Huang, W., Ganapathy, M. E., Wang, H., Kekuda, R., Conway, S. J., Leibach, F. H., & Ganapathy, V. 2000. Structure, function, and regional distribution of the organic cation transporter OCT3 in the kidney. *American journal of physiology. Renal physiology*, **279**(3), F449–F458.
- Young, A. H., Macritchie, K. A., & Calabrese, J. R. 2000. Treatment of bipolar affective disorder. *BMJ (Clinical research ed.)*, **321**(7272), 1302–1303.
- Young, James D., Yao, Sylvia Y. M., Baldwin, Jocelyn M., Cass, Carol E., & Baldwin, Stephen A. 2013. The human concentrative and equilibrative nucleoside transporter families, SLC28 and SLC29. *Molecular aspects of medicine*, **34**(2-3), 529–547.
- Zhang, L., Dresser, M. J., Gray, A. T., Yost, S. C., Terashita, S., & Giacomini, K. M. 1997. Cloning and functional expression of a human liver organic cation transporter. *Molecular pharmacology*, **51**(6), 913–921.
- Zhang, L., Schaner, M. E., & Giacomini, K. M. 1998. Functional characterization of an organic cation transporter (hOCT1) in a transiently transfected human cell line (HeLa). *The Journal of pharmacology and experimental therapeutics*, **286**(1), 354–361.

CURRICULUM VITAE - JOÃO N. S. PEREIRA

João Nuno dos Santos Pereira

Born: 13. January 1989, Torres Novas, Portugal

Nationality: Portuguese

EDUCATION

- Nov. 2011 – **PhD Student**
PhD Program in Molecular Medicine
Georg-August University of Göttingen, Germany
Thesis title:
„The role of membrane influx transporters on the metabolism and distribution of psychotropic drugs“
- Sep. 2009 – **MSc. in Biotechnology**
Oct. 2011 NOVA University of Lisbon, Portugal
Thesis title:
“Establishing a high titer transient gene expression process in conditioned media for CHO-DG44 cells”
- Sep. 2010 – **Exchange student / Master Thesis**
Aug. 2011 Swiss Federal Institute of Technology Lausanne (EPFL), Switzerland
- Sep. 2006 – **BSc. in Biochemistry**
Jul. 2009 NOVA University of Lisbon, Portugal

WORK EXPERIENCE

- Sep. 2011 – **Institute for Clinical Pharmacology**, PhD Student / Research assistant
University of Göttingen Medical Center, Georg-August University of Göttingen, Germany
- Sep. 2010 – **Laboratory of Cellular Biotechnology**, Master Student
Aug. 2011 Swiss Federal Institute of Technology Lausanne (EPFL), Switzerland
- Feb. 2009 – **Associated Laboratory REQUIMTE**, Junior Researcher
Aug. 2009 Faculty of Sciences and Technology, NOVA University of Lisbon
Project title: “Proteomic analysis from human skin – Psoriasis, a skin autoimmune disease”

PUBLICATIONS

dos Santos Pereira JN, Tadjerpisheh S, Abu-Abed M, Saadatmand AR, Weksler B, Romero IA, Couraud PO, Brockmöller J, Tzvetkov MV. The poorly membrane permeable antipsychotic drugs amisulpride and sulpiride are substrates of the organic cation transporters from the SLC22 family. AAPS Journal. **2014**

Tzvetkov MV, dos Santos Pereira JN, Meineke I, Saadatmand AR, Stingl JC, Brockmöller. Morphine is a substrate of the organic cation transporter OCT1 and polymorphisms in OCT1 gene affect morphine pharmacokinetics after codeine administration. Biochemical Pharmacology. **2013**

João Pereira, Yashas Rajendra, Lucia Baldi, David L Hacker and Florian M Wurm Transient gene expression with CHO cells in conditioned medium: a study using TubeSpin® bioreactors. BMC Proceedings **2011** (Extended abstract)

ORAL COMMUNICATIONS IN MEETINGS

Influx transporters at the blood-brain barrier: Amisulpride and sulpiride as substrates of the organic cation transporters from the SLC22 family. Bad Herrenalb Transporter and Barrier Days. Bad Herrenalb, Germany. **2014**

Characterization of sulpiride and amisulpride as substrates of the organic cation transporters from the SLC22A family. Göttingen Transporter Days. Göttingen, Germany **2013**

Drugs and drug transporters at the human blood-brain barrier. Göttingen Transporter Days. Göttingen, Germany **2012**

POSTER COMMUNICATIONS IN MEETINGS

The weakly membrane permeable antipsychotics amisulpride and sulpiride are substrates of the organic cation transporters from the SLC22 family. Hannover, Germany. **2014**

Influx transporters at the blood-brain barrier: Amisulpride and sulpiride as substrates of the organic cation transporters from the SLC22 family. Microsomes and drug oxidations. Stuttgart, Germany. **2014**

Pharmacogenetics of Drug Transport at the Blood Brain Barrier: Which Transporters for Which Drugs?. World congress of psychiatric genetics. Hamburg, Germany. **2012**

Transient gene expression with CHO cells in conditioned medium: a study using TubeSpin® bioreactors. European Society for Animal Cell Technology (ESACT) meeting. Vienna, Austria. **2011**